The potential application of canine and human mesenchymal stem cells for the treatment of spinal cord injury: an *in vitro* examination of their neurotrophic and angiogenic activities

Doctor of Philosophy

by

Ibtesam Radhi Thammer Al-delfi

Aston University

March 2017

Aston University

The potential application of canine and human mesenchymal stem cells for the treatment of spinal cord injury: an *in vitro* examination of their neurotrophic and angiogenic activities

Ibtesam Radhi Thammer Al-delfi **Doctor of Philosophy, 2017**

Thesis Summary

Traumatic spinal cord injury (SCI) is a devastating event. It causes severe damage to the nervous tissue which can be associated with partial or complete loss of movement and sensation. Recent studies suggested that the benefits of stem cell transplants for SCI may not be restricted to cell restoration alone, e.g. to replace damaged neurons, but also may be due to their capacity to stimulate endogenous cells at wound sites through paracrine activity. Mesenchymal stem/stromal cells (MSCs), in particular, are thought to have anti-inflammatory, neuroprotective, neurotrophic and angiogenic effects and may thus reduce secondary damage and promote neuroregeneration and wound healing after their administration. Experimental studies of small rodent SCI models are currently being used to investigate the MSCs as a promising option for treatments that repair damaged neuronal tissue. However, translation to human patients is still a challenging step. Dogs represent a good large animal model as the causes of SCI in dogs occur naturally and traumatically, and because of the similar scale and heterogeneity of the lesions formed. Therefore, this study aimed to investigate and compare the effects of canine and human MSCs, focused on the effects of MSC conditioned medium (MSC CM) on neurogenesis and angiogenesis using established responder cell lines, i.e. SH-SY5Y neuronal cells and EA.hy926 endothelial cells. All of the MSCs were derived from adipose tissue, and CD271 was used to isolate subset populations from human MSCs. The study has demonstrated for the first time the potentially beneficial effects of canine MSC CM in promoting SH-SY5Y neurite outgrowth and cell proliferation, as well as EA.hy926 endothelial cell proliferation, cell migration and the formation of endothelial tubules. Further experimentation demonstrated that canine and human adipose-derived MSCs exhibited such neurotrophic and angiogenic effects to a similar extent. This may have important implications for the pre-clinical assessment of MSC paracrine activity in the development of cell transplantation protocols both for dogs and humans. Finally, the study compared the neurotrophic and angiogenic effects of MSC CM from selected subpopulations of human MSCs, i.e. $CD271^+$ versus $CD271^-$ and plastic adherent MSCs; this was with a view to establishing whether a more homogeneous MSC population might differ in their paracrine activity. There was no significant difference in the neurogenic effects of these various secretomes; however, MSC CM from human $CD271^+$MSCs was found to be significantly less pro-angiogenic than human $CD271^-$ MSCs or non-selected human MSCs. In conclusion, the study supports the use of MSCs to treat naturally occurring SCI in dogs, and suggests that there is no evidence herein to support pre-selecting $CD271^+$ cells.

Key words: human MSCs, canine MSCs, MSC CM, SCI, CD271, neurogenic, angiogenic.

Dedication

In the name of Allah (God), the entirely merciful, the especially merciful

“And they ask thee concerning the soul. Say, 'The soul has been created by the command of my Lord; and of the knowledge thereof you have been given but a little**” Quran Chapter Al-Isra (17), verse (85)**

I would like to dedicate my simple efforts first to my God for guiding me and giving me a chance in this life to seek the good over the evil. Second I indeed dedicate this thesis to all the brave women and men in my country who sacrifice themselves to the defence of our beloved homeland Iraq, asking my mighty God to bring peace on it. Also, I would like to dedicate it to my beloved family.

Acknowledgements

First I would like to thank my Country Iraq for whom my prayers will never stop to bring peace on it as it was before. I would like to thank the Iraqi ministry of higher education and scientific research for sponsoring my project.

I would like to express my gratitude feeling and thanks to my supervisor Professor Eustace Johnson not just for the tremendous support, guidance and mentorship whilst supervisor me throughout my PhD but also for the kindness and humanity he has shown during these four years I knew him.

Also, I would like to thank Dr. Ann Vernallis for her help and support during the last year of my study.

I would like to thank my colleagues and friends Dr. Jonathan Sheard, Dr. Saima Begum, Dr. Nupur Kohli, Sowmya Ajay, and Oulseyi Ayinde for being a great help and support during my PhD.

Finally, I would like to thank my parents, sisters, and brothers whom never stopped their prayers for me and wished me to be successful and safe.

Abbreviations

AT MSCs	Adipose tissue-derived mesenchymal stem cells
BDNF	Brain-derived neurotrophic factor
bFGF	Basic fibroblast growth factor
BM MSCs	Bone marrow-derived MSCs
BSA	Bovine serum albumin
BSCB	Blood-spinal cord barrier
CFU-F	Colony forming unit-fibroblasts
cMSCs	Canine adipose-derived mesenchymal stem cells
CNS	Central nervous system
CR3	Complement receptor 3
DMSO	Dimethyl sulphoxide
ECM	Extracellular matrix
EGF	Epithelial growth factor
ELISA	Enzyme-linked immunosorbent assay
ESCs	Embryonic stem cells
EVs	Extracellular vesicles
FACS	Fluorescence-activated the cell sorting
FBS	Fetal bovine serum
GAGs	Glycosaminoglycans
HGF	Hepatocyte growth factor
HLA	Human leukocyte antigen
hMSCs	Human adipose-derived mesenchymal stem cells
HSCs	Haematopoietic stem cells
IBMX	3-isobutyl-1-methylxanthine
ICM	Inner cell mas
IGF-1	Insulin-like growth factor-1
iPSCs	Induce pluripotent stem cells
ISCT	International Society for Cellular Therapy
ITS	Insulin/transferrin/selenium
IVDD	Intervertebral disc disease
LNGFR	low-affinity nerve growth factor receptor
Mac-1	Macrophage-1 antigen
MACS	Magnetic-activated cell sorting
MHC	Major histocompatibility complex
miRNA	micro-RNA
MP	Methylprednisolone
MSC CM	MSC culture-conditioned medium
MSCs	Mesenchymal stem cells
MVs	Microvesicles
NEAA	(Non-essential amino acids
NGF	Nerve growth factor
NGFR	Nerve growth factor receptor
NSPCs	Neural stem/progenitor cells
PA MSCs	Plastic adherent MSCs
PMCs	Mesenchymal progenitor cells
PTPRC	Protein tyrosine phosphatase, receptor type C
RoI	Region of interest
RPE	Retinal pigment epithelium
SCI	Spinal cord injury
SD	Standard deviation
SEM	Standard error of the mean
SVF	Stromal vascular fraction
TGF-α	Transforming growth factor-alpha

TGF-β	Transforming growth factor-beta
VEGF	Vascular endothelial growth factor

List of Tables

List of Figures

Chapter One: Introduction

1. Introduction

This chapter explores the problem area that inspired the hypothesis which was tested in this study. This chapter covers several topics including; the stem cells and their different types, in particular, the MSCs and their therapeutic role in treating spinal cord injury (SCI). This chapter also explains the role of the large animal model in translating SCI research. At the end of the chapter, the aim of the study is presented. This thesis is organised as follows: chapter two discusses the chosen methodology, chapter three to five set out the results obtained by this study and chapter six discusses the results and draws conclusions.

1.1 Stem Cells

Stem cells are undifferentiated cells found in multicellular organisms. Although they make up a small portion of the body mass, their properties and capacities of developing into a variety of cell types in the body are remarkable. Stem cells can divide through mitosis and differentiate into a variety of specialised cell types. Moreover, stem cells can self-renew to produce more stem cells (Lin, 2008). Also, under certain physiological conditions *in vitro*, stem cells can differentiate into different mature cell types with specialised functions (Wells, 2002). The ability to differentiate into diverse cell types allows stem cells to serve as a repair system to continuously replenish other cells (Li and Xie, 2005). Once, a stem cell divides, each new cell has the potential to either remain as a stem cell or become another mature cell type with new specific functions (Lechler and Fuchs, 2005). In fact, it is still a challenge to understand the underlying mechanisms of stem cells to differentiate and develop into various types of cells, which in turn have important biological functions (Feng and Wang, 2012, Xu et al., 2014). However, all stem cells, regardless of their origin, have three features. Firstly, one of the fundamental properties of stem cells is they are unspecialised cells, not allowed to perform specific functions as they do not have any tissue-specific structures (Melton, 2014).

For example, a stem cell cannot work with its neighbors to pump blood through the body (like a heart muscle cell) ; it cannot carry molecules of oxygen through the bloodstream (like a red blood cell); it cannot fire electrochemical signals to other cells that allow the body to move or speak like a nerve cell (Zapata et al., 2012). However, unspecialised stem cells can give rise to specialised cells, including heart muscle cells, blood cells, or nerve cells (Kehat et al., 2001, Wichterle et al., 2002, Novotny et al., 2009). Secondly, stem cells have the capacity for dividing and renewing themselves for long periods. Stem cells may replicate many times in contrast with other mature cells such as muscles, red blood cells and nerve cells which do not usually replicate themselves (Clatworthy and Subramanian, 2001).

Proliferation is the term which describes the repeated self-replication. The *in vitro* experimental studies showed that the stem cells can replicate many times, and can yield millions of cells. These studies have used the cell doubling time assay and cell proliferation assay to show the proliferative potential of the stem cells(Bruder et al., 1997, Baksh et al., 2007). If these cells resulting from proliferation continue to be unspecialised, like their original parent stem cells, then the cells will also be capable of long-term self-renewal (Park et al., 2008). Thirdly, stem cells can give rise to specialised cells. Differentiation is the term which describes the process by which unspecialized stem cells result in specialised cells through distinctive differentiation pathways controlled by internal and external signals. Researchers in their studies are just beginning to understand the internal signals and external signals that trigger the differentiation of stem cells. The internal signals are controlled by a cell's genes, which are interspersed across long strands of DNA, and carry coded instructions for all the structures and functions of a cell. The external signals for cell differentiation include chemicals secreted by other cells, physical contact with neighbouring cells, and certain molecules in the microenvironment (Tosh and Horb, 2014). These characteristics make stem cells a good target in regenerative medicine as they hold promise in the repair and regeneration of damaged tissue (Kimbrel and Lanza, 2015). Fighting diseases is a fundamental battle, stem cells present a powerful therapy to repair injured tissue by cell therapy and tissue regeneration (Trounson and DeWitt, 2016).

There are a variety of sources of stem cells, based on the type of tissue origin. Mammalian stem cells can be classified into embryonic stem cells (ESCs), which can form specialised cells of all three germ layers, i.e., ectoderm, mesoderm and endoderm, and adult stem cells, which are more restricted in their differentiation potential (Fortier, 2005).

1.2 Types of stem cells

The potency of stem cells can be defined as the capacity to differentiate into specialised cell types (Polejaeva and Mitalipov, 2013). During adulthood life and growth of each organism, stem cells have an increased potential to develop into many different cell types in the body. They have a crucial role in replenishing other cells in the body (Avasthi et al., 2008). Stem cell potency can be classified according to the differentiation extent of stem cells to give rise to different cell types. There are three main classifications for stem cell potency; these are: totipotent, pluripotent or multipotent (Sharma et al., 2012). Totipotent stem cells are stem cells that have the ability to differentiate into all possible cell types.

The first few cells that result from the division of the zygote, which formed by the fusion of sperm cell with an egg cell, are considered as totipotent stem cells. They have the potential capacity to give rise to the whole embryo and extra embryonic structures (Figure 1.1) (Martín and Menéndez, 2012). Pluripotent stem cells are stem cells that have the ability to give rise and differentiate into almost all cell types. An example of pluripotent stem cells is ESCs that are isolated from the inner cell mass (ICM) which can give rise to all cell types that are derived from the mesoderm, endoderm, and ectoderm germ layers (Figure 1.2). Induce pluripotent stem cells (iPSCs) are another example of pluripotent stem cells (Thomson et al., 1998, Sharma et al., 2012). Multipotent stem cells are stem cells that have the capacity to differentiate and give rise to several cell types. Haematopoietic stem cells (HSCs) and mesenchymal stem cells (MSCs) are examples of multipotent stem cells (Figure1.5) (Uccelli et al., 2008).

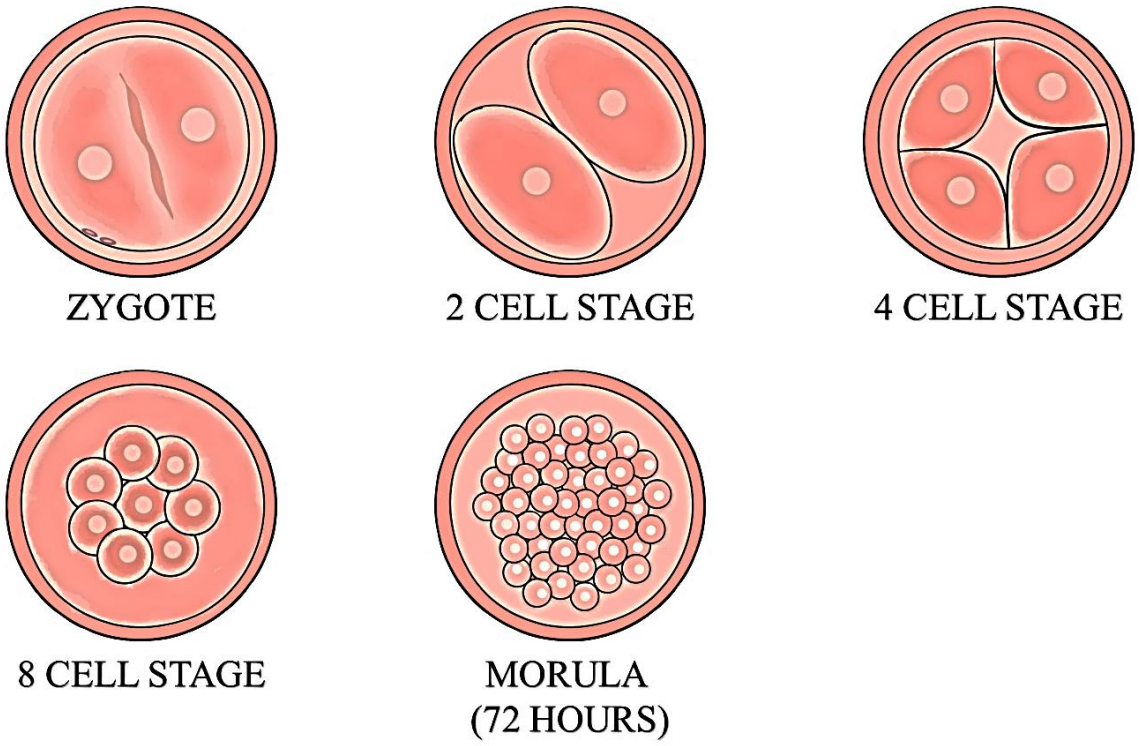

Figure 1:1 Early developmental stages of a human zygote as an example for totipotent stem cells.

Schematic illustration showing the stages of division of a fertilised egg as an example for totipotent stem cells. Each cell is capable of giving rise to a complete organism, plus the extraembryonic placental cells. Image adapted (Shutterstock, 2003).

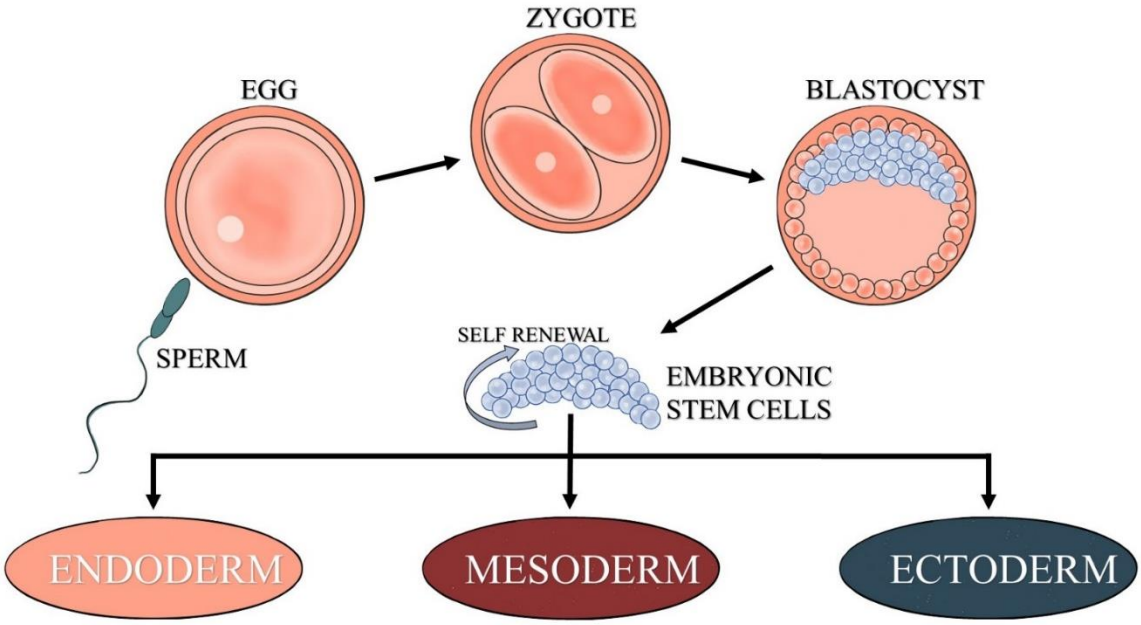

Figure 1:2 Embryonic stem cells derived from the inner cell mass as an example of pluripotent stem cells.

Schematic illustration showing the developmental stages of embryonic stem cells which are derived from the ICM and their differentiation capacity into any of the three germ layers ectoderm, mesoderm and endoderm. They do not have the ability to give rise to the extraembryonic structures the umbilical cord and placenta. Image adapted from (Chial, 2008).

1.2.1 Embryonic stem cells

In 1981, Evans and Kaufman were the first to isolate embryonic stem cells from mouse, which can be isolated from the ICM of the blastocyst at early stages of embryonic development (4-5 days after fertilisation), i.e., before implantation in the uterine wall (Evans and Kaufman, 1981). In the same year Martin, 1981 named them as ESCs (Martin, 1981). This finding led to an interest in an *in vitro* isolation of human ESCs and cell culturing by James Thomson and co-workers (Figure1.3) (Thomson et al., 1998). ESCs can be classified as pluripotent stem cells. They can be maintained and expanded in culture indefinitely under optimal conditions. As stated earlier, ESCs have the capacity to differentiate into all three embryonic germ layers endoderm, mesoderm and ectoderm which, subsequently can differentiate into different tissues (Evans and Kaufman, 1981). Thomson et al. (1998) and Odorico et al. (2001) suggested that ESCs can propagate for about 300 population doublings when growing in culture and that they can be passaged for over a year in culture (Thomson et al., 1998, Odorico et al., 2001).

ESCs have the potential uses in cell replacement therapy for transplantation medicine as they have the capacity to differentiate into cells or tissues that have been damaged by disease or injury (Thomson et al., 1998, McDonald et al., 1999, Odorico et al., 2001, Menasche et al., 2015). Thus, ESCs may represent great promise in the future in various research areas, such as human developmental biology and cell-based therapies. However, despite these advantageous characteristics of ESCs, they have disadvantages as well. One of these disadvantages is the ethical issues surrounding ESCs since, to isolate ESCs, the destruction of the human embryo is required. Also, the other disadvantage of using ESCs is the possibility of tumour formation. Many animal experiments have shown that embryonic stem cells form tumours after transplantation (Master et al., 2007).

Moreover, transplantation of ESCs requires either a histocompatibility match or the patient needs to be immunosuppressed (Swijnenburg et al., 2008).

However, Schwartz et al., 2012 showed in their preliminary report the safety of treating patients with Stargardt's macular dystrophy and dry age-related macular degeneration by transplantation of human ESC-derived retinal pigment epithelium (RPE). They reported in their study that transplantation of ESC-derived RPE cells showed no signs of hyperproliferation, tumorigenicity, ectopic tissue formation, or apparent rejection after four months. They claimed that the pre-differentiation of ESCs into RPE cells before their transplantation could reduce the chances of the formation of a tumour or being rejected by host tissues (Schwartz et al., 2012).

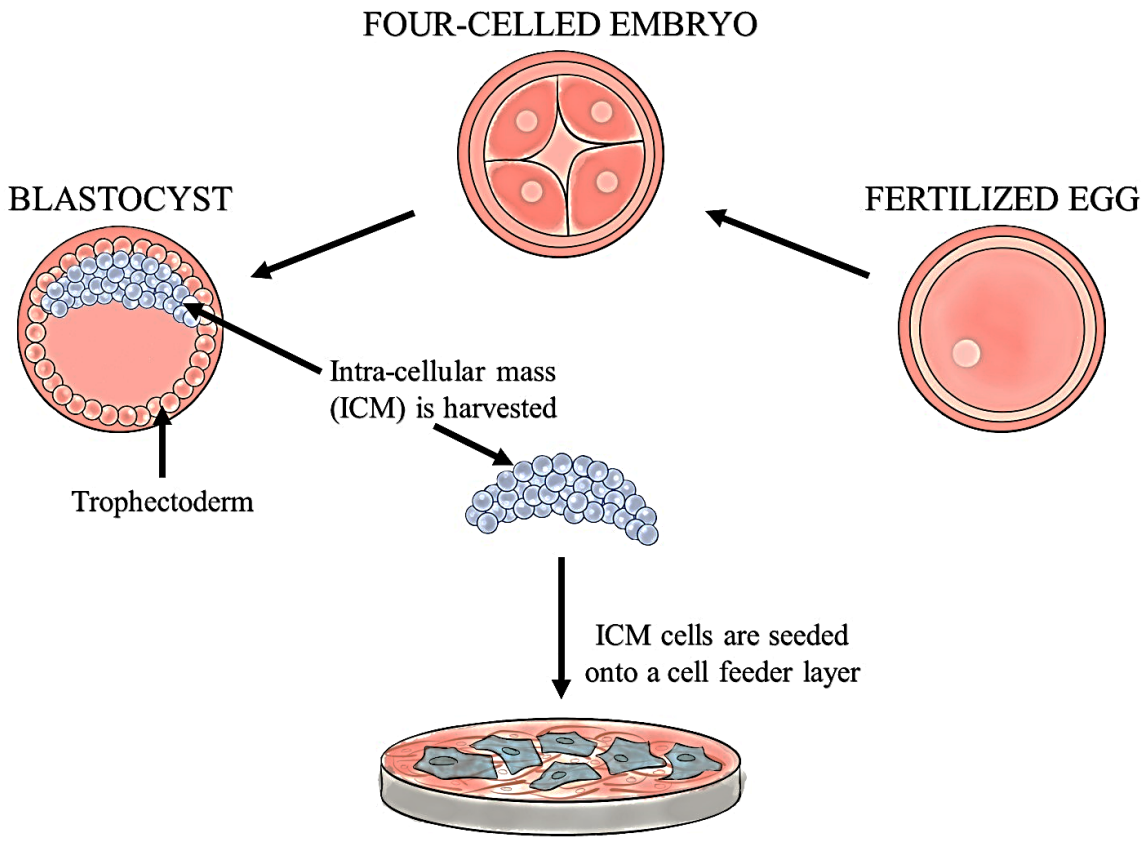

Figure 1:3 In vitro isolation of human embryonic stem cells.

The schematic illustration showing the steps from a fertilised egg obtained by IVF to the culture of ESCs are depicted. A few-celled embryo later gives rise to the blastocyst, a structure comprised of an outer cell layer, the trophectoderm, and ICM. The ICM is harvested and plated on feeder cells, to yield a population of ESCs. Image adapted from (Landry and Zucker, 2004).

1.2.2 Induced pluripotent stem cells

iPSCs are in fact adult somatic cells that have regained their pluripotency state by genetic engineering mechanisms (Takahashi and Yamanaka, 2006). These reprogrammed adult cells are similar to ESCs in that they are pluripotent and capable of differentiating to produce all of the different cells and tissues in the adult body (Okita et al., 2007). In brief, iPSCs can be generated by treating somatic cells with a combination of four reprogramming factors, including Oct4 (Octamer-binding transcription factor 4), Sox2 (Sex-determining region Y)-box2, Klf4 (Kruppel like factor-4), and c-Myc (Figure 1.4) (Takahashi and Yamanaka, 2006). The iPSCs may overcome the various ethical issues regarding the use of embryos in research and clinical medicine. Also, immune rejection is not a concern since the body considers the introduction of iPSCs as an autologous transplantation (Guha et al., 2013). However, they also have the capacity to form tumours similar to ESCs (Howe et al., 2008). Despite all the limitations and controversy, both ESCs and iPSCs are already used in ongoing clinical treatments of spinal cord injury, macular degeneration of the retina, type 1 diabetes and heart failure (Table 1.1) (reviewed in Ilic et al., 2015).

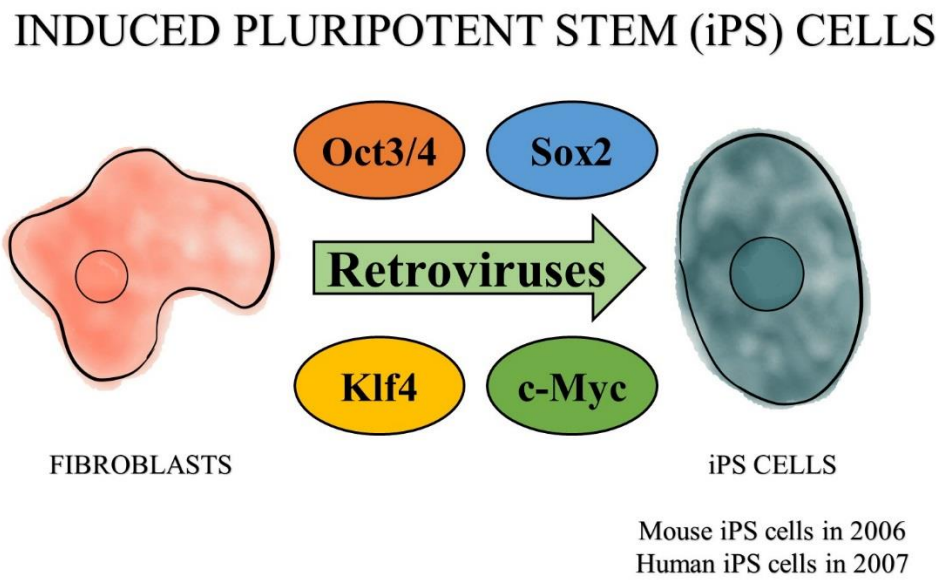

Figure 1:4 Generation of iPS cells.

The schematic illustration showing the reprogramming of adult fibroblast cells in iPS cells mediated by Oct-4, Klf4, Sox2 and c-Myc give rise to cells that resemble ESCs with embryonic potential. In 2006, Kazutoshi Takahashi and Shinya Yamanaka reprogrammed mice fibroblast cells into iPS and in 2007 they have reprogrammed human fibroblast cells into iPS. Image adapted from (Yamanaka, 2009).

Indication	Cell source	Institution	Country	Start date	Finish date	Subjects
Spinal cord injury	hESC	Geron	USA	October 2010	July 2013	5
		Asterias	USA	March 2015	June 2018	13
Immunotherapy vaccine for lung cancer	hESC	Asterias	UK	Not defined	Not defined	Not defined
Geographic atrophy secondary to myopic macular degeneration	hESC	Ocata	USA	April 2014	April 2015	Not defined
Stargardt macular degeneration of retina	hESC	Ocata	USA	July 2012	December 2030	13
			UK	November 2011	December 2015	16
Dry macular degeneration of retina	hESC	Ocata	USA	July 2012	December 2030	13
		Cell Cure Neurosciences	Israel	April 2015	August 2017	15
	iPSC	RIKEN CBD	Japan	October 2013	Not defined	6
Wet macular degeneration of retina	hESC	The London Project to Cure Blindne	UK	August 2015	October 2016	10
Diabetes type I	hESC	ViaCyte	USA	September 2014	August 2017	40
Heart failure	hESC	APHP	France	June 2013	June 2017	6

Table 1: The current clinical trial using ESCs and iPSCs.

The table shows most of the current studies ongoing or recently closed. Most of these studies have demonstrated the safety of using ESCs and iPSCs rather than efficacy. The table is adapted from (Ilic et al., 2015).

1.2.3 Adult stem cells

Most human body tissues have a stem cell population; these cells are called an adult or somatic stem cells. Adult stem cells are responsible for the replenishment of cells of the tissue or organ where they reside as well as undergoing self-renewal (Goodell et al., 2015). Adult stem cells can be found in all part of the body tissues. For example, they can be found in the brain, bone marrow, adipose tissue, peripheral blood and blood vessels, skeletal muscle, skin, teeth, heart, gut, liver, ovarian epithelium, and testis (Zuk et al., 2002, Avgustinova and Benitah, 2016). Commonly, the beneficial and therapeutic usage of adult stem cells is considered more acceptable than that of ESCs, as there are fewer ethical considerations and less controversy on the usage of adult stem cells in comparison with ESCs. This is because the isolation of adult stem cells and culture does not require the destruction of an embryo (Bongso and Richards, 2004, Larijani et al., 2012).

However, the therapeutic use of adult stem cells faces several challenges. These include issues that may be related to donor source, e.g. a genetic pre-disposition to disease. Also, limitations in the differentiation potential of the somatic stem cells (which are multipotent rather than pluripotent) compared to ESCs (Mariano et al., 2015). Also, since adult stem cells are present in small numbers within the tissues they reside, this means few cells can be released, and as high numbers of cells are needed for stem cell replacement therapies, this is another challenge of using adult stem cells (Spradling et al., 2001). Finally, during cell culture, the capacity of adult stem cells to renew themselves are not as great as with ESCs. Adult stem cells also tend to undergo senescence after long-term culture (Zimmermann et al., 2004).

Example of adult stem cells which are common in use in research is HSCs and MSCs which the later has discussed in more details in next section.

1.3 Mesenchymal stem cells

1.3.1 Sources and main characteristic features of mesenchymal stem cells

MSCs are multipotent stem cells that have the capacity to renew themselves and have the ability to differentiate into several lineages of cells including adipocytes, osteoblasts, chondrocytes, myocytes and fibroblasts (Pittenger et al., 1999). MSCs were first identified in the late 1970s, by a group led by the Russian scientist, Alexander Friedenstein (Friedenstein et al., 1970). They showed in their study that bone marrow contains a population of cells that have the characteristic of being plastic adherent, highly proliferative, and have the capacity to form a colony of fibroblasts. Hence, these cells were named colony forming unit-fibroblasts (CFU-F) (Friedenstein et al., 1981, Friedenstein et al., 1982). Friedenstein and his group found that these CFU-F spontaneously formed bone, cartilage and fibrous tissue following transplantation in diffusion chambers (Friedenstein et al., 1987). This study suggested that these cells were multipotent and can form different mature cell types of mesenchymal lineages. In 1991, Arnold Caplan proposed the term ″ mesenchymal stem cells″ for the previously termed CFU-F (Caplan, 1991). Basically, MSCs are multipotent stem cells that have the capacity to renew themselves and have the ability to differentiate into several lineages of cells including adipocytes and chondrocytes (Dennis et al., 1999), osteoblasts (Haynesworth et al., 1992), muscle (Wakitani et al., 1995, Gang et al., 2004), marrow stromal cells (Majumdar et al., 1998), tendon and ligament (Young et al., 1998, Kuo and Tuan, 2008), and other connective tissues (Studeny et al., 2004, Bhatia and Hare, 2005) (Figure 1.5).

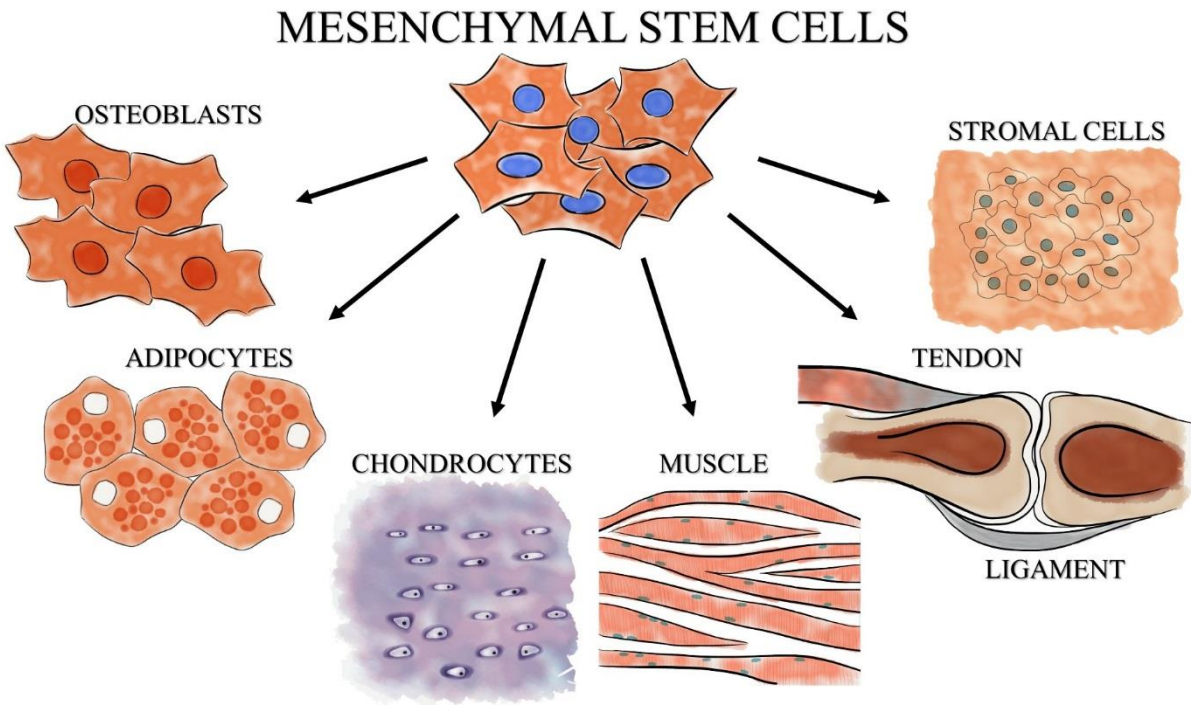

Figure 1:5 Multipotent differentiation capacity of mesenchymal stem cells.

The schematic illustration shows the differentiation capacity of MSCs into limited types of cells. Image adapted from (Das et al., 2013).

As mentioned previously, MSCs were identified for the first time in the early 1970s by Alexander Friedenstein using the bone marrow, these cells are now referred to as bone marrow-derived MSCs (BM MSCs) (Friedenstein et al., 1970). However, over the last decades many studies have demonstrated that MSCs can be found in other places in the body, e.g., brain, adipose tissue, liver, and lungs (Zuk et al., 2001, Zuk et al., 2002, Kang et al., 2010, Zou et al., 2010). The International Society for Cellular Therapy (ISCT) has suggested three minimum criteria that MSCs should display regardless of the tissue from which they are isolated. The isolated cells are termed mesenchymal stem cells if they demonstrate the following criteria; i) plastic adherence, ii) multipotent differentiation profile (i.e., adipogenic, osteogenic and chondrogenic differentiation capacity) iii) expression of a specific cell surface markers and the absence of others (Dominici et al., 2006). The cell surface markers that the isolated cells should express include; CD44, CD73, CD90 and CD105, more than 95 % of the MSC population must express these markers. Also, the isolated cells must lack expression of CD34, CD45, CD11b, CD14, CD79, CD19 and HLA class II (less than 2 % should express these markers (Horwitz et al., 2005, Dominici et al., 2006).

CD44 is a cell-surface glycoprotein involved in cell-cell interactions, cell adhesion and migration (Goodison et al., 1999, Ponta et al., 2003). CD73 is one of the several enzymes responsible for the production of extracellular adenosine, a signalling molecule that is involved in responses to inflammation and tissue injury (Hashikawa et al., 2003). CD90 also known as Thy1, is a glycosylphosphatidylinositol-linked protein involved in cell-cell and cell-matrix interactions (Rege and Hagood, 2006). CD105 also known as endoglin, is a type I membrane glycoprotein that functions as an accessory receptor for TGF-beta superfamily ligands (Varma et al., 2007).

Whereas the cell surface markers that the isolated cells should lack are; CD34 is a member of a family of single-pass transmembrane sialomucin proteins that show expression on early haematopoietic and vascular-associated tissue (Nielsen and McNagny, 2009). CD45 is Protein tyrosine phosphatase, receptor type C (PTPRC).

It was originally called leukocyte common antigen, and it is specifically expressed in haematopoietic cells (Wu et al., 2002). CD11b is a macrophage-1 antigen (Mac-1) or complement receptor 3 (CR3). It is expressed on the surface of many leukocytes involved in the innate immune system, including monocytes, granulocytes, macrophages, and natural killer cells (Hickstein et al., 1987, Xu et al., 2015). CD14 is a human gene also known as cluster of differentiation 14. The protein encoded by this gene is a component of the innate immune system. CD14 is expressed on the surface of various cells, including monocytes, macrophages, polymorphonuclear neutrophils and chondrocytes (Tobias and Ulevitch, 1993, Bas et al., 2004).

CD79 is composed of two distinct chains called CD79A and CD79B (formerly known as Ig-alpha and Ig-beta); these form a heterodimer on the surface of a B cell stabilised by disulphide bonding. CD79a and CD79b are both members of the immunoglobulin superfamily (Chu and Arber, 2001, Matnani et al., 2013). CD19 is a protein that in humans is encoded by the CD19 gene. It is found on the surface of B-cells, a type of white blood cell. CD19 is a B lymphocyte cell-surface marker which is expressed early during pre-B-cell differentiation, and this expression remains until terminal differentiation into plasma cells (Zhou et al., 1992). The human leukocyte antigen (HLA) system or complex is a gene complex encoding the major histocompatibility complex (MHC) proteins in humans. The MHCs are responsible for the regulation of the immune system in humans. HLAs are the leading cause of organ transplant rejection (Taylor et al., 2011).

The MSCs are an attractive resource not only for autologous cell therapy but also for allogenic cell therapy, as they possess immune modulatory properties and a powerful immunosuppressive potential (Zhu et al., 2008). Zuk et al., 2001 was the first who identified adipose tissue-derived mesenchymal stem cells (AT MSCs). These cells have a multi-lineage potential differentiation profile since they are capable of differentiating into adipogenic, osteogenic, chondrogenic (Zuk et al., 2001) and myogenic cells (Mizuno et al., 2002).

Also, in culture AT MSCs are characterised by their expression of a panel of markers (i.e. CD44, CD73, CD90 and CD105) and the absence of others (i.e. CD34, CD45, CD11b, CD14, CD79, CD19 and HLA class II). AT MSCs and BM MSCs are the main sources of MSCs, and they are widely used especially in autologous cell-based therapies (Hoogduijn and Dor, 2013). According to the website of (clinicaltrials.gov), there are around 369 clinical trials as of 20.03. 2017 on MSCs transplantation ranging from recruiting, enrolling by invitation to completed trails. In these studies, both autologous and allogenic MSCs have used for treating different conditions, these studies were based on showing the safety and efficacy of MSCs.

However, AT MSCs have several biologic advantages over BM MSCs in term of regenerative application for repairing injured and damaged tissue. These benefits can be ascribed to the fact that adipose tissue is a more abundant tissue than bone marrow. It is easy to access and the procedure to harvest adipose tissue has a low morbidity rate when compared with the harvesting of bone marrow (Padoin et al., 2008). Moreover, the yield of AT MSCs from adipose tissue is potentially higher than the yield from bone marrow. AT MSCs make up roughly 2% of the nucleated cells in processed lipoaspirate, wears BM MSCs constitute about 0.01% of the total nucleated cells in the bone marrow (Friedenstein et al., 1970, Li et al., 2015).

The approximate CFU-F per gram of adipose tissue is around 5000, compared with CFU-F from 1 ml of bone marrow MSCs which is around 100 to 1000 (Strem et al., 2005). Furthermore, AT MSCs have better performance in terms of proliferative capacity and secreted proteins (basic fibroblast growth factor, interferon-γ, and Insulin-like growth factor-1), and immunomodulatory effects (Li et al., 2015). These differences between both BM MSCs and AT MSCs could be due to differences in tissues origin site. In fact, heterogeneity is found not only between two MSCs population from different tissues of origin but also can be found within the MSC population itself (Noer et al., 2006, Tallone et al., 2011). As AT MSCs were used in this study, the heterogeneity of this population is further considered in the next section.

1.3.2 Heterogeneity of MSCs

Many studies suggested that MSCs are heterogeneous populations. This heterogeneity could stem from different reasons such as genetic, epigenetic, localization-relocalization, site of origin, and likely sex/gender factors (Pevsner-Fischer et al., 2011, Li et al., 2013, Hart, 2014). Therefore, using heterogeneous populations of MSCs with the presence of subpopulations could result in different outcomes. Thus, to emphasise the point, the therapeutic effect of MSCs could be achieved by using very well characterised subpopulations to lighten the variation (Phinney, 2012). AT MSCs are easily isolated from adipose tissue by collagenase digestion followed by centrifugation steps; the isolated fraction is called the stromal vascular fraction (SVF) (Zuk et al., 2001). This SVF is characterised by its highly heterogeneous nature since it has different stem cell subpopulations and more differentiated cells (differentiated endothelial cells, smooth muscle cells and pericytes) (Ho et al., 2008).

The plastic adherent outgrowth from SVF is AT MSCs which in turn are considered to be a heterogeneous population as they comprise several subset populations (Noer et al., 2006, Tallone et al., 2011, Busser et al., 2015). There are several techniques used to isolate a specific subset population from heterogeneous populations of AT MSCs. Such isolation can be carried out either by using flow cytometric sorting or immunomagnetic separation (Griesche et al., 2010, Jiang et al., 2010).

Flow cytometry is a powerful diagnostic technique which can measure the physical and chemical characteristics of single cells when they pass individually through a laser beam. Additionally, flow cytometers also have the ability to sort cells within a heterogeneous mixture. This type of flow cytometer device is known as a flow sorter and also known as fluorescence activated the cell sorting (FACS) device (Figure1.6) (Shapiro, 2004). Many studies have used FACS technology to purify MSCs from heterogeneous cell populations. Such purification is based on the identification of cell surface markers expressed by MSCs (Battula et al., 2009, Ramakrishnan et al., 2013).

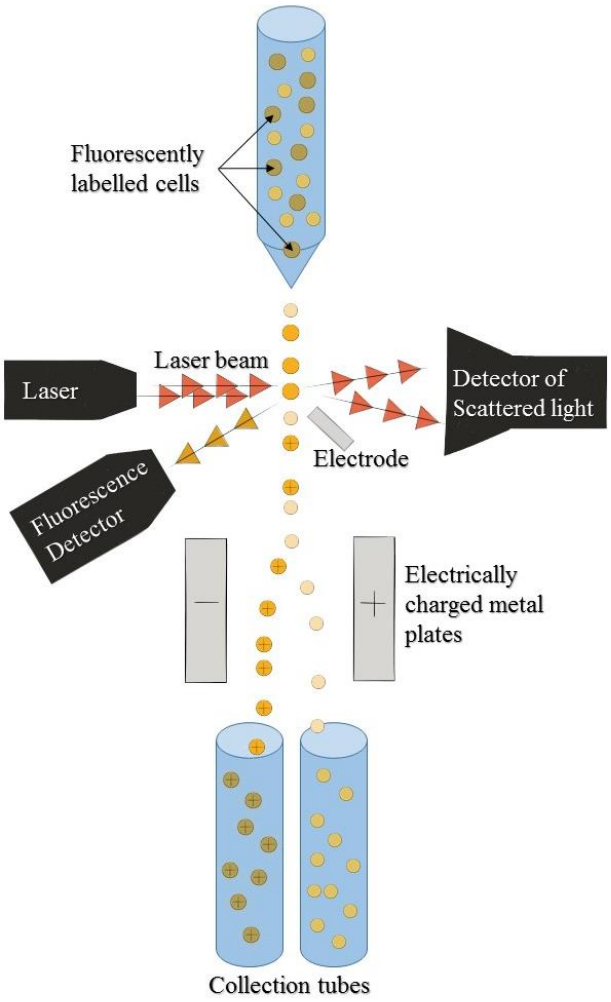

1. A mixed population of cells is labelled with a fluorescent antibody marker
2. The cell mixture leaves the nozzle in droplets
3. A laser beam strikes each droplet
4. The fluorescence detector identifies the fluorescently labelled cells by the fluorescent light emitted by the cell
5. An electrode gives a positive charge to identified cells
6. As cells drop between electrically charged plates, the cells with a positive charge move closer to the negative plate
7. The separated cells fall into different collection tubes

Figure 1:6 Cell sorting technique using fluorescence activated cell sorting FACS device.

Schematic illustration showing the steps required to isolate certain populations of cells using a FACS device as the cells were fluorescently labelled with a targeted marker resulting in highly pure population. Image adapted from (Techniques, 2004).

The immunomagnetic separation technique is the most common technique of sorting cells using magnetic forces named magnetic-activated cell sorting (MACS). The cells selected for isolation are labelled with 50 nm diameter superparamagnetic beads and sorted using a packed column (Miltenyi et al., 1990). To achieve the separation and purification of a specific subset of cells, one uses magnetic beads coated with an antibody that is known to bind to the selected cell type selectively. These magnetic beads are incubated with the sample. Once the cells- particles are formed, the mixture should pass through a small column under the influence of a strong magnetic force. In the column matrix, a high gradient magnetic field is induced as the mixture passes, leading to particle-bound cells to be retained while the untagged cells pass through (Figure 1.7). Before tagged cells can be eluted from the column and to ensure a proper purification, the column must be washed at least three times with buffer to remove all unwanted cells (Jones et al., 2002). In fact, subset isolation techniques have attracted attention in mesenchymal stem cells research; this is because the isolation of subpopulations from SVF could have potential benefit to repair specific damaged tissue.

Miranville et al., 2004 isolated CD34+/CD31− cells from the SVF of human adipose tissue obtained from three different regions (subcutaneous gluteal, subcutaneous abdominal and visceral abdominal) undergoing either lipoaspiration or lipectomy. In their study, they demonstrated that the selected cells improved postnatal neovascularization in a mouse model with an ischemic limb (Miranville et al., 2004). Boquest et al., 2005 also described the differences of AT MSCs stemness between two AT MSCs subpopulations, $CD31^+$ cells and $CD31^-$ cells, isolated from adipose tissue which was obtained by liposuction from abdominal, hip, and thigh regions. In their study, they showed that the differentiation plasticity of $CD31^-$ was higher compared with $CD31^+$ which most closely resembled microvascular cells (Boquest et al., 2005).

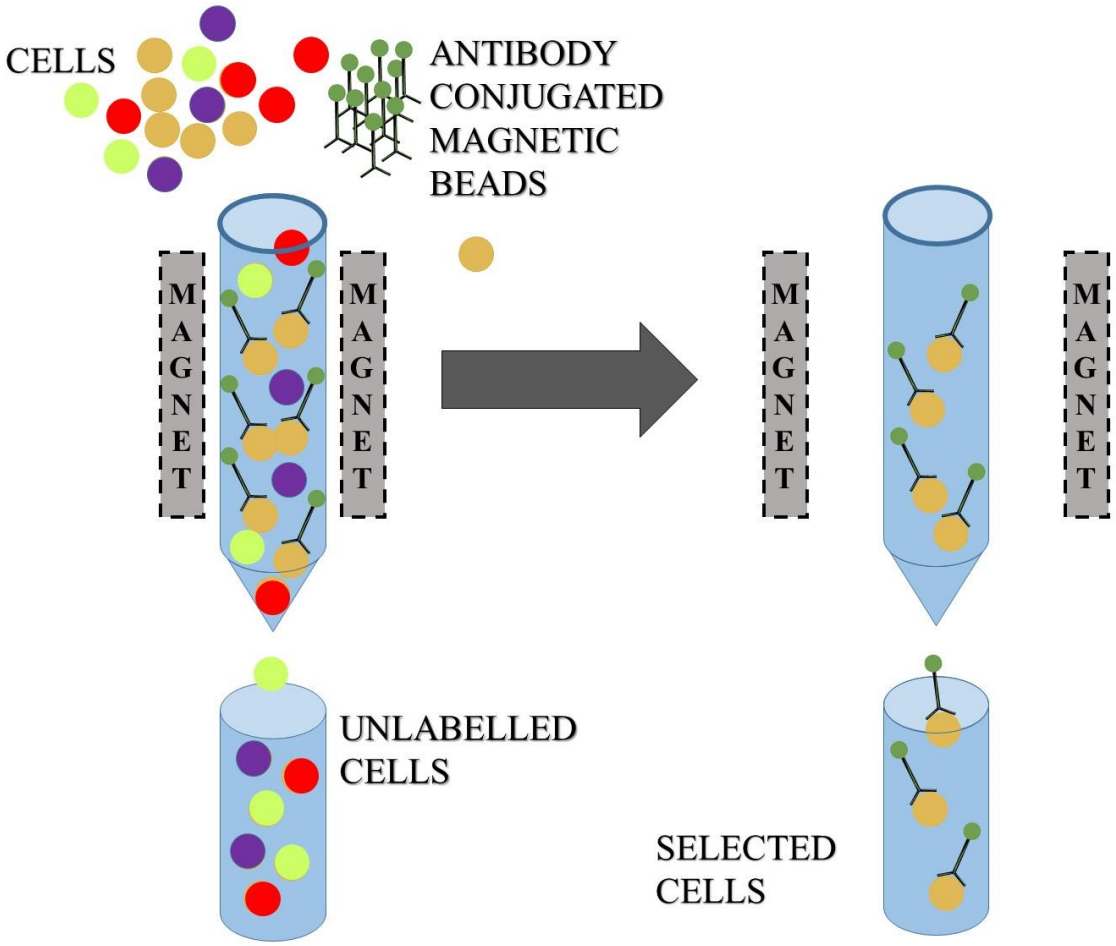

Figure 1:7 Cell sorting technique using magnetic-activated cell sorting (MACS).

The schematic illustration shows the experimental strategy using magnetic MACS beads to isolate specific subtypes of cells from the mixed population. The principles behind this technique are based on labelling cell surface antigens with superparamagnetic microbeads specific for targeted populations and a magnetic column (Steinhauser et al., 2013).

As another example of MSC cell purification, Jones et al., 2002 reported a study in which they performed a cellular purification of MSCs or as Jones et al referred these cells as mesenchymal progenitor cells (PMCs) from bone marrow by positive selection with D7-conjugated magnetic microbeads. They claimed in their study that they were able to purify a Homogeneous population of PMCs from BM based on D7-FIB+, CD45low, LNGFR+ phenotype. They suggested that this population is distinctive from haematopoietic stem cells by their lack of expression CD45 and their large size, also they claimed that the Stro-1 marker was expressed on these cells. Their study suggested that the BM PMCs contained all the CFU-F activity, also these cells have the capacity to differentiate into adipocytes, osteoblasts, and chondrocytes (Jones et al., 2002).

Interestingly, CD271 has been described as one of the most specific markers for the purification of human BM MSCs. CD271 also known as low-affinity nerve growth factor receptor (LNGFR), nerve growth factor receptor (NGFR), or p75NTR (neurotrophin receptor), belongs to the tumour necrosis factor superfamily (Quirici et al., 2002, Buhring et al., 2007). In 2002 Quirici et al., reported for the first time that the anti-CD271 antibody is specific for a subset population of multipotent BM cells. Also, they suggested in their study the use of CD271 as a marker for the selection of MSC from BM (Quirici et al., 2002, Jones and McGonagle, 2008). This finding was also supported by Jarocha et al., 2006. They suggested that the purification strategy population based on CD271 expression resulted in obtaining a subpopulation of cells that have a higher number of CFU-F colonies with higher enrichment for molecular markers of early osteogenic and adipogenic progenitors (Jarocha et al., 2008).

Moreover, CD271 is not only a marker for a specific subset of MSCs in bone marrow, but it also has been used to isolate CD271 subpopulations from other tissues sources for MSCs successfully, for example, adipose tissue, dental pulp and placenta (Álvarez-Viejo et al., 2015). Furthermore, several studies suggested that the CD271 positively selected cells have demonstrated a higher differentiation potential.

Mifune et al., 2013 demonstrated in their study that CD271 selected MSCs to have a greater differentiation potential for chondrogenesis *in vitro* and *in vivo* than plastic adherent MSCs (PA MSCs) (Mifune et al., 2013). Similarly, Alvarez et al., 2015 have successfully isolated three different subpopulations from the dental pulp using three different combinations of surface markers (CD51/CD140a, CD271, and STRO-1/CD146). They reported in their study that the isolated CD271 cells from the dental pulp displayed the greatest odontogenic potential. The isolation of CD271 positive MSCs from adipose tissue has received increased attention and favour in regenerative research. Such preferences can be ascribed to the fact that AT MSCs are isolated from fat tissue easily, have a high yield and also, these cells are easily cultured and have the capacity to differentiate into various cell lines (Zuk et al., 2002). Moreover, Cuevas-Diaz Duran et al., 2013 reported in their study that although the amount of CD271 positive MSCs decreased with age, the CD271 positive cells isolated from adipose tissue were present in all age groups and their frequency was higher than what has been found in BM. Therefore, they suggested that the CD271 positive cells selected from adipose tissue were proposed as the primary choice for tissue regeneration and autologous stem cell therapies in older subjects (Cuevas-Diaz Duran et al., 2013).

In summary, from all the above it can be concluded that MSCs are not a homogeneous population of cells. Several studies suggested that there are several stem cell subpopulations within SVF, each population could have potential benefit to repair specific damaged tissue (Calabrese et al., 2015, Latifi-Pupovci et al., 2015). Moreover, it is worth mentioning that up till now; all these previous studies have focused on and demonstrated the potential of MSC subpopulations only; no study has explored the secretomes activity of these cells. Thus, in this study and as a part of this project, the potential paracrine action of CD271 isolated cells has been examined.

1.4 The Role of the MSCs' Secretomes in Regenerative Medicine

As stated previously MSCs are characterised by their multipotent capacity. One of the most characteristic features of MSCs is their potent effect on the immune system; it is well known that

MSCs have an excellent capability to suppress immune responses (Jiang et al., 2005, Corcione et al., 2006, Casiraghi et al., 2008, Jarvinen et al., 2008). Also, one of the most distinguishing features of MSCs compared to most other cell types is that MSCs retain the ability to migrate into damaged tissues so that they can differentiate. In the other word, MSCs are clearly remarkable in possessing several regenerative properties including the homing ability to the site of damaged tissue, immunosuppressive capacity and multiple differentiation capacities as well as secreting growth factors (Figure 1.8) (Deng et al., 2011). In the past, the effective and most common accepted concept about the regenerative therapeutic effects of transplanted MSCs was by their migration and integration into the damaged tissue and differentiation into specialised cells (Kapur and Katz, 2013, Collawn and Patel, 2014). However, many experimental studies showed that only a small proportion of locally or systemically administered MSCs have participated in the healing of injured tissues (Baglio et al., 2012).

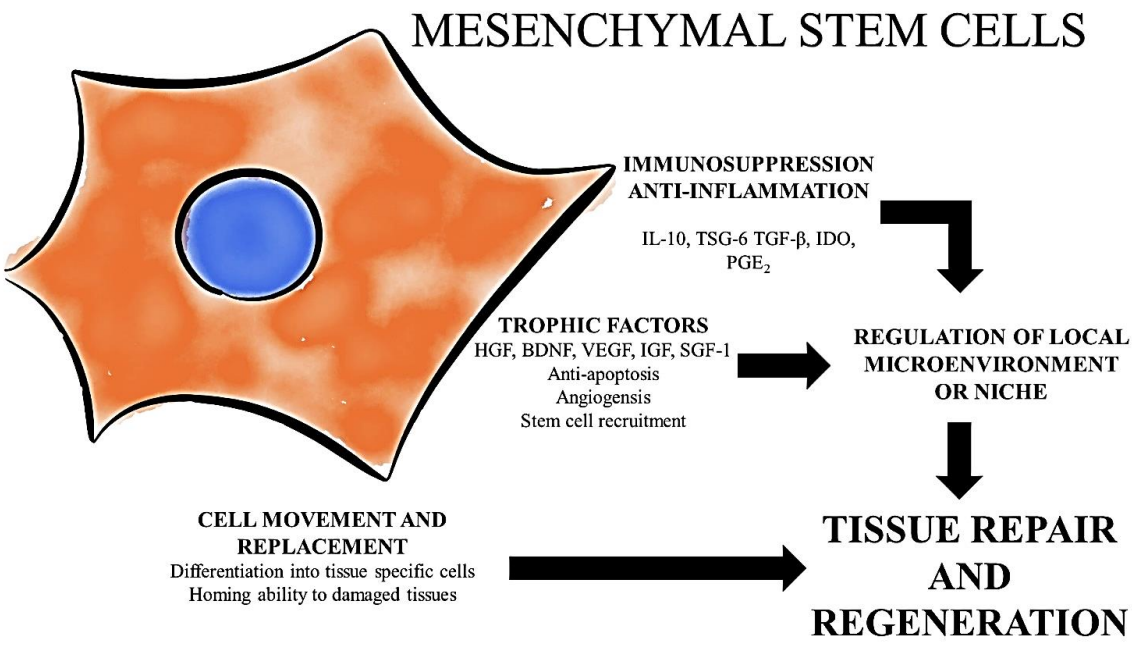

Figure 1:8 Regenerative properties of MSCs.

Schematic diagram showing the main properties that make MSCs a potential therapy for human degenerative diseases. The image is adapted from (Kim et al., 2013a).

Thus, the scientists are currently suggesting that the beneficial effects in tissue repair and regeneration are more likely indirect and depend on the paracrine activity of MSCs and not on their engraftment. Several studies proposed secretomes as the main pathway through which MSCs exert their therapeutic effects in the central nervous system (CNS) (Drago et al., 2013, Teixeira et al., 2013, Konala et al., 2016) this will be described later in this section. Interestingly, this hypothesis opens the window on novel therapeutic applications involved in the development of cell-free strategies based on the use of MSCs secretomes. The development of such strategies can ensure a treatment that is free of immune rejection and tumour formation risks and maybe even potentially better in some cases than the application of cell therapy (Kim et al., 2013a). MSCs' secretomes can be defined as a rich complex set of molecules secreted by living cells or shed from the cell surface. It is believed that the MSCs' secretomes are composed of soluble factors, cytokines, chemokines, micro-RNA (miRNA), exosomes and microvesicles (Skalnikova et al., 2011).

These secreted trophic and immunomodulatory/anti-inflammatory factors function together in a co-operative manner to generate tissue microenvironments that are ideal for repair/regeneration (Figure 1.9) (Madrigal et al., 2014). The fully characterised profile of secretomes is required for better application in regenerative medicine. Therefore, different proteomic approaches have been applied to address the characterization of growth factors, cytokines and other molecules secreted by stem cells (Skalnikova et al., 2011). Classical proteomic techniques such as 1-D or 2-D gel-based and chromatographic fractionation and protein identification using mass spectrometry, along with recent advancements in proteomic tools including protein microarrays, quantitative mass spectrometry and bioinformatics also highly sensitive antibody-based techniques are expected to enable mapping of the stem cell secretomes (Potian et al., 2003, Wang et al., 2006, Chiellini et al., 2008, Hoch et al., 2012, Kim et al., 2013b).

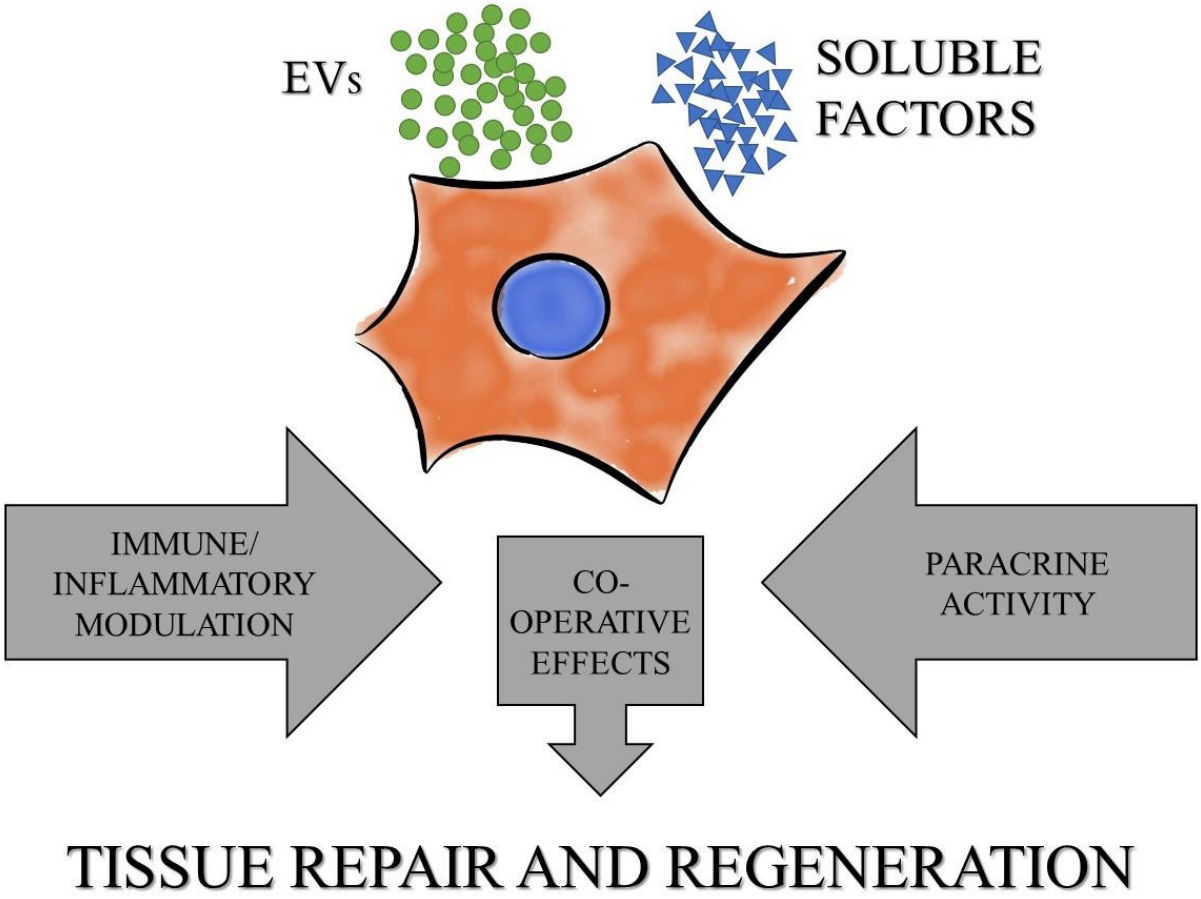

Figure 1:9 MSCs secretomes potential activities.

Schematic diagram showing a summary of the potential therapeutic roles attributed to the mesenchymal stem cells secretomes. Image adapted from (Lavoie and Rosu-Myles, 2013).

All biological functions of cells such as growth, division, differentiation, apoptosis and signalling are regulated and coordinated by secreted proteins (Skalnikova et al., 2011). Similarly, the tissue repair process requires several factors including; regulating extracellular matrix deposition, collagen synthesis, fibroblast proliferation, platelet activation, fibrinolysis and angiogenesis. Also, the tissue repair process requires immunomodulatory factors, this are often involved in suppressing T cells, activating macrophages and potentially recruiting neutrophils (Krafts, 2010).

MSCs' trophic properties have been studied for wound healing. MSCs can be recognised by their ability to secrete many vital growth factors and chemokines to induce cell proliferation and angiogenesis. These factors include; transforming growth factor-alpha (TGF-α), transforming growth factor-beta (TGF-β), hepatocyte growth factor (HGF), epithelial growth factor (EGF), basic fibroblast growth factor (bFGF) and Insulin-like growth factor-1(IGF-1) to increase fibroblast, epithelial, and endothelial cell division (Haynesworth et al., 1996, Caplan and Bruder, 2001, Collawn and Patel, 2014). Vascular endothelial growth factor (VEGF), IGF-1, EGF and angiopoietin-1 are also released to recruit endothelial lineage cell and initiate vascularization (Chen et al., 2008).

Interestingly, there is growing evidence that MSCs' secretomes also include neuroregulatory molecules such as brain-derived neurotrophic factor (BDNF) and nerve growth factor (NGF) (Teixeira et al., 2013, Teixeira et al., 2016). Wilkins et al. (2009) in their study showed that MSCs secreted several neurotrophic factors such as BDNF. In their study, they demonstrated that exposure of neurones to BDNF secreted by MSCs increased activation of AKT pathways and protected neurones from trophic factor withdrawal (Wilkins et al., 2009).

Similarly, Egashira et al., (2012) have suggested that murine and human adipose-derived MSCs have neuroprotective effects against experiment models of stroke, both *in vivo* and *in vitro* (Egashira et al., 2012).

Also, Teixeria et al., 2016, has investigated the effect of human MSCs' secretomes on neural progenitor cells in an *in vitro* and *in vivo* studies. They claimed that MSCs' secretomes prepared either in dynamic or static condition both improved proliferation and differentiation of neural progenitor cells (Teixeira et al., 2016). Although a significant part of the trophic effect of the MSCs' secretomes are due to growth factors and cytokines, recently it has also become evident that the extracellular vesicles (EVs) including exosomes (40–100 nm) and microvesicles (MVs) (100–1000 nm) have been shown to play a vital role in tissue repair (Konala et al., 2016).

The molecular composition of EVs are mainly proteins including; endosome-associated proteins (e.g., Rab GTPase, SNAREs, Annexins, and flotillin), proteins involved in biogenesis (e.g., Alix and Tsg101) and some membrane proteins including tetraspanins (e.g., CD63, CD81, CD82, CD53, and CD37) (Hemler, 2003, van Niel et al., 2006, Zoller, 2009). Additionally, the EVs are highly enriched in lipids (e.g., cholesterol, sphingomyelin, and hexosylceramides) (Brouwers et al., 2013). Moreover, EVs are also enriched with a cargo of both mRNA and miRNA (Valadi et al., 2007). Several studies have examined the regenerative therapeutic effect of EVs derived from MSCs for different diseases for example cardiovascular disease, neurological diseases and other diseases (Bian et al., 2014, Jarmalavičiūtė and Pivoriūnas, 2016). Feng et al., 2014, reported in their study where they use mouse myocardial infarction model that the delivery of miR-22, which was released by MSCs, reduced apoptosis in ischemic cardiomyocytes, reduced fibrosis and promoted cardiac function post-myocardial infarction (Feng et al., 2014).

Exosomes are fitting for neurological diseases as lipid-bound nano-vesicles exosomes act as liposomes which can cross the blood-brain barrier (Konala et al., 2016). However, MSCs' paracrine actions also have limitations that must be addressed. For example, some cytokines or chemokines, such as TNF-α and IL-6 released from MSCs may be harmful (Ward, 2009). Nevertheless, exploring the MSCs' secretomes holds great promise as a more controllable, manageable and sensible therapeutic strategy than cell-therapy.

Since MSCs have emerged in the field, intensive research has been explored on the MSCs' potential for therapy for different conditions including; cardiovascular diseases, autoimmune diseases, and liver diseases, orthopaedic injuries, and spinal cord injury (Wright et al., 2011, Kim and Cho, 2013). Many animal experiments have recorded an improvement in locomotor function after transplantation of MSCs in SCI (Ankeny et al., 2004, Ohta et al., 2004, Deng et al., 2006, Geffner et al., 2008). The main mechanism of effect in cell transplantation has been ascribed to their secretomes (Kanno et al., 2014). The recent clinical trial phase I of SCI in human showed that the transplantation of MSCs was safe and feasible (Kakabadze et al., 2016). SCI is further explored in the next section.

1.5 Spinal cord injury and regenerative medicine

1.5.1 Gross anatomy of the spinal cord

The spinal cord is a part of the central nervous system. The spinal cord is the long tubular bundle of nerves and neurones that extend from the medulla oblongata in the brainstem to the lumbar region of the vertebral column. Generally, spinal cords are characterised by their elaborate organisation and complexity. Its complexity is attributed to its critical functions. These include; sensation, autonomic and motor control (FintanSheerin, 2004).

The spinal cord can be described as a complicated processor of sensory and motor information. It can regulate the sensory inflow and is involved in the control of movements. In other words, the spinal cord looks and also functions as a cable gathering sensory information from the body to the brain and sending movement orders from the brain to the body. The spinal cord also processes sensory and motor signals (Dikopolskaya and Makarenko, 2014).

1.5.2 Causes and pathophysiology of spinal cord injury

SCI is one of the most devastating injuries that can affect the CNS. SCI causes severe damage to the nerve tissue in the spinal cord leading to a block in the communication between the brain and the body. Before proceeding onto the further explanations regarding SCI, it is worth highlighting the fact that the clinical presentation and syndromes of SCI do not necessarily correlate with the pathological findings (El Masri, 2006, Ecker et al., 2008).

A person with SCI, loses sensory, motor and reflex messages, which may not be able to get past the damage to the spinal cord (Mothe and Tator, 2012).The most common causes of traumatic SCI are motor vehicle accidents, falls at home or work-related injuries, acts of violent crime, and sports-related injuries (Devivo, 2012). Most clinicians classify the level of injuries of the spinal cord as either complete or incomplete. Simply, the fully compressed or severed spinal cord is classified as complete spinal cord injury in which the brain's ability to send signals below the point of damage is eliminated. Incomplete spinal cord injuries occur when the spinal cord is partially compressed or injured, and the brain's ability to send signals below the site of the injury is not completely removed (Kirshblum et al., 2011). However, the severity of damage or injury in the spinal cord can be classified based on the amount of spinal cord tissue damage or density of the lesion. Regardless of the cause the mechanisms underlying injury after spinal cord trauma results from, primary and secondary injury mechanisms (Webb et al., 2010).

The primary mechanism of spinal cord trauma is a mechanical injury to the spinal cord. This mechanical injury occurs as a result of impact and compression (due to column fracture and dislocation) against the spinal cord. This leads to several pathological changes at the site of injury including; severe damage to the axon, mechanical trauma causing damage to the cells, and damage to the small intramedullary vessels causing haemorrhage (Rowland et al., 2008). The primary injury leads to the secondary mechanism. The secondary mechanism of injury results in several events. These include first, electrolyte shifts in which changes in local ionic concentration occur. Second, vascular dysfunction this includes; disturbance in local and systemic blood pressure, reduction in spinal blood flow and rupture of the blood-brain barrier. Third, the release of free radicals and finally, immune system response inflammation, and apoptotic cell death (Dumont et al., 2001, Oyinbo, 2011). However, these two mechanisms are involved in four biological phases as a response to a spinal cord injury. The immediumte phase (0-2 hours) is the immediumte result of the injurious event itself.

It begins at the time of injury and lasts ~ 2 hours. This phase represents the primary mechanism of injury and is accompanied by the phenomenon of spinal shock leading to loss of function at and below the level of injury for complete injuries (Dumont et al., 2001).

The acute phase in which the secondary injury processes become dominant and can be subdivided into two stages; early acute stage (2-48 hours) which is characterised by continuing haemorrhage, increasing oedema and inflammation. Subacute stage (2 days to 2 weeks) this stage represents the most favourable time for repair mechanisms, in particular for the strategies based on cell therapies. Many experimental studies showed that active functional recovery could happen after cell transplantation during this stage compared with immediate treatment or at later time point (Keirstead et al., 2005, Karimi-Abdolrezaee et al., 2006).

The intermediate phase (2 weeks to 6 months) is characterised by the continued maturation of the glial scar and by regenerative axonal sprouting. Finally, the chronic phase (more than 6 months) takes over. This phase begins at 6 months following injury and continues throughout the lifetime of the patient. The main characteristic features of this phase are the maturation and stabilisation of the lesion through the continuation of scar formation and the development of cysts, and alterations in neural circuitries (Dumont et al., 2001).

1.5.3 The importance of nerve regeneration and revascularization in SCI recovery

Anatomically the spinal cord can be divided into five regions. The nerves in the cervical region control the muscles and glands and receive sensory input from the neck, shoulder, arm and hand. The thoracic region nerves are associated with the chest and abdominal walls. The lumbar region nerves are associated with the hip and leg. In the sacral region, the nerves are associated with the genitals and lower digestive tract. Coccygeal region nerves supply the skin over the coccyx. Spinal cord regions do not necessarily correspond to the bony regions of the spinal column (Figure 1.10) (Silva et al., 2014).

Nerve regeneration after SCI is very limited, however, a team led by Rosenzweig in California San Diego in 2010 performed an incomplete hemisection spinal cord injury on adult rhesus monkeys, administered at C7 of the spinal cord. They investigated the mechanisms underlying natural recovery after such injury. Their findings suggested that the connections between circuits in the spinal cord grew again, considerably and spontaneously, and after only 24 weeks following the mild spinal cord injury, 60 percent of the connections were fully recovered (Rosenzweig et al., 2010). Also, El Masri and colleagues demonstrated that early simultaneous active physiological conservative management of the injured spine in patients with complete motor paralysis but with sparing of pinprick sensation, 70% of those patients revealed in the first 72 h of injury recovered motor power to ambulate without surgical, pharmacological, cellular or biological intervention. Thus, based on their studies they suggested that surgical intervention is not recommended at the early stages of SCI (El Masri and Kumar, 2017).This may be due to the fact that surgical intervention at early stages of SCI may add extra trauma to the already injured tissue.

When CNS patients undergo injury, several factors are required to reconstruct neuronal circuit including; synaptic reorganisation, axonal sprouting and neurogenesis. Under the effect of injury environment, the nervous system reveals plasticity property to adapt the environmental changes (Celnik and Cohen, 2004). Particularly, the undamaged neurones and collateral axon branches can grow into the injured regions to re-establish the neuronal circuit. Although this plasticity is limited due to inhibitory factors released at the site of injury, increasing numbers of studies showed that a cell transplantation strategy could improve neuronal plasticity (Darian-Smith, 2009, Liu et al., 2012).

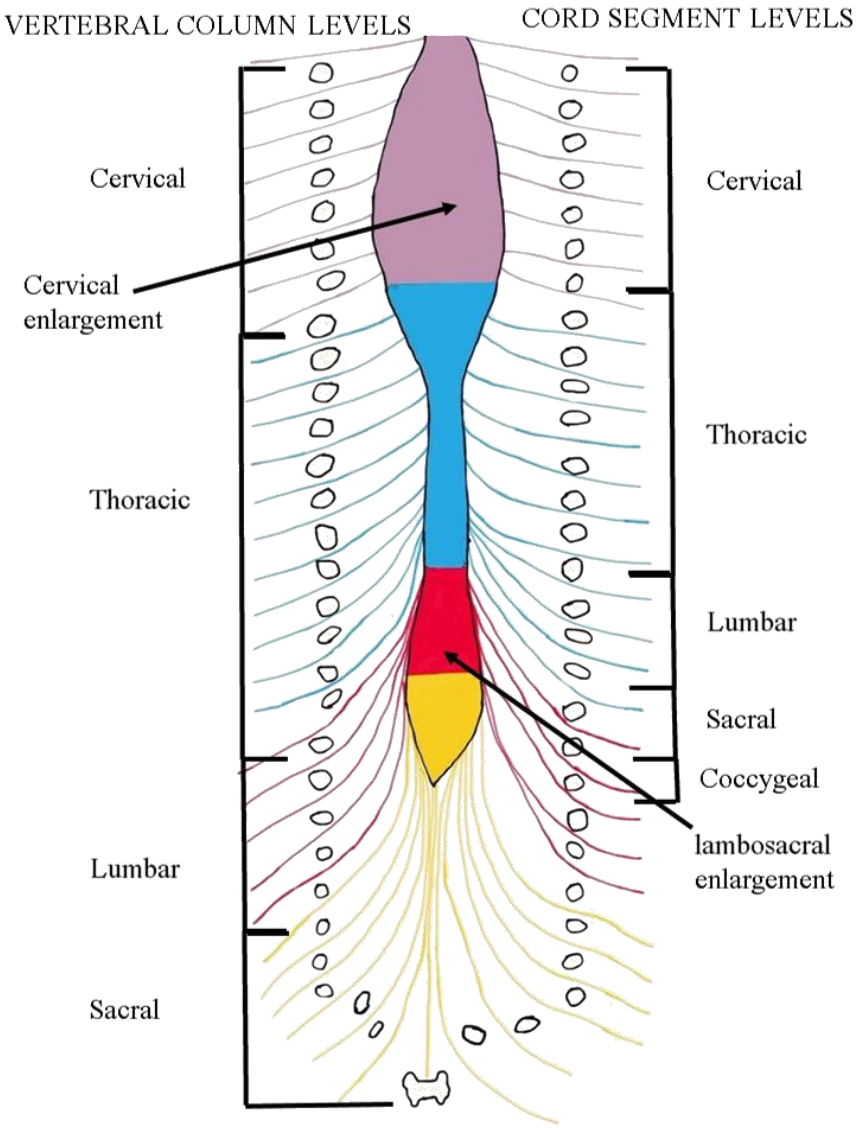

Figure 1:10 Spinal cord regions.

The schematic illustration shows the five regions of the spinal cord which are not related to the bony structure of the vertebra. Image adapted from (System, 2016).

Based on several studies either *in vitro* (Wright et al., 2007, Liu et al., 2010) or *in vivo* (Ribeiro et al., 2011, Neirinckx et al., 2015), MSCs transplantation or conditioned medium exhibited neurological effects by improving neurite outgrowth or neuronal axon sprouting from surviving axons.

Angiogenesis plays a critical role in SCI recovery by reducing secondary axonal damage due to ischaemia and also by the delivery of oxygen and nutrients to the site of regeneration and removal of metabolic waste (Loy et al., 2002, Lutton et al., 2012). Migration and proliferation of endothelial cells are important in the angiogenic process. In the spinal cord, blood vessel distribution is based on the area of supply, grey matter is characterised by its high vascularisation compared with white matter. Such variation in blood supply reflects the metabolic activity of individual areas as the grey matter is the aggregation of nerve cells bodies where the metabolic activity is very high whereas white matter is an aggregation of axons (Mautes et al., 2000). The vertebral arteries are the main source of blood to the spinal cord which undergoes a series of branching, ending in terminal capillary beds that establish the blood-spinal cord barrier (BSCB) (Fenstermacher et al., 1988). The anatomical structure of BSCB is composed of several components including; a capillary wall of endothelial cells, pericytes, astrocytes and the extracellular matrix (Mautes et al., 2000). The endothelial cells of BSCB are unlike those in the peripheral circulation (Figure 1.11). Endothelial cells of BSCB are characterised by their non-fenestrated membrane. Instead, the endothelial cells overlap and seal the paracellular spaces with tight junctions (Ng et al., 2011). Pericytes surround the endothelial cells and separate from endothelial cells by the basal lamina. Pericytes have a significant role in endothelial cells' proliferation, migration, and differentiation. Both endothelial and pericyte cells are wrapped within a layer of the basal lamina which provides physical support for the vessel wall. Astrocytes foot processes, which are juxtaposed against the basal lamina, surround the outer surface of these capillaries.

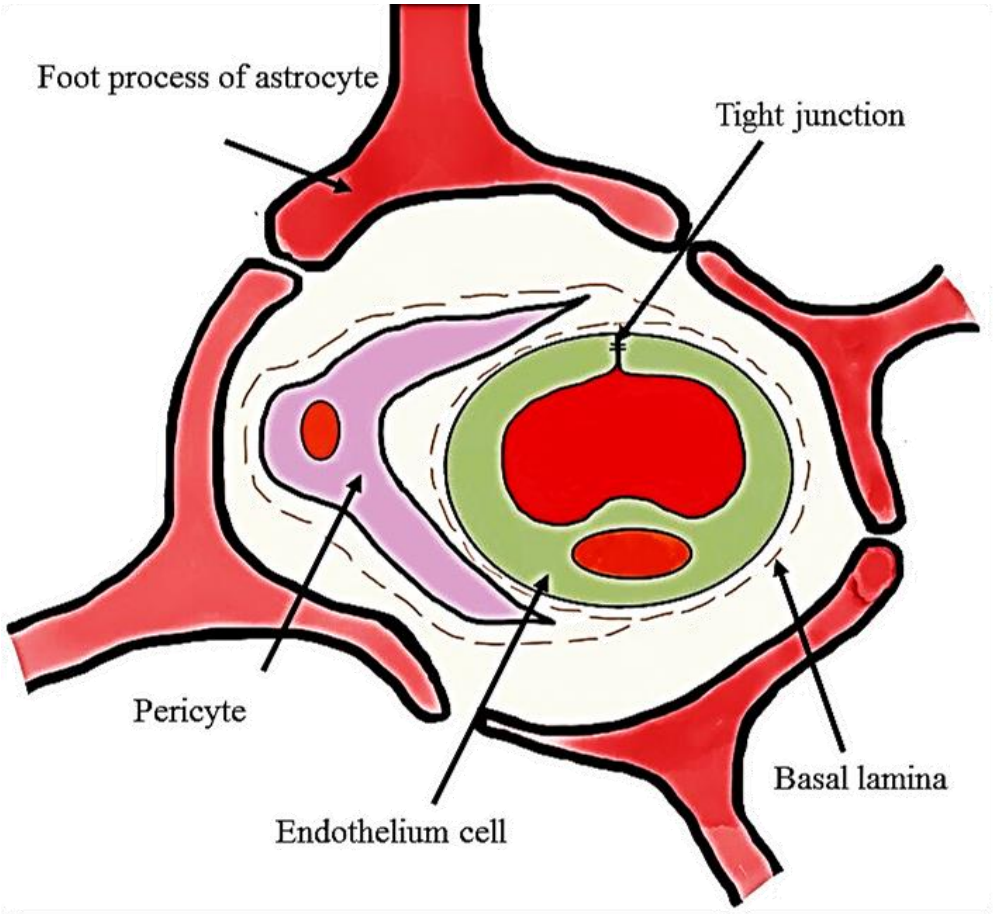

Figure 1:11 Basic cellular constituents of the BSCB.

Schematic illustration showing the basic composition of BSCB which is formed from an overlapped endothelial cell that has tightened by tight junction surrounded with pericyte, and the whole structure is wrapped with feet processes of astrocytes. Image adapted from (Abbott et al., 2006).

Astrocytes have a critical role in the formation and maintenance of the BSCB (Bartanusz et al., 2011). This concrete structure of BSCB reflects the effective role of this barrier to protect spinal cord by preventing passage of any molecules apart from the required nutrients. Therefore, lack of such protective barrier results in the influx of cellular toxic molecules including; calcium, excitatory amino acid neurotransmitters. A high concentration of glutamine and glycine can be toxic to cells. Free radicals, erythrocytes, leukocytes, and inflammatory mediators can also be toxic (Bartanusz et al., 2011, Ng et al., 2011). In fact, there is an angiogenic response that occurs after SCI in which new blood vessels are formed (Oudega, 2012). However, Whetstone et al., 2003 has reported in their study that BSCB lost its permeability and the regenerated blood vessels after injury of spinal cord do not display a typical barriers' properties (Whetstone et al., 2003). Therefore, there is a need to develop a strategy to ensure the restoration of fully functional nerves and BSCB. The restoration of a complete structural and functional BSCB may enhance the improvement of neuronal tissue as the BSCB can prevent infiltration of unwanted particles.

In fact, the cellular and molecular changes that occur during the secondary processes of SCI have a significant role in the development of pathophysiology of the lesion. Many studies claimed that the intervention may reduce secondary injury of the spinal cord by reducing the series of cascade events after spinal cord trauma and thus, an improvement in spinal cord functionality may be achieved (Dasari et al., 2014). Since the emerging of stem cells as cell-based therapy, many studies have investigated their potential activities to modulate the cascade of events of secondary injury after spinal cord trauma. For example, transplantation of MSCs in animal model studies has been shown to increase the repair of the injured spinal cord tissues (Park et al., 2011). Although, a full determination of the *in vivo* MSCs functional roles and involved molecular regulatory mechanisms are not yet completed. However, several studies suggested that the possible mechanisms through which MSCs may ameliorate the secondary injury of SCI may be due to the main characteristic features of MSCs biological activities including; migration to the damaged neuronal tissue, neuronal

differentiation, and releasing survival factors that could play a role in neuronal protection (Qu and Zhang, 2017).

Cancer cell lines are widely used as models to investigate broad biological activities. Therefore, to achieve the goals raised by this study, two cell line models have been adapted to investigate the neurogenic and angiogenic effects of MSCs conditioned medium.

These models include: **SH-SY5Y human neuroblastoma cell line**, SH-SY5Y human neuroblastoma cell line is one of the cell lines which have been widely used to understand neurogenic properties. It is the third successive subclone from the original cell line, called SK-N-SH, which was isolated from a bone marrow biopsy taken from a four-year-old female with neuroblastoma. SH-SY5Y has been extensively used as a neuronal model in most *in vitro* neurological experiments. This was conferred due to first, their ability to differentiate into a functionally mature neuronal phenotype when they are differentiated by exposure to retinoic acid followed by brain-derived neurotrophic factor in serum-free medium. Second, due to the experimental limitation of gaining primary neurone cells *in vitro*, SH-SY5Y cells considered as an alternative source for neuron cells (Yusuf et al., 2013).

EA.hy926 Human endothelial cell line, a hybrid cell line that was established by fusion of A549 cells (human cell lung carcinoma) with human umbilical vein endothelial cells (HUV-EC). Note that HUVEC is primary cells (Edgell et al., 1983). This cell line displays structural and functional characteristic features of vascular endothelial cells (Edgell et al., 1990, Bauer et al., 1992, Rieber et al., 1993). This study has adopted EA.hy926 cell line over the primary HUVECs for the following reasons, i) long life span of EA.hy926 cells compared with HUVECs as they have a short life span ii) reducing individual variation as the primary cells HUVECs are multi-donor of origin adding variability to the variability from the conditioned medium used in this study that has been also derived from different donor. Thus, using a cell line model can minimise the risk of the donor to donor variations (Bouïs et al., 2001).

1.5.4 Strategies for SCI treatment

As stated above, SCI results from severe damage to neuronal tissue resulting in dramatic disability represented in the loss of motor and sensory functions. The primary aim for SCI management is avoidance of secondary injury. Thus, the recent therapeutic strategies are aimed to reduce and control any further damage to the spinal cord after injury (Martin et al., 2015). Currently, no treatment is effective at obtaining a full recovery of function of the damaged tissue of spinal cord after injury. However, there are several strategies that claim to improve some of the functions of the spinal cord after injury. These strategies include; spinal cord decompression, spinal cord stabilisation, neuroprotective strategies and regenerative therapies. The surgical intervention to decompress spinal cord after injury within the first 24 h claim to increase the chances of improvement in motor function at later stages of injury (Dvorak et al., 2015). Similarly, spinal cord stabilisation is at least as important as spinal cord decompression. Spinal cord stabilisation may involve different surgical interventions for example; anterior and posterior surgical approaches, halo-vest cervicothoracic orthosis and external bracing or rigid collar. The surgical interventions are based on the severity of damage in ligaments and bone (Krengel et al., 1993, Furlan et al., 2011).

Neuroprotective strategies include hypothermia and pharmaceutical therapy. Several studies showed that systemic hypothermia in acute SCI has contributed to improving neurological functions. However further studies are needed before hypothermia is adopted widely (Wang and Pearse, 2015).

The evidence based on research studies suggested administration of some pharmaceutical drugs may have a beneficial effect on either minimising the secondary injury mechanism or facilitate the neurological recovery after injury. Methylprednisolone (MP) is a potent corticosteroid that inhibits inflammation and membrane lipid peroxidation. It was widely used by SCI clinicians previously. However, this drug classifies as an optional treatment as there is a controversy about the high dose of MP (Hugenholtz, 2003, Evaniew et al., 2015, Martin et al., 2015). However, several drugs are in development for treating spinal cord injury. They are either neuroprotective or neuroregenerative agents targeting specific pathological mechanisms. Riluzole is considered as one of the

neuroprotective agents which slow degeneration of motor neurones and prolongs survival (Fehlings et al., 2012). Another neuroprotective agent is minocycline which has an effect by reducing microglial activation and TNF-alpha secretion (Festoff et al., 2006). Pre-clinical studies suggested that improvement in motor function, reduction in lesion size, and preservation of axons have been achieved after the administration of minocycline after SCI attributing this improvement to its neuroprotective effects (Wells et al., 2003, Casha et al., 2012). The regenerative approaches can be achieved not only by halting secondary injury but also by inducing and amplifying repair mechanisms. Cethrin is a bacterial-derived toxin that blocks signalling from inhibitory proteins released by myelin debris present at the site of injury and promotes axonal growth *in vitro* (Fehlings et al., 2011). Protein nogo-A is one of the myelin proteins which act as an inhibitor of nerve growth factor (NGF). Recently, applying a biological strategy of neutralising monoclonal antibodies that are selective for Nogo-A has been shown to enhance the regeneration and reorganisation of the injured spinal cord (Liebscher et al., 2005, Zhao et al., 2013b).

These advances in both the understanding of spinal cord pathological mechanisms of injuries and developing therapies have shown promising results at the preclinical stage of study but failed to translate into clinic Since each therapy focuses on one specific mechanism, therefore, a combination of therapies is needed (Martin et al., 2015). Thus, various aspects of stem cells therapy for SCI have attracted research as they exert a multiple or a combination of therapeutic and trophic activities. MSCs account for a large share of investigations for their therapeutic activities for SCI; this can be attributed to their main characteristic features including; freedom from concern about ethical issues, ease of access and lack of tumour formation after transplantation (Li and Lepski, 2013, Dasari et al., 2014). Several new studies have investigated the therapeutic potential of AT MSCs by targeting a different aspect of injury mechanisms (Kolar, 2014, Hur et al., 2016). AT MSCs hold significant promise for SCI, most of the animal studies showed MSCs could contribute to repair spinal cord tissue after injury by several mechanisms. These mechanisms include; replacement of damaged nerves as a result of injury, generation of new supporting cells that are capable of formation of

myelin, reduction of the damaging inflammation that can occur after injury and secretion of protective substances as trophic factors to protect the cell from further damage at the site of injury and also absorption of free radicals (Dasari et al., 2014). However, further investigation is still required to understand the underlying mechanisms of the therapeutic effects of MSCs and to optimise the roles of MSCs in repairing SCI.

1.6 The importance of a large animal model in translating regenerative therapy for SCI

As stated above the strategy of using stem cell transplantation for SCI is rapidly evolving in regenerative medicine. However, the absence of animal models fully reflecting the phenotype of the human experience of SCI is still a challenging step in bridging the gap between translation research and human clinical trials (Harding et al., 2013).

Although, rodents represent the most traditional animal models for preclinical studies, in cell-based therapies they have their limitations. On the one hand, rodents have the advantage in experimental studies of easier management and relatively inexpensive cost. On the contrary, they have a short lifespan which does not fit with observation experiments over long periods, small organ sizes and marked physiologic differences (Cibelli et al., 2013). Rodent models do not reproduce full in certain aspects of SCI in human, as the injury is induced in the lab and it is not spontaneously and natural in occurrence. Large animal models could be the best option to investigate and translate the outcome of cell-based therapies into human clinical trials. The large animals are anatomically and physiologically similar to human in comparison with rodents which have small body size and substantially different physiology (Casal and Haskins, 2006). For example, the neuropathological sequences following SCI in human are characterised by cystic cavitation whereas in murine the lesion site is filled with non-neuronal cells (Fujiki et al., 1996, Guth et al., 1999, Byrnes et al., 2010).

Large animals like rabbits, cats, dogs, pigs, goats, sheep, and non- human primates often represent better models than rodents. The use of dogs as large animal models can bring benefits for both human

and veterinary medicine. Besides, dogs among other large animals faithfully mirror most of the disease in humans (Starkey et al., 2005). The domestic dogs share common similar features in diseases including; physiology, disease presentation and clinical response. About 400 inherited and naturally occurring diseases in dogs are similar to those found in human (Khanna et al., 2006). Diabetes, epilepsy, asthma and cancer are the most common inherited diseases. These diseases occur as a result of complex interactions between multiple genes and environmental factors, interestingly, these characteristics are shared by both human and dogs (Schneider et al., 2008). In 2005 Toh et al., announced the publication of a complete map of the dog genome. The availability of this genome map provides the opportunity to explore the genetic basis of disease susceptibility and may provide insights into disease mechanism. This may lead to the possibility of clinical trials in dogs with genetic diseases to develop new therapeutics that would improve health in both dogs and humans (Switonski and Szczerbal, 2001, Lindblad-Toh et al., 2005). Indeed, the availability of canine DNA and protein sequence make dogs a more relevant model to translate the genetic mechanisms underlying the occurrence of some genetic diseases in human than mice (Kirkness et al., 2003, Lindblad-Toh et al., 2005).

Similarly, in stem cell transplantation dogs have a crucial role as a model for many transplantation research studies (Abkowitz et al., 1996, Wagner and Storb, 1996, Horn et al., 2004). Moreover, canine SCI represents perfect models for spontaneous SCI in human. The common reasons for SCI in canine are similar to human; that can either be traumatic injury as a result of motor accidents or non-traumatic injury due to Intervertebral disc disease (IVDD) (McMahill et al., 2015). There are three methods of inducing SCI in the lab which is frequently used for experimental animal models including; transection model, compression model, and contusion model (Rosenzweig and McDonald, 2004). Each method addresses a specific question thus each one has its advantages and disadvantages. Briefly, the transection model is either a complete or partial section of the spinal cord involving an opening within the dura to induce this injury. The advantages of this method are that it provides a good setting for axon regeneration experiments and it is a suitable method for the implantation of

specific devices. The disadvantage of this method is that transection in spinal injury is very rare in humans (Zorner et al., 2010). The contusion model is induced without any disruption of the dura by instead directly hitting the spinal cord. There is a specific tool that is controlled by a computer called the impactor to generate this model. The advantage of this method is that it provides valuable information on several biomechanical parameters. The disadvantage is that it is difficult to distinguish between the survived tissue (i.e., spared tissue) and the newly regenerated tissue, as the survival tissue has a marked contribution to the recovery process of the spinal cord. Thus the moral value of this model could be to assess the safety of interventions but not to establish an efficacy (Salegio et al., 2016).

Whereas, the compression model allows for a prolonged spinal cord compression using a clip or forceps compression technique. The advantages of this model are that it is simple, inexpensive, and limited resources are necessary. The disadvantages are the lack of an acute injury to study (Cheriyan et al., 2014).

Nonetheless, the clinical lesion in human and dogs usually occur due to a mixture of both forces, contusive and compressive, which affect multiple regions of the spinal cord. While in rodents' experimental model's the lesion is only one type either contusive or compressive which are created on a single side of the spinal cord (Jeffery et al., 2006a). Also, the immune response in rodents after SCI differs compared with human and dogs. Both canine and human inflammation are dominated by microglia cells (Schmitt et al., 2000, Spitzbarth et al., 2011). In contrast, inflammation in injured rodents is dominated by T-lymphocyte (Popovich et al., 1997). Thus SCI in canine is more closely mimics the pathophysiology of SCI in human compared to rodents. Canine could be a promising model to bridge that gap between research and human clinical trials.

Although dogs may consider as better large animal model for human SCI, there are several limitations should be taken in a count as dog is quadruped that has less motor dominance by the pyramidal (corticospinal) tract, in this aspect it is difficult to use dog as model for human SCI also, difficulties in interpreting outcomes measured in animals (Jeffery et al., 2006b, McMahill et al., 2015).

1.7 Aims and objectives of the study

The major aim of this study was to investigate the regenerative activities of MSCs' secretomes and their potential benefit for SCI repair in both human and veterinary regenerative medicine. The reason for focusing on secretomes rather than the cells themselves was to establish and develop a new strategy of cell-free therapy that will be ready to use at any time, without needing to wait for two or three weeks as is the case with using the cells. As it was explained previously in the Introduction (Section 1.5.3) neurogenesis and angiogenesis play a critical role in spinal cord recovery and repair. Therefore, the thesis has firstly, investigated the regenerative activities (i.e. neurogenesis and angiogenesis activities) of canine MSCs secretomes. Secondly, the aim was to investigate the differences in these regenerative activities between human and canine MSCs secretomes. Such studies could bridge the gap between translating research into preclinical studies and clinical trials on SCI in human. Thirdly, the aim was to investigate the differences in regenerative activities among MSC subpopulation secretomes. Such investigating could explore the differences in biological actions within heterogeneous populations, which may lead to the identification of differences that can be employed to develop a specific application of treatment.

Chapter Two: Materials and Methods

2.1 Tissue culture regime and management

2.1.1 Isolation and culture of canine adipose-derived mesenchymal stem cells

Canine adipose-derived mesenchymal stem cells (cMSCs) were kindly provided by the Veterinary Tissue Bank Limited (VTB Ltd., Chirk, UK.) (Table 2.1). These cells were isolated from the inguinal fat pads of dogs undergoing MSCs transplantation in the treatment of joint pathology. Fat samples were dissected, minced and washed in phosphate buffered saline (PBS) (Gibco®, Life Technologies™, Paisley, UK). Then each sample was digested with collagenase solution (0.2% Collagenase type A, Worthington Biochemical Corporation. USA) where the sample was placed in an incubator at 37 ºC with gentle shaking for 2hrs. An equal amount of standard culture medium, i.e., DMEM/F-12 medium supplemented with 10% fetal bovine serum (FBS) and 1% penicillin/ streptomycin (all from Gibco®) was added to stop the action of collagenase, then the digested sample was filtered through a 40µm cell strainer (BD Biosciences) to remove any large debris. Following two cycles of centrifugation at 1,200 rpm for 4 minutes and resuspension of the resultant cell pellet in standard culture medium to wash away any remaining collagenase, the obtained cells were seeded in T75 tissue culture flasks (Sarstedt AG & Co. Germany) and incubated in a humidified incubator with 5% CO_2 at 37ºC. Any non-adherent cells were removed by discarding the medium at 24-72 hours post-seeding, and the adherent cells cultured as monolayer cultures through to passaging by trypsinisation into fresh T75 flasks. The culture-cMSCs at passages II-III was delivered to the research laboratories at Aston University. These cells were further cultured with standard culture medium, where they were kept incubated at 37ºC in a humidified atmosphere of 5% CO_2.

It may cross the mind how old is a dog in the human year, actually, dogs mature more quickly than human do early on. In fact, dog size and breed play a role. Smaller dogs tend to live longer than larger ones, but they may mature more quickly in the first few years of life. Table 3 shows the dog age compared to a human. Also, it is worth to mention that age and gender of donors have an influence on the potency of MSCs (Sotiropoulou et al., 2006, Duggal and Brinchmann, 2011). Donor-to-donor variation and gender-related variation have a significant impact on phenotype features and functional properties of MSCs (Siegel et al., 2013).

2.1.2 Isolation and culture of human adipose-derived mesenchymal stem cells

Following ethical approval and informed consent (LREC number 12/EE/0136), human adipose-derived mesenchymal stem cells (hMSCs) were harvested from the excised infrapatellar fat pad of the knee joints of patients having a knee replacement surgery (Table 2.1). The MSCs were isolated from adipose tissue samples following the protocol described previously by (Bunnell et al., 2008). Initially, adipose tissue samples were minced and incubated with 0.3 U/ml of collagenase type I (Sigma, Dorset, UK) for 3-4hrs in a humidified incubator at 37°C and 5% CO_2, with gentle shaking. Following collagenase digestion, an equal amount of DMEM/F-12 medium supplemented with 20% FBS and 1% penicillin/streptomycin was added to stop the reaction of collagenase. Then the digested tissue was centrifuged at 1000 rpm for 10 minutes. After removing the supernatant, the resultant cell pellet was washed in DMEM/F-12 containing 20% FBS and 1% penicillin/ streptomycin followed by further centrifugation at 1000 rpm for 10 minutes. The resultant cell pellet was resuspended and filtered through 70µm cell strainers (BD Biosciences) to remove any debris. The cells obtained following this filtering were then cultured in DMEM/ F-12 containing 20% FBS and 1% penicillin/ streptomycin in a humidified atmosphere in an incubator at 37 °C and 5% CO_2 and after 24-72 hours of incubation and non-adherent cells were washed off by a complete change of medium and the adherent cells remaining were subsequently culture expanded in T75 flasks until they reached 70%-80% confluence. The cultured adherent cells were further cultured expanded by passaging through trypsinisation and re-seeding into fresh T75 flasks, as described (Kohli et al., 2015).

MSC ID	Tissue of origin		Sex	Age
MSC from human				
MSC101	The infrapatellar fat pad of the knee joints		Female	27
MSC110	The infrapatellar fat pad of the knee joints		Female	49
MSC105	the infrapatellar fat pad of the knee joints		Male	69
MSC123	The infrapatellar fat pad of the knee joints		Female	59
MSC126	The infrapatellar fat pad of the knee joints		Female	60
MSC from canine				
		Breed		
MSC012	The inguinal fat pads	Labrador	Female	7
MSC014	The inguinal fat pads	Labrador	Female	8
MSC017	The inguinal fat pads	Spaniel	Male	2
MSC018	The inguinal fat pads	Not specified	Female	8
MSC020	The inguinal fat pads	Doberman	Male	6
MSC028	The inguinal fat pads	Plummer terrier	Female	9

Table 2: MSCs donor details.

The table shows the MSCs used in this study. Human MSCs were provided by the Royal Orthopaedic Hospital, Birmingham whereas the canine MSCs were provided by the Veterinary Tissue Bank Limited.

Size of dogs	Small 20 Ibs or less	Medium 21-50 Ibs	Large More than 50 Ibs
Age of dog (year)	**Age in human years**		
1	**15**	**15**	**15**
2	**24**	**24**	**24**
3	**28**	**28**	**28**
4	**32**	**32**	**32**
5	**36**	**36**	**36**
6	**40**	**42**	**45**
7	**44**	**47**	**50**
8	**48**	**51**	**55**
9	**52**	**56**	**61**
10	**56**	**60**	**66**
11	**60**	**65**	**72**
12	**64**	**69**	**77**
`13	**68**	**74**	**82**
14	**72**	**78**	**88**
15	**76**	**83**	**93**
16	**80**	**87**	**120**

Table 3: Dog age in human years.

The table shows dogs' age in human years based on their body mass. This table adapted from (WebMD, 2017).

2.1.3 Isolation and culture of $CD271^+$ and $CD271^-$ human adipose-derived mesenchymal stem cells

MSCs were harvested from the excised infrapatellar fat pad of the knee joints of patients having a knee replacement surgery after the ethical approval and informed consent (LREC number 12/EE/0136) by collagenase digestion, as described above. Following two steps of washing and centrifugation to remove collagenase, the resultant cell pellet was re-suspended with 10ml of DMEM/F-12 containing 20% FBS and 1% penicillin/ streptomycin and passed through A 100µm cell strainer (BD Biosciences). The filtered cell suspension was collected in a 15ml conical centrifuge tube and centrifuged at 600g for 10 minutes. Then the cell pellet was re-suspended in 5ml of DMEM/F-12 containing 20% FBS and 1% penicillin/ streptomycin and passed through a 40µm cell strainer (BD Biosciences). After that, the number of cells was determined by counting viable and non-viable cells using the method of trypan blue exclusion and a haemocytometer. Some cells were then cultured in T25 flasks to isolate MSCs based on their adherence on tissue culture plastic (PA MSCs), as described above, whilst the rest were processed for isolation based on their immunopositivity for CD271 using immunolabelling with an antibody for CD271 and magnetic beads, as described previously (Jones et al., 2002) and by the manufacturers protocol for $CD271^+$ cell isolation (Miltenyi Biotec Inc. USA). In brief, this was as follows: 1. cells were centrifuged at 300g for 10 minutes and then the supernatant completely removed; 2. any erythrocytes were lysed by treatment of the resultant cell pellet with 1ml of 1x erythrocyte lysis buffer (provided with the kit) and incubation for 10 minutes at room temperature, then the solution was further centrifuged at 300g for 10 minutes; 3. next, the supernatant was removed completely, and cells were re-suspended with 80µl of buffer (PBS pH 7.2%, 0.5% bovine serum albumin (BSA) and 2 mM of EDTA) ; 4. 10µl of FcR blocking reagent and 10µl of CD271-APC was added to the cell suspension, mixed well, and the cells were incubated at 2-8 ºC for 10 minutes; 5. at the end of the incubation period, cells were washed by adding a further 1ml of buffer and centrifuged at 300g for 10 minutes;

6. the supernatant was completely removed, the resultant cell pellet was re-suspended with 10µl of FcR blocking reagent and 20µl of anti-APC microbeads and incubated at 2-8 ºC for 15 minutes; 7. the washing step was repeated by adding 1ml of the buffer to the cells and centrifugation at 300g for 10 minutes; 8. finally, the supernatant was completely removed, and the cell pellet was re-suspended with 500µl of the buffer, preparing them for magnetic separation. 9. based on the total number of cells obtained following this procedure the appropriate MACS column and MACS separator were chosen and placed in the magnetic field. 10. the column was rinsed three times with buffer solution, then 500µl of the cell suspension was loaded onto the column. 11. unlabelled cells were collected by applying 3x3 ml of buffer to the column and eluting each time; these cells were used for this study as $CD271^-$ cells. 12. after the third buffer wash, the column was removed from the magnetic field, placed into new collection tube and a further 5ml of buffer applied onto the column and the magnetically labelled cells were immediately flushed out by firmly pushing the plunger into the column and collecting the eluent; these collected cells have been referred to as $CD271^+$ cells. 13. after this final separation and isolation procedure, all collected cells were pelleted by centrifugation and re-suspended with 5ml of DMEM/F-12 containing 20% FBS and 1% penicillin/ streptomycin and seeded in a T25 flask at 37 ºC with 5% CO_2.

2.1.4 Cell culture expansion and storage

2.1.4.1 Passaging cells

Monolayer cells in tissue culture flasks were washed with PBS and incubated with 0.25% trypsin (w/v)/EDTA (Gibco®) for 5 minutes at 37 °C with 5% CO_2. After the detachment of cells, trypsin activity was neutralised by adding an equal volume of standard medium containing 10% FBS. Then this cell suspension was centrifuged for 10 minutes at 1000 rpm to make a cell pellet. The supernatant was removed, and the pellet was re-suspended in the culture medium. A viable cell count was performed using trypan blue exclusion.

The cells were then seeded into new fresh flasks at a desired density ranging from 5000-20000 cells per cm^2 according to the experimental protocol.

2.1.4.2 Cell cryopreservation and re-culture from storage

Cells were harvested by trypsinisation following the method described above and the cell pellet after centrifugation was resuspended in cold freezing mix (10% dimethyl sulphoxide (DMSO) in FBS). The cell suspension in freezing mix was transferred into cryovials (containing 1-2 ml per vial), which were then stored overnight in a designated cryofreezing container that contained isopropyl alcohol at -80°C before transfer to storage containers at the same temperature or in liquid nitrogen. Cells were returned to culture from -80°C storage by rapidly thawing cryovials under running warm/hot tap water. Then the cells in freezing mix were transferred to a 15ml centrifuge tube, and 1ml of ice-cold standard culture medium was added to the cell suspension dropwise over one minute. The cells were left to stand for one minute at room temperature. After that, 10ml of room temperature standard culture medium was added drop-wise over 5 minutes. Then the cell suspension was centrifuged for 10 minutes at 1000 rpm. The pellet was re-suspended in the warm standard culture medium, a viable cell count was performed using trypan blue stain, and then the cells were cultured in T25/T75 flasks at 37 °C with 5% CO_2 at the desired cell density for each experiment.

2.1.4.3 Screening for mycoplasma contamination in tissue culture

Regular testing of cell cultures to ensure the absence of mycoplasma infections was performed, in conjunction with good aseptic technique, as strongly recommended (Barile et al., 1973). Mycoplasma screening was performed on every new donor cell sample received from VTB Ltd, as well as on maintained cultures routinely every 3-6 months using a commercial kit by following the manufacturer's instructions (EZ-PCR mycoplasma test kit; Geneflow, Lichfield, Staffordshire, UK). In brief, 0.5-1ml of the medium was harvested from the supernatant of each cell culture to be tested and transferred into a 2ml micro-centrifuge tube. The supernatant was centrifuged at 250g for 3

minutes to remove cellular debris, then collected into a new micro-centrifuge tube and centrifuged at 15,000g for 10 minutes. Then the supernatant was removed carefully and completely and the resultant pellet was re-suspended in 50µl of the commercial buffer solution provided, mixed thoroughly with a micro-pipette and heated to 95°C for 3 minutes. This is referred to as the "test sample". Then 35µl of dH_2O was mixed with 10µl of reaction mix and 5µl of the test sample in a sterile PCR tube. A positive template control was also prepared by adding 39µl of dH_2O that was mixed with 10µl of reaction mix and 1µl of the positive template in sterile PCR tubes. All tubes were placed into a DNA thermal cycler (Thermo Fisher Scientific, UK) and the following parameters were set to amplify the DNA: 30 seconds at 94°C, then 35 cycles of; 30 seconds at 94°C then 120 seconds at 60°C then 60 seconds at 72°C, followed by 30 seconds at 94°C, 120 seconds at 60°C and finally 5 minutes at 72°C. After that, the samples were used for agarose gel electrophoresis to determine if a PCR product had formed by loading 15µl of the sample in a 2% (w/v) agarose gel and applying 100 volts across the gel for 30-45minutes. A known DNA ladder of 100-1013 base pairs (HyperLadder™ 100bp, Bioline, London, UK) was also loaded. The gel was then visualised under UV light, and digitised images were captured using Syngene imaging software (Syngene, Cambridge, UK). The positive control for mycoplasma infection and any mycoplasma positive cultures gave a visible band at 270bp. Any mycoplasma positive MSC cultures were subsequently destroyed and all data omitted from this thesis.

2.2 Mesenchymal stem cell phenotyping

The ISCT (Dominici et al., 2006) has proposed three phenotypic criteria to define MSCs for laboratory investigations and preclinical studies, these are: (i) adherence to plastic and a stromal morphology; (ii) a CD profile that is immunonegative for CD34 and CD45, but immunopositive for CD44, CD73, CD90, CD105 and Stro-1; (iii) a multipotent differentiation capacity to form adipocytes, osteoblasts and chondrocytes after induction with appropriate induction medium. Therefore canine and human MSCs were examined for their capacity to meet these criteria.

2.2.1 Immunophenotypic characterization of MSCs using flow cytometry

Canine and human MSCs were examined for their expression of specific CD markers on the cell surface by flow cytometry, according to the availability of commercial antibodies of published specificity.

Canine MSC CD immunoprofiling.

Immunolabeling of cMSCs was performed from passage III-V as described previously (Zhang et al., 2013a). In brief; $3x10^5$ cells were trypsinised, washed and pelleted by centrifugation, then re-suspended in 200µL of 2% BSA/PBS containing 5µL of each one of the antibodies for each sample of cells prepared. Cells were incubated with each of the following antibodies conjugated to phycoerythrin (PE) or fluorescein (FITC): PE-CD34 (Cat No. 559369 BD Biosciences), FITC-CD44 (Cat No. 115440 eBiosciences), PE-CD45 (Cat No. 125451 eBiosciences), and PE-CD90 (Cat No. 125900 eBiosciences) or with antibodies that were not specific for mammalian antigens as isotype-matched controls, i.e. IgG1 mouse (Cat No.12-4714-41 eBiosciences), IgG2a rat (Cat No.11-4321-41 eBiosciences), IgG2b rat (Cat No. 11-4031-81 eBiosciences) and IgG2b rat (Cat No. 12-4031-81 eBiosciences) (isotype control respectively for each CD marker), for 30 minutes at room temperature. The cells were then washed twice with 2% BSA/PBS. Immunoreactivity for each CD marker was assessed by flow cytometry using a Beckman Coulter FC500 Flow Cytometer and data was analysed using Kaluza® Analysis Software.

Human MSC CD immunoprofiling

Immunolabelling of human MSC was performed at passages II-V as described previously (Kohli et al., 2015).

In brief, cells were harvested by trypsinisation, washed and centrifuged, and the resultant pellet re-suspended in 2% BSA/ PBS. Initially, the cells were blocked with 10% normal human immunoglobulin (Grifols, Cambridge, UK) for 1hr on ice with shaking. Then cells were washed with 1 ml of 2% BSA/PBS and centrifuged. Then 10^5 of cells were aliquoted and each of one of the following PE-conjugated mouse monoclonal anti-human antibodies: CD34, CD44, CD45, CD105 (Immunotools, Friesoythe, Germany), CD73 or CD90 (BD Biosciences, UK), CD271 (Miltenyi Biotec Inc.) was added. Separate aliquots of 10^5 cells were also incubated with isotype-matched control PE-conjugated antibodies IgG2a and IgG1 (Immunotools) to detect levels of non-specific binding and fluorescence. The extent of immunoreactivity for each CD marker was performed by flow cytometry using a Beckman Coulter FC500 flow cytometer with data analysed using Kaluza® Analysis Software.

2.2.2 Multipotential differentiation of MSCs

Canine and human MSCs were induced to differentiate along multiple mesenchymal cell lineages, i.e. adipocytes, osteoblasts and chondrocytes, at passages III-V, as described previously by (Wright et al., 2008). This was performed as follows:

Adipogenic Induction: Cells were seeded in triplicate wells at 10^4 cells per well in a 24 well plate and cultured for one week to reach confluence before starting adipogenic induction. Cells were then treated with adipogenic induction medium, which consisted of DMEM/F-12 culture medium supplemented with 10% FBS, 1% penicillin/streptomycin, 1µM dexamethasone, 1% insulin/transferrin/selenium (ITS), 0.5mM 3-isobutyl-1-methylxanthine (IBMX) and 100µM indomethacin. The medium was completely replaced with fresh induction medium every 2-3 days. Control medium consisted of the carriers alone, i.e., methanol and DMSO, at the same dilution as was used for the induction medium.

Osteogenic Induction: Cells were seeded into 24 well plates and cultured for one week as described for the adipogenic induction above. They were then treated with DMEM/F-12 medium supplemented with 10% FBS, 1% penicillin/streptomycin, 10µM beta-glycerophosphate, 50µM ascorbic acid and 10nM dexamethasone. The medium was completely replaced with fresh induction medium every 2-3 days. Control medium contained the carriers alone, i.e., methanol and cell culture water at the same dilution as was used for the induction medium.

Chondrogenic Induction: Cells were aliquoted at 25 x 10^5 cells in 1 ml of DMEM/F-12 medium supplemented with 2% FBS and 1% penicillin/streptomycin into 1.5ml microfuge tubes. These were then centrifuged in a microcentrifuge at 500g for 5 minutes until they formed a small cell pellet. After that, the cell pellets were maintained in the same culture medium further supplemented with 10nm TGF-β and 50nm ascorbic acid with fresh medium changes every 2-3 days. All cultures were maintained in a humidified atmosphere of 5% CO_2 at 37ºC for 4 weeks after the initial addition of induction medium.

2.2.3 Assessment of MSC differentiation

Oil Red O staining and quantification of lipid vacuoles for adipogenic differentiation: The formation of lipid droplets was verified by Oil Red O staining and quantified by spectrophotometry, as described previously (Ramirez-Zacarias et al., 1992). Briefly, the Oil Red O stock staining solution was prepared by dissolving 300mg of Oil Red O powder (Sigma) into 100ml of isopropanol. The stock solution can be stored for 1year at room temperature. The Oil Red O working solution was then prepared by dilution of 3 parts from the stock solution into 2 parts of distilled water; this was mixed well and left to stand for 10minutes, then filtered through Whatman paper (Whatman No.1 filter paper, Maidstone, UK), and the filtered solution was used within 3hrs. The induced cell cultures were fixed in 10% neutral buffer formalin for 1hr, the 1ml from the working Oil Red O staining solution was added for 1hr. The stain was removed, and after 3-4 washing steps in PBS to remove any unbound stain, digitised images were captured with an inverted phase contrast microscope (CETI. Medline Scientific Ltd. UK).

The relative levels of Oil Red O accumulation in each culture were further measured by a spectrophotometer (Multiskan go, Thermo Scientific. UK) after treating the stained wells with 100µl of 100% isopropanol to extract the Oil Red O from the stained cells. The plates were incubated for 15minutes on a plate shaker; then the 100µl isopropanol contained the Oil Red O stain was transferred into 96 well plates, and the absorbance (optical density - O.D.) was measured using a bench spectrophotometer at 540nm.

Alkaline phosphatase staining and quantification for osteoblastic differentiation:

Alkaline phosphatase activity is frequently used as a key marker of osteoblast differentiation (Štefková et al., 2015). To assess alkaline phosphatase activity by staining, cells were fixed with 10% neutral buffer formalin for 10 minutes. Meanwhile, staining solution was prepared by placing 25mg of naphthol-phosphate (Naphthol AS-MX phosphate: Sigma) in 0.5ml of dimethyl formamide. Then, this solution was mixed with 50ml of 0.2M Tris-HCl buffer containing 50mg of fast red TR (Sigma). After mixing well, the final solution was filtered using Whatman No. 1 filter paper (Whatman). The fixative solution was then removed, and cells were washed with PBS, then 1ml of the staining solution was added to each well for 1hr. Finally, the stain was removed, and digitised images were captured with an inverted microscope.

For the purpose of quantification, a colourimetric assay kit (BioVision, USA) was also used to determine alkaline phosphatase activity. This was performed by following the manufacturer's protocol as follows; in brief, cells were homogenised in the assay buffer. The homogenised cells were then centrifuged to remove insoluble material at 13,000g for 3minutes. Then 80µl of each of the samples was loaded into separate wells of a 96 well plate. Then 50µl of 5mM of the *p*NPP solution was added to each sample well. Following a mixing step by pipetting up and down, the wells were incubated at 25ºC for 60minutes. A standard curve was generated by diluting 40µl of 5mM of pNPP into 160µl of assay buffer to generate 1mM *p*NPP standard.

Then 0, 4, 6, 12, 16 and 20µl of this standard solution was loaded into a 96 well plate to generate 0-20 nmol/ml *p*NPP standards that could be measured by spectrophotometry. Then, the volume of all wells was brought up to 120µl by adding required volumes of assay buffer solution. Then 10µl of alkaline phosphatase enzyme was added to each well containing the *p*NPP standard, and the plates were further incubated at 25ºC for 60minutes. Following this incubation period, 20µl of the stop solution was added into each standard and sample well to stop all the reactions. The levels of alkaline phosphatase activity in all wells were measured by O.D. at 405nm in a microplate spectrophotometer.

Glycosaminoglycan staining and quantification for chondrogenic differentiation:

Glycosaminoglycans (GAGs) are a major component of the extracellular matrix (ECM) of cartilage, and their generation is a key indicator of chondrogenic differentiation (Sasisekharan et al., 2006). The deposition of GAGs in the ECM in 3D chondrogenic-induced pellet cultures was demonstrated by harvesting and sectioning the cell pellets and toluidine blue staining for the metachromatic staining that demonstrates the presence of GAGs (Wright et al., 2008). Briefly, 3D pellet cultures were harvested at day 28 of differentiation and fixed with 10% neutral buffer formalin overnight followed with two steps of washing with PBS. After fixation, the 3D pellets were processed for histological sectioning as follows. The pellets were immersed in 70%, 90% and 100% solutions of ethanol (in water), respectively, for 30minutes per each concentration. Then the pellets were immersed in 100% xylene for 30 minutes. The pellets were carefully transferred to a base mould, which was then filled with melted paraffin wax (VWR International Ltd., Poole, UK) and left to stand at 60ºC for a minimum of 12hrs. After this time fresh, melted paraffin wax was added after aspiration of the old paraffin from the pellets, and embedding cassettes (Thermo Electron Corporation, Basingstoke, UK) were placed on top of the base moulds. The cassette and base moulds were transferred to an ice block and left to stand for 10 minutes.

Finally, the paraffin-embedded 3D pellet blocks were stored at room temperature for further histological purposes. Three-micron thick tissue sections were prepared using a standard rotary microtome (HM325, Thermo Scientific) placed on glass slides and allowed to dry using a hotbox at 70ºC.

Then the sections were dewaxed with 100% xylene for 5 minutes and rehydrated in serial dilutions of 100%, 90%, 70% ethanol (in water) for 2 minutes per each concentration, and then washed in tap water. These sections were then stained with 0.4% staining solution of toluidine blue (Sigma) in 0.2M sodium acetate buffer (pH3.75-4.25), which was added to the sections for 10minutes. After 10 minutes incubation, the sections were washed with tap water for 1minute, then again passed through a graded series of 70%, 90%, 100% of ethanol (in water) for dehydration, being immersed for 2 minutes per each concentration. After a clearing step with 5 minutes in 100% xylene, the slides were mounted in Pertex mounting medium (Sigma). Digitised images of the toluidine blue stained sections were captured using an inverted microscope.

The amount of GAGs in the 3D pellets was quantified using the 1, 9-dimethyl methylene blue (DMMB) dye binding spectrophotometric assay (Farndale et al., 1982, Farndale et al., 1986). In brief, this was performed, as more recently described (Wright et al., 2008). The 3D chondrogenic-induced pellet cultures and control pellet cultures were washed with PBS and digested overnight with papain at 60ºC. A DMMB solution was prepared as follows; 16mg of DMMB powder, 3.04g of glycine and 1.6g of NaCl were dissolved in 95ml of 0.1M acetic acid, and the volume was increased to 1L with water, then filtered (0.45µm filter, Sigma) and stored in a brown bottle to protect the solution from light. A standard curve for GAG levels was prepared by dissolving 40µg/ml of chondroitin sulphate from shark cartilage (Sigma) to generate 0, 8, 16, 24, 32, 36, 40µg/ml chondroitin sulphate standards. In 96 well plates, 50µl of each standard and test samples were mixed each with 200µl of the DMMB solution; then absorbance was measured at 595nm after incubation of the plate for 5minutes at room temperature using a bench spectrophotometer.

2.3 The generation of MSC culture-conditioned medium (MSC CM)

Canine and human MSCs were seeded at a seeding density of $1.5x10^6$ cells in T75 tissue culture flasks in DMEM/F-12 medium supplemented with 10% FBS and 1% penicillin/streptomycin for 24hrs to permit cell adhesion. After this time, the standard culture medium was discarded, and the cultures were washed three times in PBS before feeding with 15ml of DMEM/F-12 culture medium supplemented with 1% ITS, 1% non-essential amino acids (NEAA) and 1% penicillin/streptomycin, but without any serum present. The MSC cultures were then incubated at 37ºC in a humidified atmosphere of 5% CO_2 for 3 days. The MSC culture-conditioned medium (MSC CM) was collected and filtered through a sterile filter (0.20µm, Minisart® C€, Germany) to remove any cell debris or fragments. The MSC CM was aliquoted and stored at -80ºC for further experimentation. Control medium (i.e. serum-free DMEM/F-12 with the same supplements, but with no cells present) was similarly incubated in T75 culture flasks for 3 days, then harvested, filtered and stored. During culture under serum-free conditions, there was no evidence of loss of cell viability as determined by cells either losing plastic adherence or floating or becoming phase dark when examined under phase contrast microscopy. In Chapter Five, the conditioned medium prepared from three human MSC subpopulations examined have been referred to as PA MSC CM, $CD271^+$ MSC CM, and $CD271^-$ MSC CM.

2.4 Assessment of the paracrine activity of canine and human MSC CM on neuronal and endothelial cell cultures

The effects of MSC CM on neurogenesis and angiogenesis were assessed since these two activities play a major role in SCI repair (Cantinieaux et al., 2013). The cell lines, SH-SY5Y neuronal cells and EA.hy926 endothelial cells were used as potential responder cells, as previous research has reported that MSC CM generated from bone marrow-derived MSC CM have been shown to induce differentiation of both cell lines (Wright et al., 2010, Walter et al., 2015).

Both cell lines derived from tumour cells and are human in origin. As described in the Introduction (1.5.3.), SH-SY5Y and EA.hy926 cells have been widely used as models to investigate neuronal and endothelial biological activities.

2.4.1 Assessment of neurogenesis using SH-SY5Y neuronal cells

The SH-SY5Y cell line was used as a neuronal model to investigate and assess the paracrine activity of canine or human MSC CM, as discussed in the Introduction (Section 1.5.3) and reported previously (Wright et al., 2010). SH-SY5Y cells were routinely grown in DMEM/F-12 supplemented with 15% FBS, penicillin/streptomycin and 1% of NEAA and 1% of ITS. For each experiment, SH-SY5Y cells were harvested at 70-80% confluence by treatment with 0.025% trypsin/EDTA, and then centrifuged at 1000rpm for 10 minutes prior to seeding the cells at a density of $1x10^4$ cells per well in 24 well plates and incubated overnight at 37°C in a humidified atmosphere of 5% CO_2 to allow the cells to adhere. The next day, the SH-SY5Y cells were treated either with 1ml of MSC CM or with serum-free control medium and the cultures incubated in the Cell IQ Imaging Platform (CM Technologies Ltd, Finland) for live cell digitised imaging and analysis, where at least 3 wells per sample were analysed and where one image/well was captured prior to and after incubation for a 3day period. The growth and morphological differentiation of SH-SY5Y cells were determined using these captured images and the Cell IQ image analyser software, as described in more detail in Section 2.5, but in brief this allowed for the determination of the total number of viable SH-SY5Y cells per image and the extent of SH-SY5Y neurite outgrowth, i.e. neurite length per cell.

2.4.2 Immunofluorescence staining of SH-SY5Y cells for β-III tubulin

Beta-III tubulin is a marker of neuronal differentiation (Dwane et al., 2013) that was used to further examine the effects of MSC CM on SH-SY5Y cells. SH-SY5Y cells were seeded on sterilised glass coverslips at a density of $1x10^4$ cells; one coverslip each was placed in a 6 well plate. Cells were allowed to adhere overnight by incubating the plates at 37 °C in a humidified atmosphere of 5% CO_2. Then cells were then washed three times with serum-free DMEM/F-12 medium, and 1ml of MSC CM (from either canine or human MSC cultures) or 1ml of serum-free control medium was added. The plates were then further incubated at 37°C in a humidified atmosphere of 5% CO_2 for three days after which the medium was removed, and the cells were fixed with 10% neutral buffer formalin for 1hr. Then the cells were washed twice with PBS and blocked with a blocking solution of 2% BSA in PBS for 1hr before adding a primary antibody of mouse monoclonal anti-beta III tubulin (TU-20: Cat. No. ab7751, Abcam) at a 1:500 dilution in blocking buffer that also contained the permeabilisation reagent, 0.1% Triton X -100. The plates were incubated with the primary antibody for 2hrs at 4°C, and parallel plates were incubated in the same permeabilisation solution with no antibody present. After three steps of washing with PBS, the SH-SY5Y cells were then incubated with a secondary antibody, which was rhodamine Red-X-AffiniPure donkey anti-mouse IgG (H+L) (Cat. No. 715-295-150, Stratech Ltd, address) at a 1:200 dilution for 1hr at 4°C in a humidified container that was light protected. After three further washing steps with PBS, 20-30µl of the antifading agent Vectashield was pipetted onto clean glass slides. The coverslips were rinsed with distilled water and mounted with the cells facing down on the glass slides. Digitised images were acquired using a Leica DMI4000 digital microscope, as shown in Chapters 3-4. There was no immunopositivity seen in control coverslips of SH-SY5Y cells that were incubated in the absence of the primary antibody.

2.4.3 Assessment of angiogenesis using EA.hy926 endothelial cells

2.4.3.1 Scratch assay using EA.hy926 endothelial cells

Migration and proliferation of endothelial cells are necessary for the angiogenesis process (Norton and Popel, 2016). Scratch assays of EA.hy926 cells combined with digitised image analysis have been used previously to examine the effects of bone marrow-derived MSC CM on both aspects of angiogenic activity (Walter et al., 2015).

Therefore, a similar approach was adopted in this research. EA.hy926 cells were seeded in DMEM/F-12 supplemented with 10% FBS and 1% penicillin/streptomycin in 24 well plates at a density of $5x10^4$ cells per well and incubated at 37 °C in a humidified atmosphere of 5% CO_2 for 48hrs to permit the formation of 100% confluent monolayers. Then the culture medium was removed, and the monolayers were scratched with a 200µl sterile pipette tip to leave a scratch with a gap in the monolayer. The wells were then washed immediately with PBS to remove any non-adherent cells or debris and then 1ml of MSC CM or serum-free control medium was added into the wells. The plates were placed for live cell imaging in the Cell IQ platform to collect digitised images for 2 days. As described in more detail in Section 2.5.1, these digitized images were analyzed using the Cell IQ analyser software to measure (i) the rate of scratch wound closure, (ii) the number of dividing cells per image, (iii) the number of non-dividing cells per image, and (iv) to track the extent of cell migration of individual cells.

2.4.3.2 Endothelial tubule formation assay

The extent to which MSC CM promoted endothelial tubule formation was examined by culturing EA.hy926 cells on a substrate of Matrigel, which is a well characterised *in vitro* model of this aspect of angiogenesis (Donovan et al., 2001, Ponce, 2001, Guidolin et al., 2004, Khoo et al., 2011).

This was performed as follows. Growth factor-reduced Matrigel (Corning. USA) was kept on ice in the fridge at 4°C overnight, then 50µl aliquots were plated into 96-well plates and incubated for 30minutes in a humidified atmosphere of 5% CO2 at 37°C. Stock cultures of EA.hy926 cells grown in DMEM/F-12 supplemented with 10% FBS and penicillin/streptomycin were washed with serum-free DMEM/F-12 three times and then detached from tissue culture plastic with 0.25% trypsin/EDTA. Harvested cells were then centrifuged at 1000 rpm for 10minutes, and the resultant cell pellets were re-suspended in 1ml of serum-free DMEM/F-12 before counting by trypan blue exclusion in a haemocytometer. Then 2 x 10^4 viable cells per well were re-suspended in 200µl of MSC CM or serum-free control medium and loaded on the top of the aliquots of Matrigel. Following incubation in a humidified atmosphere at 37°C and 5% of CO_2 for 1day, phase-contrast digitised images were captured from three different randomly selected positions in each well using the Cell IQ live imaging platform. From these digitised images, image analysis was performed, as described in more detail in section 2.5.1, to determine the total tubule length per image and a total number of branching points per image was using the Cell IQ analyser software.

2.4.4 Cell viability assessment using MTT assay

The MTT assay is a colourimetric assay for assessing cell metabolic activity. The principle of this assay is based on the capability of NAD(P)H-dependent cellular oxidoreductase enzymes, which under defined conditions reflect the number of viable cells present, to reduce the tetrazolium MTT dye 3-(4,5-dimethylthiazol-2-yl)-2,5-diphenyltetrazolium bromide to its insoluble formazan, which has a purple colour. Thus, in this study, the MTT assay was performed to assess further the effects of MSC CM on SH-SY5Y and EA.hy926 cell proliferation, by determining the numbers of viable, i.e. metabolically active cells present. This was performed as follows: SH-SY5Y cells and EA.hy926 cells were seeded at a density of 5x10^3 cells per well into 96 well plates and treated with 200µl of MSC CM or serum-free control medium for three or two days respectively.

Following the treatment period, 20µl of 5mg/ml MTT solution was added to each well and incubated for 3-4hrs at 37°C in a humidified atmosphere of 5% CO_2. Then carefully and without disturbing the cells, the medium was removed. The plates were left for 10 minutes to dry then 100µl of DMSO was added. The MTT assay was performed in the dark since the MTT reagent is sensitive to light. The absorbance of each well, including blanks containing MTT alone (no cells), were measured at 492 nm and background at 650nm a plate reader.

2.5 Microscopy and Image Analysis

2.5.1 The Cell IQ live cell imaging machine

The Cell IQ is an automated live-cell imaging apparatus, which provides an environment that enables cells to remain viable, i.e. in an incubator at 37ºC and atmosphere of 5% CO_2, while also collecting digitised images of the cells, a single snapshot at a time. The system can provide for long-term analysis of cells, and its software can be applied to the digitised images collected automatically to identify and quantify changes in cell phenotype. The system can be used to collect both phase contrast data and fluorescence data in different wavelengths and combinations thereof. The accompanying analyser software is powerful and has been applied to examine multiple changes in cell phenotype, including cell viability (Cao et al., 2016), cell proliferation (Rämö et al., 2016), cell migration (Bray and Slevin, 2015), individual cell tracking (Jansson et al., 2012), and specific changes for different cell lineages, e.g. increases in neurite outgrowth from neurons (Palazzolo et al., 2012), and endothelial tubule formation (Bray and Slevin, 2015). Any morphological parameter that cannot be identified by the naked eye can be analysed and quantified by Cell-IQ analyser software. It is possible to analyse structures composed of groups of cells either in 2D or 3D in cell culture, e.g. scratch wound closure, endothelial tube length and branch points, embryo and oocyte tracking. Such analysis is achieved by using the software to develop an analysis protocol for each parameter to be quantified.

Because of the advantages of using the Cell IQ platform, regarding accumulated extensive, accurate and objective data on changes in cell phenotype, the platform was used to examine the effects of MSC CM on SH-SY5Y neuronal cells and EA.hy926 endothelial cells. More routine examinations of stock cell cultures, e.g. for passaging cells and trypan blue exclusion measures of stock cell viability, were performed using an inverted phase contrast microscope.

2.5.2 The Cell IQ analysis protocol for SH-SY5Y viable cell numbers and neurite outgrowth

After treating SH-SY5Y cells with MSC CM or with serum-free control medium, the plates were set for imaging using the Cell IQ live cell imaging platform and digitised images captured under phase contrast using an X10 objective, where one image per well (in triplicate wells) was captured at the end of 3-day time courses. At the end of the incubation period, these images were processed for further analysis using the Cell IQ analyser software. Digitised images were uploaded and opened in the analyser software window. By following the steps provided in the Cell IQ analyser user manual, the protocol was developed using an initial sample "library" of morphological features of the imaged cells that were designated as neurites or viable neuronal cell bodies (distinguished as phase-bright) versus cell debris or non-cellular background (Figure 2.1).

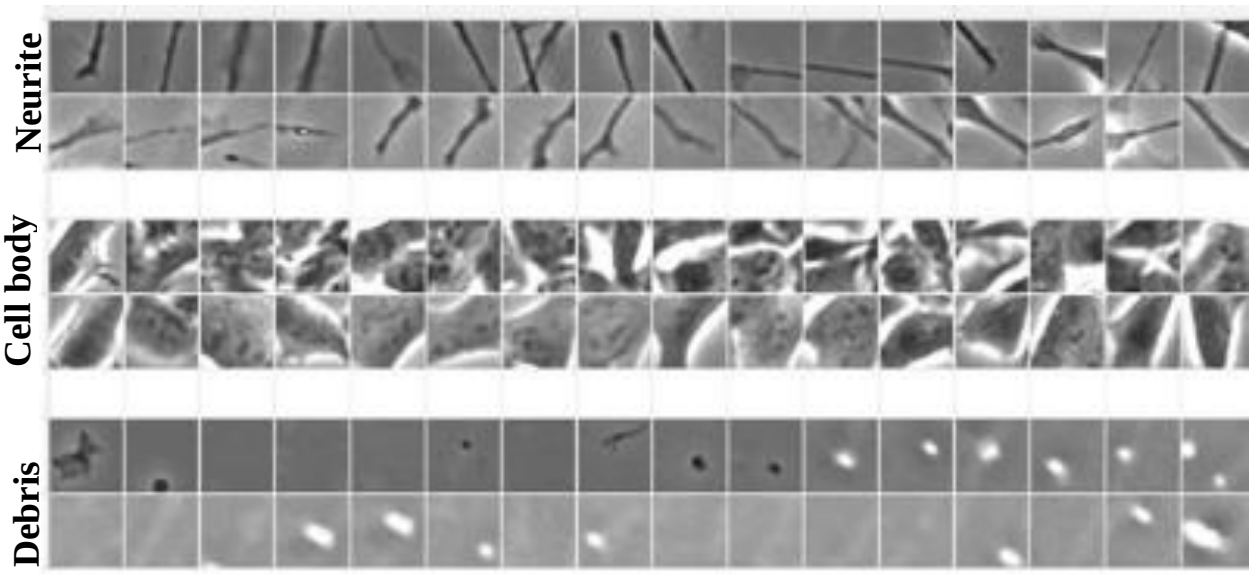

Figure 2:1 Digitised phase contrast images of SH-SY5Y neuronal cells used as a reference library for the image analysis software to distinguish morphological features.

Representative images are shown of the sample library through segmentation and classification based on morphological differences. The process of generating the image analysis protocol was performed initially by selecting the "cell classifier" + "neurite finder". The classes identified were neurites (top panels), cell bodies and debris of background (bottom panels). These are magnified images derived from digitised images collected using a phase contrast X10 objective, then further magnified using the image analysis software.

2.5.3 The Cell IQ analysis protocol for EA.hy926 viable cell numbers, scratch wound closure and individual cell migration

EA.hy926 cells were treated with MSC CM after performing a scratch as described in section 2.4.2.1; then the plate was incubated in the Cell IQ platform for digitised image acquisition under phase contrast using the x10 objective. Images were generated by selecting at least one region of interest (RoI) per well and captured at the same RoI every 15minutes over a two-day period to the point of scratch wound closure. Measurements of wound closure, viable cell numbers (distinguished as phase bright cells) and cell migration/movement were obtained by using Cell IQ analyser software and following the instructions provided by the user manual guide. In brief, the scratch wound closure analysis was based on previously published protocols (Walter et al., 2010, Bray and Slevin, 2015), which utilised threshold levels and selected parameters as shown in Figure 2.2. The Threshold tool selects the area that contains viable cells covering the entire digitised then the selected parameters can be set to identify and remove any debris from the scratch area or fill in gaps in the non-scratched area. The results generated for the scratch wound area have been indicated by the purple boundary line seen in Figure 2.2, while the width of the scratch at exactly the centre of the image is shown by a blue line. The results used were derived from the scratch area as a proportion of the original scratch wound area. This was to avoid the use of the scratch width, which varied along the scratch length. The measurement of cell proliferation was also performed using the Cell IQ analyser by counting the number of dividing and non-dividing cells in the digitised images collected for each of the scratch wounds over time. This measurement was achieved by generating a cell identification protocol based on a library of sample images, which were classified according to their morphological appearance (Figure 2.3). The same cell identification protocol was also used to track viable cell movement and to measure the total distance of cell migration from the edge of the scratch wound towards the wound centre. These measurements were quantified over the two days of imaging period.

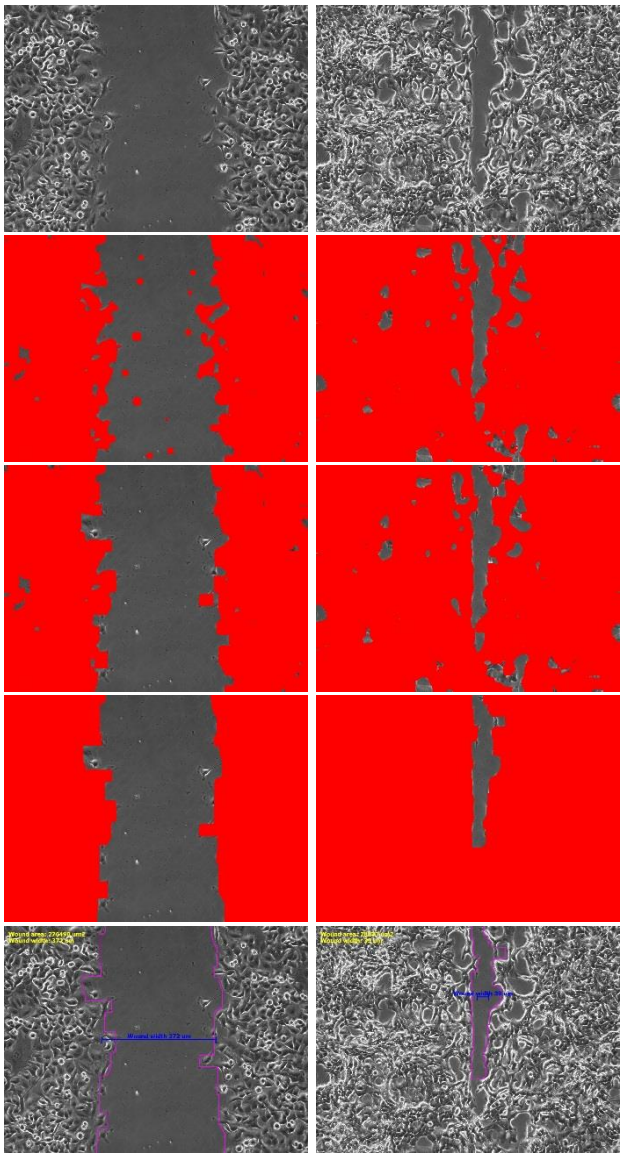

Figure 2:2 The imaging protocol used to measure EA.hy926 cell scratch wound closure.

Representative digitised images are shown of the processing steps undertaken for scratch wound area analysis that was used to measure the percentage of wound closure over time. This measurement was based on a "threshold level" that initially identified the area of the digitised image that was covered by cells. Images from the left panels indicate a representative scratch wound created at day 0, while the images in the right panels are representative images of the same scratch at day 2. Images from top panels to the bottom panels represent the processing steps: i) setting the threshold ii); removing debris in the scratched area; iii) eliminating gaps from the non-scratched area; (iv) finally, the resultant images used to calculate the scratch wound area as a proportion of the original scratch area.

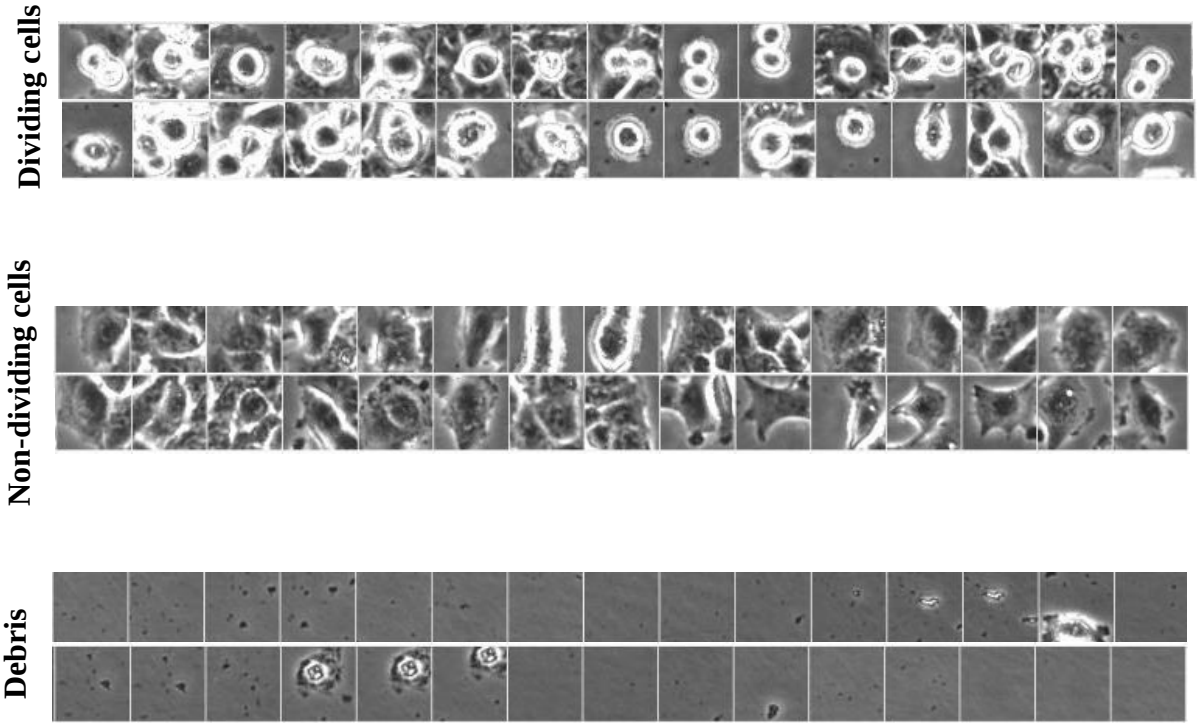

Figure 2:3 The imaging protocol used to measure viable EA.hy926 cell division and proliferation.

Representative images are shown from the sample library that was used to identify and quantify the numbers of dividing and non-dividing cells present in each of the digitised images of EA.hy926 cells in the scratch wound assays. As illustrated above, the cells were classified as dividing and non-dividing cells based on their morphological appearance, with dividing cells appearing phase bright and rounded up or undergoing mitosis, while non-dividing cells were also phased bright but flattened and without any clear mitotic changes taking place.

2.5.4 The imaging protocol used to measure EA.hy926 tube formation

Digitised images were captured of EA.hy926 cells cultured on Matrigel in the presence of MSC CM versus serum-free control medium for 1day. These digitised images were then analysed to measure the total tubule length and total branch point count per image using the Cell IQ analyser software. For each well (there were 5 wells per sample tested), 3 images were captured randomly from the well and then the threshold tool and selected parameters enabled the required measurements to be determined (Figure 2.4). Initially, the threshold tool was used to identify areas of the images that contained cells. Then followed by removal of all debris or small single objects, including single cells or short lengths of connected cells in sequence, and the removal of cell connections that were less than the width of one cell. The numbers of branch points were counted whenever longer sequences of cells (classified as tubules) connected with shorter sequences of cells (tubules); these were only scored once per connection.

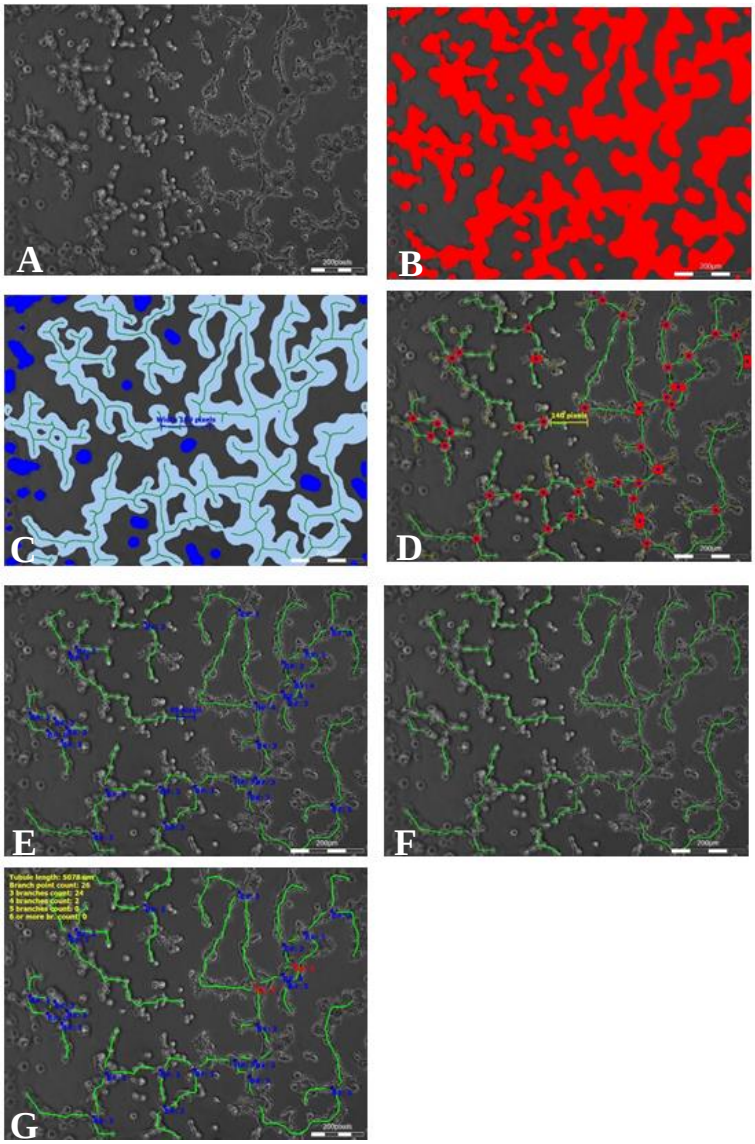

Figure 2:4 The imaging protocol used to measure EA.hy926 tube formation.

Representative images show the processing steps that were applied to develop the analysis protocol for measuring endothelial tubule length and for counting the number of endothelial tubule branch points. The measurement was based on initially thresholding the areas that were covered by cells and that were connected to other cells. Top panels: A) original image; B) applied threshold to identify all cells; C) step required to identify debris, single cells and short lengths of unconnected cell sequences; D) identification of branch points and removal of small sequences of cells identified in the previous step; E) performing the branch counts; F) an optional step to classify the endothelial tubule as thin or thick; G) the resultant image that was used to determine the final measurement for tubule length and branch point count.

2.6 ELISA analysis

Canine and human MSC CM were analysed for the presence of VEGF protein by enzyme-linked immunosorbent assay (ELISA) using a commercially available kit (R&D Systems; Minneapolis, MN, USA) according to the manufacturer's instructions. In brief, this involved bringing all the reagent to room temperature. The working standards were prepared by dilutions as 1000, 500, 250, 125, 62.5, 31.3, 15.6, and 0 pg/ml after having reconstituted the VEGF in 2000 pg/ml with calibrator diluent. 50µl of assay diluent was added to each well coated with a monoclonal antibody against VEGF, followed by adding 200µl of standard or sample per well and the plate was incubated for 2hrs. after incubation, each well was aspirated then washed three times with wash buffer after the last wash step a complete removal of any remaining wash buffer was performed by aspirating or decanting. Then 200µl of the anti-VEGF conjugate was added to each well and incubated for 2hrs at room temperature followed by repeating the same aspiration/ wash steps described earlier. This was followed by adding 200µl of substrate solution to each well and incubated for 20minutes protected from light. Finally, 50µl of stop solution was added to each well, and 450 nm optical density was determined using microplate reader.

2.7 Statistical analysis

At least three independent experiments were performed for all analysis, i.e. using canine and human MSCs and MSC CM that was derived from at least three different patients (for each species) versus at least three separately generated serum-free control medium. Data has presented as the mean ± the standard error of the mean (SEM). For one experimental readout, i.e. the quantitative determination of alkaline phosphatase activity shown in Chapter 5, it was only possible to measure levels in n=2 MSC donors; therefore this data has been presented as the mean ± standard deviation (SD). All data were examined for normal distributions and then analysed using parametric tests (normally distributed data) or non-parametric tests (non-normally distributed data) accordingly.

The tests used were an independent samples t-test or Mann-Whitney *U* test, one-way ANOVAs and two-way ANOVAs. A *p* value below 0.05 was considered significant. Statistical analysis was performed using Prism software (GraphPad Software Inc., La Jolla, CA, USA).

Chapter 3: An *in vitro* investigation of the neurotrophic and angiogenic paracrine activities of cMSCs

3.1 Aim and background

The most common causes for SCI in dogs are IVDD or vehicle accidents (Bonner and Smith, 2013). Regardless of the cause of the SCI in both cases, the resultant pathology will lead to primary and secondary injury. Excellent recovery after injury can be achieved by preventing secondary injury, promoting regeneration and sprouting of remaining axons, enhancing the remaining function of any preserved neural circuitry, replacing destroyed spinal cord tissue and promoting revascularisation (Thuret et al., 2006). However, the recovery level depends on the severity of the injury, the more severe the injury, the less efficient the recovery. Although cure from paralysis is still difficult to achieve, recent research studies have suggested novel methodologies for SCI treatment, one of which is the use of MSCs as a cell-based therapy (Park et al., 2012a). Different studies suggested that transplanted MSCs exert therapeutic activity through their secretomes (Drago et al., 2013, Neirinckx et al., 2015, Bollini et al., 2013).

As described in Chapter 1, dogs represent an excellent opportunity in which it is possible to examine how cell therapies may benefit SCI patients. Given the evidence that rodent and human MSCs exert paracrine activity in promoting nerve growth and angiogenesis (Wright et al., 2007, Wright et al., 2014, Walter et al., 2015). Therefore, this study has investigated the capacity of canine MSCs to exert paracrine activities on models of nerve growth and angiogenesis. As stated above, to achieve a good recovery the regeneration of destroyed axons and CNS tissue revascularization is required. This chapter reports on the initial characterisation of cMSCs according to the criteria of the ISCT (Dominici et al., 2006) and on the effects of canine MSC secretomes, in the form of culture conditioned medium, on the SH-SY5Y neuroblastoma cells and the EA.hy926 endothelial cells.

3.2 Phenotypic verification of cMSC by multipotential differentiation and immunophenotype

Differentiation capacity of cMSCs

Cells were originally provided by the Veterinary Tissue Bank at passage II-III, then culture expanded as monolayer cultures in standard culture medium (DMEM/F-12 supplemented with 10% FBS, and 1% penicillin and streptomycin, as described in Chapter 2(Section, 2.1.1). These cultures of culture expanded cMSCs were plastic-adherent and displayed a stromal appearance. At passages III-V, cMSC cultures were induced to undergo differentiation towards adipogenic, osteogenic and chondrogenic lineages. As shown in Figure 3.1, cMSCs were able to differentiate along all three lineages. For adipogenic and osteogenic differentiation there was no evident loss of cell viability. However, for chondrogenic pellet cultures some cell death was apparent (as determined by Live/Dead staining and confocal microscopy), but nonetheless, there was also clear evidence of extracellular metachromatic staining with toluidine blue, indicative of glycosaminoglycan deposition and chondrogenic differentiation (Figure 3.1).

Immunophenotyping for CD markers

The expression of a panel of CD markers was examined for cMSCs (n=4 dogs; passages III-V) by flow cytometry. The cMSCs were notably immunopositive for CD44 and CD90 while being immunonegative for CD34 and CD45. This finding is in line with the minimal phenotypic CD pattern for the identification of MSCs (Figure 3.2) (Table 3.1) (Dominici et al., 2006).

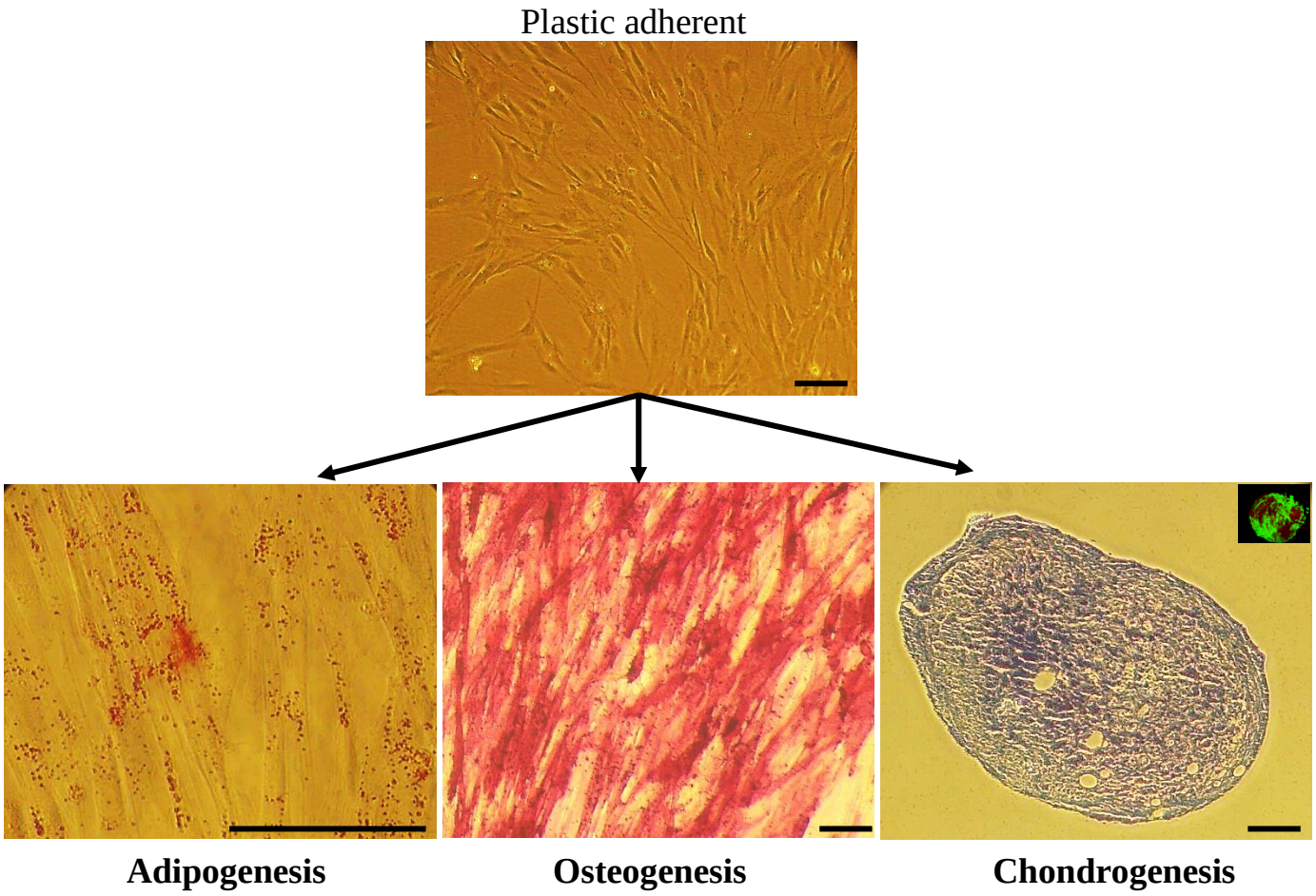

Figure 3:1 Differentiation of cMSCs along mesenchymal lineages.

Representative images are shown of plastic adherent, fibroblastic cells under phase contrast microscopy before treatment with inducers of differentiation (top panel) and after induction to become Oil Red O-positive adipocytic cells, alkaline phosphatase-positive osteoblastic cells, and toluidine blue-stained cartilaginous extracellular matrix and cells, as indicated (bottom panels). There was an evident loss of cell viability during the chondrogenic differentiation of MSCs in 3D-pellet cultures (visualised following Live/Dead staining and confocal microscopy; inset, bottom left panel). Scale bars = 100µm.Original magnification X10 for plastic adherent, osteogenesis, and chondrogenesis images. Original magnification X40 for adipogenesis image. Data shown are representative of inductions of cMSCs from four separate dogs.

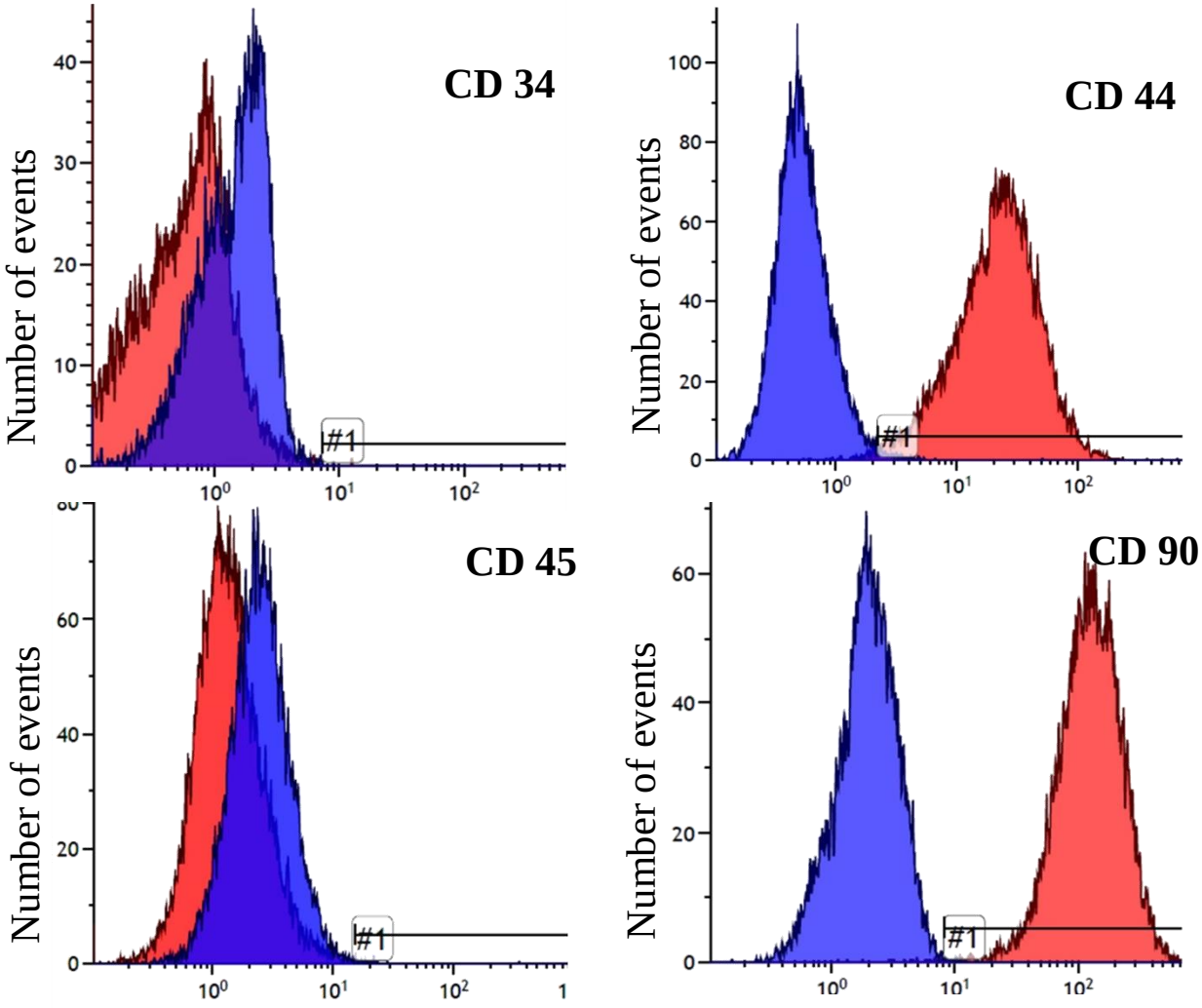

Figure 3:2 Immunophenotypic verification of cMSCs following CD immunostaining.

Representative histograms are shown flow cytometric analysis of cMSCs following immunocytochemical staining for CD34, CD44, CD45 and CD90. Immunoreactivity following immunocytochemical staining with irrelevant isotype-matched control antibodies has been shown in blue, while immunoreactivity for each of the CD markers has been shown in red. Data shown are representative of the CD profiles of cMSCs from four separate dogs.

Percentage expression of CD markers					
Cell type	**Patient ID**	**CD34**	**CD44**	**CD45**	**CD90**
Canine MSCs	cMSC 012	0.6	99.31	0.1	96.3
	cMSC 014	0.3	82.1	0.1	90.9
	cMSC 017	0.1	81.7	0.1	92.7
	cMSC 028	0.3	90.35	0.04	96.3
Mean		0.33	88.37	0.18	94.05
SEM		0.11	4.16	0.075	1.35

Table 4: CD immunopositivity of cMSCs.

The percentages of cMSCs that were immunoreactive for specific CD markers. The cells were largely immunonegative for CD34 and CD45, but immunopositive for CD44 and CD90. Summative data has been shown as the mean±SEM of four independent experiments (i.e. 4 different donor dogs).

3.3 The effects of cMSC CM on SH-SY5Y neuronal cells

Following cell characterisation for minimal criteria of MSCs phenotype, the investigation of paracrine activities was performed. The neurotrophic activity was examined using SH-SY5Y cells.

3.3.1 cMSC CM enhanced SH-SY5Y cell proliferation and neurite outgrowth

SH-SY5Y cells were seeded at $1x10^4$ cells per well in triplicate wells of 24 well plates in DMEM/F-12 containing 15% FBS and 1% penicillin and streptomycin and left overnight to allow for cell adherence. After removal of the serum containing medium and washes in serum-free medium, cells were treated with cMSC CM versus serum-free control medium. A single digitised phase contrast image of each well was generated after placing the culture plates in the Cell IQ live cell imaging platform at the end of the 3-day time course (see Figure 3.3 for representative images). These images were then used, along with the Cell IQ analyser software, to measure the number of viable cells present and the extent of neurite outgrowth per cell. As shown in Figure 3.4, there were significant increases in both the number of cells present and neurite outgrowth in cMSC CM when compared with control (p= 0.0036 for cell number and p= 0.0055 for neurite outgrowth/cell, respectively) (Figure 3.4).

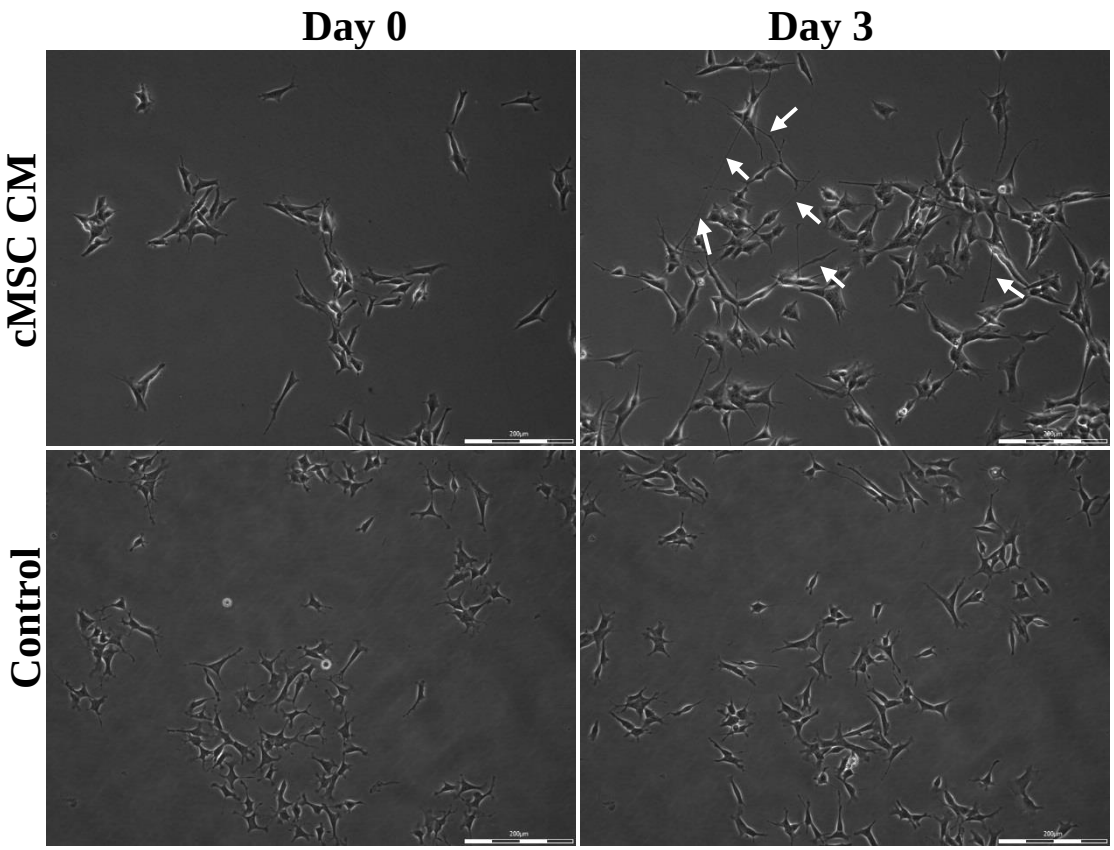

Figure 3:3 The appearance of SH-SY5Y cells cultured for 3 days in the presence of cMSC CM versus control medium.

Representative images show there was an apparent increase in SH-SY5Y cell numbers and increased neurite outgrowth (arrowed) in cMSC CM compared with control cultures. Scale bars = 200µm. These images were performed on cMSC CM from three separate donors.

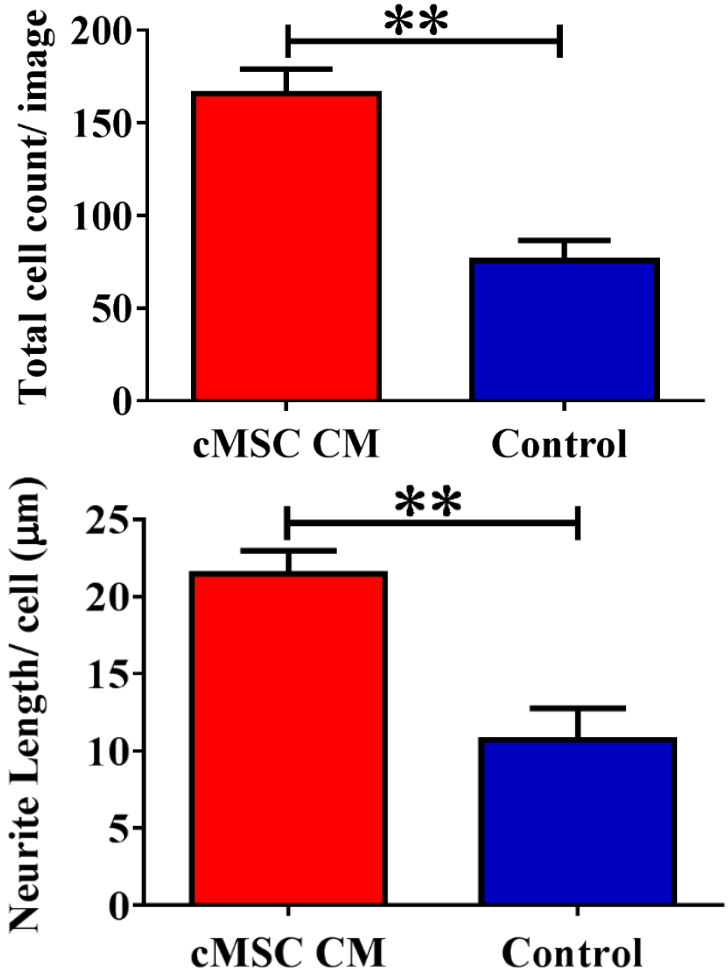

Figure 3:4 cMSC CM significantly increased SH-SY5Y cell proliferation and neurite outgrowth.

SH-SY5Y cells were treated with cMSC CM or serum-free medium for 3 days when digitised phase contrast images were captured and analysed using the Cell IQ imaging platform and software. There was a significant increase in both the number of viable cells present and the extent of neurite outgrowth per cell in cMSC CM at the 3-day time point compared with the control cultures. Each bar represents the mean±SEM of 5 independent experiments (i.e. using cMSC CM from 5 separate dogs). **indicates $p \leq 0.01$. Mann-Whitney U test used to determine the significant differences.

3.3.2 cMSC CM induced immunopositivity for the mature neuronal marker, βIII-tubulin in SH-SY5Y cells

To further examine the differentiation status of SH-SY5Y cells, the cells were tested for their immunopositivity for the mature neuronal marker, βIII-tubulin (Meyer et al., 2004). As shown in Figure 3.5, SH-SY5Y cells were βIII-tubulin immunopositive following their treatment with cMSC CM for 3 days but were largely immunonegative in control medium at the same time point. Figure 3.6 demonstrates that there were significantly greater numbers of βIII-tubulin immunopositive SH-SY5Y cells when cultured in the presence of cMSC CM compared with control cultures (p= 0.0002).

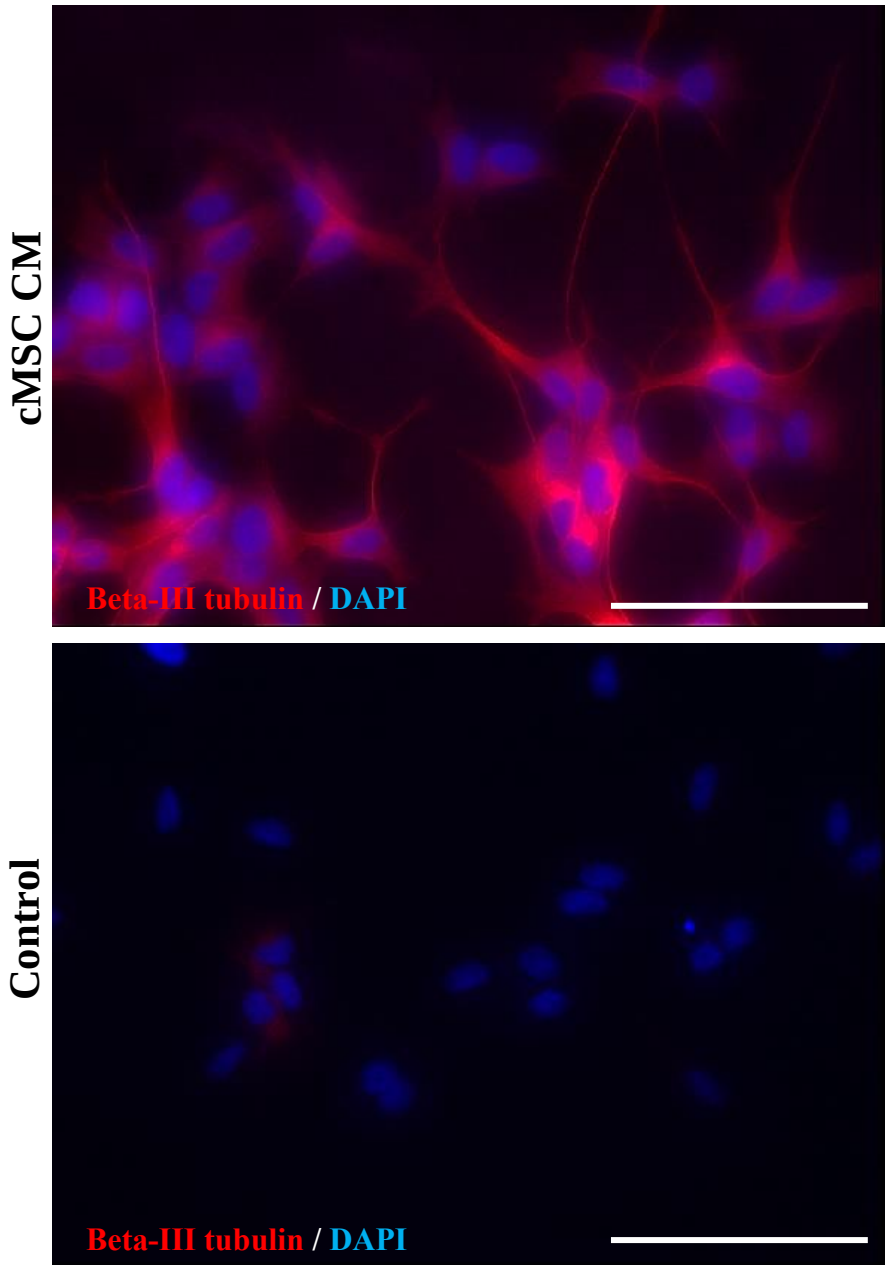

Figure 3:5Treating SH-SY5Y human neuroblastoma cells with cMSC CM induced beta-III tubulin immunopositivity.

Representative images are shown of SH-SY5Y cells following immunocytochemical staining for beta-III tubulin. As shown, there was a clear increase in immunopositivity in cells cultured in the presence of cMSC CM compared with control cultures. Scale bar = 100µm. Original magnification X40. These images were performed on cMSC CM from 3 separate donors.

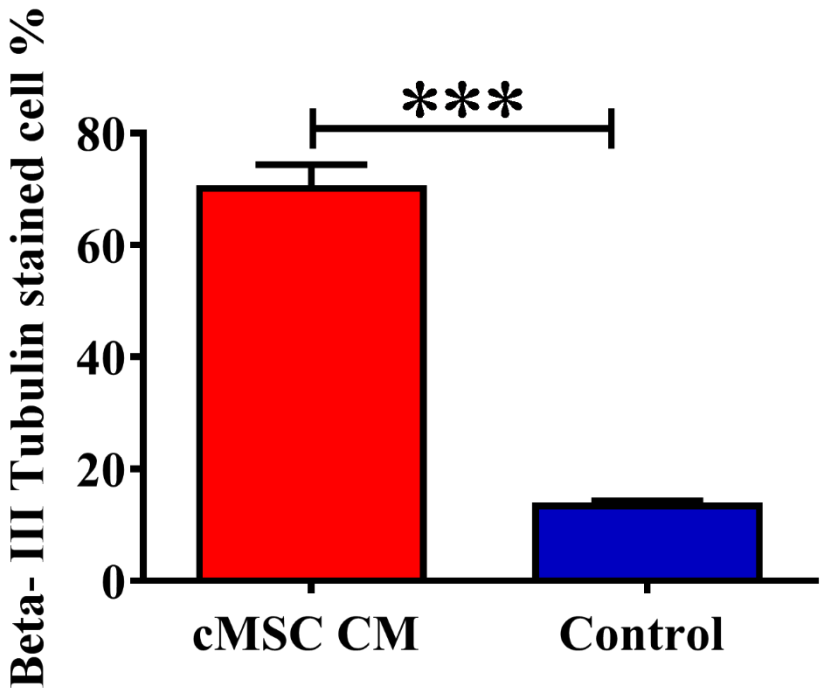

Figure 3:6 cMSC CM significantly increased the proportion of SH-SY5Y neuronal cells that were beta-III tubulin immunopositive.

As shown, there was a marked increase in the percentage of SH-SY5Y cells cultured in cMSC CM versus control medium that was beta-III tubulin immunopositive. The proportion of beta-III immunopositive SH-SY5Y cells present was determined by scoring a minimum of 500 cells from digitised images, each collected from 5 randomly selected fields in each of 3 wells per medium tested. Each bar represents mean±SEM from three independent experiments, i.e. after culturing cells in cMSC CM from 3 separate dogs versus control medium. ***indicates $p \leq 0.001$. Mann-Whitney U test used to determine the significant differences.

3.3.3 Assessment of SH-SY5Y viable cell numbers using the MTT assay

The MTT assay was used to further examine the number of viable SH-SY5Y cells present in cMSC CM versus control medium in a 96 well plate format. As shown in Figure 3.7, there appeared to be more viable SH-SY5Y cells present after culturing in cMSC CM for 3 days compared with control medium. These cultures were subsequently processed to assess viable cell number using the MTT assay, which measures non-specific esterase activity in viable cells (Hansen et al., 1989, Denizot and Lang, 1986). As shown in Figure 3.8, there was a significantly greater level of absorbance, indicative of increased numbers of viable SH-SY5Y cells in cMSC CM versus control medium (p= 0.0009).

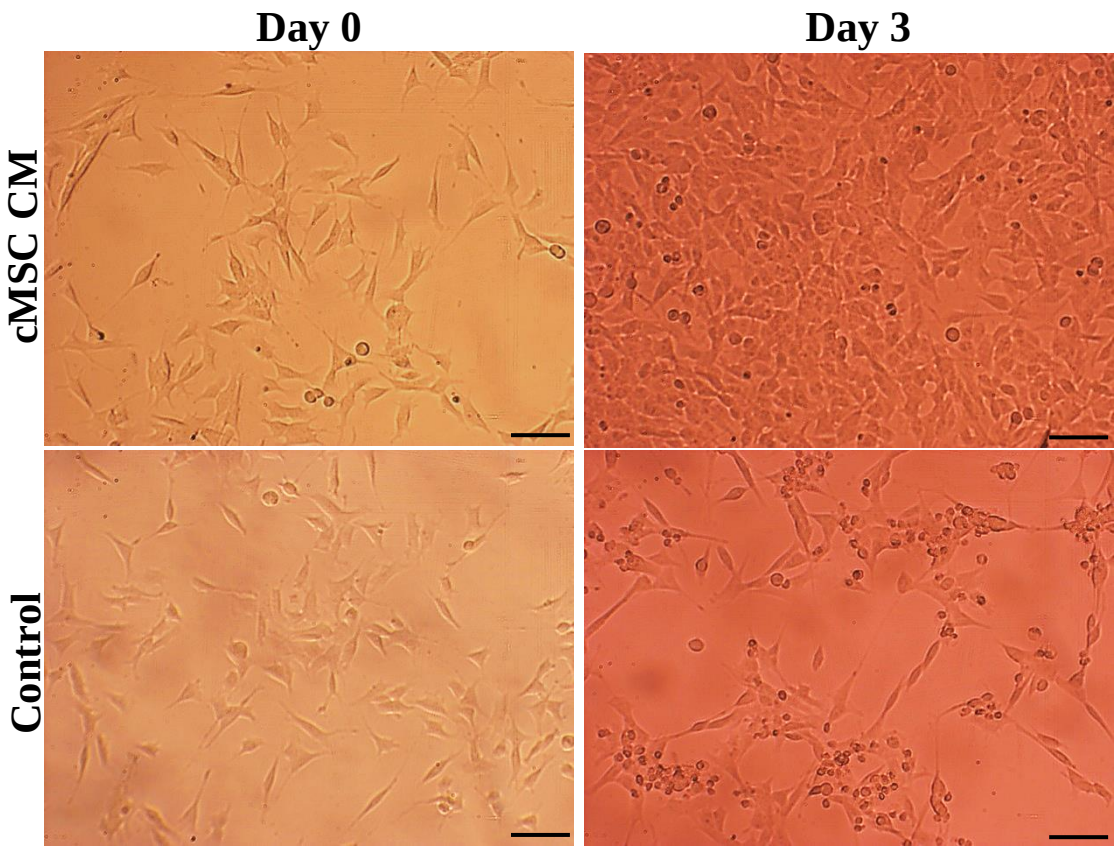

Figure 3:7 The effects of cMSC CM on SH-SY5Y neuronal cell proliferation.

Representative images have been shown to the relative increase in SH-SY5Y cell numbers when cultured for 3 days in cMSC CM versus control medium. Scale bar = 100µm. Original magnification X10. These images were performed on cMSC CM from 3 separate donors.

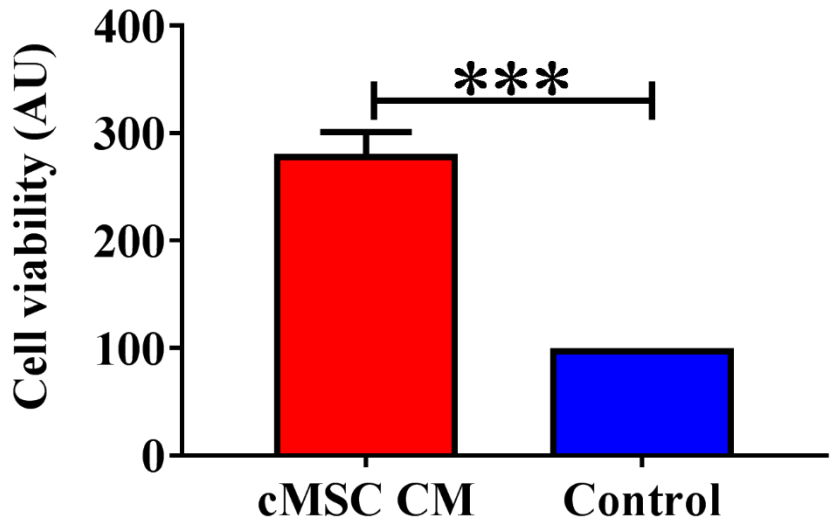

Figure 3:8 The MTT assay confirmed that culturing SH-SY5Y neuronal cells in cMSC CM versus control medium significantly increased the number of viable SH-SY5Y cells present.

MTT assays were performed to assess viable cell numbers. The results showed a significant increase in the number of viable SH-SY5Y cells in cMSC CM versus control medium at 3 days. Each bar represents mean±SEM from three independent experiments, i.e. using cMSC CM from 3 separate dogs. ***indicates $p \leq 0.001$. Mann-Whitney U test used to determine the significant differences.

3.4 The effects of cMSC CM on EA.hy926 endothelial cells

3.4.1 cMSCs CM increased EA.hy926 endothelial cell migration and proliferation

The effects of soluble factors secreted into the conditioned medium by cMSCs on EA.hy926 cells were examined using a scratch assay. Confluent layers of EA.hy926 endothelial cells were scratched using a yellow pipette tip, and the medium was replaced with either cMSC CM or serum-free control medium. Then, the rates of EA.hy926 endothelial cell migration and proliferation were monitored and quantified using the Cell IQ Imaging platform. Results showed that there was a significant increase in scratch wound closure (as a percentage of the original scratch width) when compared with control cultures (p=0.0409) (Figures 3.9 and 3.10). To determine whether cMSC CM played a role in promoting cell migration to induce wound closure, cells from both sides of wound edges were tracked by using Cell IQ analyser software. A minimum of three cells for each of triplicate scratch wound from each of three independent experiments (i.e. testing cMSC CM from three separate dogs) was randomly selected. Their patterns of migration were tracked by collecting digitised images every 15 minutes over a 2-day time course, after which the total distance that each cell had migrated during this period was measured. These results showed that there was a significant increase in the extent of cell migration in the closure wound area when the cells were treated with cMSC CM compared with control medium (p= 0.0001) (Figure 3.11).

Additional analysis using the cell IQ analyser software was performed on tracked cells to determine the numbers of dividing, and non-dividing cells present within the scratch wound area in each image collected every 15 minutes over the two-day time course. This data showed that the number of both dividing and non-dividing EA.hy926 cells present within the scratch wound area were significantly higher when treated with cMSC CM compared with control medium (p= 0.0127 for dividing cells, p =0.0001 for non-dividing cells) (Figure 3.12). EA.hy926 cell proliferation was also determined using a 96 well plate format and the MTT assay. Representative images in Figure 3.13 show evidence of EA.hy926 endothelial cells proliferating to a greater extent after treatment with cMSC CM compared with control medium after 2 days of incubation.

The MTT assay of these cultures also showed a significant difference in the number of viable EA.hy926 cells present in cultures treated with cMSC CM compared with control medium after 2 days of treatment (p= 0.0001) (Figure 3.14).

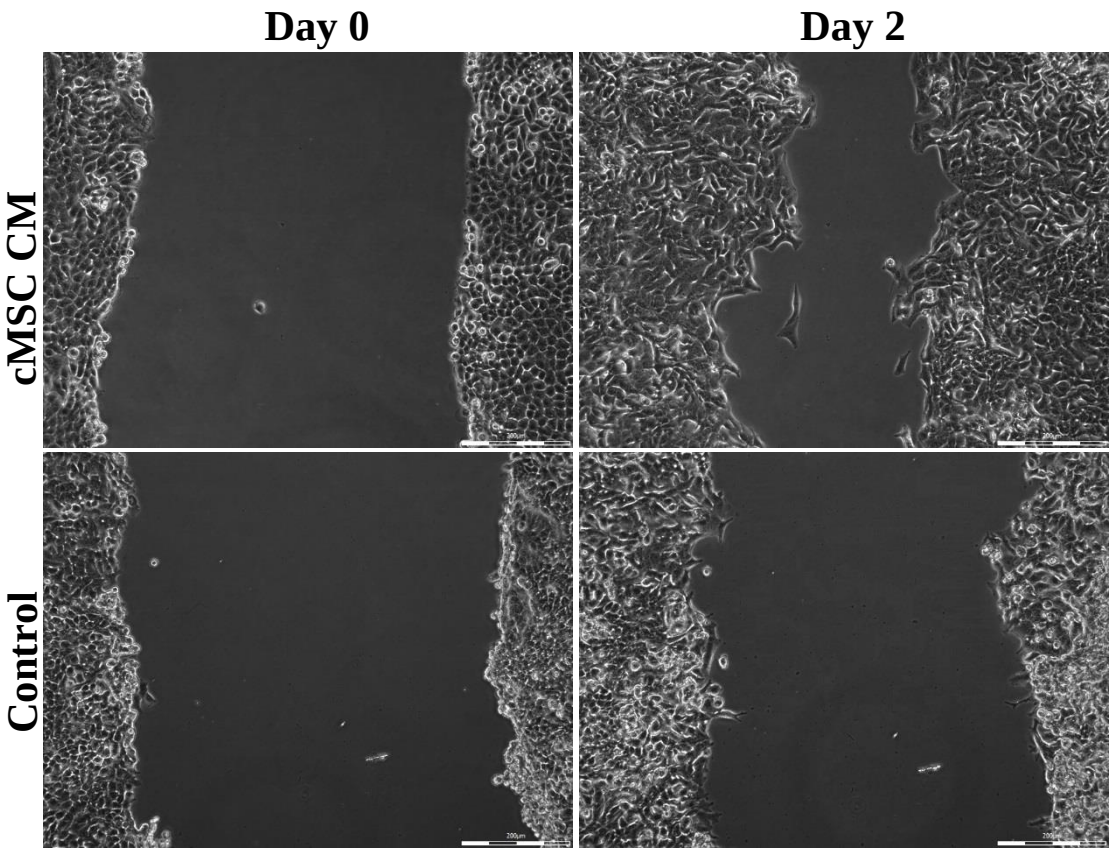

Figure 3:9 The effects of cMSC CM on EA.hy926 endothelial cells in scratch assays.

Representative images are shown EA.hy926 endothelial cell scratch assays, which were treated with cMSC CM or serum-free control medium for 2 days after scratching. EA.hy926 cells were seeded into multiple wells of 24 well plates and cultured in a standard culture medium until confluent and then scratched using a yellow pipette tip. After washing with PBS, the cultures were then fed with cMSC CM or serum-free control medium. Scale bars = 200µm. These images were performed on cMSC CM from 3 separate donors.

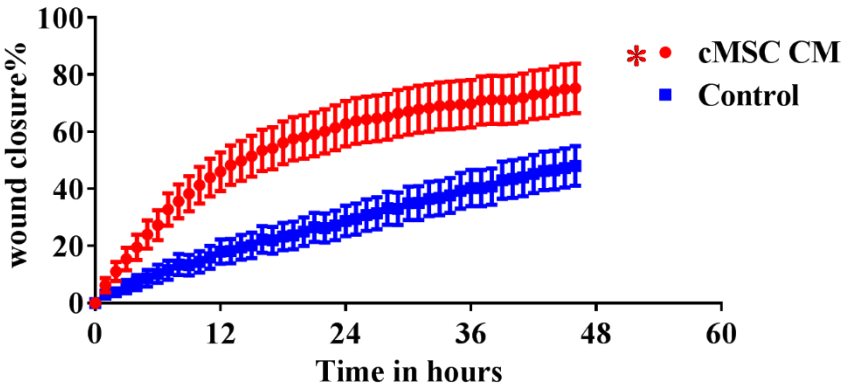

Figure 3:10 cMSC CM significantly increased the rate of wound closure in EA.hy926 endothelial scratch assays.

The Cell IQ platform was used for live imaging of wound closure in EA.hy926 endothelial cell scratch wound assays in the presence of cMSC CM versus serum-free control medium. Digitised images were generated over 2 days of incubation and the Cell IQ imaging software used to measure the extent to which the wound had closed (as a proportion of its original scratch area). There was a significant increase in the rate of wound closure in cMSC CM compared to the control medium. Each bar represents mean±SEM of 3 independent experiments, i.e. using cMSC CM from 3 separate dogs. * (red start) indicates $p \leq 0.05$. Two-way ANOVA with a Sidak's multiple comparisons test used to determine the significant differences.

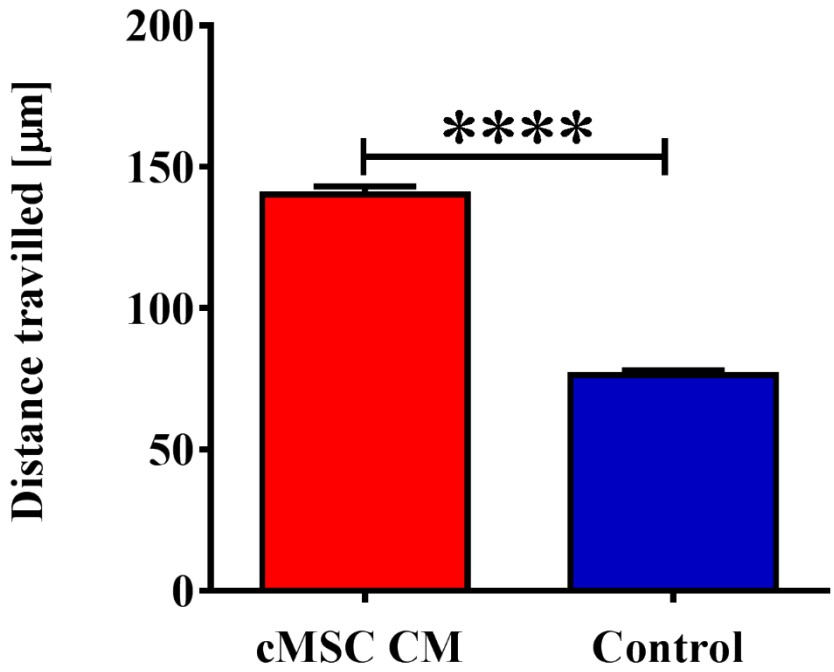

Figure 3:11 cMSC CM significantly increased EA.hy926 endothelial cell migration.

Image analysis of the collected digitised images was used to measure the distance that EA.hy926 endothelial cells migrated from the edge of the scratch towards the centre of the wound over a period of 2 days in the presence of cMSC CM versus serum-free control medium. As shown, there was a significant increase in distance travelled in cMSC CM versus control medium during this time. Each bar represents the mean±SEM of 3 independent experiments (i.e. 3 different dog donors) of 3 replicates per each experiment. ****indicates $P \leq 0.0001$. Mann-Whitney U test used to determine the significant differences.

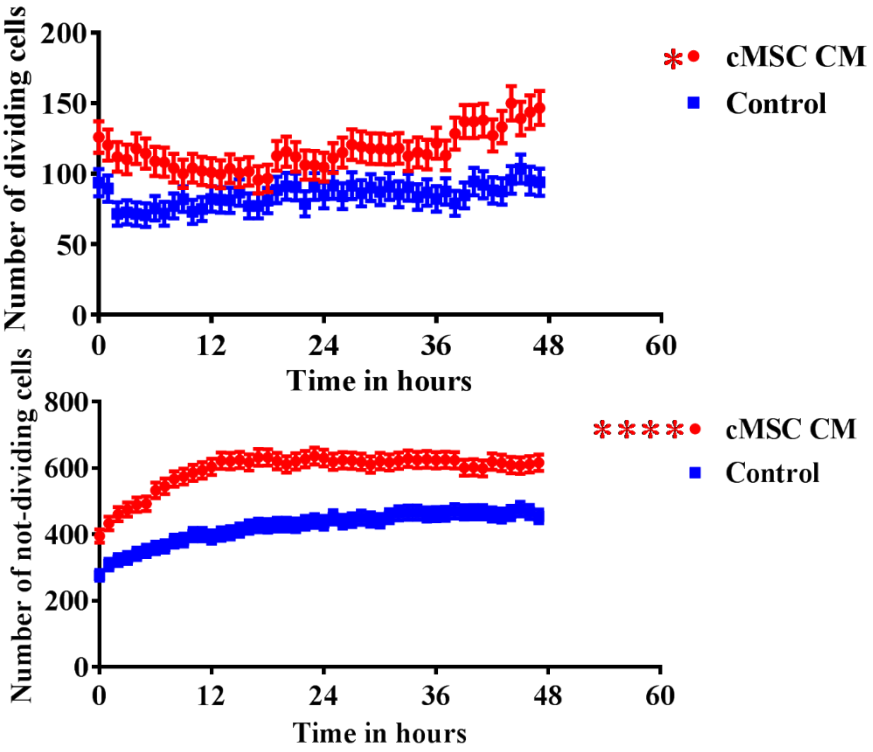

Figure 3:12 The stimulatory effects of cMSC CM on EA.hy926 endothelial cell numbers in the scratch wound area resulted from increased cell migration and cell proliferation.

The increased numbers of EA.hy926 endothelial cells present in the closure of scratch wounds, seen in Figures 3.9 and 3.10, could have been through increased cell migration (as shown in Figure 3.11) and increased cell proliferation. Therefore further analysis was performed to track the number of dividing and non-dividing cells present in the wound area. As shown, there was a significant increase in both cell populations, indicating that cMSC CM stimulated EA.hy926 endothelial cell migration and cell proliferation. Each bar represents mean±SEM from 3 independent experiments, i.e. using cMSC CM from 3 separate dogs. * (red star top panel) indicates $P \leq 0.05$ and **** (four red stars bottom panel) indicates $P \leq 0.0001$. Two-way ANOVA with a Sidak's multiple comparisons test used to determine the significant differences.

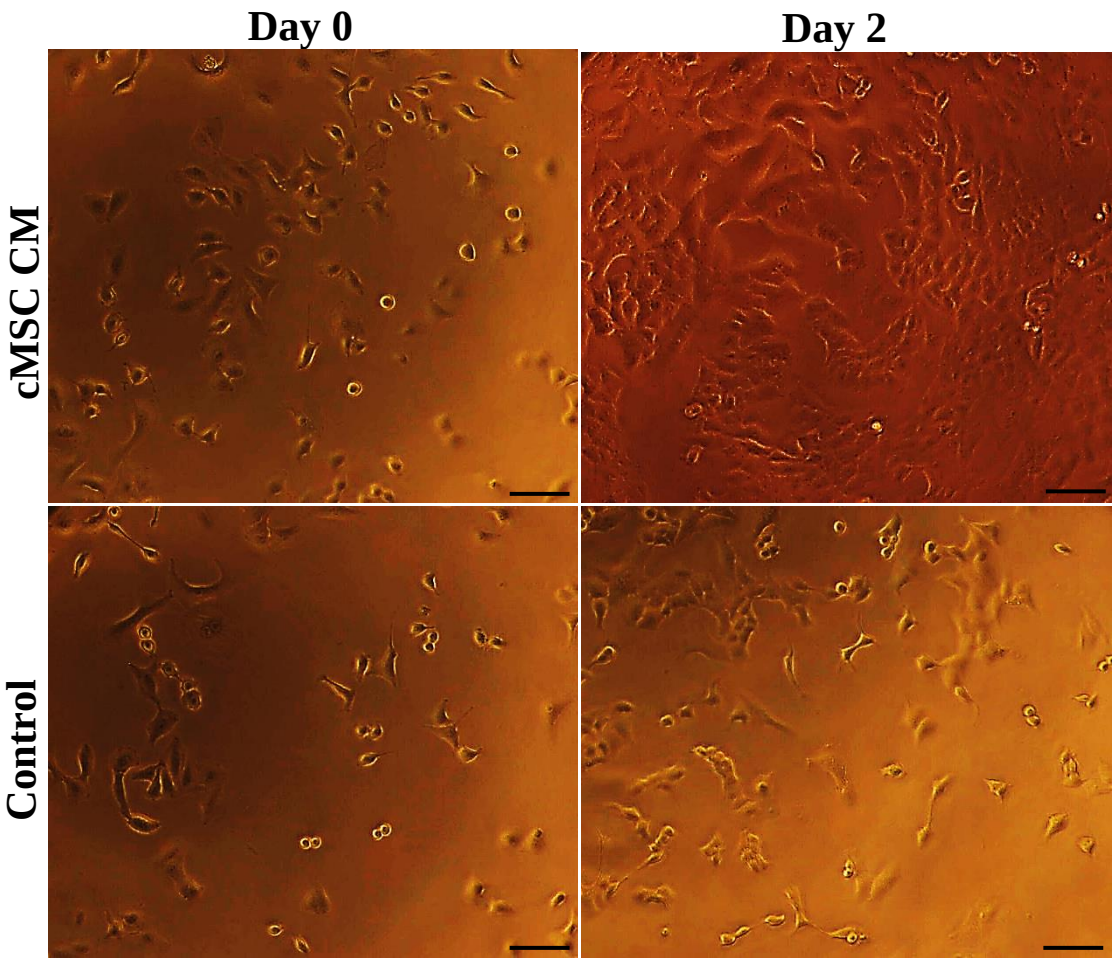

Figure 3:13 cMSC CM promoted EA.hy926 endothelial cell proliferation in 96 well plates.

Representative images are shown of EA.hy926 cells cultured in cMSC CM or serum-free control medium. As shown, there was an apparent increase in the number of EA.hy926 cells present in cMSC CM versus control medium at 2 days of culture. Scale bars = 100µm. Original magnification X10. This analysis was performed on cMSCs from 3 separate donors.

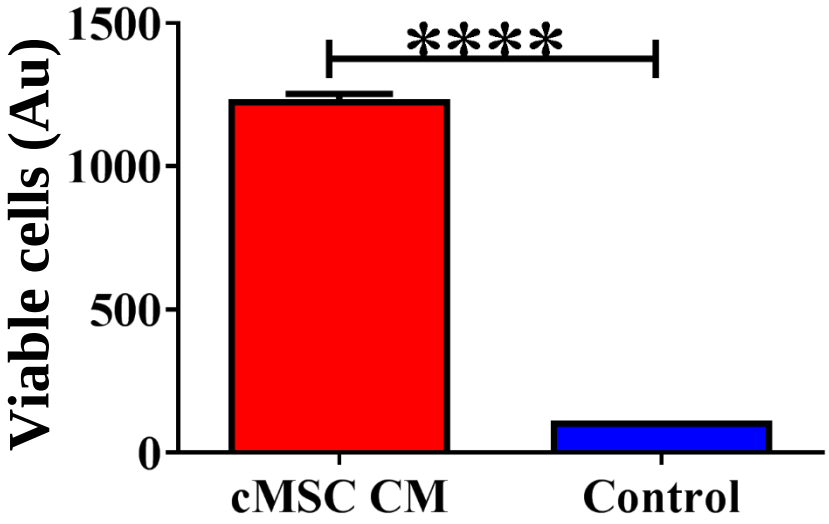

Figure 3:14 The MTT assay confirmed that culturing EA.hy926 endothelial cells in cMSC CM versus control medium significantly increased the number of viable EA.hy926 cells present.

MTT assays were performed to assess viable cell numbers. The results showed a significant increase in the number of viable EA.hy926 cells in cMSC CM versus control medium at 2 days. Each bar represents mean±SEM from 3 independent experiments, i.e. using cMSC CM from 3 separate dogs of five replicates per each experiment. ****indicates $p \leq 0.0001$. Mann-Whitney U test used to determine the significant differences.

3.4.2 The effects of cMSC CM on EA.hy926 endothelial tubule formation

Angiogenesis is a normal and vital process in growth and development, as well as in wound healing. When a new tissue is formed, it is vital that it has blood supply for its growth and sustenance. For this, the formation of blood vessels or angiogenesis is important. The effect of cMSC CM was examined further using an *in vitro* assay for endothelial tubule formation. EA.hy926 endothelial cells were cultured on three-dimensional Matrigel (with reduced growth factors) in cMSC CM or serum-free control medium. As shown in Figure 3.15, culturing EA.hy926 cells in cMSC CM induced the formation of tubule-like structures, with more of these structures present in the cMSC CM compared with control medium. After one day of treatment with cMSC CM or serum-free control medium, phase contrast images were captured and analysed using the Cell IQ cell imaging platform and software. As shown in Figure 3.16, there were significant increases in both the total tubule length per image (p= 0.0082) and the number of tubule branch points per image (p= 0.0307) in cMSC CM versus control medium.

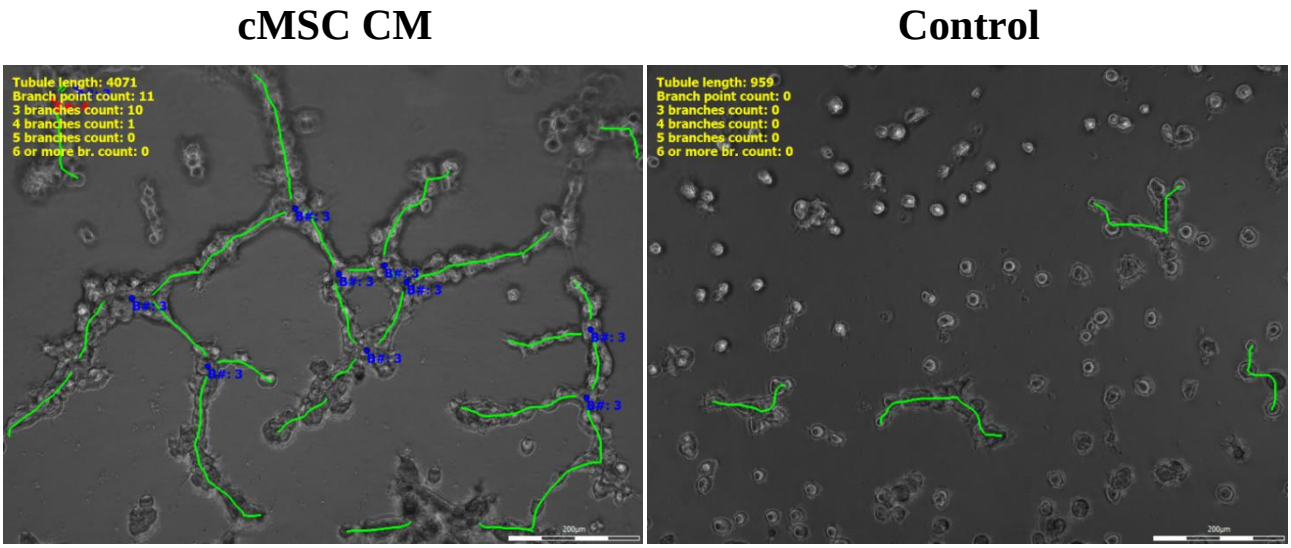

Figure 3:15 The effects of cMSC CM on EA.hy926 endothelial cells cultured on Matrigel.

Representative images are shown of EA.hy926 endothelial cells cultured on Matrigel in the presence of cMSC CM or serum-free control medium. These images were subsequently analysed using the Cell IQ imaging software to determine the length (indicated by green lines) and the number of branch points (indicated by blue dots) seen in endothelial tubule-like structures. Scale bars = 200µm. This analysis was performed on cMSCs from 3 separate donors.

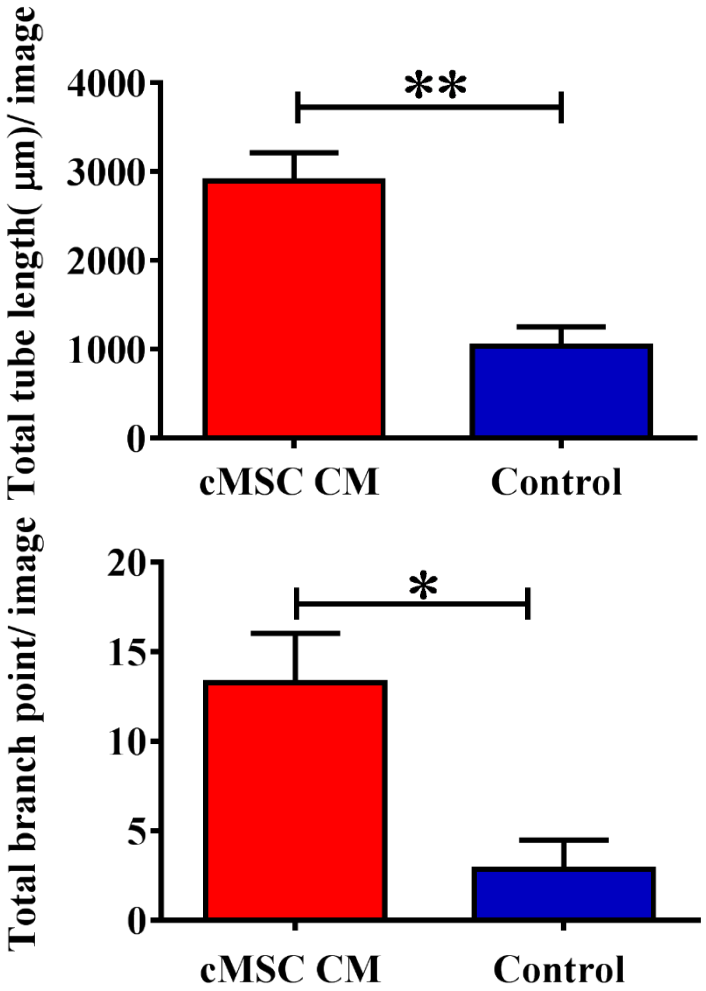

Figure 3:16 cMSC CM significantly increased EA.hy926 endothelial tubule formation.

Image analysis of the collected digitised images (see Figure 3.15) was used to measure both the total length of tubules formed (per image) and the number of endothelial tubule branch points (per image). As shown, there were significant increases in both of these parameters when EA.hy926 cells were cultured on Matrigel for 2 days in cMSC CM versus control medium. Each bar represents the mean±SEM of 3 independent experiments, i.e. using cMSC CM from 3 separate dogs. Top panel: **indicates $p \leq 0.01$. Bottom panel: *indicates $p \leq 0.05$. Unpaired t-test with Welch's correction used to determine the significant differences.

3.5 Discussion

MSCs are traditionally characterised by their capacity for self-renewal and multipotent potential to differentiate into three lineages: adipocytes, osteoblasts and chondrocytes (Caplan, 1991). The rare population of MSCs established from bone marrow (BM) by their preferential adhesion to tissue culture plastic constitute only 0.001% -0.01% of the total nucleated cells in the bone marrow (Friedenstein et al., 1970). Adipose tissue (AT), like BM, is derived from mesenchyme and has supportive stroma that is easily isolated (Zuk et al., 2002). Throughout the last decade, AT MSCs have been achieving mounting attention in regenerative medicine (Zuk et al., 2001, Hong et al., 2010). AT MSCs have similar characteristics to BM MSCs, which are the classical cells source for tissue regeneration, but AT MSCs may have advantages since they are more genetically stable in long-term culture than BM MSC (Fernyhough et al., 2008, Liu et al., 2011).

The ISCT has proposed minimal criteria to define MSCs. These are adherence to plastic, specific surface antigen (Ag) expression for example CD73, CD90 and CD105, and low or no expression of CD34, CD45, CD11b, CD14, CD19, CD79a and HLA-DR., multipotent differentiation potential into the three mesenchymal lineage cell types of adipocytes, osteoblasts and chondrocytes, at least *in vitro* (Dominici et al., 2006). The immunophenotyping of the canine culture expanded and plastic adherent cells seen in this study was supportive of these cells being characterised as MSCs. They were positive for certain surface antigen markers specific for CD44 and CD90. Also, these cells showed negativity for the haematopoietic CD markers CD34 and CD45. The study has only examined these four canine specific CD markers as they were commercially available. However, this study showed that cMSCs poorly differentiate into adipocytes, this might be as a result of using an established protocol which was suitable for hMSCs, but might not be suitable for cMSCs. Recently, cell therapy has been considered as an efficient method to repair injuries such as SCI (Quertainmont et al., 2012). Different studies suggested that cell replacement is not the sole way for transplanted stem cells to boost tissue repair *in vivo* (Madrigal et al., 2014).

It is, in fact, becoming increasingly accepted that the mechanism of the therapeutic effect of MSC transplants in particular could be related to the ability of these cells to secrete a varied array of factors, including growth factors, cytokines, chemokines, metabolites and bioactive lipids, that have paracrine activity (Pluchino et al., 2005, Caplan and Correa, 2011, Paul and Anisimov, 2013). Moreover, several recent studies have suggested that the secretomes of AT MSCs can have a stimulatory effect on wound healing (Walter et al., 2010, Lopatina et al., 2011, Zhao et al., 2013a).

Having established that canine MSCs could be culture expanded from adipose tissue, this study aimed to examine the potential neurotrophic effect and angiogenic effect of canine AT MSCs secreted factors in cMSC CM. The purposes of this study were first to determine the effects of cMSC CM on neurite growth and cell survival using the SHSY-5Y neuroblastoma cell line. Secondly, to identify effects of cMSC CM on endothelial cell migration, proliferation and tubule formation using the EA.hy926 endothelial cell line. The Cell IQ live cell image capture platform and analysis software was used for these studies, as has been performed previously (Pandya et al., 2006, Ucuzian and Greisler, 2007, Bokara et al., 2016), along beta-III tubulin immunopositivity as a marker of neuronal differentiation (Brohlin et al., 2012) and MTT assays for viable cell numbers (Morgan, 1998). The data obtained by this study showed that cMSC CM significantly increased SH-SY5Y neurite outgrowth, proliferation and differentiation when these cells were cultured in cMSC CM generated under serum-free conditions versus serum-free control medium. These findings support the hypothesis raised by this study, i.e., that the cMSCs secretomes are neurotrophic. Similarly, Neuhuber et al., 2005 in their study claimed that MSCs secreted factors which mediate the axonal outgrowth and enhance the recovery after SCI (Neuhuber et al., 2005). Wright et al., 2014 presented in their MSCs as a suitable candidate and an option of treatment for chronic SCI as they claimed that MSCs encourage the neurite outgrowth overcoming the inhibitory factors which are common in the chronic lesion (Wright et al., 2014).

Moreover, Pires et al. (2014), in their study, showed the secretomes of both BMSCs and Warton jelly-derived MSCs was capable of sustaining SH-SY5Y cell survival throughout their differentiation into a neuronal phenotype. Such finding can support the evidence on the capacity of AT MSCs to secrete neuroprotective and neurotrophic growth factors (Pires et al., 2014).

When the spinal cord is injured, the local blood vascular supply also will be ruptured, and the primary injury mechanism leads further to haemorrhage at the site of injury. This disturbance in the vasculature of the spinal cord causes necrotic damage to the endothelial cells, and subsequently, there is a decrease in blood vessel density (Ng et al., 2011). This decreased vascularization may be considered detrimental to SCI recovery, as several studies have suggested that functional improvement after SCI might be related to increases in blood vessel density (Glaser et al., 2006, Kaneko et al., 2006, Rauch et al., 2009). Hence, this study also evaluated whether cMSC CM promote endothelial cell migration and blood vessel formation. A handful of studies has confirmed that AT MSC CM from other species promotes wound healing and formation of new blood vessels (Estrada et al., 2009, Ranganath et al., 2012). Also, *in vitro* studies demonstrated that MSCs from a variety of sources could secrete angiogenic, anti-apoptotic and mitogenic factors for endothelial cells such as VEGF, HGF, angiopoietin-1, adrenomedullin and IGF-1 (Kinnaird et al., 2004, Schinkothe et al., 2008). In particular, this study showed the effect of cMSC CM on the proliferation, migration, and tube formation of EA.hy926 endothelial cells. The results showed that cMSC CM significantly increased the closure rate of scratch wounds compared to non-conditioned control medium. Furthermore, detailed live cell image analysis demonstrated that increased EA.hy926 endothelial cell proliferation and cell migration contributed to the wound closure process. The data also showed that cMSC CM induced the formation of endothelial tube-like capillaries in a Matrigel assay. These findings are supportive of the conclusion that cMSCs are also angiogenic.

In summary, this study has used established *in vitro* models to examine the paracrine activity of cMSCs. It demonstrated that cMSC CM was both neurotrophic and angiogenic. Further studies are required to identify mechanisms of action, although a significant number of studies have already

shown that MSCs from a variety of different sources and across species secrete neurotrophic and angiogenic factors (Timmers et al., 2011, Cantinieaux et al., 2013, Sun et al., 2013, Zhang et al., 2013b). Also, it would also be important to confirm that the canine MSCs exert similar trophic effects on canine neurones and canine endothelial cells, especially if cMSCs were to be used clinically. The stimulatory activities reported here support the application of cMSCs as a therapeutic option in veterinary regenerative medicine, e.g. to treat SCI. Furthermore, as discussed previously, the investigation of cMSC CM on these cell models and in the treatment of SCI in dogs could help to develop cell-based regenerative strategies for the treatment of humans. Since many aspects of canine diseases and injury are functionally and structurally similar to those described in humans (Starkey et al., 2005). A second important consideration, therefore, in this translational pathway, is to examine how the paracrine activity of canine MSC and human MSC compare, which is the focus of the next research chapter.

Chapter 4: An *in vitro* comparison of the neurogenic and angiogenic paracrine activities of human versus canine MSCs

4.1 Background and aims

SCI can be a devastating condition in humans and other species since it causes direct damage to the neuronal tissue accompanied by the loss of motor and sensory function. Current treatments involve surgery to decompress and stabilise the spinal cord, treatments that avoid secondary complications and that may promote rehabilitation (Tator, 2006). However, functional neurological recovery after serious injury, i.e. injury involving chronic and complete loss of motor and sensory function, is still rare and effective treatment has not yet emerged. On the other hand, recent evidence, based on studies focused on stem cells as a therapy for SCI, have shown some promising results. For example, experimental and clinical studies demonstrated the possible use of ESC-derived oligodendrocyte precursor cells (Keirstead et al., 2005), neural stem/progenitor cells (NSPCs) (Tsuji et al., 2011), iPSCs (Oh et al., 2015, Salewski et al., 2015)or MSCs (Matos et al., 2016, Rathinasabapathy et al., 2016) as a potential cell transplantation therapy for SCI.

However, MSCs may be preferable over other stem cells for many strategies promoting tissue repair for a variety of reasons. First, there is less concern about the ethical issues of using MSCs in comparison with ESCs. Second, studies have suggested that MSCs are suitable for allogenic transplantation procedures since they are immuno-privileged, which make the risks of rejection and complications more unlikely (Gupta et al., 2013, Vega et al., 2015). Third, the possibility of obtaining MSCs in quantity required for clinical application in comparison with many other types of adult stem cells, e.g. neural stem cells or olfactory cells, make them preferable (Le Blanc and Pittenger, 2005, Morte et al., 2013). Fourth, MSCs do not carry the same risk of forming teratomas compared to ES cells (Tipnis et al., 2010, López-Iglesias et al., 2011, Rong et al., 2012). As stem cells emerge as potential cell-based therapies, pre-clinical assessment of their regenerative activity is required. Therefore, there is a clear awareness of the need for animal models that fully reflect the target diseases to be investigated by using stem cells (Plews et al., 2012). Different studies reported that the application of mouse models in regenerative medicine has many limitations (Cibelli et al., 2013).

This could be because mice have short lifespans in comparison to humans and also there are significant anatomical and physiological differences between human and mouse (Schneider et al., 2008). In contrast, large animal models more closely resemble important aspects of human anatomy, physiology and pathology than mouse models. In this regard, it may be considered that dogs represent a promising translational model for many human diseases (Qeska et al., 2013, Hicks et al., 2015, Park et al., 2016). Similarly to SCI in human, SCI in dogs may lead to severe neuronal tissue damage resulting in loss of motor and sensory functions (Starkey et al., 2005, McMahill et al., 2015). In addition, a number of studies have tested the safety and occasionally, efficacy of cell transplantation therapies in dogs with SCI, examining the outcome of different transplanted cell types, including autologous canine olfactory cells (Jeffery et al., 2006a, Granger et al., 2012) and canine MSCs (Jung et al., 2009, Sarmento et al., 2014). The mechanisms of action of canine MSCs in the treatment of dogs with SCI are currently unknown. For this reason, the previous chapter examined whether canine MSCs secrete factors that are neurotrophic and angiogenic, using established cell model systems. However, the longer term aim is to evaluate the potential of MSCs to treat humans with SCI, wherein the effects of canine MSCs in dogs with SCI would represent part of the translational pathway from evaluating cell phenotyping and reparative activity *in vitro*, through to clinical treatment. As a step along this pathway, it is worthwhile comparing the neurotrophic and angiogenic effects of canine MSCs with human MSCs. Such knowledge would be invaluable in trying to estimate their potential for regenerative effects when transplanted.

This chapter aims to address and understand the differences in the behaviour of MSCs secretomes from both canine and human donors. Therefore, experiments were performed to investigate the neurotrophic and angiogenic activity for human MSCs in comparison with canine MSCs secretomes, where the cells were isolated and cultured from adipose tissue in both cases and all experimentation was performed independently of that shown in Chapter 2 and Chapter 3. Cell assays were undertaken to examine the effects of MSC CM on SH-SY5Y neuronal cells and EA.hy926 endothelial cells, following the methods established in Chapter 3.

The outcome of these investigations might provide benefits for veterinary and human medicine and also might be helpful to bridge the gap between translational research and human clinical trials.

4.2 Characterisation of hMSCs and cMSCs

4.2.1 Growth characteristic and differentiation capacity of hMSCs and cMSCs

Human and canine MSCs were plastic adherent and displayed a spindle-shaped fibroblast-like morphology (Figure 4.1), matching the criteria for an MSC phenotype established by the ISCT (Dominici et al., 2006). Both hMSCs and cMSC were assessed for their ability to differentiate the following induction in culture into three mesodermal lineages, i.e. to form adipocytes, osteoblasts and chondrocytes. As shown in Figure 4.1, hMSCs and cMSCs demonstrated some differentiation capacity to form adipocytes (indicated by staining intracellular lipid droplets with Oil Red O), osteoblasts (indicated by staining for alkaline phosphatase activity) and chondrocytes (indicated by staining the paraffin sections of chondrogenic 3D cell pellets with toluidine blue for glycosaminoglycan deposition) (Figure 4.1). However, there was less evidence of greater lipid accumulation in the cMSCs compared with hMSCs.

4.2.2 Immunophenotype

According to the ISCT criteria, MSCs should be immunopositive for the cluster of differentiation (CD) markers, CD73, CD90 and CD CD105, and lack immunopositivity for CD11b, CD14, CD19, CD34, CD79α and HLA-DR (Dominici et al., 2006). Some of these markers were included in this study, according to the availability of antibodies recognising the canine antigens, and the CD profiles were assessed using flow cytometry. The results showed that the large majority of cultured hMSCs and cMSCs were immunopositive for CD44 and CD90, but were immunonegative for haematopoietic markers, i.e. CD34 and CD45 (Figure 4.2). For hMSCs 91.83%±3.92% and 97.81%±0.52% of cells were CD44 and CD90 immunopositive, respectively, while only 1.14%±1.08% and 0.06%± 0.02% of cells were CD34 and CD45 immunopositive, respectively (mean±SEM).

Similarly, cMSCs were 90.57%±1.52% immunopositive for CD44 and 99.20%±0.22% immunopositive for CD90, but only 5.79%±5.58% and 0.04%±0.00% of cells were immunopositive for CD34 and CD45, respectively (mean±SEM) (Table 4-1).

In summary, this data demonstrated that the processes of isolating and culturing hMSCs and cMSCs from adipose tissue generated a population of cells that met with the ISCT criteria for being considered MSCs.

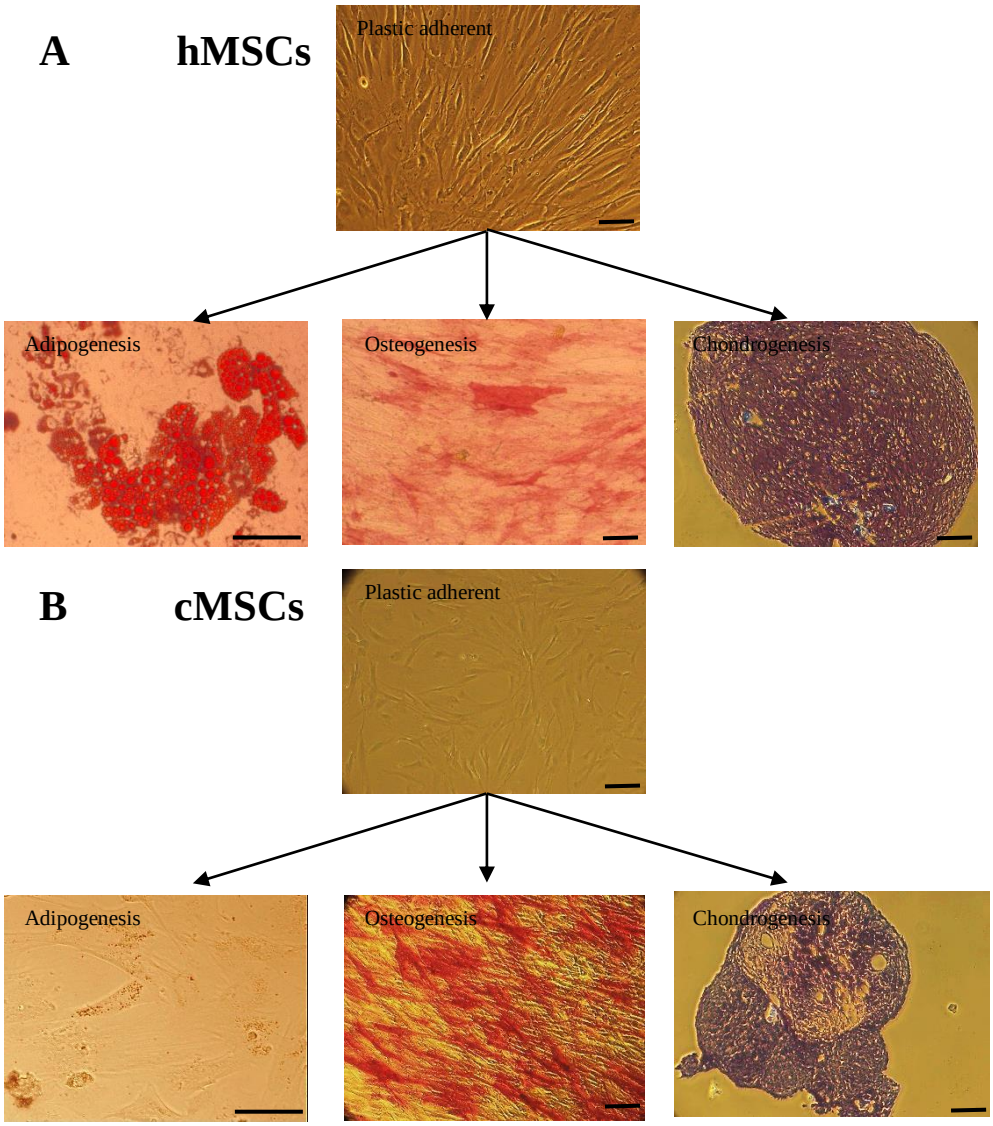

Figure 4:1 The appearance and differentiation potential of hMSCs and cMSCs.

Representative images are shown of hMSCs (top panels A) and cMSCs (bottom panels B). Both cell types were plastic adherent and fibroblastic in appearance under phase contrast microscopy. Furthermore, hMSCs and cMSCs underwent differentiation into the mesodermal lineages, adipocytes, osteoblasts, and chondrocytes. Scale bars = 100µm with original magnification X10 for plastic adherent, osteogenesis, and chondrogenesis images. Scale bar = 50µm with original magnification X40 for adipogenesis image. This analysis was performed on hMSCs and cMSCs from 3 separate donors of human or canine.

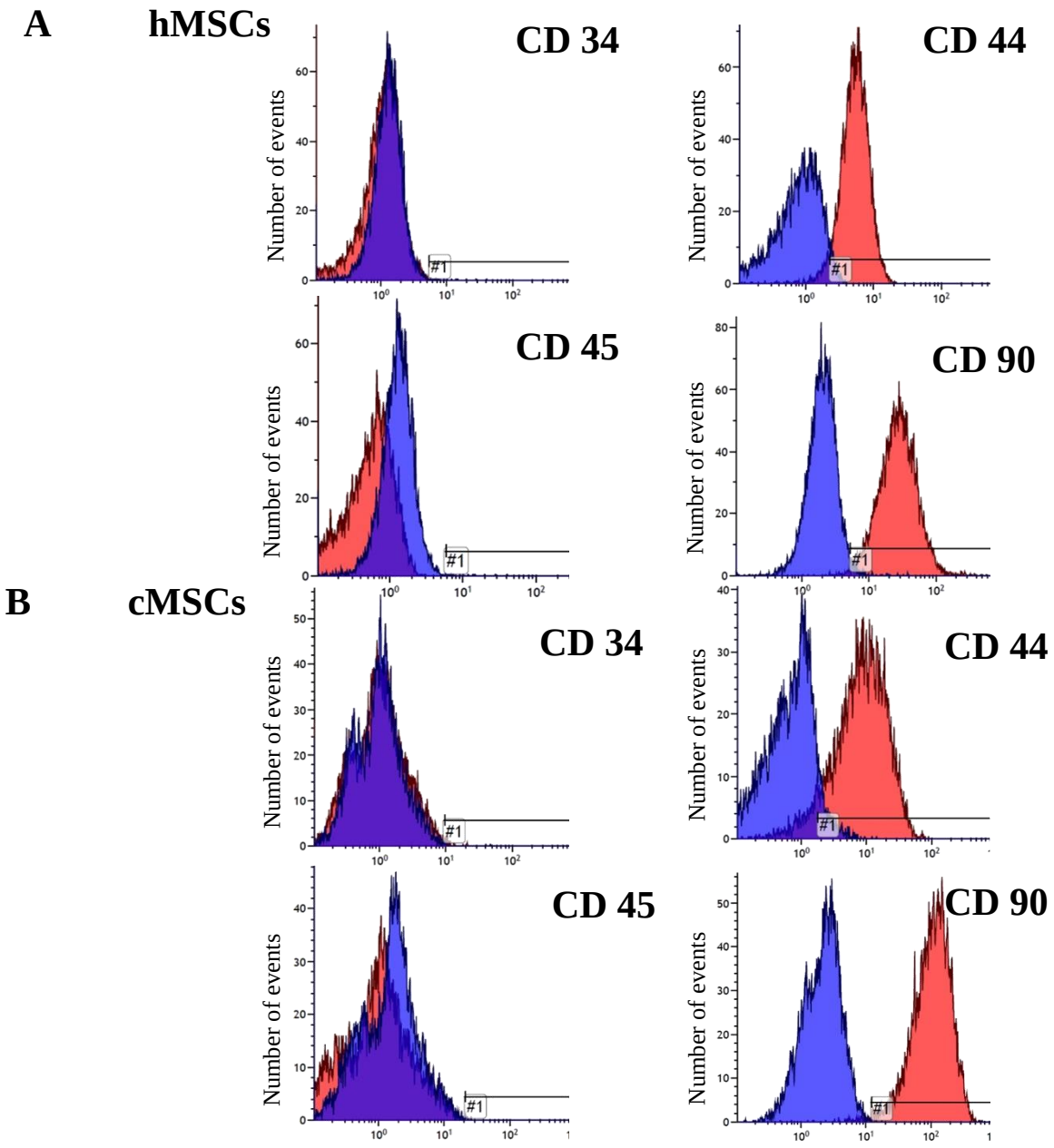

Figure 4:2 Flow cytometry analysis of CD markers phenotypic for MSCs.

Representative histograms are shown of the extent of immunopositivity seen for CD34, CD44, CD45 and CD90 in hMSCs (top panels A) and cMSCs (bottom panels B). As shown, both human and canine MSCs were immunonegative for CD34 and CD45, but they were immunopositive for CD44 and CD90. Immunostaining for each CD marker is shown in red, whilst control staining with irrelevant isotype-matched antibodies (as described in chapter two, section 2.2.1) is shown in blue. This analysis was performed on hMSCs and cMSCs from 3 separate donors.

Percentage expression of CD markers for hMSCs					
Cell type	Patient ID	CD34	CD44	CD 45	CD90
Human MSC	hMSC101	0.04	83.99	0.04	97.54
	hMSC110	3.30	95.72	0.04	97.08
	hMSC123	0.09	95.78	0.10	98.83
Mean		1.14	91.83	0.06	97.81
SEM		1.08	3.92	0.02	0.52

Percentage expression of CD markers of cMSCs					
Cell type	Patient ID	CD34	CD44	CD45	CD90
Canine MSC	cMSC 018	0.03	92.57	0.04	98.86
	cMSC 020	16.97	87.59	0.04	99.62
	cMSC 028	0.39	91.54	0.04	99.13
mean		5.79	90.57	0.04	99.20
SEM		5.58	1.52	0	0.22

Table 5: The proportions of hMSCs and cMSCs that were immunopositive for CD markers. The percentages of hMSCs (top panel) and cMSCs (bottom panel) for each of the CD markers. As shown, this analysis was performed on hMSCs and cMSCs from 3 different donors.

4.3 A comparison of the neurotrophic effects of hMSCs and cMSCs conditioned medium

4.3.1 Human and canine MSC CM promoted neurite outgrowth and neuronal cell proliferation of SH-SY5Y cells

The effects of hMSC CM and cMSC CM on SH-SY5Y neuroblastoma cells were examined using the same methodology previously described in Chapter 2 (Section 2.4.1) and Chapter 3. In brief, the SH-SY5Y cells were seeded in 24 well plates and incubated for 24 hours to allow for cells to adhere. Following medium change and treatment with either hMSC CM, cMSC CM or serum-free medium (in control cultures), the plates were incubated in the Cell IQ live cell imaging platform for 3 days for digitised image collection (Figure 4.3). At the end of incubation period, these images were analysed using the Cell IQ analyser software.

The data obtained showed that both human and canine MSC CM have a marked neurotrophic effect, enhancing neuronal cell growth and neurite outgrowth from SH-SY5Y cells compared to control cultures. The results showed that human and canine MSC CM significantly increased the number of SH-SY5Y cells present after 3 days in culture compared with control medium (p= 0.0288 for hMSC CM and p= 0.0168 for cMSC CM). However, there was no significant difference between the effects of human and canine MSC CM in this regard (p= 0.8865). Also, both human and canine MSC CM significantly increased neurite outgrowth of SH-SY5Y cells compared with control medium (p= 0.0042 for hMSC CM and p= 0.0098 for cMSC CM), but there was no significant difference between the effects of human and canine MSC CM (p= 0.6819) (Figure 4.4).

Therefore, hMSC and cMSC were shown to have significant neurotrophic activity, which was similar.

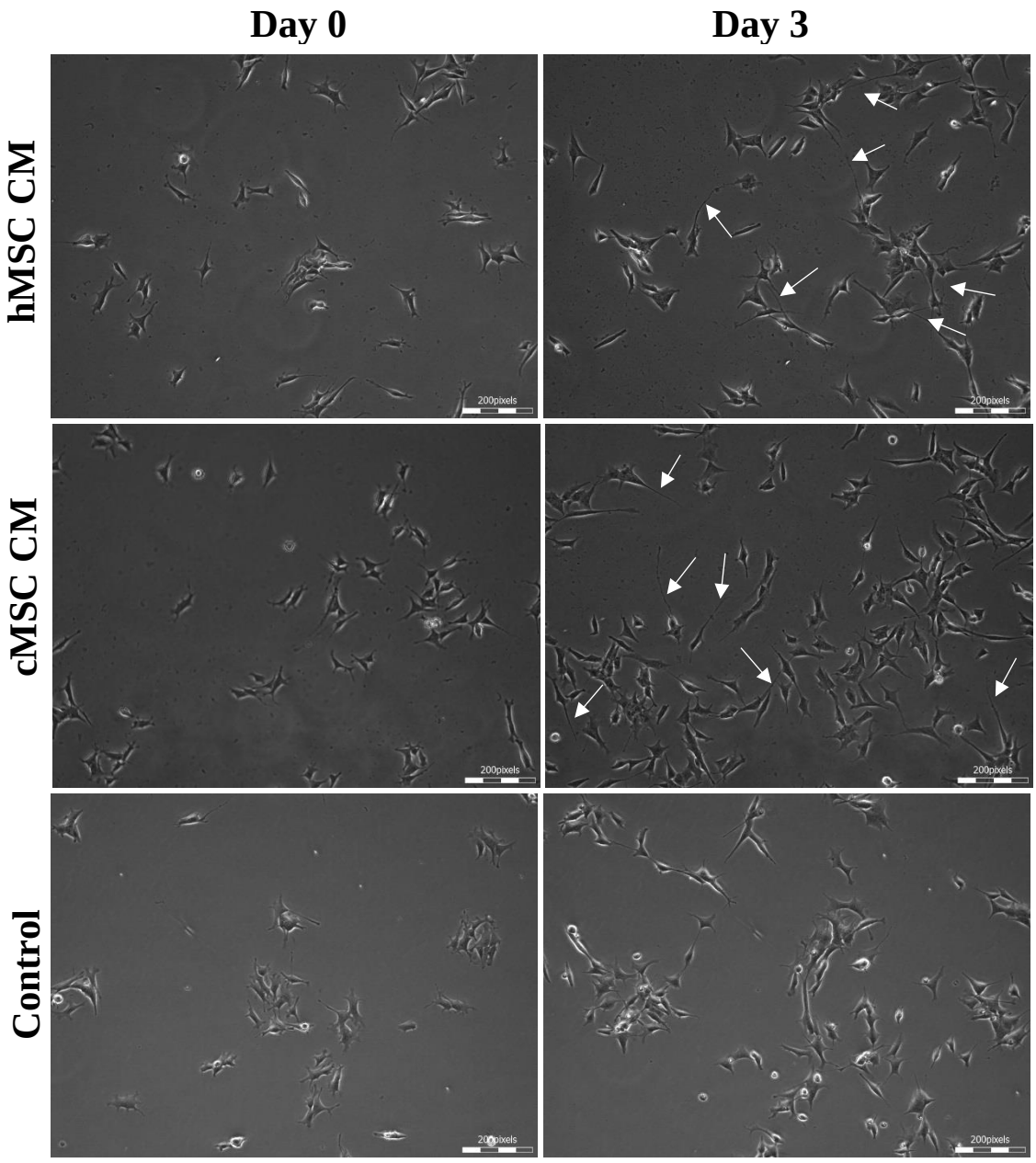

Figure 4:3 Human MSC CM and canine MSC CM increased neuronal cell numbers and neurite outgrowth in SH-SY5Y neuroblastoma cells.

Representative digitised images captured by the Cell IQ live cell imaging platform have been shown. As shown, hMSC CM and cMSC CM increased neurite outgrowth (arrows) and neuronal cell proliferation compared with control medium. Scale bar = 200µm. These images were collected using hMSC and cMSC CM from 3 separate donors.

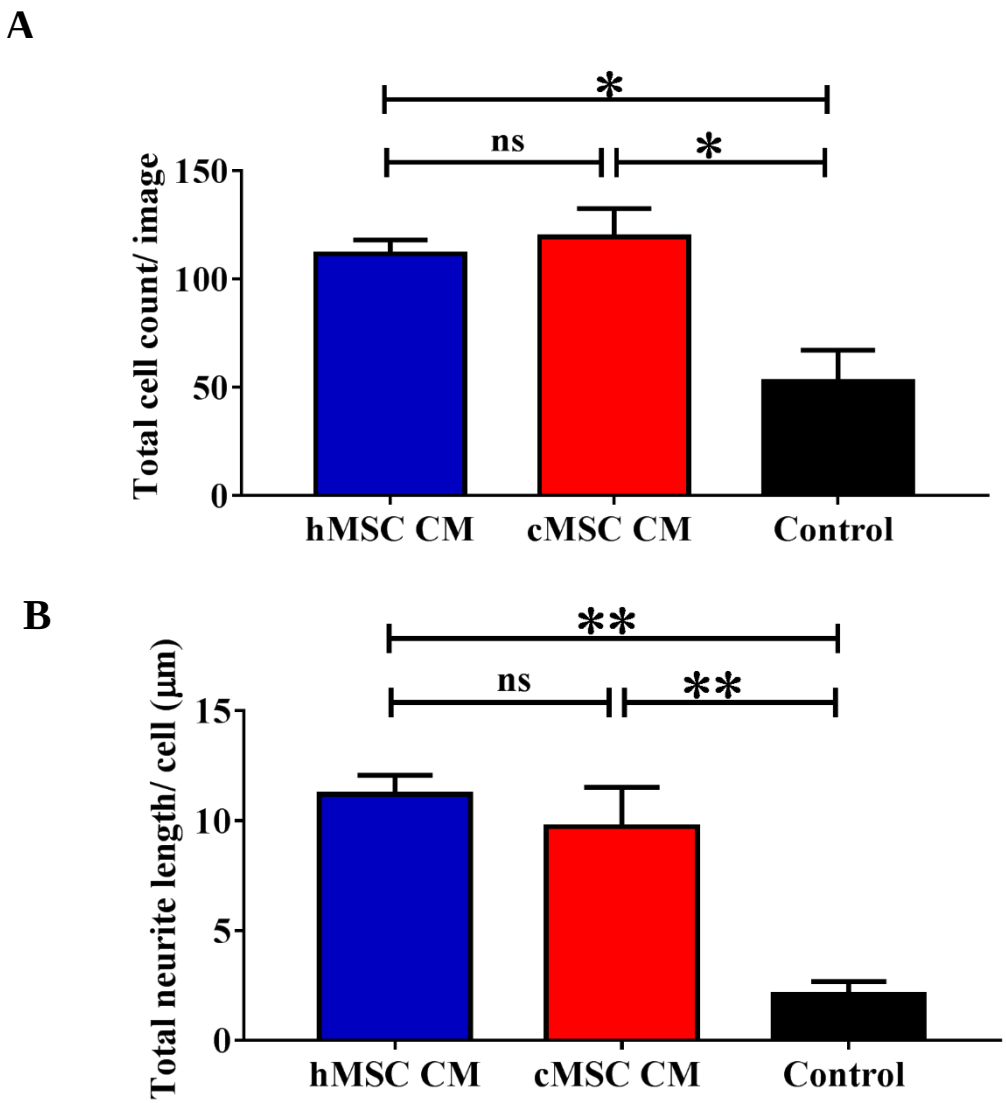

Figure 4:4 Human MSC CM and canine MSC CM significantly increased SH-SY5Y cell numbers and neurite outgrowth.

The results showed that hMSC CM and cMSC CM had a similar effect of increasing cell proliferation and neurite outgrowth of SH-SY5Y cells. Each bar represents the mean±SEM from 3 independent experiments (i.e. 3 different donors) of 3 replicates per each individual experiment. *indicates $p \leq 0.05$ (top panel A); and **indicates $p \leq 0.01$ (bottom panel B). One way- ANOVA with Tukey's multiple comparisons test used to determine the significant differences.

4.3.2 hMSC CM and cMSC CM enhanced immunopositivity for the mature neuronal marker βIII-tubulin in SH-SY5Y neuronal cells

βIII-tubulin is a marker of neuronal differentiation (Dwane et al., 2013), which was detected by immunocytochemistry. This analysis demonstrated that βIII-tubulin appeared to be present to a greater extent in SH-SY5Y cells when they were treated with hMSC CM and cMSC CM compared with control medium (Figure 4.5). The proportions of βIII-tubulin immunopositive SH-SY5Y cells were significantly increased versus controls when cultured for three days in hMSC CM (p= 0.0018) and cMSC CM (p= 0.0013). There was no significant difference in the proportions of βIII-tubulin immunopositive SH-SY5Y cells present in either hMSC CM versus cMSC CM (p= 0.4674) (Figure 4.6).

Therefore, hMSC and cMSC secreted factors that appeared to induce neuronal differentiation to a similar extent.

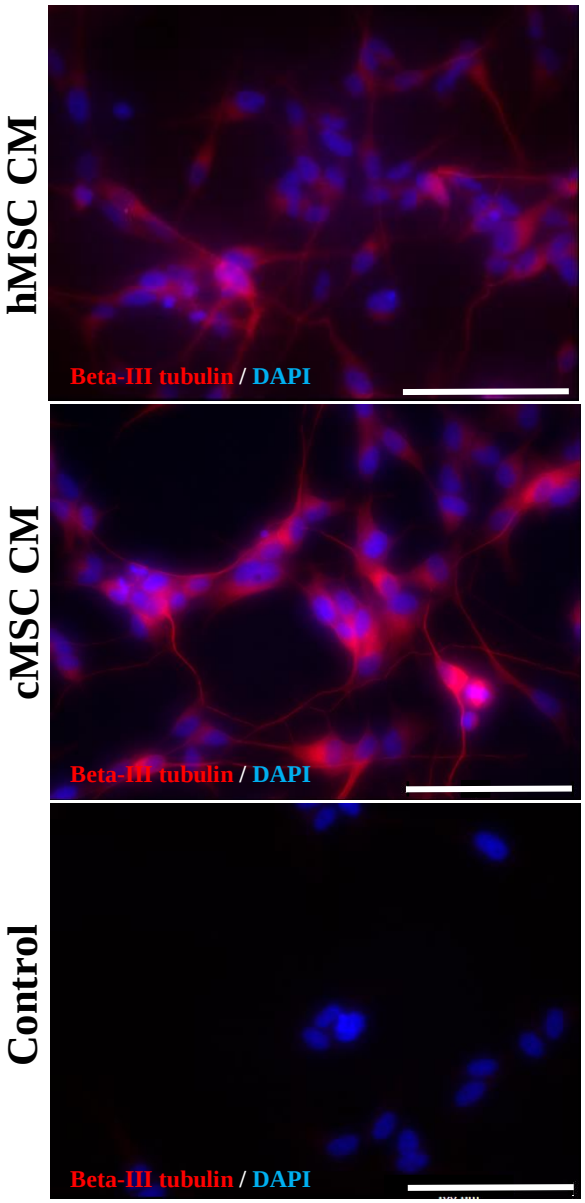

Figure 4:5 The effects of hMSC CM and cMSC CM on beta-III tubulin immunopositivity in SH-SY5Y cells.

Representative images are shown of SH-SY5Y cells treated with hMSC CM or cMSC CM or control medium for 3 days and immunostained for beta-III tubulin. As shown there was an apparent increase in immunopositivity when cultured in the presence of MSC CM. Scale bar = 100µm. Original magnification X40. These images were collected using hMSC CM and cMSC CM from 3 separate donors.

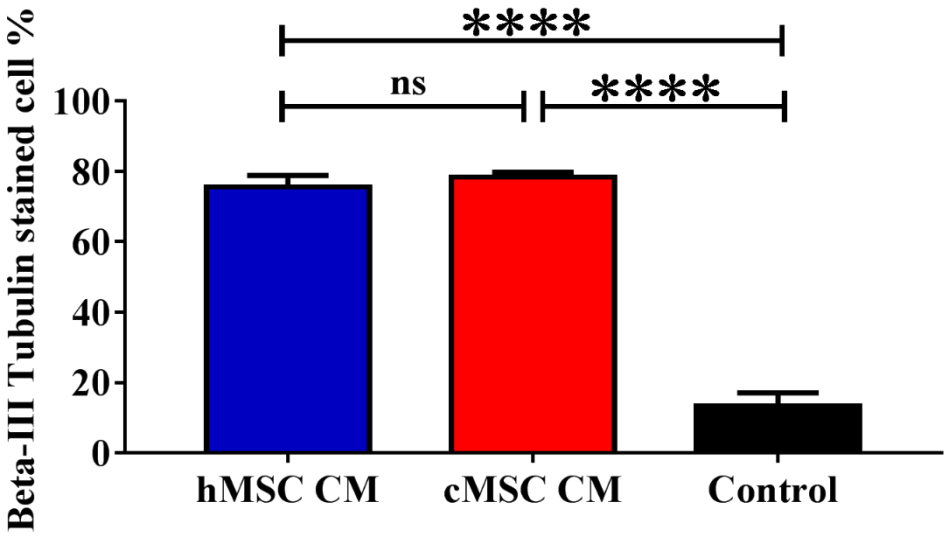

Figure 4:6 Human MSC CM and canine MSC CM significantly increased the proportion of SH-SY5Y cells that were beta-III immunopositive.

The proportion of beta-III immunopositive SH-SY5Y cells present was determined by scoring a minimum of 500 cells from digitised images, each collected from 5 randomly selected fields in each of three wells per medium tested. Each bar represents the mean±SEM from 3 independent experiments, i.e. testing hMSC CM and cMSC CM from 3 separate donors. ****indicates $p \leq 0.0001$. One way- ANOVA with Tukey's multiple comparisons test used to determine the significant differences.

4.3.3 Assessment of SH-SY5Y viable cell numbers using the MTT assay

The MTT assay was used to further examine the number of viable SH-SY5Y cells present in cMSC CM versus control medium in a 96 well plate format. As shown in Figure 4.7, there appeared to be more viable SH-SY5Y cells present after culturing in hMSC CM or cMSC CM for 3 days compared with control medium. These cultures were subsequently processed to assess viable cell number using the MTT assay, which measures non-specific esterase activity in viable cells (Denizot and Lang, 1986, Hansen et al., 1989). As shown in Figure 4.8, there was a significantly greater level of absorbance, indicative of increased numbers of viable SH-SY5Y cells in hMSC CM (p= 0.0016) and cMSC CM (p=0.0060) versus control medium whereas, the absorbances showed no significant difference between hMSC CM and cMSC CM (p= 0.3548).

Therefore, the data suggested that hMSC and cMSC secreted factors appeared to support neuronal growth and survival to a similar extent.

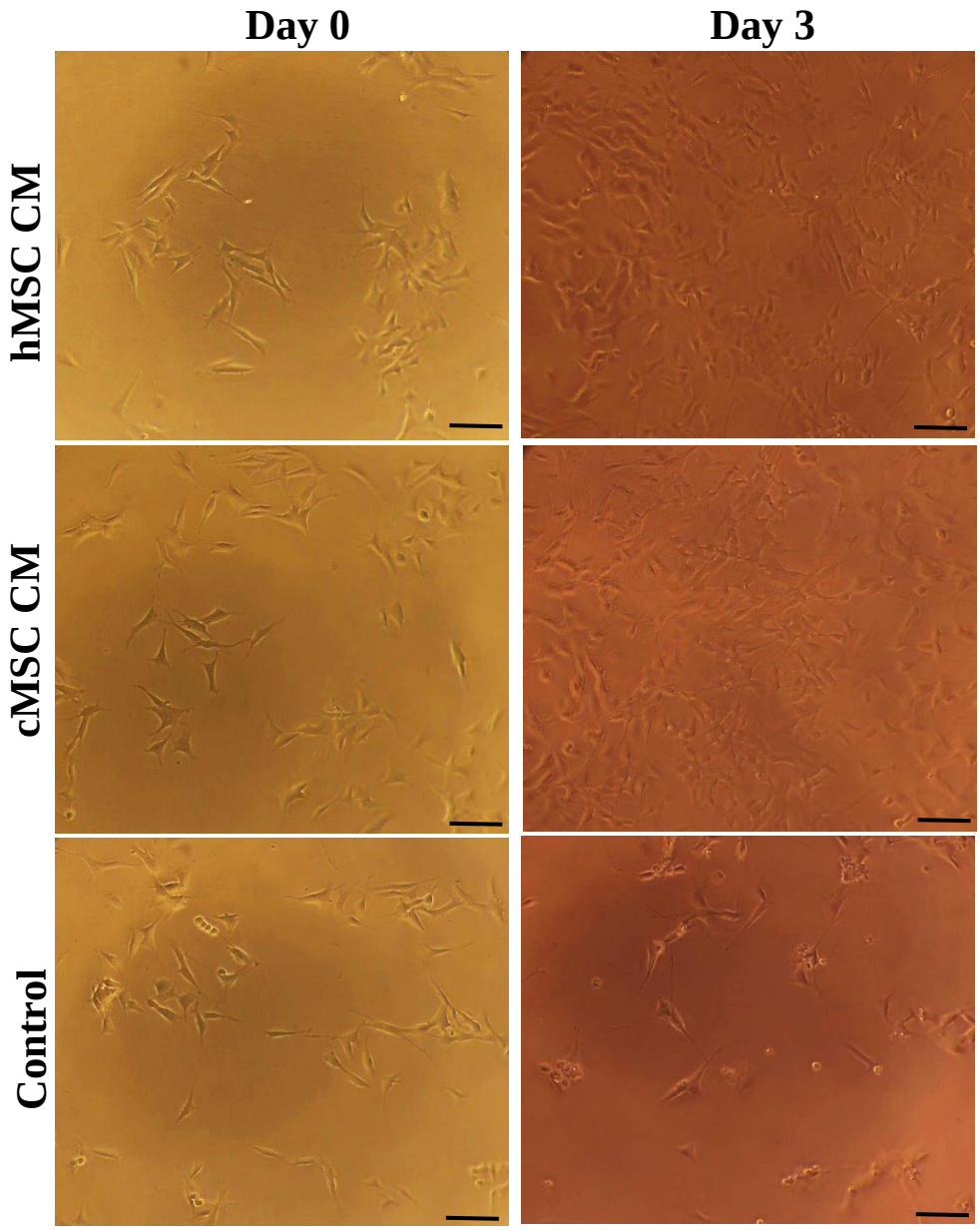

Figure 4:7 The effects of hMSC CM and cMSC CM on SH-SY5Y neuronal cell proliferation. Representative images demonstrate the relative increase in SH-SY5Y cell numbers when cultured for 3 days in hMSC CM or cMSC CM versus control medium. Scale bar = 100µm. Original magnification X10. These images were collected from hMSC CM and hMSC CM from 3 separate donors.

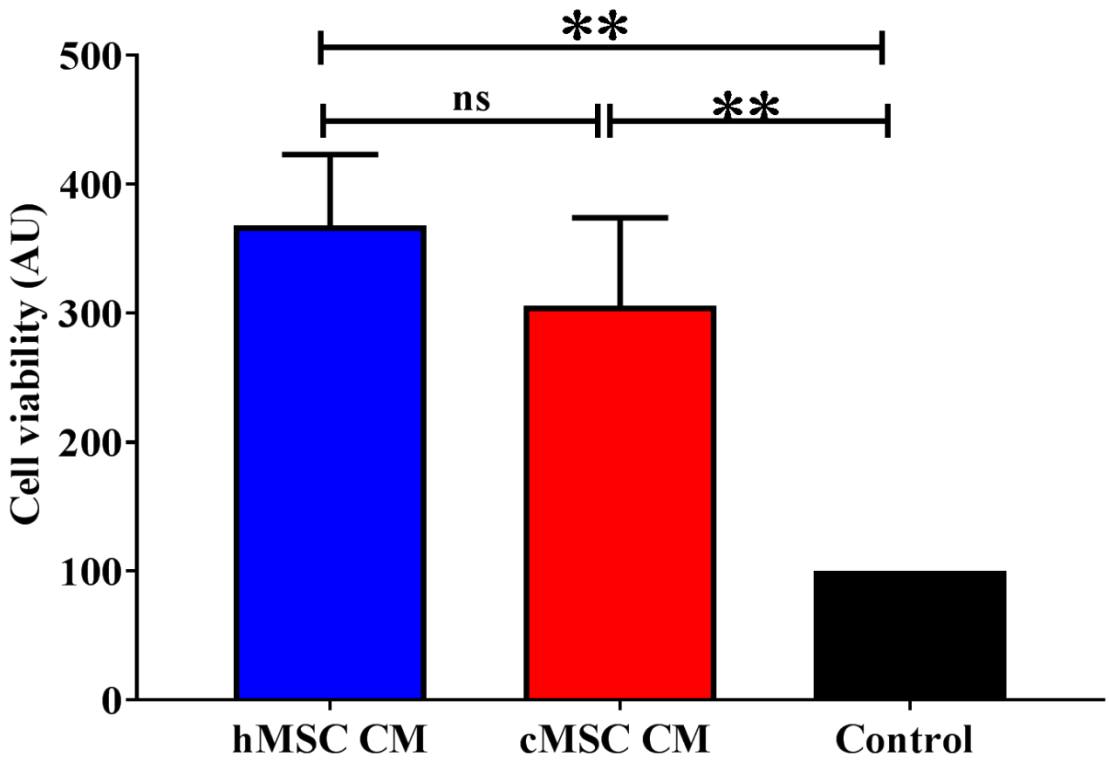

Figure 4:8 The MTT assay confirmed that culturing SH-SY5Y neuronal cells in hMSC CM or cMSC CM versus control medium significantly increased the number of viable SH-SY5Y cells present.

MTT assays were performed to assess viable cell numbers. The results showed a significant increase in the number of viable SH-SY5Y cells in hMSC CM or cMSC CM versus control medium at 3 days. Whereas, hMSC CM or cMSC CM had a similar effect. Each bar represents the mean±SEM from 3 independent experiments, i.e. testing hMSC CM and cMSC CM from 3 separate donors. **indicates $p \leq 0.01$. One way- ANOVA with Tukey's multiple comparisons test was used to determine the significant differences.

4.4 The comparative of effects of hMSC CM and cMSC CM on EA.Hy926 endothelial cells.

4.4.1 Human and canine MSCs CM increased the migration and proliferation of EA.hy926 endothelial cells

The angiogenic effects of human and canine MSC CM on EA.hy926 endothelial cells were examined by using scratch assays, and live cell image analysis with the Cell IQ imaging platform (Figure 4.9), as described in Chapter 2 (Section. 2.4.3.1) and Chapter 3. The results showed that both human MSC CM (p=0.0001) and canine MSC CM (p= 0.0242) significantly enhanced the rates of scratch wound closure compared to control medium. In contrast, there was no significant difference in the rate of wound closure between the hMSC CM versus cMSC CM (p= 0.1897) (Figure 4.10).

To determine whether MSC CM played a role in stimulating EA.hy926 cell migration versus proliferation to induce wound closure, cells from the sides of wound edges were tracked by using the Cell IQ analyser software. Each scratch wound assay was performed in triplicate in each of the 3 independent experiments and a minimum of 3 cells at the edge of the scratch per replicate scratch were tracked to plot their movement into the scratch wound area every 15 minutes over a 2 days period. This meant a total of 27 cells for each condition (hMSC CM, cMSC CM and control medium) were tracked. The total distance each cell had migrated from day 0 to day 2 was measured and demonstrated that hMSC CM and cMSC CM significantly enhanced the extent to which cells migrated in the wound area compared to control medium (p= 0.0001 in both cases), but that there was no significant difference between the human and canine MSC CM (p= 0.3155) (Figure 4.11).

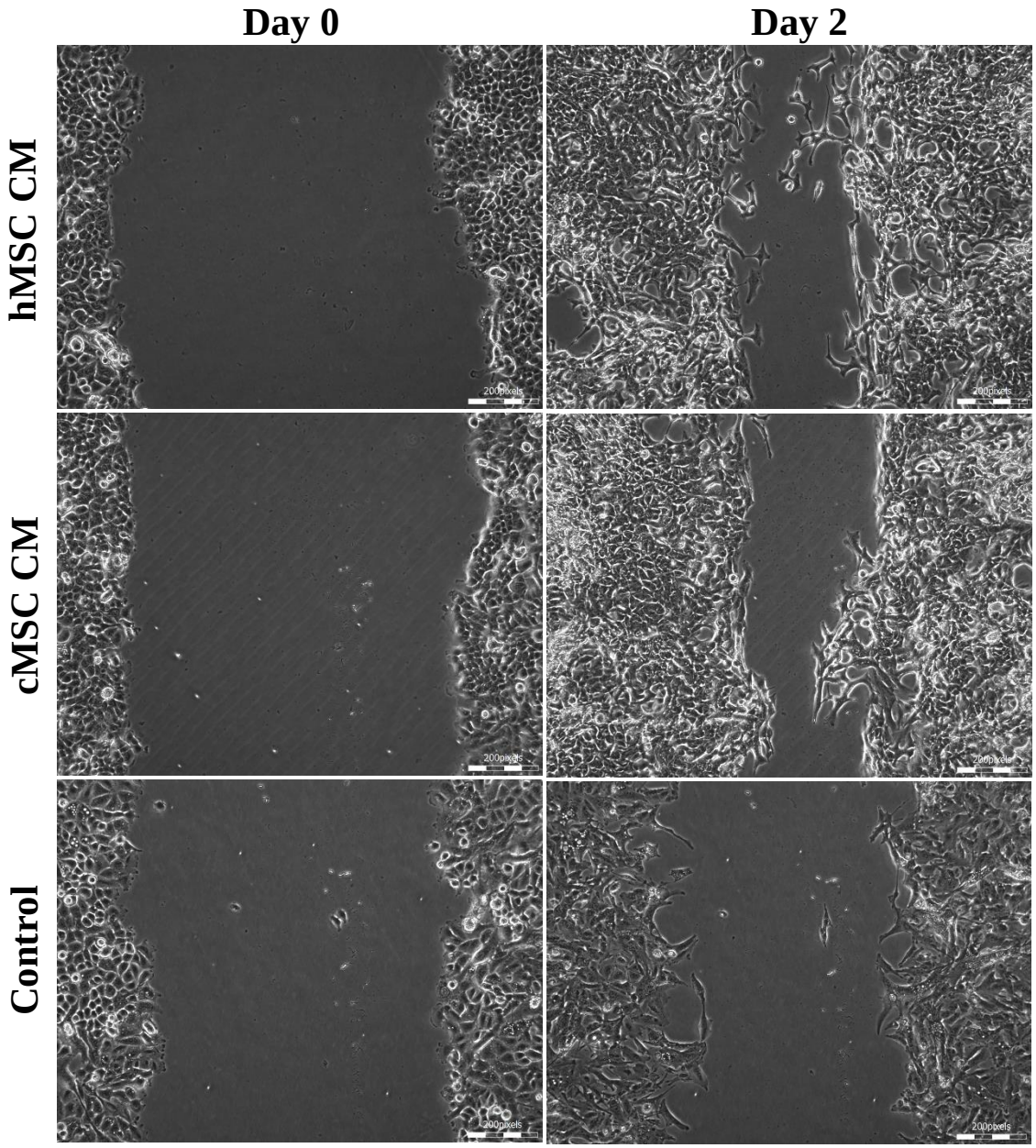

Figure 4:9 The effects of hMSC CM and cMSC CM on EA.hy926 endothelial cells in scratch assays.

Representative images are shown EA.hy926 endothelial cell scratch assays, which were treated with hMSC CM, cMSC CM or serum-free control medium for 2 days after scratching. EA.hy926 cells were seeded into multiple wells of 24 well plates and cultured in a standard culture medium until confluent and then scratched using a yellow pipette tip. After washing with PBS, the cultures were then fed with cMSC CM or serum-free control medium (Control). Scale bars = 200µm. These images were collected using hMSC and cMSC CM from 3 separate donors.

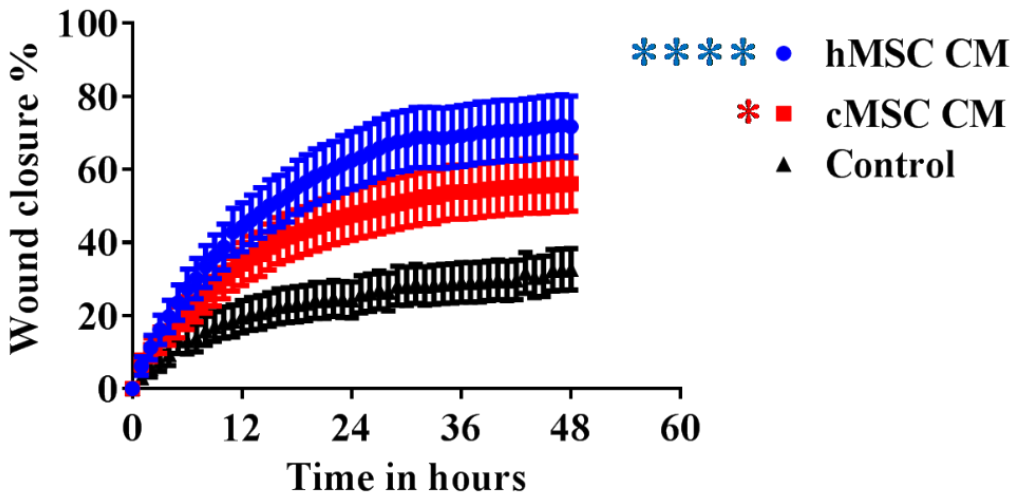

Figure 4:10 Human and canine MSC CM significantly increased the rate of wound closure in EA.hy926 endothelial scratch assays.

The Cell IQ platform was used for live imaging of wound closure in EA.hy926 endothelial cell scratch wound assays in the presence of hMSC CM or cMSC CM versus serum-free control medium. Digitised images were generated over 2 days of incubation and Cell IQ imaging software was used to measure the extent to which the wound had closed (as a proportion of its original scratch area). There was a significant increase in the rate of wound closure in hMSC CM and cMSC CM compared to the control medium, whereas no significant difference between hMSC CM and cMSC CM. Each bar represents mean±SEM of 3 independent experiments, i.e. using hMSC CM and cMSC CM from 3 separate donors. *indicates $p \leq 0.05$, and ****indicates $p \leq 0.0001$.Blue stars represent hMSC CM vs control, and red stars represent cMSC CM vs control. A Two-way ANOVA with Tukey's multiple comparisons tests used to determine the significant differences.

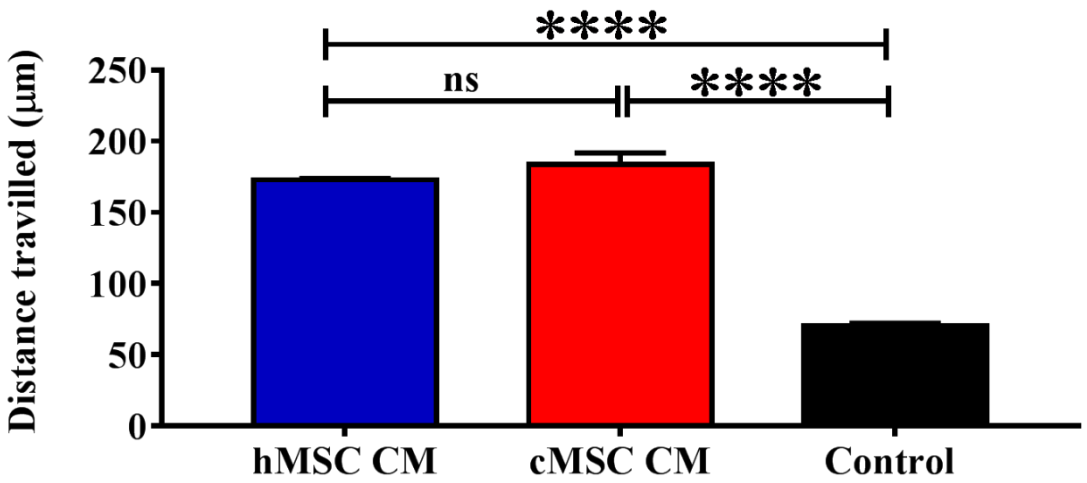

Figure 4:11 Human and canine MSC CM significantly increased EA.hy926 endothelial cell migration.

Image analysis of the collected digitised images was used to measure the distance that EA.hy926 endothelial cells migrated from the edge of the scratch towards the centre of the wound over a period of 2 days in the presence of hMSC CM or cMSC CM versus serum-free control medium. As shown, there was a significant increase in distance travelled in hMSC CM and cMSC CM versus control medium during this time. Each bar represents mean±SEM of 3 independent experiments, i.e. using hMSC CM and cMSC CM from 3 separate donors. ****indicates $p \leq 0.0001$. One way ANOVA with Tukey's multiple comparisons tests used to determine the significant differences.

The numbers of dividing and non-dividing EA.hy926 cells within each of the digitised images collected in each of the scratch wound assays were also identified using live cell image analysis. This demonstrated that hMSC CM and cMSC CM significantly increased the numbers of dividing and non-dividing cells present within the scratch wound assays compared with control medium (p= 0.0001 for dividing cells in both MSC CM, p= 0.0001 for non-dividing cells in hMSC CM; p= 0.0003 for non-dividing cells in cMSC CM) (Figure 4.12). However, there was no significant difference in the effects of hMSC CM versus cMSC CM (dividing cells p= 0.1006; non-dividing cells p= 0.9379). Moreover, the effects of human and canine MSC CM versus control medium on EA.hy926 cell proliferation was further determined by inverted Phase contrast microscopy and by MTT assay to determine the number of viable cells present after treatment in 96 well plates. The results showed that the hMSC CM (p= 0.0035) and cMSC CM (p= 0.0244) significantly increased the number of viable EA.hy926 cells over a 2 day period compared with control medium, but that there was no significant difference between the human and canine MSC CM (p= 0.2276) (Figures 4.13 and 4.14).

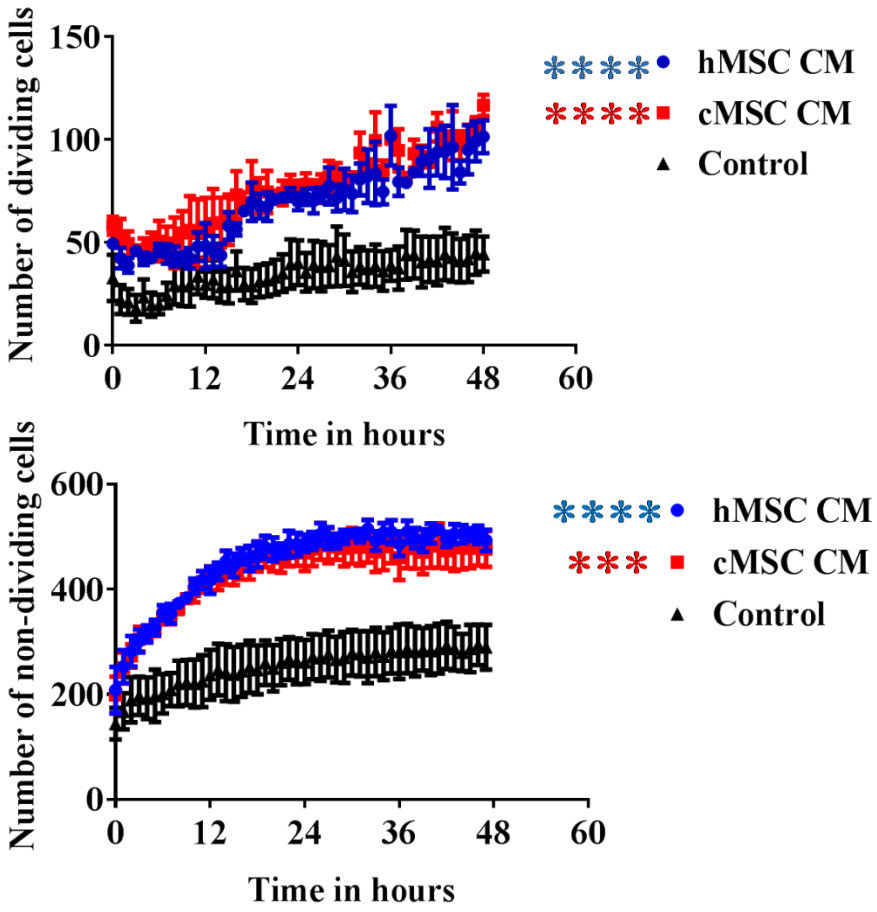

Figure 4:12 Human and canine MSC CM increased the numbers of EA.hy926 endothelial cells in the scratch wound site.

The number of dividing versus non-dividing EA.hy926 endothelial cells present in the whole area of the digitised images collected of each scratch wound assay was determined over a 2 day period using live cell image analysis. As shown, there were marked increases in both dividing and non-dividing cells when cultured in the MSC CM versus control medium. Results have been shown as mean±SEM from 3 independent experiments, i.e. testing MSC CM harvested from 3 donors versus control medium. *** indicates $p \leq 0.001$ and **** indicates $p \leq 0.0001$. Blue stars represent hMSC CM vs control, and red stars represent cMSC CM vs control. Two-way ANOVA with a Tukey's multiple comparisons test used to determine the significant differences.

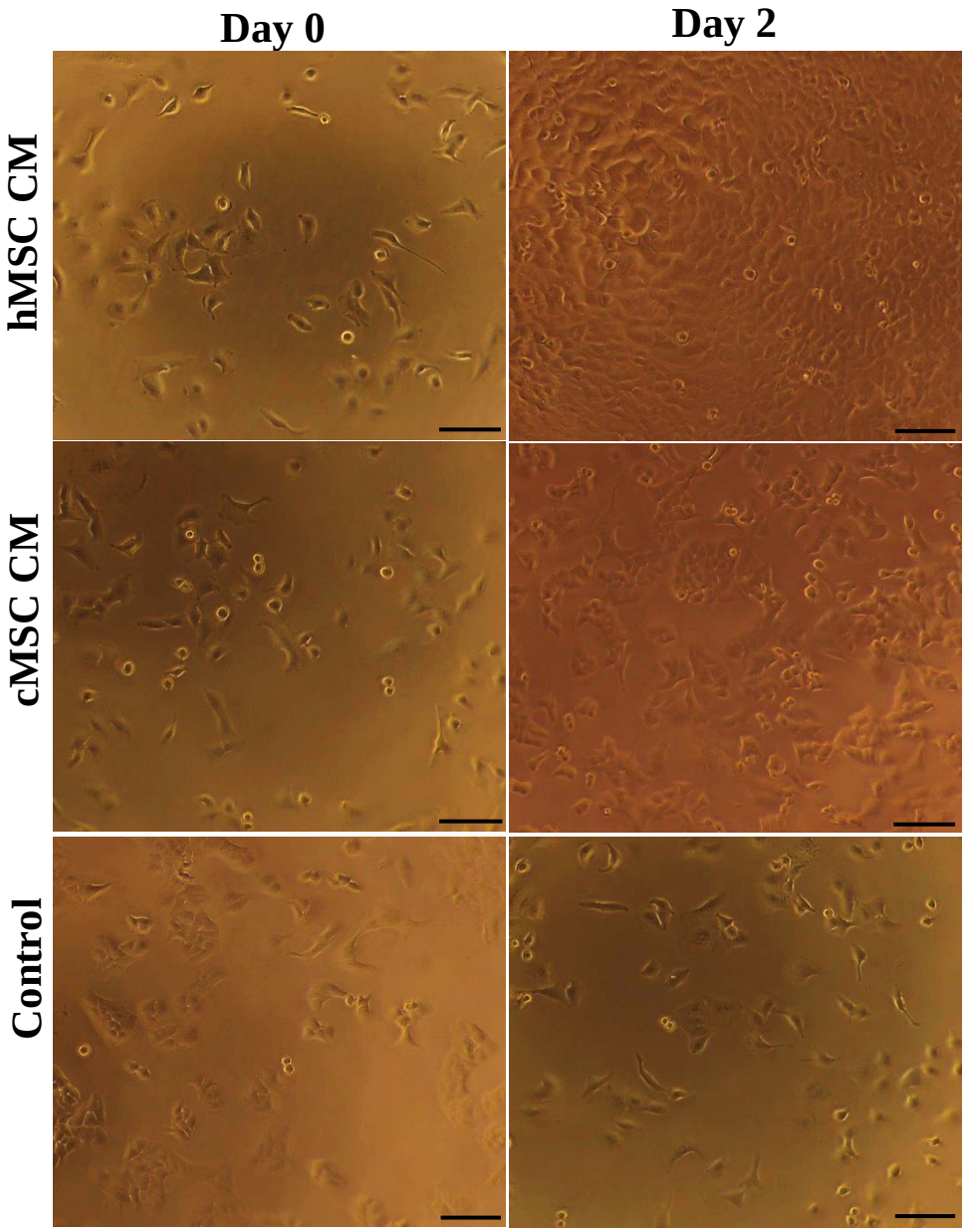

Figure 4:13 Human and canine MSC CM promoted EA.hy926 endothelial cell proliferation. Representative images are shown of EA.hy926 cells cultured in 96 well plates in the presence of hMSC CM or cMSC CM versus control medium for a 2 day period. As shown, there was an increase in the presence of viable EA.hy926 cells with time, which was most marked in cells cultured in MSC CM. Scale bars = 100µm. Original magnification X10.This image was collected from hMSC CM and cMSC CM from 3 separate donors.

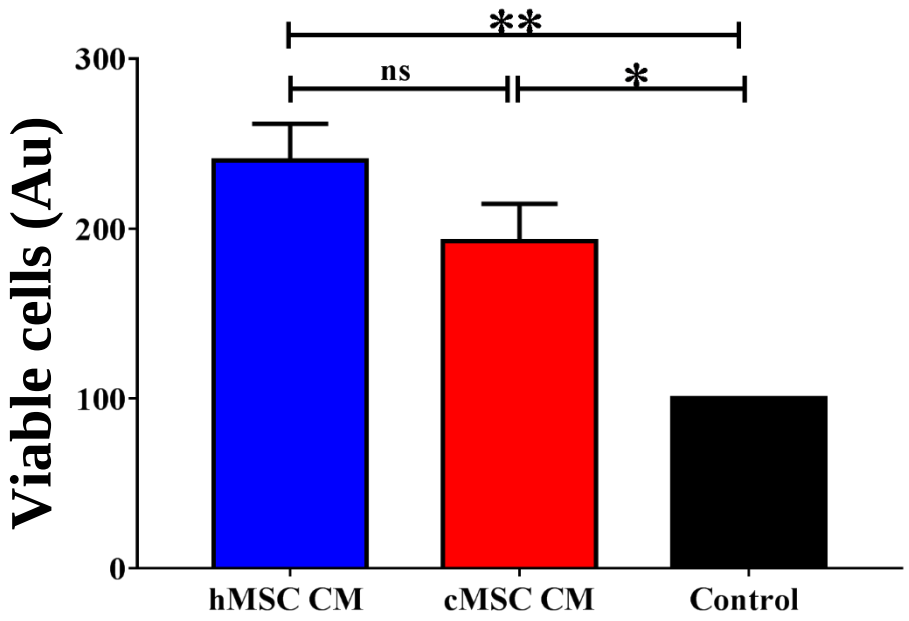

Figure 4:14 The MTT assay confirmed that culturing EA.hy926 endothelial cells in cMSC CM versus control medium significantly increased the number of viable EA.hy926 cells present.

MTT assays were performed to assess viable cell numbers. The results showed a significant increase in the number of viable EA.hy926 cells in human and canine MSC CM versus control medium at 2 days. Whereas, human and canine MSC CM had a similar effect. Each bar represents the mean±SEM from 3 independent experiments, i.e. testing hMSC CM and cMSC CM from 3 separate donors. *indicates $p \leq 0.05$ and **indicate $p \leq 0.01$. One way- ANOVA with Tukey's multiple comparisons test used to determine the significant differences.

4.4.2 Human and canine MSC CM stimulated endothelial tubule formation in Matrigel assays

The angiogenic activity of human and canine MSC CM was further assessed using Matrigel assays to examine endothelial tubule formation by EA.hy926 cells, as has been reported in other studies testing different angiogenic factors (Ponce, 2001, Ponce, 2009, Khoo et al., 2011). The extent of tubule formation and endothelial tubule branch formation was determined by capturing digitised images after EA.hy926 cells had been cultured on Matrigel in hMSC CM, cMSC CM or control medium, and using the Cell IQ image analysis software (see Chapter 2, 2.5.4). As shown in Figure 4.15, human and canine MSC CM induced the formation of tubule-like structures by EA.hy926 endothelial cells to a markedly greater extent than culturing the cells on Matrigel in control medium. Angiogenic activity was quantified by measuring total tubule length and branch point count for each of the digitised images captured. The results showed that both the human and the canine MSC CM significantly increased these parameters compared to control medium (Figure 4.16). Hence, there was a significant increase in total tubule length (hMSC CM versus control, p= 0.0034; cMSC CM versus control, p= 0.0080) and the number of branch points (hMSC CM versus control, p= 0.0163; cMSC CM versus control, p= 0.0298). In contrast, there was no significant difference between hMSC CM versus cMSC CM for either total tubule length or branch point counts (p= 0.6665, p= 0.8611. respectively). Taken together, this data demonstrated that human and canine MSC CM had a marked and significant stimulatory angiogenic effect on EA.hy926 endothelial cells.

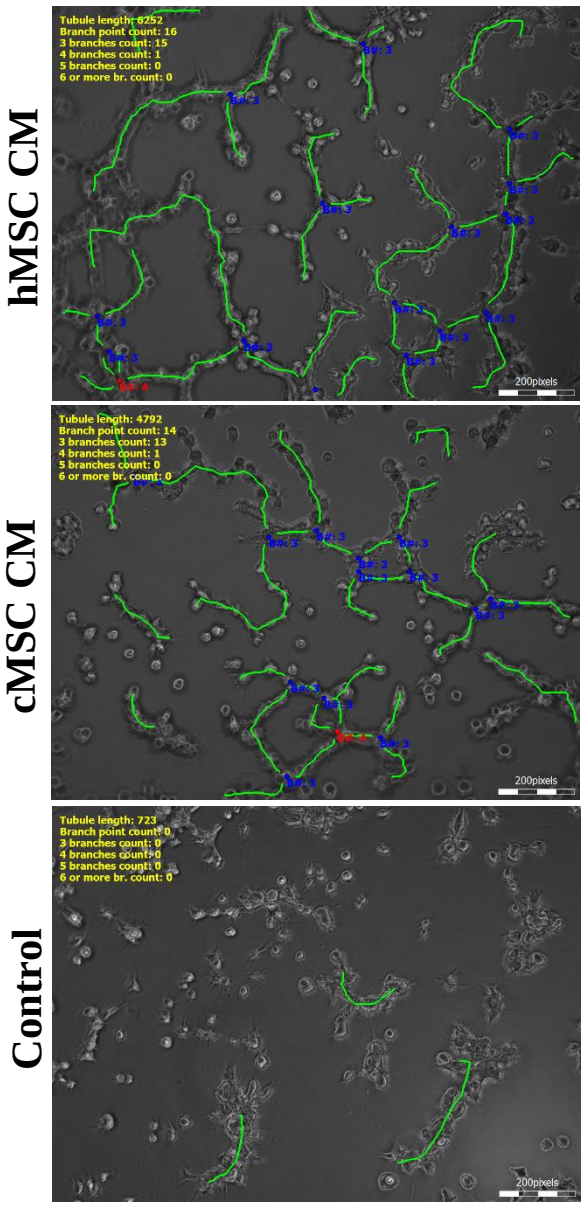

Figure 4:15 The effects of human and canine MSC CM on EA.hy926 endothelial cells cultured on Matrigel.

Representative images are shown of EA.hy926 endothelial cells cultured on Matrigel in the presence of hMSC CM or cMSC CM versus serum-free control medium. These images were subsequently analysed using the Cell IQ imaging software to determine the length (indicated by green lines) and the number of branch points (indicated by blue and red dots) seen in endothelial tubule-like structures. Scale bars = 200µm. This analysis was performed on hMSC CM and cMSC CM from 3 separate donors.

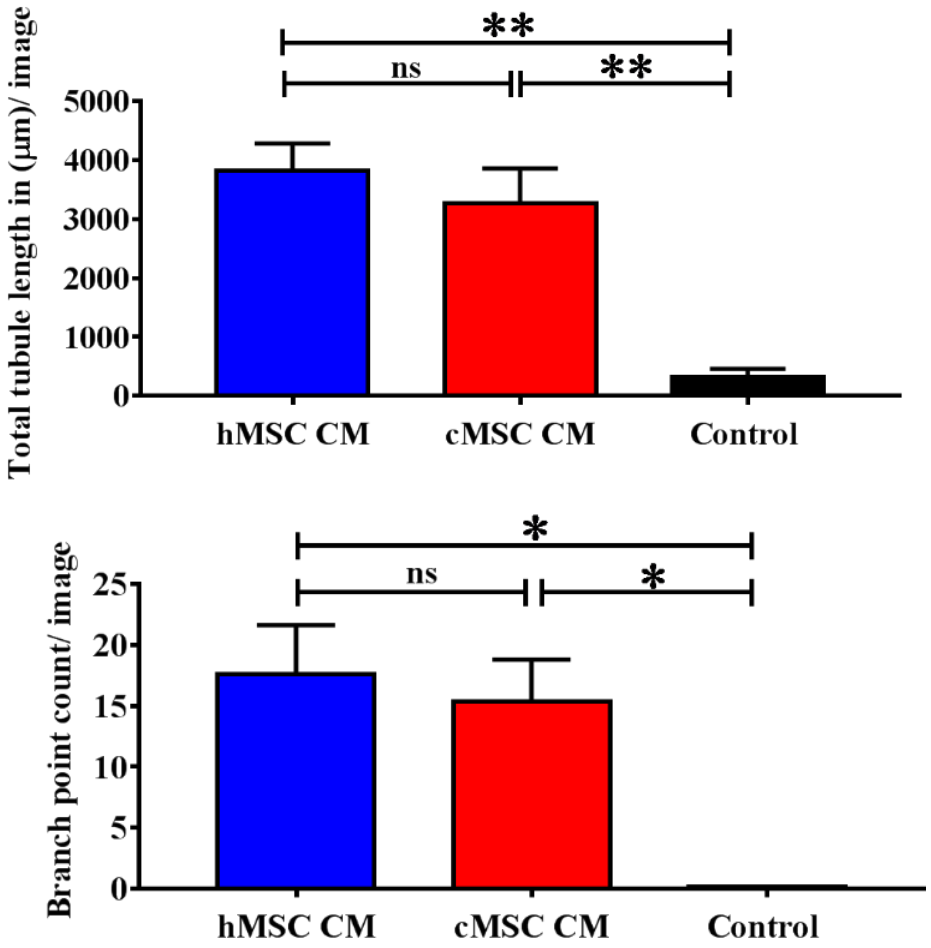

Figure 4:16 Human and canine MSC CM significantly increased EA.hy926 endothelial tubule formation.

Image analysis of the collected digitised images (see Figure 4.15) was used to measure both the total length of tubules formed (per image) and the number of endothelial tubule branch points (per image). As shown, there were significant increases in both of these parameters when EA.hy926 cells were cultured on Matrigel for 1 day in hMSC CM and cMSC CM versus control medium. Each bar represents the mean±SEM from 3 independent experiments, i.e. testing hMSC CM and cMSC CM from 3 separate donors. Top panel: **indicates $p \leq 0.01$. Bottom panel: *indicates $p \leq 0.05$. One way-ANOVA with Tukey's multiple comparisons test used to determine the significant differences.

4.5 Discussion

MSCs have been intensively studied for their potential therapeutic activity for a large number of conditions, particularly CNS damage such as SCI (Mariani and Facchini, 2012, Oliveri et al., 2014, Razeghian Jahromi et al., 2016). Recently it has become more accepted that transplanted MSCs exert a therapeutic effect through their paracrine activities on endogenous cells present at the sites of injuries (Teixeira et al., 2013, Konala et al., 2016). MSCs have the ability to secrete different kinds of reparative proteins including growth factors, cytokines, chemokines as well as extracellular vesicles (Kupcova Skalnikova, 2013, Kalinina et al., 2015). However, the translation of research into cell-based therapy into the clinic requires a good animal model for SCI, which anatomically, physiologically and pathologically resembles human SCI. Dogs, among many other animal models, including rodents, are a powerful model for the study of human diseases and pre-clinical and clinical research leading therapy (Rowell et al., 2011).

In the previous Chapter, the results demonstrated that canine MSCs exert paracrine activity by stimulating neuronal outgrowth and endothelial growth and migration. To help develop a translational pathway from establishing the potential effect of canine MSC transplants in dogs with SCI to human MSC transplants in humans with SCI, the aim of this study was to compare the paracrine activities of human MSCs with canine MSCs. Having established that the human and canine MSCs examined, which were isolated and cultured from adipose tissue, met the minimal criteria of the MSC phenotype described by the ISCT (Dominici et al., 2006), the study then examined their paracrine activity using MSC CM.

Results obtained by this study showed that both the human and canine MSC CM similarly promoted SH-SY5Y neuronal cell proliferation, cell survival, neurite outgrowth and neuronal differentiation. These findings suggest that human and canine MSCs exert neurotrophic effects through their secretomes in a similar manner and to a similar extent.

Traumatic SCI causes damage and disruption to the blood vessels that supply the spinal cord and the early re-establishment of blood vessels can minimise the loss of neuronal tissue after injury (Kundi et al., 2013). Therefore, this Chapter, like the studies undertaken in Chapter 3, also compared the angiogenic effects of human and canine MSC CM. This demonstrated that both the human and the canine MSCs had a significant stimulatory effect on EA.hy926 endothelial cells, indicating an angiogenic paracrine activity. Similar to the effects on SH-SY5Y cells, there were no marked or significant differences between hMSC CM versus cMSC CM. These findings suggest that human and canine MSCs exert angiogenic effects through their secretomes in a similar manner and to a similar extent.

However, a clear caveat to concluding that the human and canine MSCs have similar paracrine activity is that the responder cell lines tested, i.e. SH-SY5Y neuronal cells and EA.hy926 endothelial cells are of human origin and derived from tumours. This means that the responses of these cells to cross-species growth factors may differ from their response to cells of the same species, plus they may vary in response from normal primary neurones or endothelial cells. The importance of the findings shown in this chapter, including possible areas that require further experimentation and validation, will be discussed in more detail in Chapter six.

In the next Chapter, experiments were performed to examine whether there may be an optimal population of human MSCs for CNS repair. This was done again as a part of the translational pathway to human clinical trials, e.g. for the treatment of SCI, because of the known heterogeneity of MSCs in terms of activity and because of the reported donor-donor variation in the effects of MSCs (Sivasubramaniyan et al., 2012, Walter et al., 2015). The generation of a more homogenous MSC population of known paracrine activity would be advantageous as the application of these cells goes to the clinic.

Chapter 5: An *in vitro* examination of the neurotrophic and angiogenic paracrine activities of human adipose-derived MSC subpopulations

5.1 Background and aims

MSCs are heterogeneous populations of non-haematopoietic multipotent cells. The main sources for MSCs are bone marrow or adipose tissue (Hass et al., 2011). The most popular and classical method to isolate and generate MSCs from tissues is by plastic adherence. The plastic adherent method is used to obtain MSCs after tissue processing, i.e., after using density gradient centrifugation of bone marrow to obtain mononucleated cells (Pittenger et al., 1999) or following collagenase digestion to obtain the stromal vascular fraction from adipose tissue (Zuk et al., 2002). The isolated cells are then put into the culture medium, and those which successfully attach to plastic following isolation are then culture expanded (after removal of non-adherent cells) as cell monolayers. These adherent monolayer cell populations are recognised as MSCs. However, they are still reported being heterogeneous in nature (Ho et al., 2008, Phinney, 2012).

Cell sorting techniques allow the achievement of more highly purified subpopulations of MSCs than their selection based on plastic adherence (Tondreau et al., 2005, Buhring et al., 2007, Battula et al., 2009). Furthermore, the identification and purification of MSC subpopulations before culturing them may allow for a better understanding of their biological functions (Jones et al., 2002, Tormin et al., 2011).

A popular marker to prospectively isolate MSCs from bone marrow and adipose tissue is CD271. The receptor belongs to the tumour necrosis factor superfamily (Quirici et al., 2002, Buhring et al., 2007). Several studies have revealed that selected $CD271^+$ MSCs have shown high osteogenic and chondrogenic differentiation capacities compared with plastic adherent selected cells (Jones et al., 2010, Cuthbert et al., 2015).

This suggests that using $CD271^+$ MSCs in orthopaedic cell replacement therapies for damaged bone and cartilage may have a more beneficial effect regarding tissue regeneration than plastic adherent selected MSCs (Mifune et al., 2013).

However, there is currently a lack of information regarding the paracrine effects of $CD271^+$ MSCs' on the biological functions of various cell types, including nerves and blood vessels, which may have application in other wound repair scenarios, e.g. for CNS damage. Therefore, this study was conducted for the first time a comparison investigation to examine the paracrine effects of three human adipose-derived MSC subpopulations, including plastic adherent MSCs (i.e., PA MSCs), CD271-selected MSCs (i.e., $CD271^+$ MSCs), and those cells which were $CD271^-$, but were selected for plastic adherence after the removal of the $CD271^+$ MSCs, i.e. the $CD271^-$ MSCs. For further purposed of comparison, this investigation of sub-population paracrine activities involved looking for the effects of MSC CM on neurogenesis and angiogenesis using the SH-SY5Y and EA.hy926 cell model systems previously utilised in Chapters 3 and 4.

5.2 Characterization of MSC subpopulations

5.2.1 Morphological appearance and differentiation of PA MSCs, CD271$^+$ MSCs, and CD271$^-$ MSCs

As described in Chapter 2 (Section 2.1.3), the human MSC subpopulations were isolated using the MACS technique, culture expanded and assessed to see if they matched the ISCT minimal criteria for MSC phenotype (Dominici et al., 2006). The PA MSCs, CD271$^+$ MSCs and CD271$^-$ MSCs all manifested a plastic adherent and fibroblastic appearance during culture expansion (Figure 5.1). Furthermore, all three MSC subpopulations differentiated into adipocytes as detected by Oil Red O staining (Figure 5.2). Moreover, the amount of Oil Red O accumulation was quantified by releasing the dye from lipid droplets using isopropanol 100% (Chapter 2, Section 2.2.3). Results shown in Figure 5.3 demonstrate that all three MSC subpopulations significantly increased the amount of lipid content in response to adipose-differentiation inductions compared with control cultures, but that there were no significant differences in the amount of lipid formation amongst the three MSCs sub-populations. A Two-way ANOVA with Tukey's multiple comparisons test was used to determine the differences amongst these three groups. This data was obtained from three independent experiments, i.e. examining each MSC subpopulation from three different MSC donors.

The three MSCs sub-populations were also assessed for their capacity to differentiate into osteoblasts (Chapter 2, Section 2.2.3) by staining and quantifying for ALP activity (Figure 5.4 and Figure 5.5). As shown in Figure 5.4, there was a marked increase in the presence of ALP-positive MSCs after osteogenic induction compared to control cultures. The results shown in Figure 5.5 demonstrated that ALP levels were significantly increased in osteogenic treated PA MSCs and CD271$^+$ MSCs versus their respective control cultures.

There was no significant difference between osteogenic treated PA MSCs and osteogenic treated $CD271^+$ MSCs. However, osteogenic treated PA MSCs and $CD271^+$ MSCs had significantly higher levels of ALP activity compared with osteogenic treated $CD271^-$ MSCs. Furthermore, the osteogenic treated $CD271^-$ MSCs showed no significant difference when compared with their control cultures. A two-way ANOVA with Tukey's multiple comparisons test was used to determine levels of differences amongst these three groups. The data was obtained from two independent experiments, i.e., examining MSC subpopulations from two different donors with three replicates for each donor and each experiment were performed and pooled.

The three MSCs sub-populations were also assessed for their capacity to differentiate into chondrocytes. As described in Chapter 2 (Section 2.2.3), the differentiation capacity was assessed by the accumulation of GAGs in the extracellular matrix of pellet cultures which were stained with toluidine stain (Figure 5.6). This demonstrated that an apparent increase in metachromatic staining within the chondrogenic treated cell pellets versus control cell pellets in all MSC subpopulations. The amount of GAGs in digested pellets after 28 days in culture was quantified by using the DMMB assay. The resulting data in Figure 5.7 showed that there was an increase in GAG content in the chondrogenic treated pellets versus control for all MSC subpopulations, but that there were no significant differences amongst the three MSC subpopulations. A Two-way ANOVA with Tukey's multiple comparisons test was used to determine the differences amongst these three groups. This data was obtained from three independent experiments, i.e., with MSC subpopulations from three different donors.

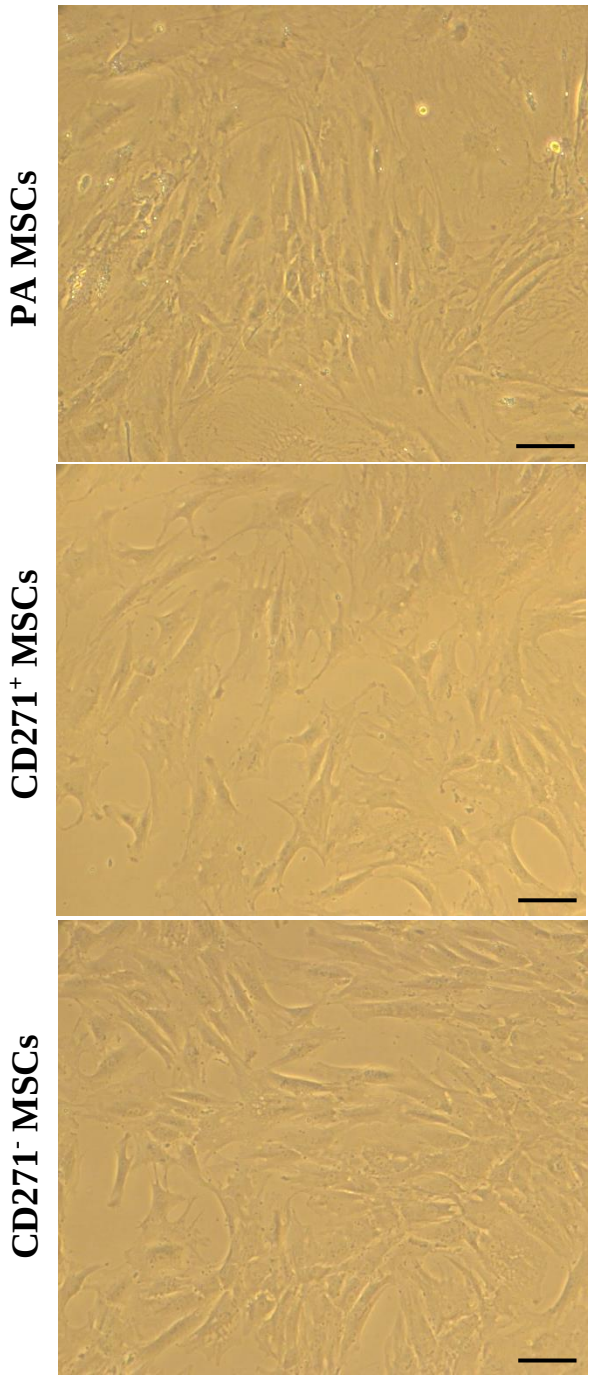

Figure 5:1 The fibroblastic appearance of MSC subpopulations.

Representative phase contrast images are shown of PA MSCs, $CD271^+$ MSCs and $CD271^-$ MSCs growing as plastic adherent cells in culture. Scale bar = 100 µm. Original magnification X10. This analysis was performed on MSC subpopulations from three separate donors.

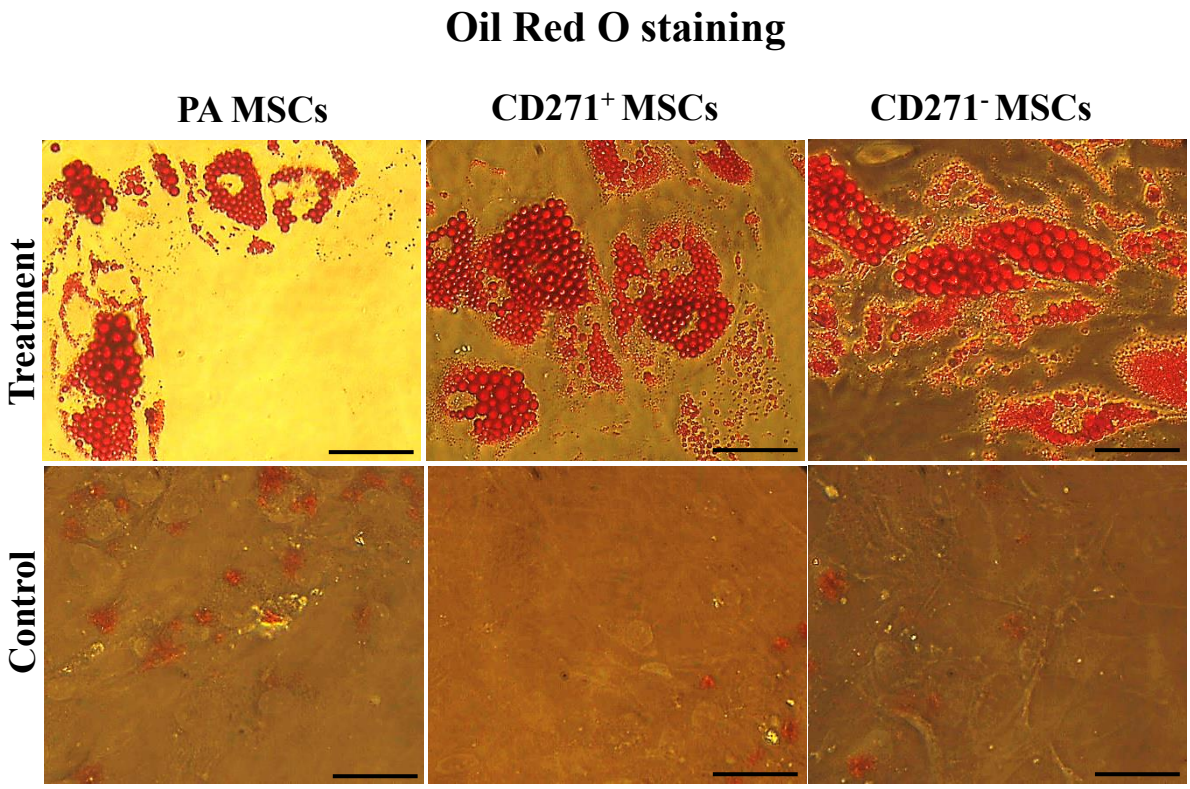

Figure 5:2 Adipogenic differentiation of MSC subpopulations.

Representative phase contrast images are shown of PA MSCs, $CD271^+$ MSCs and $CD271^-$ MSCs. All three MSC subpopulations displayed the ability to differentiate into adipocytes after their treatment with adipogenic induction medium. Oil Red O staining was used to indicate the accumulation of fat droplets in the cell cytoplasm. Scale bar = 50 µm. Original magnification X40. This analysis was performed on MSC subpopulations from three separate donors.

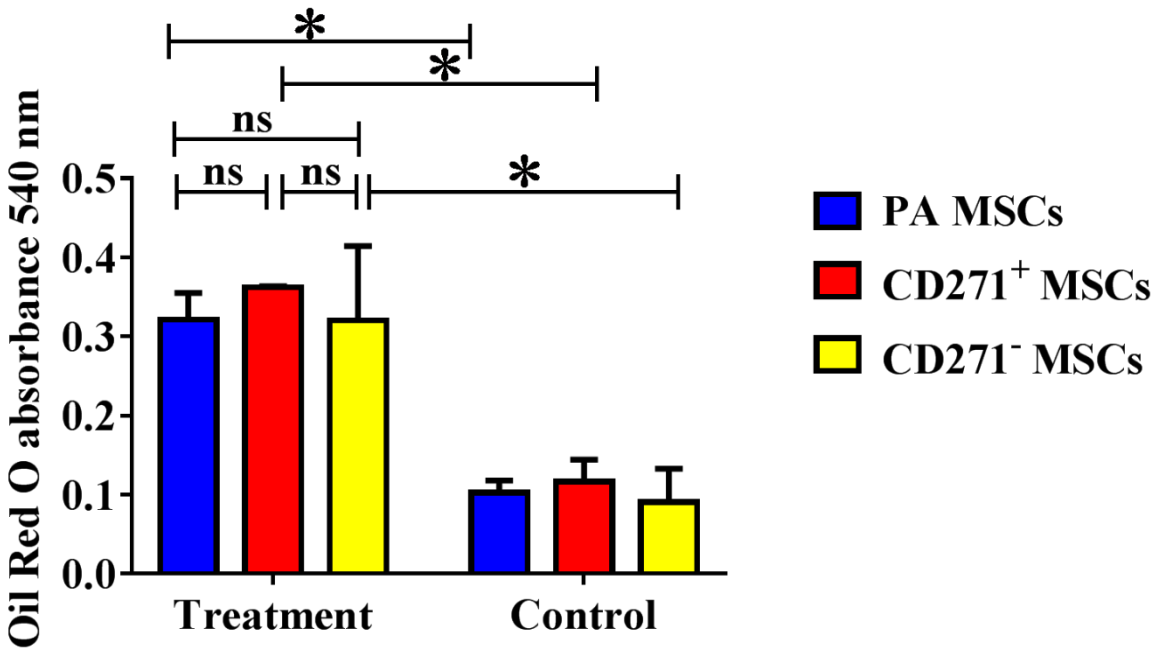

Figure 5:3 The extent of lipid accumulation in MSC subpopulations.

The amount of lipid accumulated after the differentiation of PA MSCs, $CD271^+$ MSCs and $CD271^-$ MSCs was quantified by spectrophotometry. Each bar represents the mean±SEM from three independent experiments, i.e. testing the MSC subpopulations from three different donors. As shown there was an increase in lipid content in MSCs that had been treated with adipogenic induction medium versus controls. *indicates $p \leq 0.05$. Two way-ANOVA with Tukey's multiple comparisons tests were used to determine significant differences.

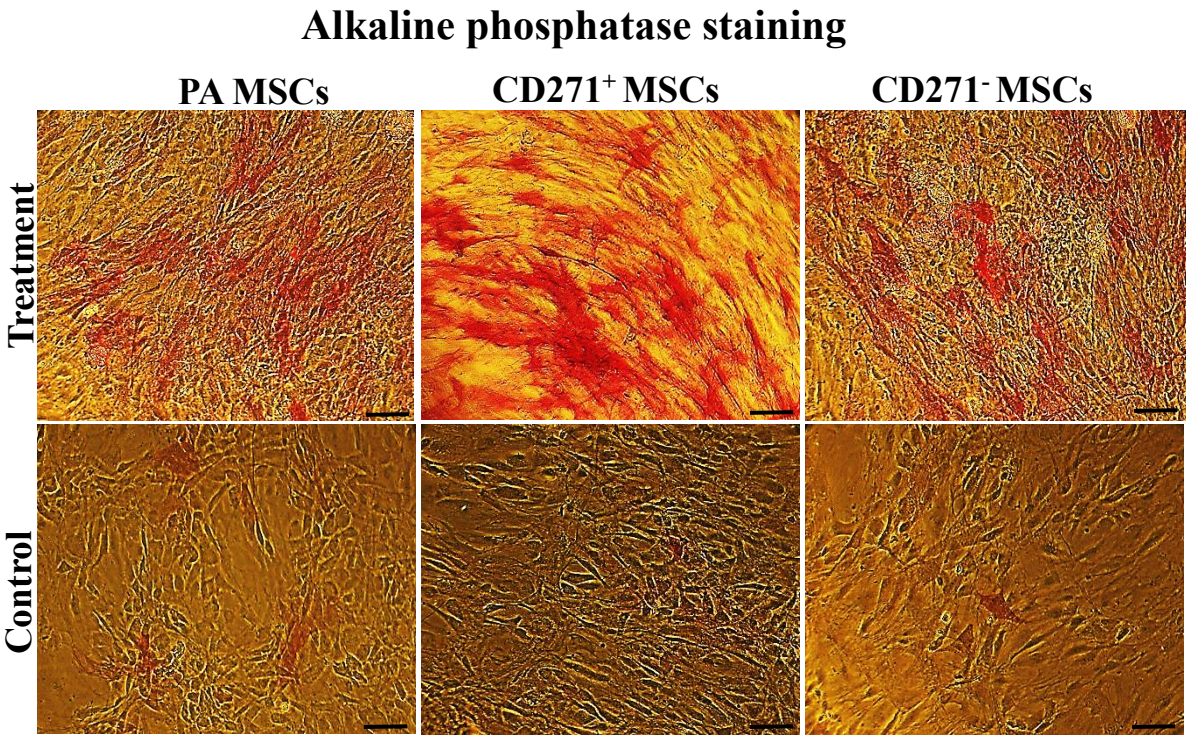

Figure 5:4 Osteogenic differentiation of MSC subpopulations.

Representative phase contrast images are shown of PA MSCs, $CD271^+$ MSCs and $CD271^-$ MSCs after differentiating into osteoblasts following treatment with osteogenic induction medium. The differentiation capacity was indicated by staining for alkaline phosphatase activity. Scale bar = 100 µm. Original magnification X10. These images were collected from two independent experiments, i.e., examining MSC subpopulations from two different donors.

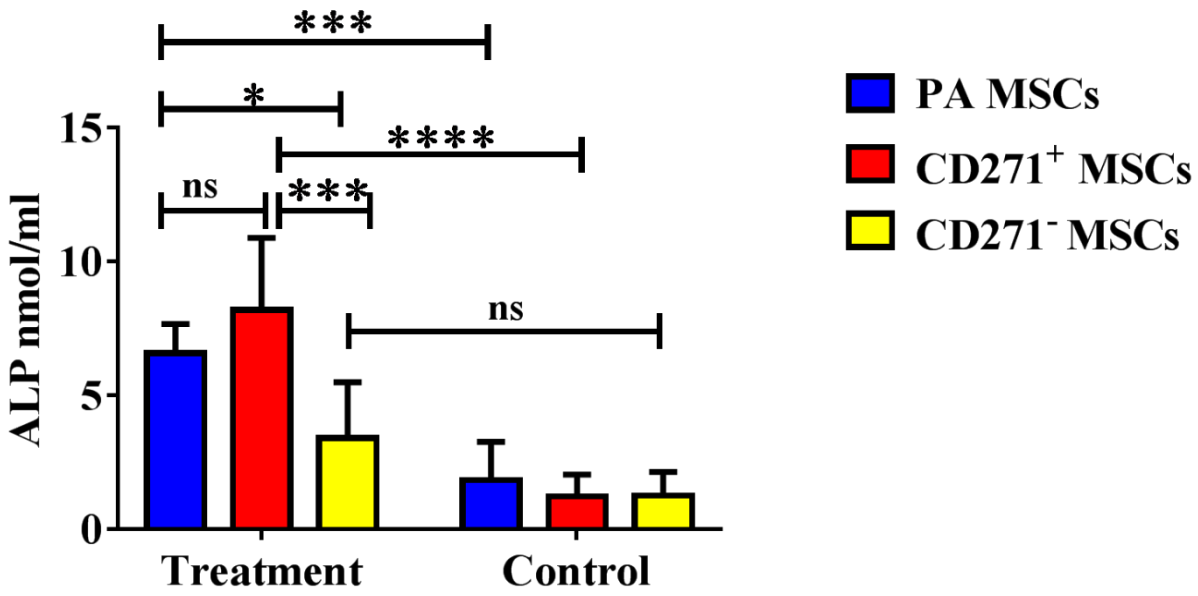

Figure 5:5 Quantification of ALP activity for MSCs sub-populations.

The amount of ALP activity in PA MSCs, $CD271^+$ MSCs and $CD271^-$ MSCs was quantified by spectrophotometry. Each bar represents the means±SD from the pooled data of two independent experiments, i.e., testing the MSC subpopulations from two different donors where there were three replicates per donor for each condition of each experiment. *indicates $p \leq 0.05$, ***indicates $p \leq 0.001$, and ****indicates $p \leq 0.0001$. A Two-way ANOVA with Tukey's multiple comparisons test was used to determine significant differences.

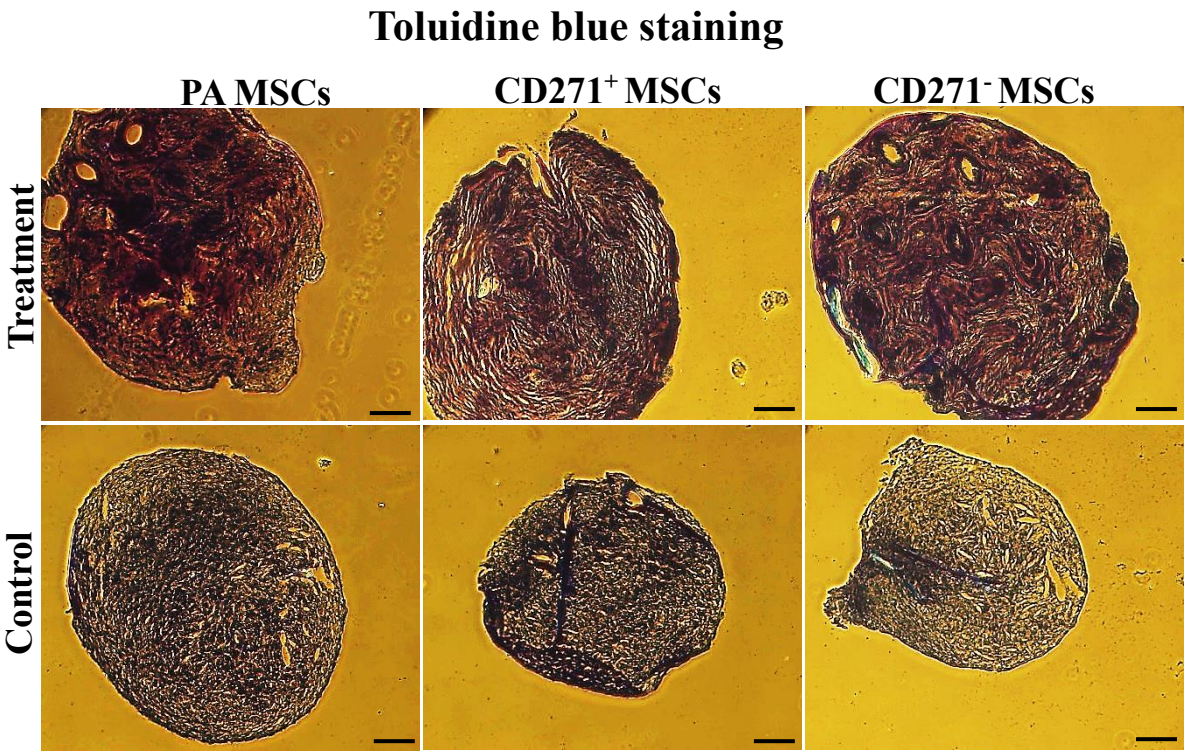

Figure 5:6 Chondrogenic differentiation of MSC subpopulations.

Representative phase contrast images are shown of PA MSCs, $CD271^+$ MSCs and $CD271^-$ MSCs in pellet cultures which had been induced to undergo chondrogenesis (treated) versus control and stained with toluidine blue stain to identify GAG content. Scale bar = 100 µm. Original magnification X10. This analysis was performed on MSC subpopulations from three separate donors.

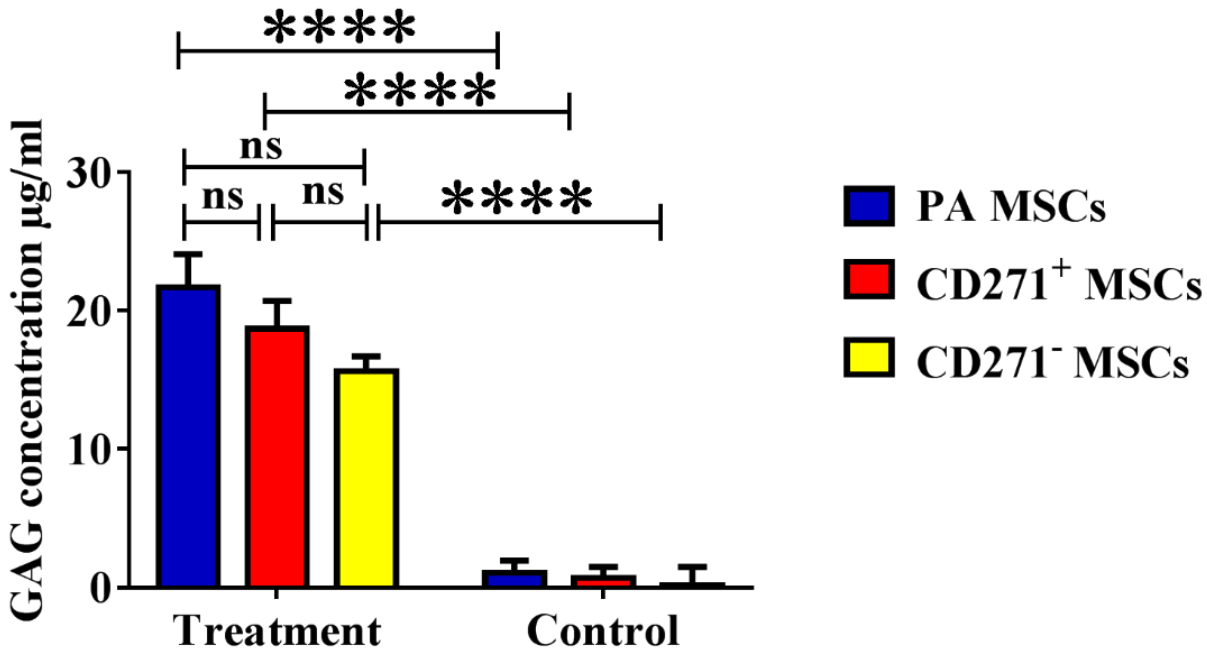

Figure 5:7 Quantification of GAGs in the MSC subpopulations.

The amount of accumulated GAGs in the extracellular matrix from the differentiated and non-differentiated pellets of PA MSCs, $CD271^+$ MSCs and $CD271^-$ MSCs were measured using the DMMB assay. Each bar represents the mean±SEM from three independent experiments, i.e., testing the MSC subpopulations from three different donors of three replicates per donor for each experiment. ****indicates $p \leq 0.0001$. A Two-way ANOVA with Tukey's multiple comparisons test was used to determine significant differences.

5.2.2 Immunophenotypic CD profiling characterization of MSC subpopulations

The common cell surface markers for MSCs which have been established by ISCT as defining markers were quantified for the three MSC subpopulations. The three MSC subpopulations at passage II were processed for flow cytometry analysis. The results showed that all these three MSC subpopulations were immunonegative for haematopoietic markers, which were CD34 and CD45 and immunopositive for MSC-specific cell-surface antigens which are not expressed by haematopoietic cells, these were CD44, CD73, CD90 and CD105 (Figure 5.8). The data gathered by this study showed that all three MSC subpopulations were immunonegative for CD34. The percentage of cells which were detected as positive for CD34 (mean±SEM) were as the following; PA MSCs 0.67±0.66%, $CD271^+$ MSCs 3.86±3.84%, and $CD271^-$ MSCs 3.45±0.96%. Similarly, the MSC subpopulations were showed immunonegative for CD45. The percentage of cells which were detected as positive for CD45 (mean±SEM) were as the following; PA MSCs 0.02±0.02%, $CD271^+$ MSCs 1.41±1.38%, and $CD271^-$ MSCs 0.10±0.05%. Also, the flow cytometry data showed that the three MSCs sub-populations were immunopositive for CD44, CD73, CD90, and CD105. The percentage of cells which were detected as positive for CD44 (mean±SEM) were as the following; PA MSCs 97.68±0.95%, $CD271^+$ MSCs 97.61± 1.19%, and $CD271^-$ MSCs 97.34± 0.42%. The percentage of cells which detected as positive for CD73 (mean±SEM) were as the following; PA MSCs 95.73±2.50%, $CD271^+$ MSCs 99.48±0.18%, and $CD271^-$ MSCs 99.56±0.15%. The percentage of cells which detected as positive for CD90 (mean±SEM) were as the following; PA MSCs 98.15±1.38%, $CD271^+$ MSCs 99.53±0.12% and $CD271^-$ MSCs 99.47±0.23%. The percentage of cells which were detected as positive for CD105 (mean±SEM) were as the following; PA MSCs 92.39±6.38%, $CD271^+$ MSCs 99.19±0.47% and $CD271^-$ MSCs 99.13±0.30%.

Furthermore, the expression of CD271 cell surface marker was examined at the same passage (i.e. passage II) for all three MSCs sub-populations PA, $CD271^+$, and $CD271^-$.

The flow cytometry data showed that although $CD271^+$ selected MSCs were positively selected for this marker, they lost the expression of this CD marker at an early passage in expanded tissue culture only about 0.06±0.04% were positive for CD271 marker. Additionally, PA MSCs and $CD271^-$ MSCs were also examined for their capacity to express CD271 cell surface marker. The results showed that PA MSCs and $CD271^-$ MSCs showed negative immunoreaction for CD271 cell surface marker (0.94±0.91% and 0.05±0.02% respectively) (Table 5.4). The data presented mean±SEM was obtained from three independent (i.e. three different donors).

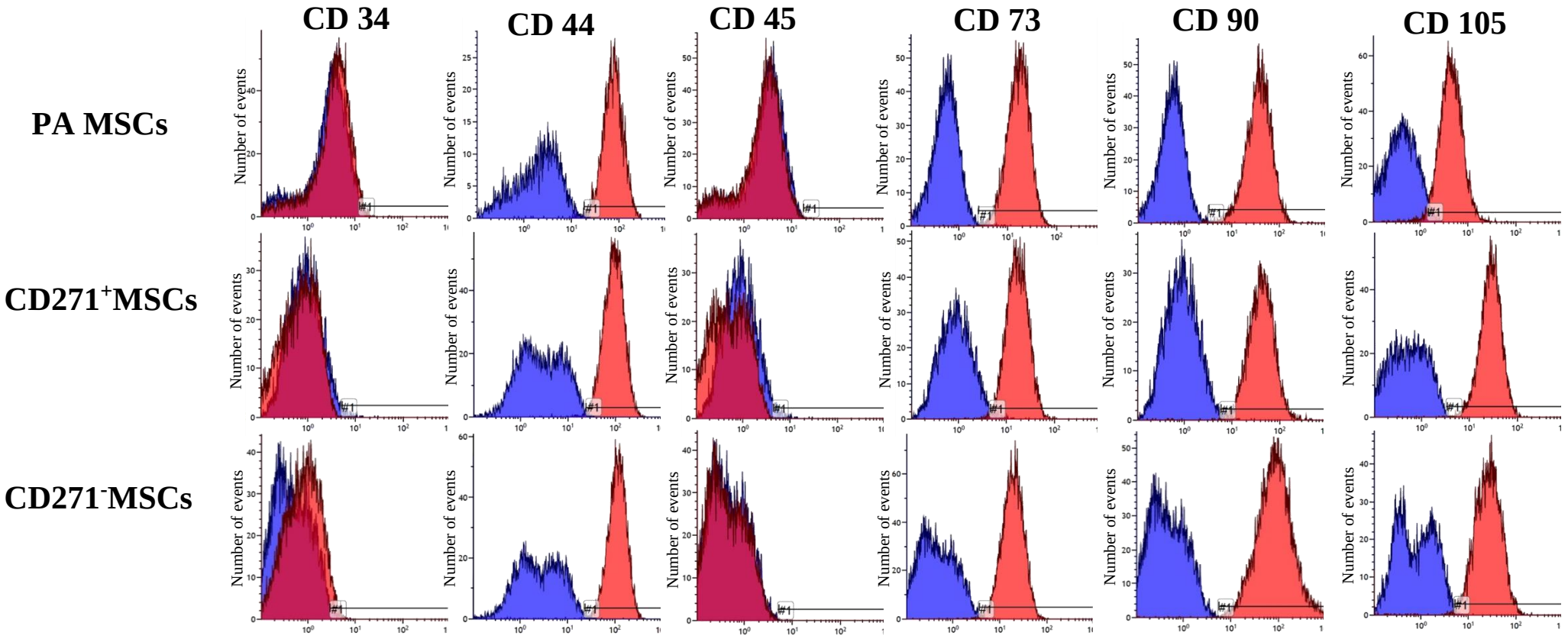

Figure 5:8 (A) Flow cytometry analysis of CD markers expressed by MSC subpopulations.

Representative images are shown of three experiments for CD profiling for MSC subpopulations. The MSC subpopulations were negative for CD34 and CD45, but they were positive for CD44, CD73, CD90 and CD105 (red histograms). IgG1 and IgG2a isotype staining were used as negative controls (blue histograms).

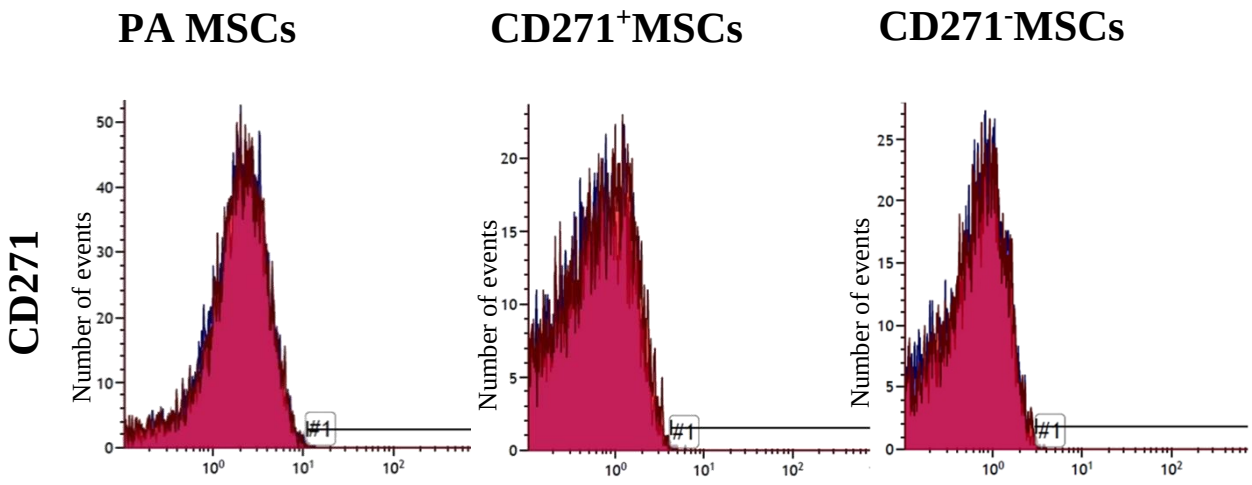

Figure 5:8 (B) Flow cytometry analysis of CD271 marker expressed by the three MSC subpopulations. Representative images for CD271 expression of MSC subpopulations are shown the expression of CD271 after being culture expanded. The $CD271^+$ MSCs lost the capacity to express the CD271 at the early passage of culture expansion. Similarly PA MSCs and $CD271^-$ MSCs were negative for CD271 (red histogram). IgG1 isotype staining groups were used as negative controls (blue histogram; overlap between red and blue appears as magenta). Data were obtained from three independent experiments, where the three MSC subpopulations were in passage II.

	CD34%	CD44%	CD45%	CD73%	CD90%	CD105%	CD271%
PA MSCs 105	0.01	98.53	0.01	99.78	99.48	99.65	2.76
PA MSCs 123	1.99	95.78	0.06	91.16	95.4	79.68	0.05
PA MSCs 126	0.02	98.72	0	96.26	99.57	97.85	0
mean	0.67	97.68	0.02	95.73	98.15	92.39	0.94
SEM	0.66	0.95	0.02	2.50	1.38	6.38	0.91
$CD271^+$ MSCs 105	0.01	99.2	0.06	99.3	99.49	99.88	0.03
$CD271^+$ MSCs 123	0.02	98.33	0.01	99.31	99.36	98.3	0.15
$CD271^+$ MSCs 126	11.54	95.29	4.16	99.83	99.76	99.4	0.01
mean	3.86	97.61	1.41	99.48	99.53	99.19	0.06
SEM	3.84	1.19	1.38	0.18	0.12	0.47	0.04
$CD271^-$ MSCs 105	1.57	97.88	0.19	99.75	99.1	98.61	0.08
$CD271^-$ MSCs 123	4.67	96.52	0.06	99.26	99.43	99.12	0.04
$CD271^-$ MSCs 126	4.12	97.62	0.04	99.67	99.89	99.65	0.02
mean	3.45	97.34	0.10	99.56	99.47	99.13	0.05
SEM	0.96	0.42	0.05	0.15	0.23	0.30	0.02

Table 6: Immunoreactivity of the three MSC subpopulations for cell surface markers.

The table shown is the percentage of cells that are immunoreactive from the three MSC subpopulations for specific CD markers. The cells showed negative immunoreaction for CD34 and CD45 and positive immunoreaction for CD44, CD73, CD90 and CD105. Also, the three MSC subpopulations showed negative immunoreaction for CD 271. Data shown is mean±SEM of three independent experiments.

5.3 Neurotrophic effect of MSC subpopulations conditioned medium

5.3.1 MSC CM from all MSC subpopulations promoted neurite outgrowth and neuronal survival of SH-SY5Y cells

The neurotrophic effects of MSC CM from MSC subpopulations were examined by performing an *in vitro* assay using SH-SY5Y cells. The representative phase contrast images in Figure 5.9 show SH-SY5Y that were seeded in 24 well plates as described in Chapter 2 (Section 2.4.1.1) and treated with conditioned medium from either PA MSC CM, $CD271^+$ MSC CM, and $CD271^-$ MSC CM or serum-free medium as a control. The plates were incubated in the Cell IQ live cell imaging platform for three days. At the end of the incubation period, images were analysed by using the Cell IQ analyser software. The data obtained showed that the MSC CM from MSC subpopulations has a similar neurotrophic effect. The Cell IQ analysis showed that the MSC CM from MSC subpopulations significantly increased the neurite outgrowth of SH-SY5Y cells compared with control medium (p= 0.0039, p= 0.0006, and p= 0.0014 respectively). However, there was no significate differences on promoting neurite outgrowth from SH-SY5Y amongst MSC CM from MSC subpopulations (PA MSC CM vs $CD271^+$ MSC CM p= 0.4023, PA MSC CM vs $CD271^-$ MSC CM p= 0.8096 and $CD271^+$ MSC CM vs $CD271^-$ MSC CM p= 0.8673). Also all three MSCs PA, $CD271^+$, and $CD271^-$ CM significantly increased cell number compared with control medium (p= 0.0005, p= 0.0008, and p= 0.0016 respectively). There was no significant differences amongst MSC CM from MSC subpopulations on increasing the cell number (PA MSC CM vs $CD271^+$ MSC CM p= 0.9762, PA MSC CM vs $CD271^-$ MSC CM p= 0.7108 and $CD271^+$ MSC CM vs $CD271^-$ MSC CM p= 0.9037) (Figure 5.10). This data was obtained from three independent experiments, i.e., with MSC subpopulations from three different donors.

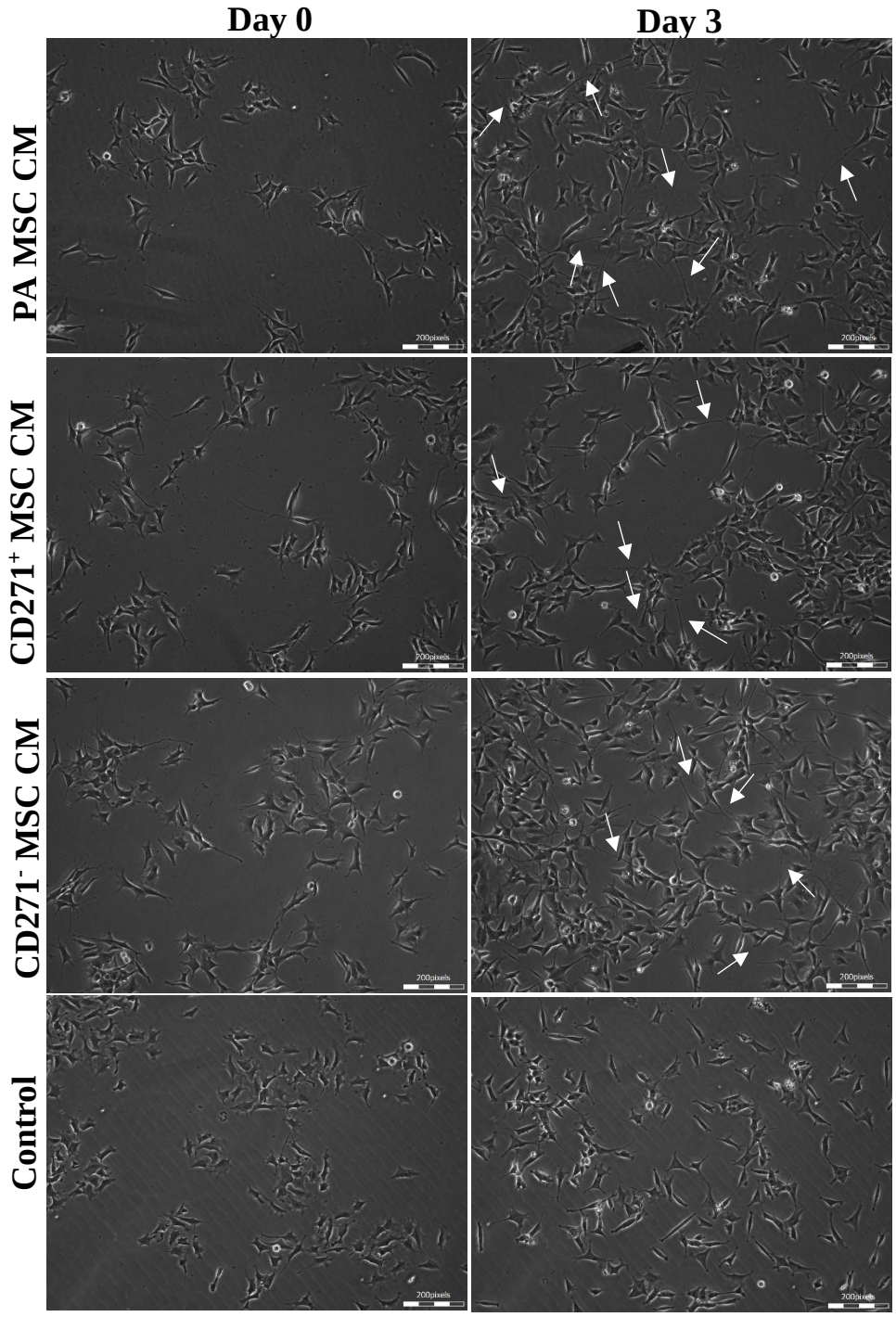

Figure 5:9 The effects of the three MSCs sub-populations PA, CD271$^+$, and CD271$^-$ CM on SH-SY5Y cells neurite outgrowth and neuronal cell proliferation.

Representative images are shown of SH-SY5Y neuronal cells following culture for 3 days in the presence of three MSCs sub-populations PA, CD271$^+$, and CD271$^-$ CM or in control serum-free medium. As shown, there was clear evidence of increased neurite outgrowth (arrows) and cell numbers in PA CM, CD271$^+$ CM and CD271$^-$ CM compared with control cultures. Scale bar = 200µm.

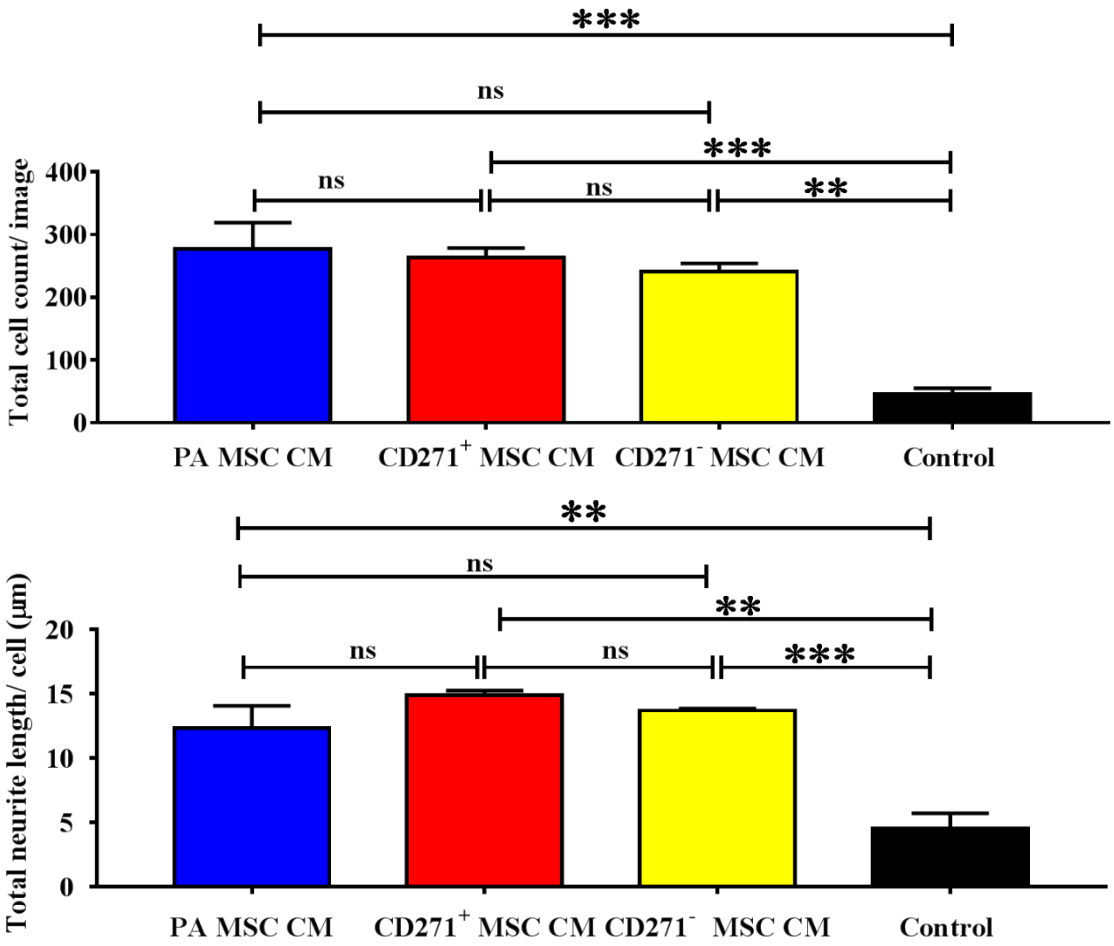

Figure 5:10 Quantitative analysis showing the effect of MSC CM of three MSC subpopulations on cell proliferation and neurite outgrowth from SH-SY5Y cells.

SH-SY5Y cells were treated with MSC CM of MSC subpopulations or serum-free medium as control when digitised phase contrast images were captured and analysed using the Cell IQ imaging platform and software. There was a significant increase in both neurite outgrowth and cell numbers from SH-SY5Y cells compared with the control medium. However, there was no significant difference amongst the three groups. Each bar represents the mean±SEM of three independent experiments, i.e., testing the MSC subpopulations from three different donors of three replicates per each experiment. **indicate $p \leq 0.01$ and ***indicate $p \leq 0.001$. One way- ANOVA with Tukey's multiple comparisons test used to determine the significant differences.

5.3.2 Assessment of SH-SY5Y viable cell numbers using the MTT assay

Cell growth and cell viability rate were determined by the using the colourimetric MTT assay. As described in Chapter 2 (Section 2.4.3.) and as the representative images shown in Figure 5.11, the SH-SY5Y cells were seeded in 96 well plates and treated with either PA MSC CM, $CD271^+$ MSC CM, $CD271^-$ MSC CM or serum-free medium as a control for 3 days. The data showed that all three MSC CM of MSC subpopulations had a similar effect on SH-SY5Y cell growth and cell viability. There was no significant differences in their effect to promote cell growth and to increase the cell viability rate of SH-SY5Y cells during the period of incubation (PA MSC CM vs $CD271^+$ MSC CM p= 0.6755, PA MSC CM vs $CD271^-$ MSC CM p= 0.2030, and $CD271^+$ MSC CM vs $CD271^-$ MSC CM p= 0.2633). On the other hand, the data showed that the MSC CM of MSC subpopulations effect was significantly different when compared with control medium (p= 0.0007, p= 0.0009 and p= 0.0049 respectively) (Figure 5.12). The data obtained from three independent experiments, i.e., testing the MSC CM of subpopulations from three different donors of five replicates per each experiment.

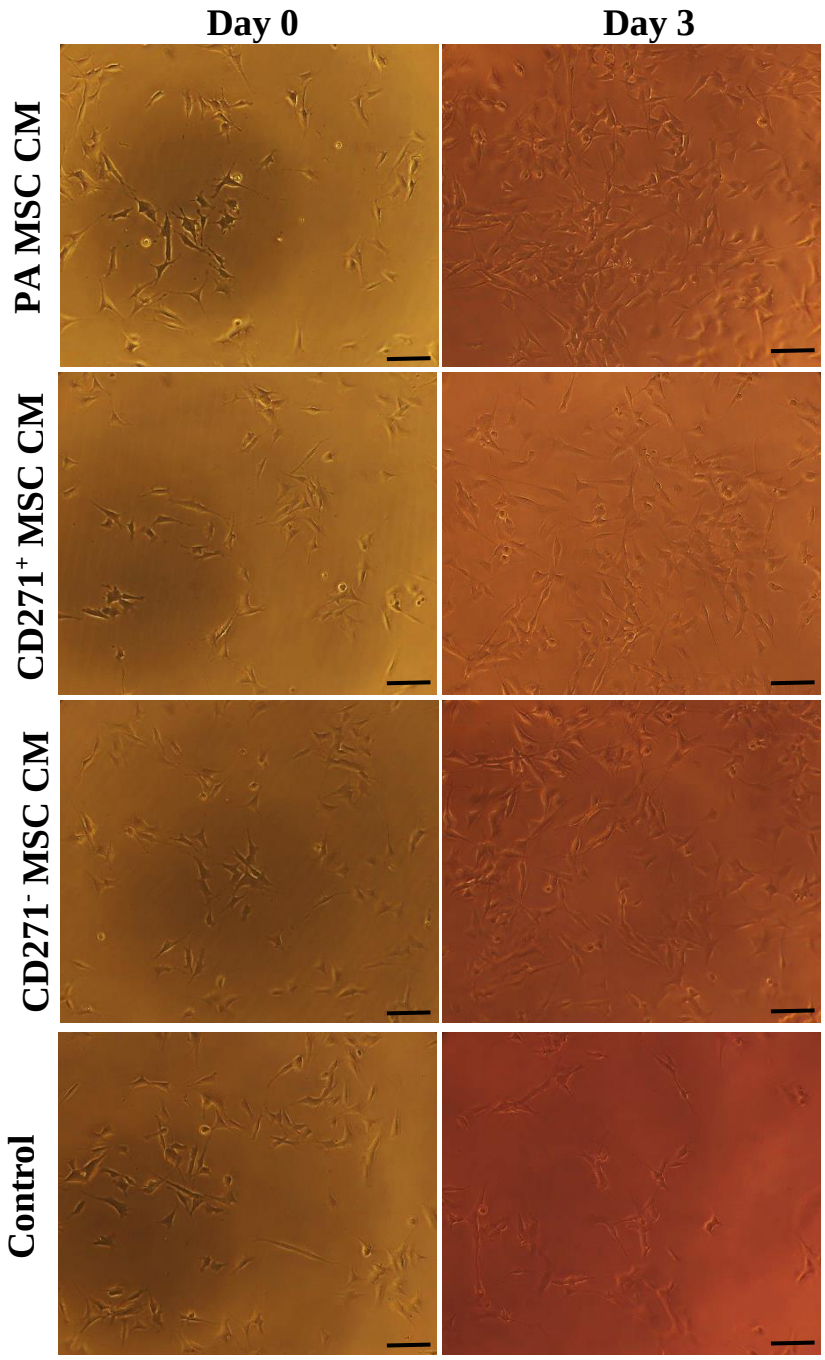

Figure 5:11 Cell growth and cell viability of SH-SY5Y cells.

Representative images are shown of the relative increase in SH-SY5Y cell numbers when cultured for three days after their treatment with conditioned medium from the three MSC subpopulations versus control medium. Cell growth and cell viability were assessed by MTT assay. Scale bar = 100µm. Original magnification X10. The images were collected from three independent experiments (i.e. three different donors).

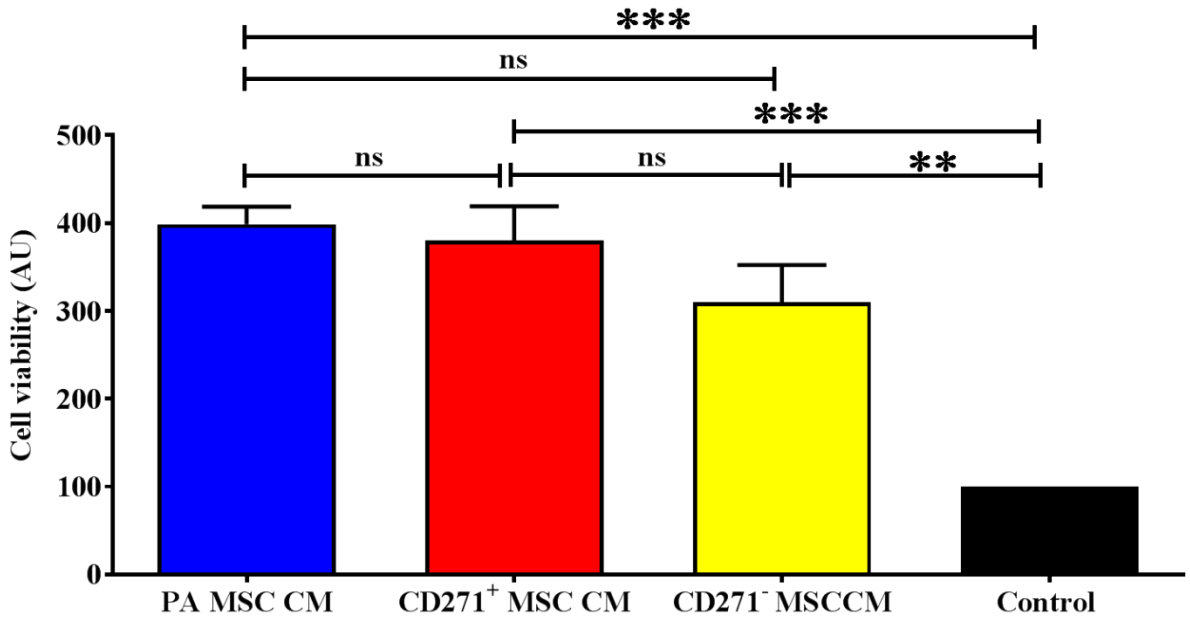

Figure 5:12 The MTT assay confirmed that culturing SH-SY5Y neuronal cells in MSC CM of MSC subpopulations versus control medium significantly increased the number of viable SH-SY5Y cells present.

MTT assays were performed to assess viable cell numbers of SH-SY5Y cells after treating with PA MSC CM, $CD271^+$ MSC CM, and $CD271^-$ MSC CM versus serum-free medium as a control for three days. The conditioned medium from the three MSC subpopulations had the similar influence, and they were significantly stronger in promoting cell viability rate as compared with control medium. Each bar represents the mean±SEM from three independent experiments, i.e., testing the MSC CM of subpopulations from three different donors of five replicates per each experiment. **indicates $p \leq 0.01$ and ***indicate $p \leq 0.001$. A One-way- ANOVA with Tukey's multiple comparisons tests used to determine the significant differences.

5.4 The effects of MSC CM of MSC subpopulations on EA.hy926 endothelial cells

5.4.1 MSC subpopulations promoted EA.hy926 endothelial cell migration and proliferation to different extents

The angiogenic effects of the MSC CM of MSC subpopulations on EA.hy926 cells were examined by using a scratch assay. The representative images in Figure 5.13 show the confluent layers of EA.hy926 cells that were scratched using a yellow pipette tip, and after three repetitive washing steps with PBS, the medium was replaced with either PA MSC CM, $CD271^+$ MSC CM, $CD271^-$ MSC CM or serum-free medium as a control. Then, the migration/ movement and proliferation of the EA.hy926 cells to close the scratch wound were monitored and quantified using the Cell IQ Imaging Platform. The result showed both PA MSC CM and $CD271^-$ MSC CM had the same effect of promoting wound closure compared with $CD271^+$ MSC CM which showed less effect in promoting wound closure. The results showed there was no significant difference between PA MSC CM and $CD271^-$ MSC CM (p= 0.9991). Whereas, both PA MSC CM and $CD271^-$ MSC CM showed significant differences when compared with $CD271^+$ MSC CM (p= 0.0204, p= 0.0304 respectively). The PA MSC CM and $CD271^-$ MSC CM also showed significant differences in increasing wound closure rate when compared with control (p= 0.0001 and p= 0.0001 respectively) while, $CD271^+$ MSC CM showed no significant difference when compared with control (p= 0.1221) (Figure 5.14). To determine whether the MSC CM of MSC subpopulations played a role in cell movement and migration to improve wound closure, cells from both sides of wound edges were tracked by using the Cell IQ analyser software. Three cells per each scratch wound from three replicate per each of three independent experiments were randomly selected. This meant a total of 27 cells for each condition (PA MSC CM, $CD271^+$ MSC CM, $CD271^-$ MSC CM, and control medium) were tracked. Cells were tracked for their movement every 15 minutes and over two days, total distance starting from the day 0 to day 2 was measured. The results showed both PA MSC CM and $CD271^-$ MSC CM similarly enhanced cells migration in wound area and there was no significant difference in their effect (p= 0.9991).

Whereas, both PA MSC CM and CD271$^-$ MSC CM showed significant differences in their effect when compared with CD271$^+$ MSC CM (p= 0.0367, p= 0.0306 respectively).

The data obtained in this study also showed that both PA MSC CM and CD271$^-$ MSC CM significantly increased the cell movements when compared with control (p= 0.0089, p= 0.0075 respectively) while CD271$^+$ MSC CM showed no significant difference when compared with control medium (p= 0.7231) (Figure 5.15). Further analysis has been done using Cell IQ analyser software to examine the rate of proliferation of EA.hy926 cells. For the purpose of quantification, cells were classified and quantified as dividing and non-dividing. Cells were counted every 15 minutes over two days. The results showed all MSC CM of MSC subpopulations similarly promoted cell proliferation. The results showed that there was no significant differences in their effect on the rate of dividing cells (PA MSC CM vs CD271$^+$ MSC CM p= 0.4809, PA MSC CM vs CD271$^-$ MSC CM p= 0.4809 and CD271$^+$ MSC CM vs CD271$^-$ MSC CM p= 0.9999). But, all MSC CM of MSC subpopulations showed significant differences when compared with control medium (p= 0.0001, p= 0.0094, and p= 0.0094 respectively). However, for non-dividing cells, the results showed there was no significant differences between PA MSC CM and CD271$^-$ MSC CM (p= 0.9996) but, both PA MSC CM and CD271$^-$ MSC CM showed significant differences when compared with CD271$^+$ MSC CM (p= 0.0228, p= 0.0304 respectively). Moreover, all MSC CM of the three MSC subpopulations were significantly higher when compared with control medium (all p= 0.0001) (Figure 5.16). The data was obtained from three independent experiments (i.e. three different donors) of three replicates per each experiment. The cell viability activities were further determined by using the MTT assay. The representative images are shown in Figure 5.17, displaying the EA.hy926 cells which were seeded in 96 well plates and treated with either PA MSC CM, CD271$^+$ MSC CM, CD271$^-$ MSC CM or serum-free medium as a control for two days. The data showed that MSC CM of the three MSC subpopulations had the same effect on EA.hy926 cell growth and cell viability and there was no significant differences in their effect on promoting cell growth and to increase the cell viability rate of EA.hy926 cells during the period of incubation (PA MSC CM vs CD271$^+$ MSC CM p= 0.9717, PA MSC CM vs CD271$^-$ MSC CM p= 0.9719 and CD271$^+$ MSC CM vs CD271$^-$ MSC CM p=

0.9999). On the other hand, the data showed that the effect of MSC CM of the three MSC subpopulations was significantly different when compared with control medium (p= 0.0382, p= 0.0211, and p= 0.0212 respectively) (Figure 5.12). The data obtained from three independent experiments (i.e. three different donors) of five replicates per each experiment.

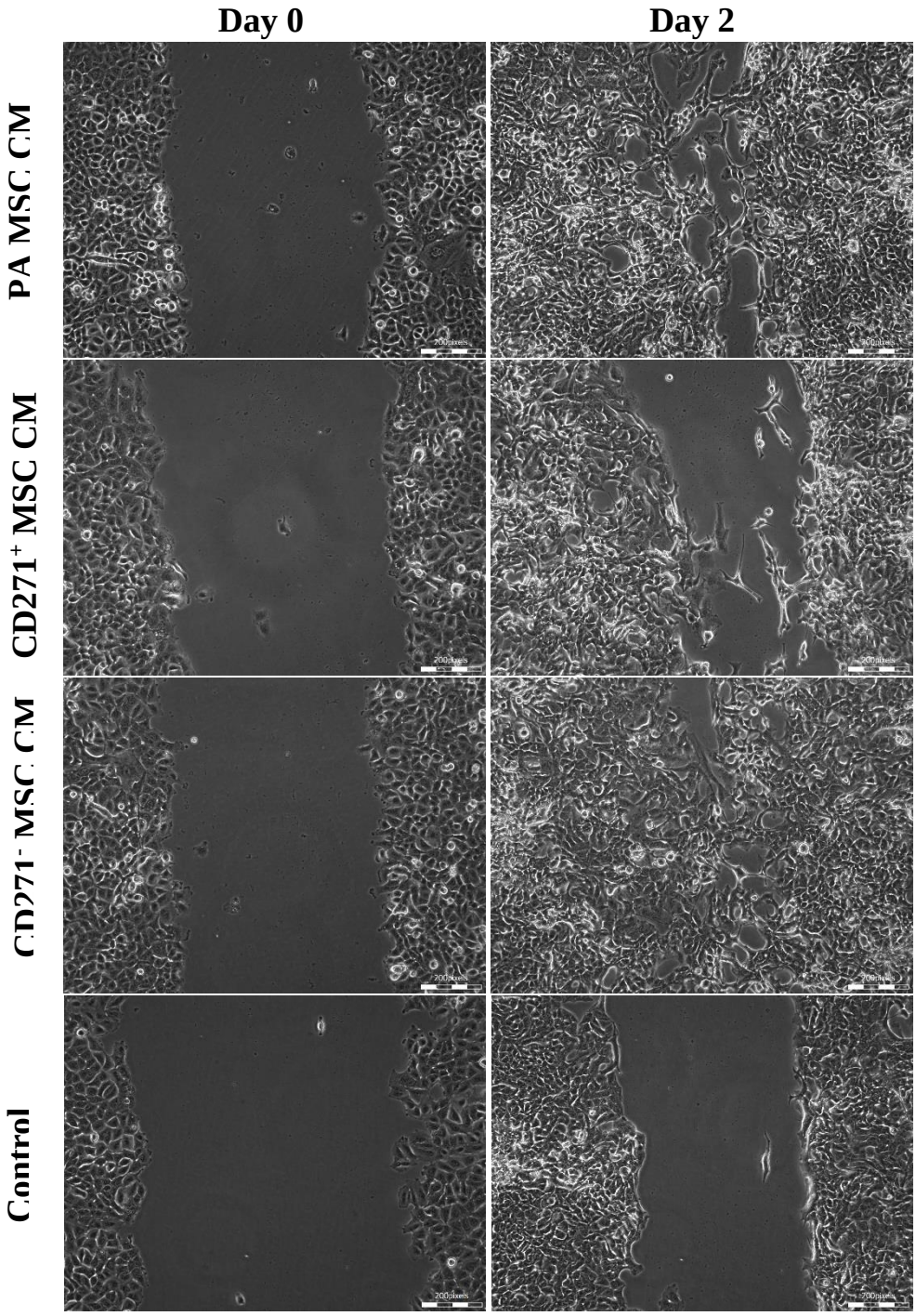

Figure 5:13 The effect of the three MSCs sub-populations PA, CD271^{+}, and CD271^{-} CM on wound closure.

Representative images of monolayer EA.hy926 cells in scratch assays which were treated with the three MSCs sub-populations PA, CD271^{+}, and CD271^{-} CM or control medium for two days. Scale bar =200µm. The images were collected from three independent experiments (i.e. three different donors).

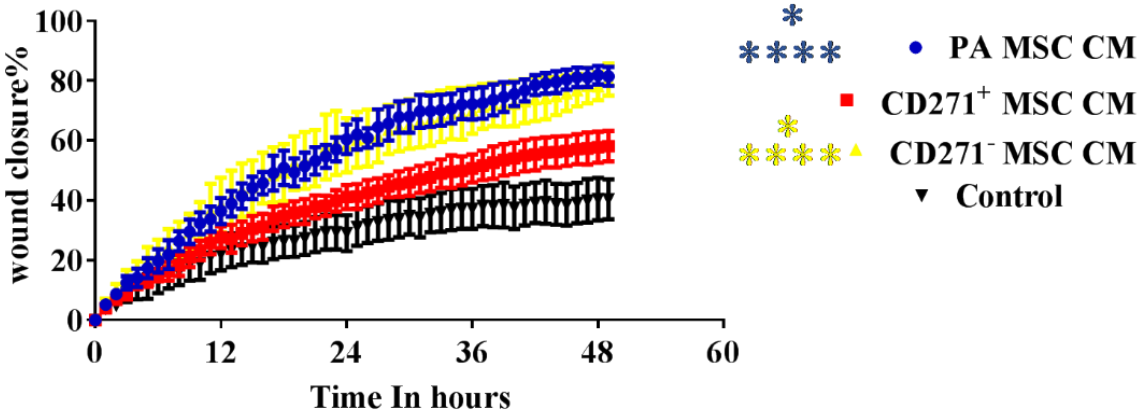

Figure 5:14 Effect of MSC CM of the three MSC subpopulations on EA.hy926 cells migration and proliferation in closing the scratch.

The Cell IQ platform was used for live imaging. Images were generated over two days of incubation. PA MSC CM and $CD271^-$ MSC CM similarly increased wound closure percentage and that was significant when they compared with $CD271^+$ MSC CM (blue star and yellow star *indicates $p \leq 0.05$). The PA MSC CM and $CD271^-$ MSC CM showed significant differences when compared with control medium (blue stars and yellow stars ****indicates $p \leq 0.0001$). Whereas, $CD271^+$ MSC CM showed no significant difference compared with control medium. Each bar represents the mean±SEM of three independent experiments, i.e., testing the MSC CM of subpopulations from three different donors of three replicates per each experiment. A Two-way- ANOVA with Tukey's multiple comparisons tests used to indicate the significant differences.

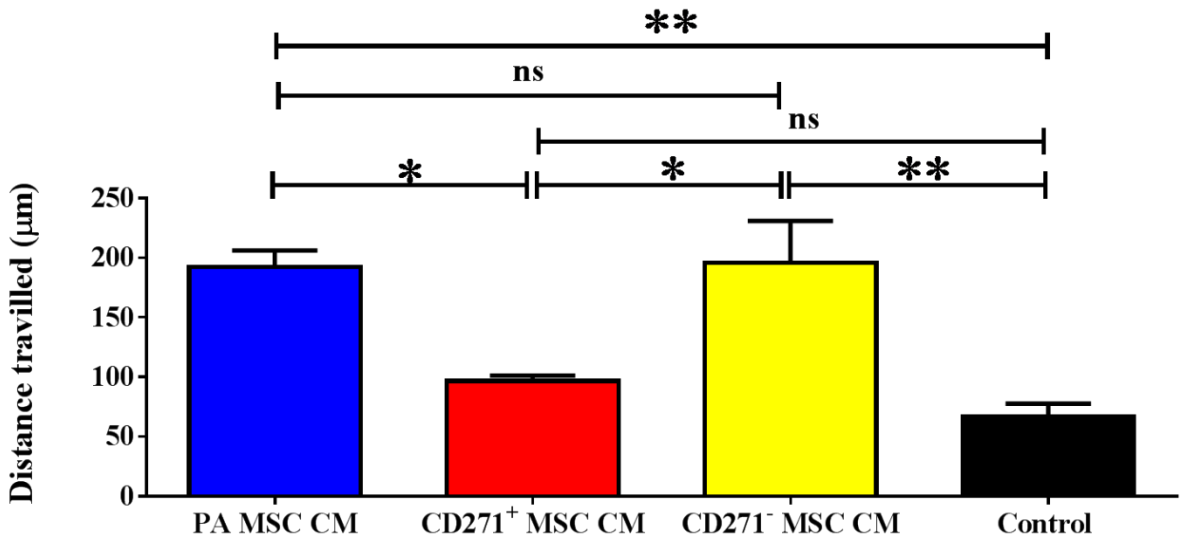

Figure 5:15 The MSC CM of the three MSC subpopulations significantly increased EA.hy926 endothelial cell migration.

Image analysis of the collected digitised images was used to measure the distance that EA.hy926 endothelial cells migrated from the edge of the scratch towards the centre of the wound over a period of two days in the presence of PA MSC CM, $CD271^{+}$MSC CM, $CD271^{-}$ MSC CM or serum-free control medium. As shown, there was a significant increase in distance travelled in PA MSC CM and $CD271^{-}$ MSC CM versus $CD271^{+}$ MSC CM and control medium during this time. Each bar represents the mean±SEM of three independent experiments of three randomly selected cells of each three replicates per of each experiment. *indicates $p \leq 0.05$ and **indicate $p \leq 0.01$. A One-way-ANOVA with Tukey's multiple comparisons test used to indicate the significant differences.

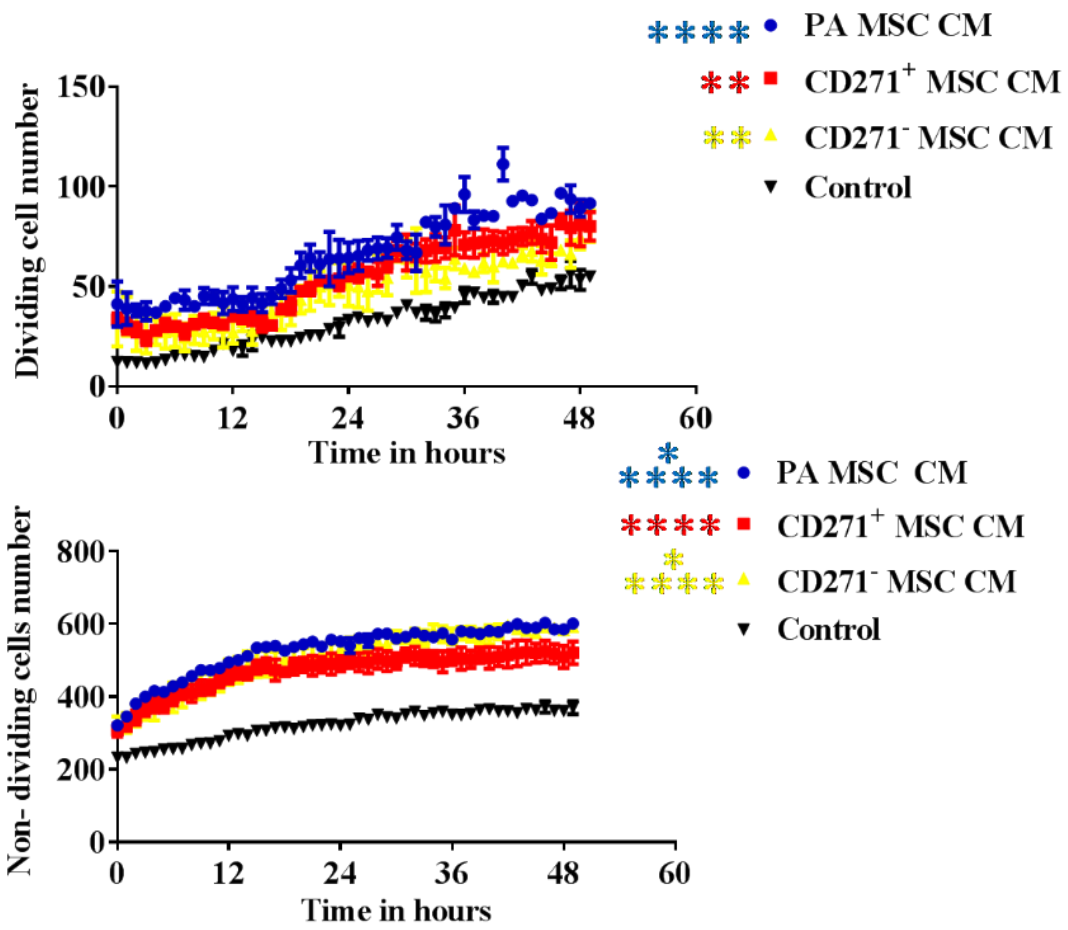

Figure 5:16 The effect of the three MSCs sub-populations PA, CD271^{+}, and CD271^{-} CM on EA.hy926 cells proliferation.

This analysis was performed to track the number of dividing and non-dividing cells present in the wound area. The data on number of dividing cells showed no significant difference amongst the three MSCs populations whereas there was a significant difference when compared with control medium (top panel: blue stars ****indicates $p \leq 0.0001$, red stars and yellow stars** $p \leq 0.01$). The data on non-dividing cells showed that PA CM and CD271^{-} CM were significantly higher compared with CD271^{+} CM (bottom panel: blue and yellow star *indicates $p \leq 0.05$).However, the 3 MSCs populations were significantly higher compared with control medium (bottom panel: blue, red, and yellow stars ****indicates $p \leq 0.0001$). Each bar represents the mean±SEM from three independent experiments, i.e., testing the MSC CM of subpopulations from three different donors of three replicates per each experiment. Two-way- ANOVA with Tukey's multiple comparisons test used to indicate the significant differences.

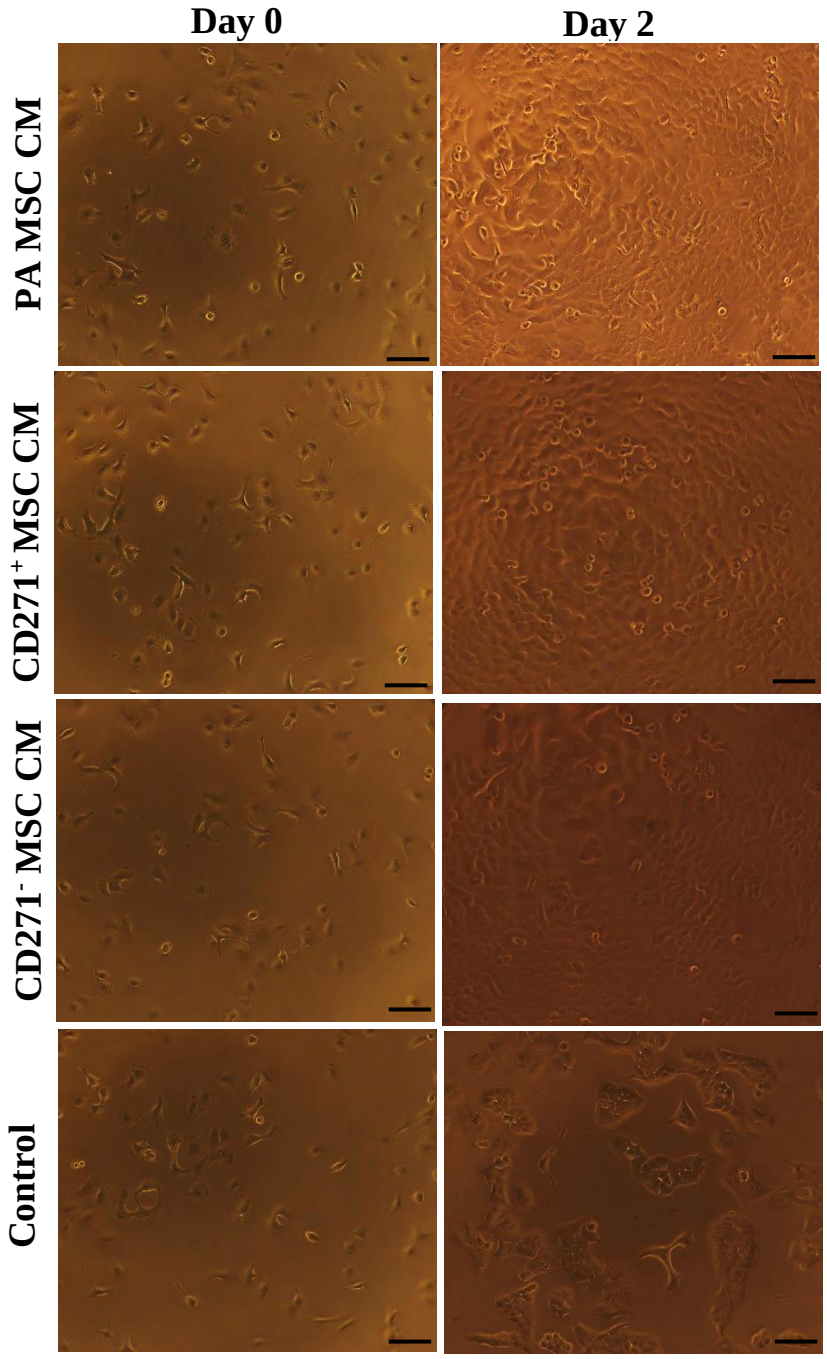

Figure 5:17 The MSC CM of the three MSC subpopulations promoted EA.hy926 endothelial cell proliferation in 96 well plates.

Representative images are shown of EA.hy926 cells cultured in PA MSC CM, $CD271^+$ MSC CM, and $CD271^-$ MSC CM or serum-free control medium. As shown, there was an apparent increase in the number of EA.hy926 cells present in PA, $CD271^+$, and $CD271^-$ CM versus control medium at 2 days of culture. Scale bars = 100µm. Original magnification X10. The images were collected from three independent experiments (i.e. three different donors).

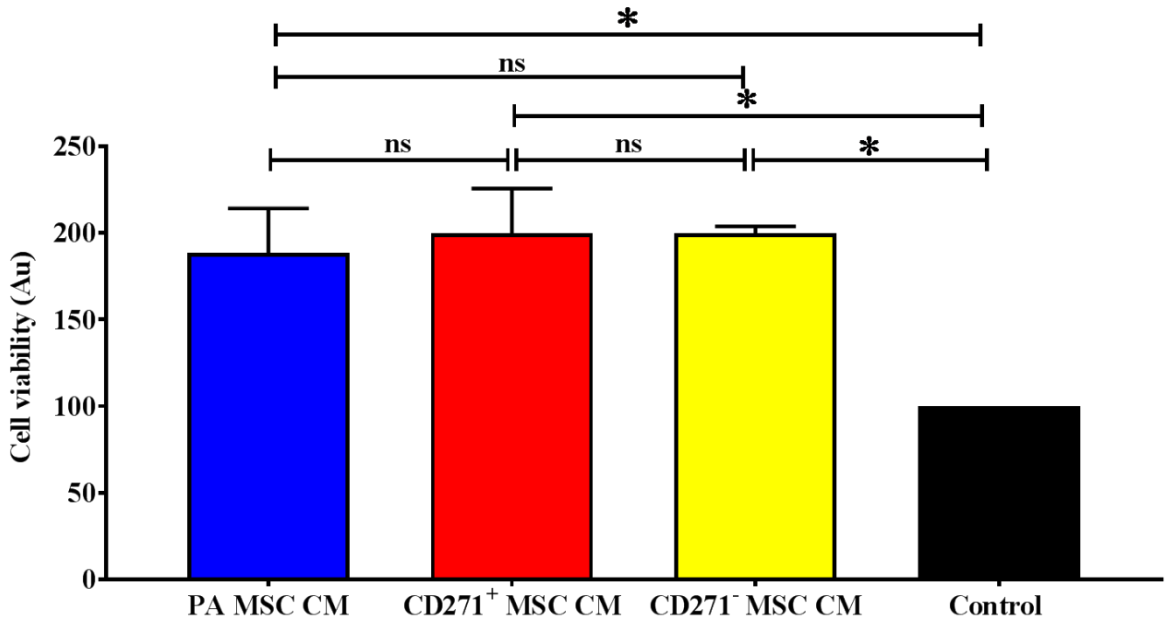

Figure 5:18 The MTT assay confirmed that culturing EA.hy926 endothelial cells in PA MSC CM, CD271$^+$ MSC CM, and CD271$^-$ MSC CM versus control medium significantly increased the number of viable EA.hy926 cells present.

MTT assays were performed to assess viable cell numbers. The results showed a significant increase in the number of viable EA.hy926 cells in PA MSC CM, CD271$^+$ MSC CM, and CD271$^-$ MSC CM versus control medium at two days. Each bar represents the mean±SEM of three independent experiments, i.e., testing the MSC CM of subpopulations from three different donors of five replicates per each experiment. *indicates $p \leq 0.05$. A One-way- ANOVA with Tukey's multiple comparisons test used to indicate the significant differences.

5.4.2 The effect of MSC CM of the three MSC subpopulations to induced morphogenesis of EA.hy926 cells *in vitro*

The paracrine activity of the three MSC subpopulations to induce tube formation from EA.hy926 cells was examined. The assessment of the regenerative capacity of the MSC CM of MSC subpopulations was performed by establishing an *in vitro* assay for tube formation using reduced growth factors Matrigel. The representative images in Figure 5.19 show the EA.hy926 cells cultured on three-dimensional Matrigel and treated with either PA MSC CM, $CD271^+$ MSC CM, $CD271^-$ MSC CM or serum-free medium as a control for one day. Plates were set in the Cell IQ live imaging platform to generate images for the purpose of measurements. The PA MSC CM showed a higher ability to induce the formation of tube-like capillaries from EA.hy926 cells as compared with $CD271^+$ MSC CM and $CD271^-$ MSC CM. The $CD271^-$ MSC CM showed stronger ability to induce the formation of tubule-like capillaries from EA.hy926 cells when compared with $CD271^+$ MSC CM. The results showed that $CD271^+$ MSC CM had the poor effect of inducing the formation of tube-like capillaries from EA.hy926 cells. The data was generated by measuring total tubule length and branch point count using Cell IQ analyser software as described previously in Chapter 2 (Section 2.5.4). The data showed there were significant differences in PA MSC CM effect compared with $CD271^+$ MSC CM (for total tube length p= 0.0001, for total branch point count p= 0.0001). Also, the data showed significant differences between PA MSC CM and $CD271^-$ MSC CM in total tubule length (p= 0.03209) and in total branch count (p= 0.0001). In addition $CD271^-$ MSC CM promoted the tube formation as compared to $CD271^+$ MSC CM significantly (for total tube length p= 0.0032, and for total branch point count p= 0.0.0365). Moreover, both PA MSC CM and $CD271^-$ MSC CM showed significant differences when compared with control medium for total tube length (p= 0.0001, p= 0.0016 respectively) and for branch point count (p= 0.0001, p= 0.0275 respectively).

While, $CD271^+$ MSC CM showed no significant difference when compared with control medium for both total tube length and branch point count (p= 0.9355, p= 0.9795 respectively) (Figure 5.20). The data was obtained from three independent experiments (i.e. three different donors) of five replicates per each experiment.

The amount of VEGF in the MSC CM of the MSC subpopulations was detected by using ELISA. The results showed that there were no significant differences amongst the three MSC CM of MSC subpopulations regarding containing VEGF in their conditioned medium. The amount of VEGF was estimated at a concentration of 307.935 pg/ml for PA MSC CM, 381.018 pg/ml for $CD271^+$ MSC CM, and 362.737 pg/ml for $CD271^-$ MSC CM (Figure 5.21). This data was obtained from two independent experiments (i.e. two different MSC donors).

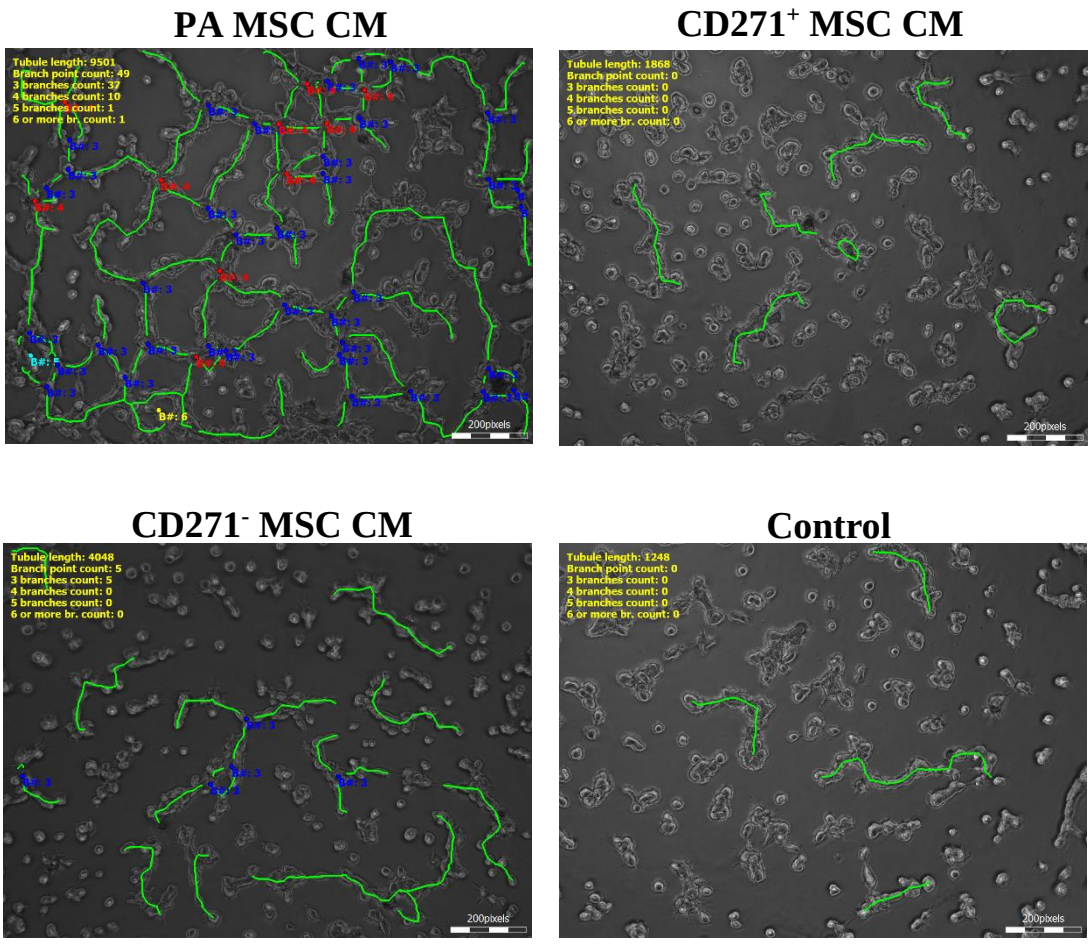

Figure 5:19 The effects of the MSC CM of MSC subpopulations on EA.hy926 endothelial cells cultured on Matrigel.

Representative images are shown of EA.hy926 endothelial cells cultured on Matrigel in the presence of MSC CM of MSC subpopulations or serum-free control medium. These images were subsequently analysed using the Cell IQ imaging software to determine the length (indicated by green lines) and the number of branch points (indicated by blue and red dots) seen in endothelial tubule-like structures. Scale bars = 200µm. The images were collected from three independent experiments (i.e. three different MSC donors).

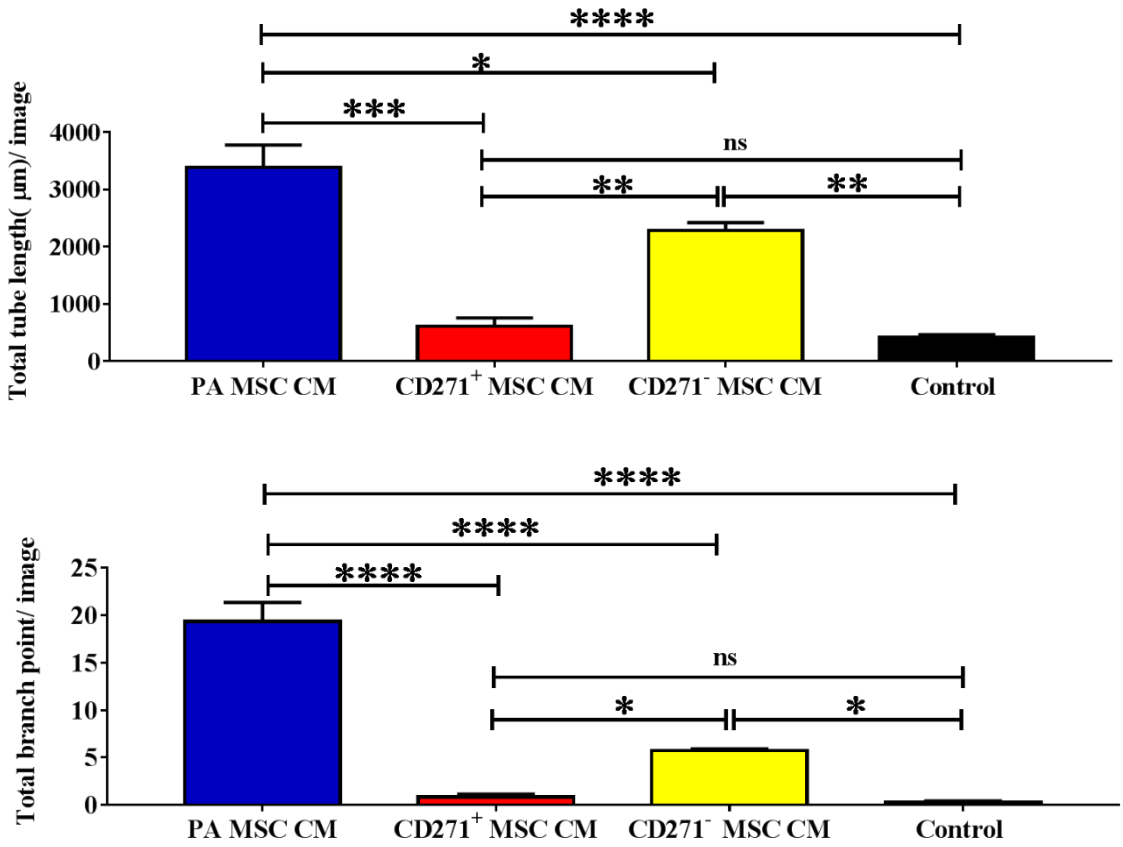

Figure 5:20 The MSC CM of the three MSC subpopulations significantly increased EA.hy926 endothelial tubule formation.

Image analysis of the collected digitised images (see Figure 5.19) was used to measure both the total length of tubules formed (per image) and the number of endothelial tubule branch points (per image). As shown, PA MSC CM significantly improved the total tubule length and total branch point compared with $CD271^+$ MSC CM and $CD271^-$ MSC CM. Also, $CD271^-$ MSC CM had a significant effect compared with $CD271^+$ MSC CM. Each bar represents the mean±SEM of three independent experiments, i.e., testing the MSC CM of subpopulations from three different donors of five replicates per each experiment. *indicates $p \leq 0.05$, ** indicates $p \leq 0.01$, ***indicates $p \leq 0.001$, and ****indicates $p \leq 0.0001$. A One-way- ANOVA with Tukey's multiple comparisons test used to determine the significant differences.

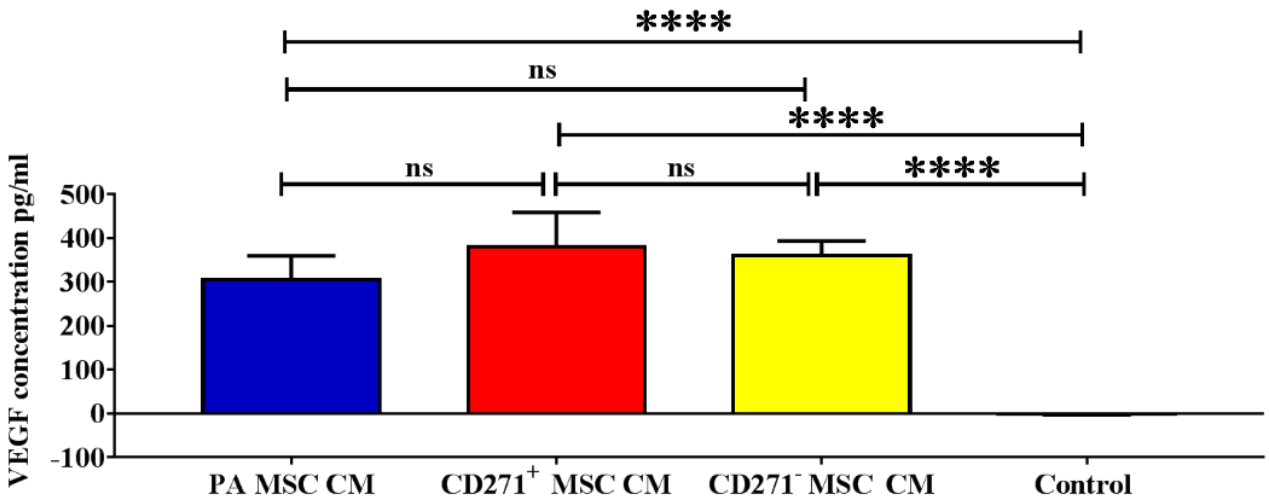

Figure 5:21 The detection of VEGF in the three MSC subpopulations conditioned medium using quantitative ELISA.

The detection of VEGF in the two donors of MSC subpopulations conditioned medium was determined using a quantitative ELISA kit. Using the equation (R2 = 0.9991 as calculated by Excel) approximately (means±SD) 306±53 pg/ml of VEGF in PA MSC CM, 380±78 pg/ml of VEGF in $CD271^+$ MSC CM and 359±33 pg/ml VEGF in $CD271^-$ MSC CM were detected. Each bar represents the means±SD of two independent experiments, i.e., testing the MSC CM of subpopulations from two different donors of two replicates per each experiment. ****indicates $p \leq 0.0001$. A One-way-ANOVA with Tukey's multiple comparisons test used to indicate the significant differences.

5.5 Discussion

MSCs are a heterogeneous population with regenerative therapeutic activities, which have been ascribed to their secretion of paracrine factors (Jayaraman et al., 2013). However, different studies have stated that MSCs exhibited donor-donor and intra-population heterogeneity (Méndez-Ferrer et al., 2010, Morando et al., 2012). Some studies showed that a CD271 positive purified population of MSCs could exert different differentiation potentials related to bone and cartilage repair (Jones et al., 2010, Cuthbert et al., 2015). Unfortunately, there is a lack of information on understanding the functional activities of MSCs at subpopulation levels for their paracrine activities in stimulating nerve growth and angiogenesis.

Therefore, this comparative study was performed to examine the biological differences, if any, in the regenerative paracrine activities of PA, $CD271^+$ and $CD271^-$ human adipose-derived MSC subpopulations on SH-SY5Y neuronal and EA.hy926 endothelial cell model systems.

The three MSC subpopulations were first examined for their capacity to exert an MSC phenotype according to the ISCT criteria (Dominici et al., 2006). The results showed that all three MSC subpopulations were plastic adherent when expanded with a stromal appearance. Furthermore, all three MSC subpopulations differentiated into adipocytes, osteoblasts and chondrocytes. There were no significant differences in their capacity to differentiate into adipocytes. However, PA MSCs and $CD271^+$ MSCs had a significantly greater level of ALP activity after osteogenic treatment than $CD271^-$ MSCs. The increased osteogenic capacity of $CD271^+$ BM MSCs has previously been reported (Cuthbert et al., 2015), which supports the current observation of adipose-derived $CD271^+$ MSCs, although it should be noted that in this previous study the $CD271^+$ MSCs differentiated to form osteoblasts to a significantly greater extent even than PA BM MSCs.

Furthermore, the three MSC subpopulations differentiated to a similar extent, as measured by GAG content, into chondrocytes after inducing the culture pellets with induction medium. Some studies suggested that $CD271^+$ MSCs have more chondrogenic differentiation capacity compared with PA MSCs (Mifune et al., 2013). However, the tissue of origin might be the reason for such differences in chondrogenic potentiality as Mifune et al., 2013 used BM MSCs.

Moreover, the three MSC subpopulations were examined for their ability to express specific cell surface markers. The flow cytometry results showed that the three MSC subpopulations shared very similar expression levels of standard MSCs markers such as CD44, CD73, CD90, and CD105, but lacked expression to haematopoietic cell surface markers such as CD34 and CD45 (Table 5.4). Hence, it can be concluded that all three subpopulations of MSCs met the ISCT criteria and can justifiably be termed MSCs. Although MSCs from different tissue sources share similar morphological appearance and differentiation capacities, their immunophenotype may show differences in their expression of CD markers. For example, several studies have suggested that AT MSCs have the ability to express CD34 when tissue culture expanded at early passages (Strioga et al., 2012, Ammar et al., 2015).This may explain the results of CD profiling for AT MSCs 126 donor used in this study as they showed some positivity for CD34.

This study also examined the expression of CD271 by $CD271^+$ positively selected cells as well as the PA MSCs and $CD271^-$ cells after cultivation. The flow cytometry data obtained by this study showed that all MSC subpopulations were immunonegative for CD271 at passage II. Hence it can be concluded that the $CD271^+$ MSCs lost CD271 at early stages of culture expansion. Similarly, Churchman et al., 2012 showed that $CD271^+$ BM MSCS also lost the expression of CD271 as they were culture expanded (Churchman et al., 2012). Thus, it seems that CD271 is lost from adipose MSCs as well as BM MSCs during cell culture expansion. The reasons for the loss of CD271 expression are currently unknown, although other researchers have suggested that the prevalence of $CD271^+$ MSCs *in vivo* may relate to microenvironmental and physiological factors (Cattoretti et al., 1993, Churchman et al., 2012). Whilst it would have been advantageous to confirm that the MACS

technique has successfully isolated $CD271^+$ cells, it was not possible to test CD271 positivity in the freshly isolated cell population due to limitations in cell numbers available after purification. However, other studies have demonstrated that the proportion of $CD271^+$ cells yielded after purification from BM or adipose tissue was ~ 0.5% of all mononucleated cells present (Jones et al., 2006, Alvarez-Viejo et al., 2013).

Various studies have reported that the secretomes of MSCs exert a beneficial impact on damaged tissue and have ascribed this effect to a wide range of different bioactive secreted molecules including growth factors, cytokines, chemokines and EVs (Lee et al., 2014, Lopatina et al., 2014, Wright et al., 2014, Kalinina et al., 2015). However, these previous studies have examined the secretomes from heterogeneous MSC populations. As alluded to earlier, this study has examined for the first time the neurotrophic and angiogenic activities of MSC subpopulations according to their isolation, which was based on PA and CD271 immunopositivity. By using *in vitro* assays with SH-SY5Y cells, it has been shown that the MSC CM of all MSC subpopulations significantly stimulated SH-SY5Y neurite outgrowth and neuronal cell survival and proliferation. There were no significant differences amongst the three MSC subpopulations in this neurotrophic effect. This finding of enhanced SH-SY5Y neurite outgrowth was based on the morphological appearance of the cells, and a further experimental confirmation to validate the effects of MSC CM in promoting neuronal differentiation, e.g., through increased Beta-III tubulin immunopositivity would be beneficial. Nonetheless, the data shown in this chapter further supports the hypothesis that MSCs are neurotrophic through their secretion of neurotrophic factors and suggests that MSC subpopulations have a similar capacity in this regard. Further studies to identify the presence and levels of different known neurotrophic factors in the MSC CM, and confirmation of their activity, e.g. through the use of blocking antibodies or through gene knockdown strategies, in promoting SH-SY5Y neuronal differentiation and growth are also warranted and would help explain potential mechanisms of action.

Interestingly, the investigations of angiogenic activity amongst these three MSC subpopulations conditioned medium have shown very clear variances in their biological effect on endothelial cells.

In EA.hy926 endothelial cell scratch wound assays, the results showed that both the PA MSC CM and the $CD271^-$ MSC CM significantly increasing scratch wound closure rates compared with the $CD271^+$ MSC CM and control medium.

This variance in effects amongst the MSC CM of the MSC subpopulations was examined further by tracking cell movements and counting dividing and non-dividing cells in the scratch wound area. The conditioned medium from $CD271^+$ MSCs showed a lower biological effect on increasing cell movement towards the centre of the scratch wound area compared with PA MSC CM and $CD271^-$ MSC CM. This finding may further interpret through the findings of dividing and non-dividing cells. Whereas the $CD271^+$ MSC CM had a similar effect on the number of dividing cells, but their effect on non-dividing cells was less when compared with the effects of PA MSC CM and $CD271^+$ MSC CM. The explanation for such difference could attributed to the fact that the cells might be under the influence of other factors that might restrict or inhibited their movement or directed them into random directions rather than towards the other side of scratch (i.e. the centre of scratch wound area) or could be as a result of the lack of other factors affecting cell movement. Therefore, further studies to identify the presence and levels of different known cytokines and growth factors that play a role in the mediation of cell migration is required (Chen et al., 2008).

Furthermore, the results of the tube formation assay using Matrigel reduced growth factors confirmed the angiogenic effect of the MSC subpopulation conditioned medium. Whereas the $CD271^+$ MSC CM again showed poor enhancement on the formation of tube-like capillaries from EA.hy926 cells, meanwhile, PA MSC CM and $CD271^-$ MSC CM revealed a stronger effect. In this assay, it is obvious that PA MSC CM and $CD271^-$ MSC CM showed a different biological effect when compared with their effect in the scratch wound assay. Herein the PA MSC CM significantly promoted the tube formation compared with $CD271^-$ MSC CM, whereas in the scratch wound assay there were no significant differences in their effect on EA.hy926 cell proliferation and migration and wound closure rate. The explanation of such differences in the biological activities might be related to the fact that although the $CD271^+$ population has a poor angiogenic effect but, their presence in the heterogeneous

population has a role to direct or regulate the other population to exert their biological effect. Hence these findings support the hypothesis raised in this study where the isolation of a more homogenous population could exert differences in their biological effects. Such findings highlight the benefit of isolating certain MSCs subsets to treat an injury where specific biological activity is required. This finding also further support the findings of Mifune et al., 2013 findings as they suggested that $CD271^+$ MSCs showed better hyaline cartilage repair *in vivo*, where the lack of neovascularization promotion is required.

Nonetheless, the detection of VEGF in the conditioned medium of the three MSC subpopulations using an enzyme-linked immunosorbent assay showed the three MSC subpopulations secreted VEGF to a similar extent. This finding may suggest that although VEGF plays the main role in the neovascularization process, other factors are required to achieve a fully functional vascularization (or lack of inhibitors).

In conclusion, this study has demonstrated for the first time that the purified MSCs derived from adipose tissue culture could exert a different biological effect. The MSCs subpopulations showed MSC phenotypes which have been established by the ISCT. The MSC CM of the three MSC subpopulations exerted a neurogenic effect to a similar extent, whereas, their angiogenic paracrine effect has shown remarkable differences among the three subpopulations. The $CD271^+$ MSC CM had a poor effect on enhancing neovascularization by the EA.hy926 cells. The demonstration of poor neovascularisation enhancement by $CD271^+$ MSC CM might explain their suitability to repair cartilage as the hyaline cartilage is an avascular tissue (Mifune et al., 2013). Finally, the data obtained by this study may suggest that the isolation and purification of a certain subpopulation of MSCs previously identified *in vivo* could result in isolation of a subpopulation that has the capacity of exerting more tailored biological activities. Also, the consequence of such purification will allow an increase in the efficiency of clinical applications of MSCs to treat and repair specific kind of injured tissues.

Chapter 6: Discussion

Since the emergence of MSCs in the field of regenerative medicine as a cell-based treatment, numerous investigations have been done on their therapeutic capacity to treat a broad range of diseases. Such interest can be attributed to their characteristic features including; fewer ethical issues than those surrounding ESCs as their extraction does not require destruction of an embryo, relative ease of access from patient sources, lack of immune rejection if applied autologously, and lack risk of tumour formation (Bongso and Richards, 2004, Larijani et al., 2012). In recent years, MSCs derived from adipose tissue have received more attention than those derived from bone marrow in terms of regenerative applications for repairing injured and damaged tissues. Such attention can be ascribed to the fact that adipose tissue is a more abundant tissue, again ease of access, and the harvesting of adipose tissue has a low morbidity rate when compared with the harvesting of bone marrow. Also, the number of the cells released from adipose tissue is higher compared to bone marrow (Padoin et al., 2008). It also has recently become more accepted that the MSCs exert their potential therapeutic activities through their secretomes (Teixeira et al., 2013). The trophic activities of secretomes of MSCs have been addressed in different aspects of regenerative medicine including SCI. It is well known that the recovery after SCI is elusive. Many experimental studies in animals showed encouraging results of recovery and regaining some functions after transplantation of MSCs in the injured spinal cord (Lim et al., 2007, Park et al., 2012b, Li and Lepski, 2013, Dasari et al., 2014). It is worth mentioning that in the absence of an animal model fully reflecting the SCI in human, it can be a challenging step to bridge the gap between experimental studies evaluating the effects of MSCs in rodent models through the translation research that leads clinical trials in human. Therefore, the research described in this study was aimed to evaluate and improve several strategies for application of secretomes of MSCs as a treatment for SCI. These strategies were:

- Examining the secretomes' activities of MSCs derived from canine adipose tissue using established assays for neurotrophic and angiogenic.

- Comparing the neurotrophic and angiogenic activity of canine and human MSCs in a step-by-step approach to help validate dogs as a clinically relevant large animal model for SCI treatments.
- Examining the regenerative paracrine activities of subset populations of human MSCs to increase the likelihood and efficiency of MSC-based clinical applications to treat and repair SCI, where avoiding cell heterogeneity is potentially advantageous.

The MSCs used in this study were derived from canine and human adipose tissue. The investigation of canine MSCs in this study was for the following reasons. First, such investigation can bring benefit to both human and veterinary regenerative medicine as a means of treating dogs with SCI. This in itself is a potential clinical application. Second, dogs represent a better large animal model for human treatment than rodents as dogs share some similarities with humans in terms of wound causation, pathophysiology and disease presentation and scale (Starkey et al., 2005, Khanna et al., 2006, McMahill et al., 2015). Third, if canine MSCs are shown to have a therapeutic effect in dogs with SCI, then understanding and comparing their activity with human MSCs may help inform how best to apply the human MSCs in the clinical setting.

The therapeutic potential of MSCs has been widely investigated for various diseases including mainly tissue injury and immune disorders (Patel et al., 2013). Dogs are valuable animal models since most of the disease is naturally occurring similar to humans. The transplantation and regenerative activities of canine MSCs have been studied in many clinical trials for a naturally occurring disease like keratoconjunctivitis Sicca (Villatoro et al., 2015), and SCI (Penha et al., 2014). Interestingly the research on cMSCs is based on investigations of the potential therapeutic effect of the cells only; there is a lack of information about the secretomes' action of canine MSCs. Thus, the study data presented in chapter 3 of results has described for the first time the potential therapeutic activities of canine MSCs secretomes for in stimulating neurogenesis and angiogenesis, which supports their application as a treatment for SCI in the dog.

The canine MSCs were initially examined for their capacity to display MSCs phenotype, according to the minimal criteria proposed by the ISCT to define MSCs. These criteria are: i) adherence to plastic, ii) specific cell surface antigen expression, for example immunopositivity for CD73, CD90 and CD105, immunonegativity for CD34, CD45, CD11b, CD14, CD19, CD79a and HLA-DR., iii) multipotent differentiation potential into the three mesenchymal lineage cell types of adipocytes, osteoblasts and chondrocytes, at least *in vitro* (Dominici et al., 2006), where the cMSCs have matched these criteria. Largely, the canine MSCs have matched these criteria, although there was some difference from human MSC phenotypes in that a proportion of canine MSCs were CD34 immunopositive. This demonstrated that the cells that were isolated and culture expanded from the inguinal fat pads of a number of dogs could be classified as MSCs.

Recent studies suggested that the mechanism of MSCs therapeutic effects might not work through differentiation of transplanted MSCs at the site of injury. In fact, MSCs exert their therapeutic effect through their secretomes that have a varied array of proteins including growth factors, cytokines, chemokines, metabolites and bioactive lipids (Kupcova Skalnikova, 2013). These secretory molecules have a role in tissue repair and regeneration after injury (Pluchino and Cossetti, 2013). In experimental studies, MSC CM have demonstrated the activities that required for tissue repair (Walter et al., 2010, Isakson et al., 2015). Therefore, MSCs represent one of the most promising cells for cell-based therapy application in human and veterinary regenerative medicine (DiMarino et al., 2013).

The rational basis of the study presented in Chapter 3 was first to characterise the MSC phenotype, as discussed, then to determine the effects of cMSC CM on neurite outgrowth and neuronal cell growth and survival, using the SH-SY5Y neuroblastoma cell line, and, on endothelial cell migration, proliferation and tubule formation using the EA.hy926 endothelial cell line. The findings suggested that cMSC CM exerted neurogenic and angiogenic effects.

These findings support the hypothesis raised by this study of considering the trophic activity of cMSC CM as potential therapies for SCI. The findings could shed light on the benefits of secretomes of

cultured cMSCs as an alternative for cell therapy with a view toward a trial in SCI repair in veterinary regenerative medicine since the regain of neuronal survival, axonal growth and revascularisation play the main role in repair processes for the injured spinal cord (Quertainmont et al., 2012). However, mechanisms of action of cMSCs are still poorly identified and have not been fully addressed in this study. Therefore, further investigation is required on the identification of the conditioned medium composition.

The preliminary data (in Appendix Figure 7.1) showed for the first time the isolation of exosomes from cMSC CM. Both concentration and diameter of these exosomes were measured using the qNano machine. This preliminary data suggested the requirement for future work including the examining of the functionality of these isolated exosomes, as human exosomes have shown a potential effect on angiogenesis and neurogenesis (Zhang et al., 2015, Kim et al., 2016).

In human regenerative medicine, there is an urgent need for a large animal model mirroring the phenotype of the target disease and bridging the gap between translation research and human clinical trials (Harding et al., 2013). As mentioned earlier in this chapter, dogs are considered as a good model to represent SCI in human, for the reasons described above and in Chapter One (Section 1.5). These are briefly, long life span, large body mass and naturally occurring diseases. SCI lesions are very similar to humans as both SCI occur due to traumatic injuries because of car accidents or non-traumatic injuries due to IVDD (McMahill et al., 2015). The findings in chapter four of results support the proposal of considering dogs with SCI as a model for human SCI. To summarise these findings of work, it was clearly demonstrated that both human and canine MSCs underwent tri-lineage differentiation into adipocytes, osteoblasts and chondrocytes. Although cMSCs showed poor adipogenic differentiation, this could be ascribed to the composition of the induction medium composition which was more suitable to human MSCs rather than cMSCs. The reason behind the chosen human induction medium to induce adipogenesis in cMSCs was to avoid variations of experimental conditions. In future using induction medium specific or suitable for cMSCs is recommended. Also, both human and canine MSCs have shown a lack of expression of

haematopoietic CD markers such as CD34 and CD45, but they showed positive expression to most of MSCs' CD markers such as CD44 and CD90 to a similar extent. Hence, this suggested that cMSCs have the capacity to exert an MSC phenotype to a similar extent to hMSCs in culture expanded.

The comparative examination of MSC CM from both human and canine showed interesting findings for their neurogenic and angiogenic paracrine activities as SH-SY5Y cells, and EA.hy926 cells were used as a model system to test these two activities respectively. Both morphological analysis using Cell IQ analysis software and immunohistochemistry for B-III tubulin staining showed both human and canine MSC CM had a neurotrophic effect on neurite outgrowth and neuronal survival from the SH-SY5Y cells line to a similar extent.

Similarly, the examining of angiogenic effects of both human and canine MSC CM in scratch wound assay and tube formation assay suggested that human and canine MSC CM exerted their angiogenic effect to a similar extent. Due to this similarity in paracrine effects from both human and canine MSC CM, a comparison of the protein sequences was performed. The amino acid sequences for NGF and VEGF were sought since NGF plays a key role in neurogenesis and VEGF is the key role for angiogenesis. This comparison was done to examine the extent of similarity between human and canine in terms of protein sequences of these growth factors. Figure 6.1 and 6.2 shows that these two human and canine growth factors are homologous. Alignment of human and canine NGF and VEGF amino acid sequences revealed a high degree of sequence homology. Interestingly, the detection of VEGF in conditioned medium from both human and canine MSCs using a human ELISA kit has shown that although the ELISA kit was specific for quantitative determination of VEGF in human samples, it has detected VEGF in the canine sample as well. VEGF in cMSC CM was detected at a concentration 229.58 pg/ml, and VEGF in human MSC CM was detected at concentration 378.39 pg/ml (measuring VEGF is a first step toward characterising the secretomes).

Although the findings in this study could encourage the idea of adopting a dog as a model in translation research for cell-based therapy (i.e. treatment using MSCs), however, clearly there is a need for an *in vivo* study to confirm the potential effect of cMSC CM. Also, both cell models, i.e.,

SH-SY5Y cell and EA.hy926 cells used in this comparative study are of human origin and derived from tumours. Thus, responses of these cells to cross-species growth factors may differ from their response to primary neuronal and endothelial cells of the same species. Therefore, these findings may highlight the importance of establishing neuronal and endothelial cells originating from canine as a model system for such investigation. Also and as stated earlier in this section, further investigation on the mechanisms of action of cMSC CM is required and also a further proteomic profile for cMSC CM is recommended. As described in the introduction (section 1.4) human MSC CM is known be composed of various growth factors, cytokines, and ECM (Walter et al., 2010, Kupcova Skalnikova, 2013). It is likely that cMSC CM contains similar factors.

Also, despite these advantages of using cell lines in research they also have their disadvantages, represented by the fact that cell lines after continuous passaging over a period of time can show genotypic and phenotypic variations. Therefore, researchers should be careful about only relying on data generated with cell lines. Hence, the primary cells are believed to be more biologically relevant tools than cell lines for studying human and animal biology. Although, primary cells have a limited lifespan, they resemble tissue characteristics and their mutation capacity is low compared with cell lines that have an infinite life span and that lose tissue characteristics and their mutation capacity is high (Hughes et al., 2007).

Interestingly, primary cells have also been used in the investigation of the potential effect of conditioned medium of MSCs. Wright et al 2007 and 2014 tested the MSCs secretomes effect on neurite outgrowth using dorsal root ganglia and spinal cord model. Based on their studies they suggested that MSCs have impact effect on promoting neurite outgrowth despite the presence of inhibitory factors (Wright et al., 2007, Wright et al., 2014).

Score	Expect	Method	Identities	Positives
422 bits(1085)	2e-151	Compositional matrix adjust.	219/241(91%)	223/241(92%)

```
Canine  1    MSMLFYTLITALLIGIRAEPHPESHVPAGHAIPHAHWTKLQHSLDTALRRARSAPAGAIA  60
             MSMLFYTLITA LIGI+AEPH ES+VPAGH IP AHWTKLQHSLDTALRRARSAPA AIA
Human   1    MSMLFYTLITAFLIGIQAEPHSESNVPAGHTIPQAHWTKLQHSLDTALRRARSAPAAAIA  60

Canine  61   ARVTGQTRNITVDPKLFKKRRLRSPRVLFSTHPPPVAADAQDLDLEAGSTASVNRTHRSK  120
             ARV GQTRNITVDP+LFKKRRLRSPRVLFST PP  AAD QDLD E G  A  NRTHRSK
Human   61   ARVAGQTRNITVDPRLFKKRRLRSPRVLFSTQPPREAADTQDLDFEVGGAAPFNRTHRSK  120

Canine  121  RSSSHPVFHRGEFSVCDSVSVWVGDKTTATDIKGKEVMVLGEVNINNSVFKQYFFETKCR  180
             RSSSHP+FHRGEFSVCDSVSVWVGDKTTATDIKGKEVMVLGEVNINNSVFKQYFFETKCR
Human   121  RSSSHPIFHRGEFSVCDSVSVWVGDKTTATDIKGKEVMVLGEVNINNSVFKQYFFETKCR  180

Canine  181  DPTPVDSGCRGIDSKHWNSYCTTTHTFVKALTMDGKQAAWRFIRIDTACVCVLSRKAGRR  240
             DP PVDSGCRGIDSKHWNSYCTTTHTFVKALTMDGKQAAWRFIRIDTACVCVLSRKA RR
Human   181  DPNPVDSGCRGIDSKHWNSYCTTTHTFVKALTMDGKQAAWRFIRIDTACVCVLSRKAVRR  240

Canine  241  A  241
             A
Human   241  A  241
```

Figure 6:1 Alignment of NGF amino acid sequences of canine (NCBI Reference Sequence: NP_001181879.1) and human (NCBI Reference Sequence: NP_002497.2).

Differences are marked in the human sequence by highlighting the residues in yellow.

Score	Expect	Method	Identities	Positives	Gaps
377 bits(969)	8e-132	Compositional matrix adjust.	205/215(95%)	207/215(96%)	1/215(0%)

```
Canine  1    MNFLLSWVHWSLALLLYLHHAKWSQAAPMA-GGEHKPHEVVKFMDVYQRSYCRPIETLVD  59
             MNFLLSWVHWSLALLLYLHHAKWSQAAPMA GG    HEVVKFMDVYQRSYC PIETLVD
Human   181  MNFLLSWVHWSLALLLYLHHAKWSQAAPMAEGGGQNHHEVVKFMDVYQRSYCHPIETLVD  240

Canine  60   IFQEYPDEIEYIFKPSCVPLMRCGGCCNDEGLECVPTEEFNITMQIMRIKPHQGQHIGEM  119
             IFQEYPDEIEYIFKPSCVPLMRCGGCCNDEGLECVPTEE NITMQIMRIKPHQGQHIGEM
Human   241  IFQEYPDEIEYIFKPSCVPLMRCGGCCNDEGLECVPTEESNITMQIMRIKPHQGQHIGEM  300

Canine  120  SFLQHSKCECRPKKDRARQEKKSIRGKGKGQKRKRKKSRYKPWSVPCGPCSERRKHLFVQ  179
             SFLQH+KCECRPKKDRARQEKKS+RGKGKGQKRKRKKSRYK WSVPCGPCSERRKHLFVQ
Human   301  SFLQHNKCECRPKKDRARQEKKSVRGKGKGQKRKRKKSRYKSWSVPCGPCSERRKHLFVQ  360

Canine  180  DPQTCKCSCKNTDSRCKARQLELNERTCRCDKPRR  214
             DPQTCKCSCKNTDSRCKARQLELNERTCRCDKPRR
Human   361  DPQTCKCSCKNTDSRCKARQLELNERTCRCDKPRR  395
```

Figure 6:2 Alignment of VEGF amino acid sequences of canine (NCBI Reference Sequence: NP_001003175.2) and human (NCBI Reference Sequence: NP_001165095.1).

Differences are marked in the human sequence by highlighting the residues in yellow.

It is worth mentioning that MSCs reveal differences in their biological properties based on their tissue of source (Elahi et al., 2016). In fact, recently, there is a clear interest in using AT MSCs in different aspects of research in regenerative medicine over the BM MSCs. This can be as a result of the fact that AT MSCs possess several features that make AT MSCs preferable, these include; ease of access and the harvesting of adipose tissue has a low morbidity rate when compared with the harvesting of bone marrow (Padoin et al., 2008). Also, for their high quantity of MSCs released from adipose tissue compared with yields from bone marrow. Besides, AT MSCs are characterised by their high proliferation capacity and secreted proteins (basic fibroblast growth factor, interferon-γ, and Insulin-like growth factor-1), and immunomodulatory effects (Li et al., 2015). However, AT MSCs are a highly heterogeneous population. SVF released from collagenase processed adipose tissue is composed of different stem cells subpopulations and fully differentiated cells (differentiated endothelial cells, smooth muscle cells and pericytes) (Ho et al., 2008).

Since CD271 has emerged as a CD marker for isolation of subpopulations within MSCs, many studies; have focused on their differentiation capacity regardless of their secretomes' activities (Quirici et al., 2002). Hence, in Chapter Five of results, and as a continuation in the loop of the translational pathway to human clinical trials, the study aimed to highlight the $CD271^+$ MSC CM neurogenic and angiogenic activities compared with the whole population of MSCs, i.e., PA MSC CM and $CD271^-$ MSC CM. The development of homogenous MSC population of known paracrine activity would allow an increase in the efficiency of clinical applications of MSCs to treat and repair injuries including SCI.

The MSC subpopulations were first examined to determine if they match the ISCT criteria. The three MSC populations had an equivalent capacity to differentiate into adipocytes and chondrocytes. Whereas they showed variances in their capacity to differentiate into osteoblasts as the PA MSCs and $CD271^+$ MSCs exerted a high level of ALP. This observation was supported by other researchers (Cuthbert et al., 2015) although in their study the $CD271^+$ MSCs had greater osteogenic activity even when compared to PA MSCs.

This study has examined the ALP expression from 2 MSC donors following their osteogenic induction, therefore, increasing the number of repeat experiment is recommended. As the limited number of MSC donors (i.e., 2 MSC donors) used in this experiment could be the reason for unmarked differences of osteogenic differentiation between $CD271^+$ MSCs and PA MSCs. Moreover, the three MSC subpopulations shared very similar expression levels of standard MSC markers such as CD44, CD73, CD90, and CD105, but lacked expression of haematopoietic cell surface markers such as CD34 and CD45. Hence, from all above it is possible to conclude that all MSC subpopulations exerted the MSCs phenotype.

Interestingly, $CD271^+$ selected MSCs lost their capacity to express the CD271 cell surface marker at an early passage, i.e., passage II. Similarly, Churchman et al., 2012 in their study showed that the BM MSCs $CD271^+$ also lost the expression of CD271 as the culture expanded. They assumed this may relate to the physiologic requirements for bone remodelling, and hence the production of osteoblasts, may stimulate CD271 cells *in vivo*. Growing as monolayers in culture and *in vitro* environment conditions could also be the reason behind such loss rather than functional differences between cells (Tormin et al., 2011). Hence, these findings could suggest that the culture expanded MSCs lost the expression of CD271 in even earlier passages. Although the mechanism underlying the loss of expression of CD271 is still unknown, but researchers have suggested that the presence of $CD271^+$ MSCs *in vivo* may relate to microenvironmental and physiological factors (Cattoretti et al., 1993, Churchman et al., 2012).

As stated earlier the aim of this study was to develop a strategy based on the generation of a homogenous MSC population of known paracrine activity which could be advantageous in the application of these cells as therapy for SCI. The three MSC subpopulations' conditioned medium showed neurogenic effects on SH-SY5Y neuroblastoma cells to a similar extent. However, this finding of enhanced SH-SY5Y neurite outgrowth was based on the morphological appearance of the cells, therefore, further experimental confirmation to validate the effects of MSC CM in promoting neuronal differentiation, e.g., through increased Beta-III tubulin immunopositivity would be

beneficial to emphasise the SH-SY5Y cells differentiation. Whereas, the finding of angiogenic activity amongst MSC subpopulations conditioned medium showed an interesting observation.

In the scratch wound assay and tube formation assay, the $CD271^+$ MSC CM showed less angiogenic activity. In the EA.hy926 endothelial scratch wound assay, Cell IQ results showed that $CD271^+$ MSC CM had a low angiogenic effect compared with PA MSC CM and $CD271^-$ MSC CM. This finding was a further corroborated by the tube formation assay as the $CD271^+$ MSC CM showed the poor angiogenic effect on enhancing formation of tube-like capillaries from EA.hy926 cells in Matrigel reduced growth factor assay when compared with PA MSC CM and $CD271^-$ MSC CM. Hence, this finding may support the hypothesis raised in this study as the homogenous population of MSCs exerted different biological effects compared to the heterogeneous population.

The data in this study indicated that the isolation strategy based on CD271 expression resulted in a cell population which has a low paracrine activity of angiogenic activity, although VEGF (which plays the main role in angiogenesis) was secreted by these subpopulations at a similar concentration. These findings encourage that further understanding of the mechanisms of action of MSC CM could be obtained through screening for the presence of other endogenous regulators that are involved in the process of angiogenesis.

This finding has answered the question raised in this study as to whether the subset of MSCs population exhibit a different pattern of action. This supports the idea of selecting specific homogenous populations to repair a specific kind of injury. MSCs $CD271^+$ might not be recommended for SCI repair, but it could be useful for repairing tissue where the requirement for new blood vessels are not necessary such as repairing articular cartilage, as this subpopulation in other studies showed a high capacity for chondrogenesis capacity (Mifune et al., 2013). In addition to the isolation of subpopulations using CD271 CD marker, on different occasions, many researchers have used different CD markers to investigate their biological activities. For example, isolation of MSCs subpopulation based on their expression of CD 105. In fact, CD105 is a receptor that plays an important role in development and remodelling of blood vessels (Duff et al., 2003).

Many studies claimed that CD105 MSCs have more myogenic potentiality. Both *in vitro* and *in vivo* studies suggested that CD105 MSCs differentiation into myoblast-like cells after myogenic induction and differentiation into muscle cells after their transplantation into damaged skeletal muscles in rats (Conconi et al., 2006, Ranganath et al., 2012). Another example for CD marker used to sort specific subset population of MSCs is CD146. The studies suggested that the localization of this subpopulation of MSCs is perivascular (Crisan et al., 2008).

Conclusion

In conclusion, from all of the results described above, there are three key findings presented in this thesis. In Chapter 3 of results, the study has demonstrated for the first time that the secretomes of cMSCs exert neurogenic and angiogenic effects in an *in vitro* assays. These results highlight the desirability of using cMSCs secretomes in further studies of wound healing in dogs, e.g. following SCI. These encouraging findings suggested considering dogs with SCI as a model for SCI in human, the results in chapter four showed for the first time the similarity in neurogenic and angiogenic activities in human and canine MSCs secretomes. Finally, the findings in chapter five of this study have demonstrated for the first time that the secretomes of purified cells of MSCs culture could exert a different biological effect. Thus this study may suggest that the usage of such purified cells will allow an increase in the efficacy of clinical applications of MSCs to treat and repair specific kind of injured tissues.

References

ABBOTT, N. J., RONNBACK, L. & HANSSON, E. 2006. Astrocyte-endothelial interactions at the blood-brain barrier. *Nat Rev Neurosci,* 7**,** 41-53.

ABKOWITZ, J. L., CATLIN, S. N. & GUTTORP, P. 1996. Evidence that hematopoiesis may be a stochastic process in vivo. *Nat Med,* 2**,** 190-7.

ALVAREZ-VIEJO, M., MENENDEZ-MENENDEZ, Y., BLANCO-GELAZ, M. A., FERRERO-GUTIERREZ, A., FERNANDEZ-RODRIGUEZ, M. A., GALA, J. & OTERO-HERNANDEZ, J. 2013. Quantifying mesenchymal stem cells in the mononuclear cell fraction of bone marrow samples obtained for cell therapy. *Transplant Proc,* 45**,** 434-9.

ÁLVAREZ-VIEJO, M., MENÉNDEZ-MENÉNDEZ, Y. & OTERO-HERNÁNDEZ, J. 2015. CD271 as a marker to identify mesenchymal stem cells from diverse sources before culture. *World Journal of Stem Cells,* 7**,** 470-476.

AMMAR, H. I., SEQUIERA, G. L., NASHED, M. B., AMMAR, R. I., GABR, H. M., ELSAYED, H. E., SAREEN, N., RUB, E. A.-E., ZICKRI, M. B. & DHINGRA, S. 2015. Comparison of adipose tissue- and bone marrow- derived mesenchymal stem cells for alleviating doxorubicin-induced cardiac dysfunction in diabetic rats. *Stem Cell Research & Therapy,* 6**,** 148.

ANKENY, D. P., MCTIGUE, D. M. & JAKEMAN, L. B. 2004. Bone marrow transplants provide tissue protection and directional guidance for axons after contusive spinal cord injury in rats. *Exp Neurol,* 190**,** 17-31.

AVASTHI, S., SRIVASTAVA, R., SINGH, A. & SRIVASTAVA, M. 2008. Stem cell: past, present and future--a review article. *Internet Journal of Medical Update,* 3**,** 22-31.

AVGUSTINOVA, A. & BENITAH, S. A. 2016. Epigenetic control of adult stem cell function. *Nat Rev Mol Cell Biol,* 17**,** 643-658.

BAGLIO, S. R., PEGTEL, D. M. & BALDINI, N. 2012. Mesenchymal stem cell secreted vesicles provide novel opportunities in (stem) cell-free therapy. *Front Physiol,* 3**,** 359.

BAKSH, D., YAO, R. & TUAN, R. S. 2007. Comparison of Proliferative and Multilineage Differentiation Potential of Human Mesenchymal Stem Cells Derived from Umbilical Cord and Bone Marrow. *STEM CELLS,* 25**,** 1384-1392.

BARILE, M. F., HOPPS, H. E., GRABOWSKI, M. W., RIGGS, D. B. & DELGIUDICE, R. A. 1973. THE IDENTIFICATION AND SOURCES OF MYCOPLASMAS ISOLATED FROM CONTAMINATED CELL CULTURES. *Annals of the New York Academy of Sciences,* 225**,** 251-264.

BARTANUSZ, V., JEZOVA, D., ALAJAJIAN, B. & DIGICAYLIOGLU, M. 2011. The blood–spinal cord barrier: Morphology and Clinical Implications. *Annals of Neurology,* 70**,** 194-206.

BAS, S., GAUTHIER, B. R., SPENATO, U., STINGELIN, S. & GABAY, C. 2004. CD14 is an acute-phase protein. *J Immunol,* 172**,** 4470-9.

BATTULA, V. L., TREML, S., BAREISS, P. M., GIESEKE, F., ROELOFS, H., DE ZWART, P., MULLER, I., SCHEWE, B., SKUTELLA, T., FIBBE, W. E., KANZ, L. & BUHRING, H. J. 2009. Isolation of functionally distinct mesenchymal stem cell subsets using antibodies against CD56, CD271, and mesenchymal stem cell antigen-1. *Haematologica,* 94**,** 173-84.

BAUER, J., MARGOLIS, M., SCHREINER, C., EDGELL, C.-J., AZIZKHAN, J., LAZAROWSKI, E. & JULIANO, R. L. 1992. In vitro model of angiogenesis using a human endothelium-derived permanent cell line: Contributions of induced gene expression, G-proteins, and integrins. *Journal of Cellular Physiology,* 153**,** 437-449.

BHATIA, R. & HARE, J. M. 2005. Mesenchymal stem cells: future source for reparative medicine. *Congest Heart Fail,* 11**,** 87-91; quiz 92-3.

BIAN, S., ZHANG, L., DUAN, L., WANG, X., MIN, Y. & YU, H. 2014. Extracellular vesicles derived from human bone marrow mesenchymal stem cells promote angiogenesis in a rat myocardial infarction model. *J Mol Med (Berl),* 92**,** 387-97.

BOKARA, K. K., KIM, J. H., KIM, J. Y. & LEE, J. E. 2016. Transfection of arginine decarboxylase gene increases the neuronal differentiation of neural progenitor cells. *Stem Cell Research,* 17**,** 256-265.

BOLLINI, S., GENTILI, C., TASSO, R. & CANCEDDA, R. 2013. The regenerative role of the fetal and adult stem cell secretome. *Journal of clinical medicine,* 2**,** 302-327.

BONGSO, A. & RICHARDS, M. 2004. History and perspective of stem cell research. *Best Pract Res Clin Obstet Gynaecol,* 18**,** 827-42.

BONNER, S. & SMITH, C. 2013. Initial management of acute spinal cord injury. *Continuing Education in Anaesthesia, Critical Care & Pain*.

BOQUEST, A. C., SHAHDADFAR, A., FRONSDAL, K., SIGURJONSSON, O., TUNHEIM, S. H., COLLAS, P. & BRINCHMANN, J. E. 2005. Isolation and transcription profiling of purified uncultured human stromal stem cells: alteration of gene expression after in vitro cell culture. *Mol Biol Cell,* 16**,** 1131-41.

BOUÏS, D., HOSPERS, G. A. P., MEIJER, C., MOLEMA, G. & MULDER, N. H. 2001. Endothelium in vitro: A review of human vascular endothelial cell lines for blood vessel-related research. *Angiogenesis,* 4**,** 91-102.

BRAY, E. & SLEVIN, M. 2015. Evaluating In Vitro Angiogenesis Using Live Cell Imaging. *In:* SLEVIN, M. & MCDOWELL, G. (eds.) *Handbook of Vascular Biology Techniques.* Dordrecht: Springer Netherlands.

BROHLIN, M., KINGHAM, P. J., NOVIKOVA, L. N., NOVIKOV, L. N. & WIBERG, M. 2012. Aging Effect on Neurotrophic Activity of Human Mesenchymal Stem Cells. *PLOS ONE,* 7**,** e45052.

BROUWERS, J. F., AALBERTS, M., JANSEN, J. W., VAN NIEL, G., WAUBEN, M. H., STOUT, T. A., HELMS, J. B. & STOORVOGEL, W. 2013. Distinct lipid compositions of two types of human prostasomes. *Proteomics,* 13**,** 1660-6.

BRUDER, S. P., JAISWAL, N. & HAYNESWORTH, S. E. 1997. Growth kinetics, self-renewal, and the osteogenic potential of purified human mesenchymal stem cells during extensive subcultivation and following cryopreservation. *Journal of Cellular Biochemistry,* 64**,** 278-294.

BUHRING, H. J., BATTULA, V. L., TREML, S., SCHEWE, B., KANZ, L. & VOGEL, W. 2007. Novel markers for the prospective isolation of human MSC. *Ann N Y Acad Sci,* 1106**,** 262-71.

BUNNELL, B. A., FLAAT, M., GAGLIARDI, C., PATEL, B. & RIPOLL, C. 2008. Adipose-derived Stem Cells: Isolation, Expansion and Differentiation. *Methods (San Diego, Calif.),* 45**,** 115-120.

BUSSER, H., NAJAR, M., RAICEVIC, G., PIETERS, K., VELEZ POMBO, R., PHILIPPART, P., MEULEMAN, N., BRON, D. & LAGNEAUX, L. 2015. Isolation and Characterization of Human Mesenchymal Stromal Cell Subpopulations: Comparison of Bone Marrow and Adipose Tissue. *Stem Cells Dev,* 24**,** 2142-57.

BYRNES, K. R., FRICKE, S. T. & FADEN, A. I. 2010. Neuropathological Differences Between Rats and Mice after Spinal Cord Injury. *Journal of magnetic resonance imaging : JMRI,* 32**,** 836-846.

CALABRESE, G., GIUFFRIDA, R., LO FURNO, D., PARRINELLO, N. L., FORTE, S., GULINO, R., COLAROSSI, C., SCHINOCCA, L. R., GIUFFRIDA, R., CARDILE, V. & MEMEO, L. 2015. Potential Effect of CD271 on Human Mesenchymal Stromal Cell Proliferation and Differentiation. *International Journal of Molecular Sciences,* 16**,** 15609-15624.

CANTINIEAUX, D., QUERTAINMONT, R., BLACHER, S., ROSSI, L., WANET, T., NOEL, A., BROOK, G., SCHOENEN, J. & FRANZEN, R. 2013. Conditioned medium from bone marrow-derived mesenchymal stem cells improves recovery after spinal cord injury in rats: an original strategy to avoid cell transplantation. *PLoS One,* 8**,** e69515.

CAO, Y., RISLING, M., MALM, E., SONDÉN, A., BOLLING, M. F. & SKÖLD, M. K. 2016. Cellular High-Energy Cavitation Trauma – Description of a Novel In Vitro Trauma Model in Three Different Cell Types. *Frontiers in Neurology,* 7**,** 10.

CAPLAN, A. I. 1991. Mesenchymal stem cells. *J Orthop Res,* 9**,** 641-50.
CAPLAN, A. I. & BRUDER, S. P. 2001. Mesenchymal stem cells: building blocks for molecular medicine in the 21st century. *Trends Mol Med,* 7**,** 259-64.
CAPLAN, A. I. & CORREA, D. 2011. The MSC: an injury drugstore. *Cell Stem Cell,* 9**,** 11-5.
CASAL, M. & HASKINS, M. 2006. Large animal models and gene therapy. *Eur J Hum Genet,* 14**,** 266-72.
CASHA, S., ZYGUN, D., MCGOWAN, M. D., BAINS, I., YONG, V. W. & HURLBERT, R. J. 2012. Results of a phase II placebo-controlled randomized trial of minocycline in acute spinal cord injury. *Brain,* 135**,** 1224-36.
CASIRAGHI, F., AZZOLLINI, N., CASSIS, P., IMBERTI, B., MORIGI, M., CUGINI, D., CAVINATO, R. A., TODESCHINI, M., SOLINI, S., SONZOGNI, A., PERICO, N., REMUZZI, G. & NORIS, M. 2008. Pretransplant infusion of mesenchymal stem cells prolongs the survival of a semiallogeneic heart transplant through the generation of regulatory T cells. *J Immunol,* 181**,** 3933-46.
CATTORETTI, G., SCHIRO, R., ORAZI, A., SOLIGO, D. & COLOMBO, M. 1993. Bone marrow stroma in humans: anti-nerve growth factor receptor antibodies selectively stain reticular cells in vivo and in vitro. *Blood,* 81**,** 1726-1738.
CELNIK, P. A. & COHEN, L. G. 2004. Modulation of motor function and cortical plasticity in health and disease. *Restor Neurol Neurosci,* 22**,** 261-8.
CHEN, L., TREDGET, E. E., WU, P. Y. & WU, Y. 2008. Paracrine factors of mesenchymal stem cells recruit macrophages and endothelial lineage cells and enhance wound healing. *PLoS One,* 3**,** e1886.
CHERIYAN, T., RYAN, D. J., WEINREB, J. H., CHERIYAN, J., PAUL, J. C., LAFAGE, V., KIRSCH, T. & ERRICO, T. J. 2014. Spinal cord injury models: a review. *Spinal Cord,* 52**,** 588-95.
CHIAL, H. 2008. Gene-Based Therapeutic Approaches. *Nature Education* 1**,** 210.
CHIELLINI, C., COCHET, O., NEGRONI, L., SAMSON, M., POGGI, M., AILHAUD, G., ALESSI, M. C., DANI, C. & AMRI, E. Z. 2008. Characterization of human mesenchymal stem cell secretome at early steps of adipocyte and osteoblast differentiation. *BMC Mol Biol,* 9**,** 26.
CHU, P. G. & ARBER, D. A. 2001. CD79: a review. *Appl Immunohistochem Mol Morphol,* 9**,** 97-106.
CHURCHMAN, S. M., PONCHEL, F., BOXALL, S. A., CUTHBERT, R., KOUROUPIS, D., ROSHDY, T., GIANNOUDIS, P. V., EMERY, P., MCGONAGLE, D. & JONES, E. A. 2012. Transcriptional profile of native CD271+ multipotential stromal cells: evidence for multiple fates, with prominent osteogenic and Wnt pathway signaling activity. *Arthritis Rheum,* 64**,** 2632-43.
CIBELLI, J., EMBORG, M. E., PROCKOP, D. J., ROBERTS, M., SCHATTEN, G., RAO, M., HARDING, J. & MIROCHNITCHENKO, O. 2013. Strategies for Improving Animal Models for Regenerative Medicine. *Cell stem cell,* 12**,** 271-274.
CLATWORTHY, J. P. & SUBRAMANIAN, V. 2001. Stem cells and the regulation of proliferation, differentiation and patterning in the intestinal epithelium: emerging insights from gene expression patterns, transgenic and gene ablation studies. *Mech Dev,* 101**,** 3-9.
COLLAWN, S. S. & PATEL, S. 2014. Adipose-Derived Stem Cells, their Secretome, and Wound Healing. *Journal of Cell Science & Therapy,* 2014.
CONCONI, M. T., BURRA, P., DI LIDDO, R., CALORE, C., TURETTA, M., BELLINI, S., BO, P., NUSSDORFER, G. G. & PARNIGOTTO, P. P. 2006. CD105(+) cells from Wharton's jelly show in vitro and in vivo myogenic differentiative potential. *Int J Mol Med,* 18**,** 1089-96.
CORCIONE, A., BENVENUTO, F., FERRETTI, E., GIUNTI, D., CAPPIELLO, V., CAZZANTI, F., RISSO, M., GUALANDI, F., MANCARDI, G. L., PISTOIA, V. & UCCELLI, A. 2006. Human mesenchymal stem cells modulate B-cell functions. *Blood,* 107**,** 367-72.

CRISAN, M., YAP, S., CASTEILLA, L., CHEN, C. W., CORSELLI, M., PARK, T. S., ANDRIOLO, G., SUN, B., ZHENG, B., ZHANG, L., NOROTTE, C., TENG, P. N., TRAAS, J., SCHUGAR, R., DEASY, B. M., BADYLAK, S., BUHRING, H. J., GIACOBINO, J. P., LAZZARI, L., HUARD, J. & PEAULT, B. 2008. A perivascular origin for mesenchymal stem cells in multiple human organs. *Cell Stem Cell,* 3**,** 301-13.

CUEVAS-DIAZ DURAN, R., GONZ, #XE1, LEZ-GARZA, M. T., CARDENAS-LOPEZ, A., CHAVEZ-CASTILLA, L., CRUZ-VEGA, D. E. & MORENO-CUEVAS, J. E. 2013. Age-Related Yield of Adipose-Derived Stem Cells Bearing the Low-Affinity Nerve Growth Factor Receptor. *Stem Cells International,* 2013**,** 9.

CUTHBERT, R. J., GIANNOUDIS, P. V., WANG, X. N., NICHOLSON, L., PAWSON, D., LUBENKO, A., TAN, H. B., DICKINSON, A., MCGONAGLE, D. & JONES, E. 2015. Examining the Feasibility of Clinical Grade CD271+ Enrichment of Mesenchymal Stromal Cells for Bone Regeneration. *PLOS ONE,* 10**,** e0117855.

DARIAN-SMITH, C. 2009. Synaptic Plasticity, Neurogenesis, and Functional Recovery after Spinal Cord Injury. *The Neuroscientist : a review journal bringing neurobiology, neurology and psychiatry,* 15**,** 149-165.

DAS, M., SUNDELL, I. B. & KOKA, P. S. 2013. Adult mesenchymal stem cells and their potency in the cell-based therapy. *J Stem Cells,* 8**,** 1-16.

DASARI, V. R., VEERAVALLI, K. K. & DINH, D. H. 2014. Mesenchymal stem cells in the treatment of spinal cord injuries: A review. *World Journal of Stem Cells,* 6**,** 120-133.

DENG, J., ZOU, Z. M., ZHOU, T. L., SU, Y. P., AI, G. P., WANG, J. P., XU, H. & DONG, S. W. 2011. Bone marrow mesenchymal stem cells can be mobilized into peripheral blood by G-CSF in vivo and integrate into traumatically injured cerebral tissue. *Neurol Sci,* 32**,** 641-51.

DENG, Y. B., LIU, X. G., LIU, Z. G., LIU, X. L., LIU, Y. & ZHOU, G. Q. 2006. Implantation of BM mesenchymal stem cells into injured spinal cord elicits de novo neurogenesis and functional recovery: evidence from a study in rhesus monkeys. *Cytotherapy,* 8**,** 210-4.

DENIZOT, F. & LANG, R. 1986. Rapid colorimetric assay for cell growth and survival. *Journal of Immunological Methods,* 89**,** 271-277.

DENNIS, J. E., MERRIAM, A., AWADALLAH, A., YOO, J. U., JOHNSTONE, B. & CAPLAN, A. I. 1999. A quadripotential mesenchymal progenitor cell isolated from the marrow of an adult mouse. *J Bone Miner Res,* 14**,** 700-9.

DEVIVO, M. J. 2012. Epidemiology of traumatic spinal cord injury: trends and future implications. *Spinal Cord,* 50**,** 365-72.

DIKOPOLSKAYA, N. & MAKARENKO, N. 2014. Anatomy of the Central Nervous System Textbook for students studying.

DIMARINO, A. M., CAPLAN, A. I. & BONFIELD, T. L. 2013. Mesenchymal Stem Cells in Tissue Repair. *Frontiers in Immunology,* 4**,** 201.

DOMINICI, M., LE BLANC, K., MUELLER, I., SLAPER-CORTENBACH, I., MARINI, F., KRAUSE, D., DEANS, R., KEATING, A., PROCKOP, D. & HORWITZ, E. 2006. Minimal criteria for defining multipotent mesenchymal stromal cells. The International Society for Cellular Therapy position statement. *Cytotherapy,* 8**,** 315-7.

DONOVAN, D., BROWN, N., BISHOP, E. & LEWIS, C. 2001. Comparison of three in vitro human 'angiogenesis' assays with capillaries formed in vivo. *Angiogenesis,* 4**,** 113-121.

DRAGO, D., COSSETTI, C., IRACI, N., GAUDE, E., MUSCO, G., BACHI, A. & PLUCHINO, S. 2013. The stem cell secretome and its role in brain repair. *Biochimie,* 95**,** 2271-2285.

DUFF, S. E., LI, C., GARLAND, J. M. & KUMAR, S. 2003. CD105 is important for angiogenesis: evidence and potential applications. *Faseb j,* 17**,** 984-92.

DUGGAL, S. & BRINCHMANN, J. E. 2011. Importance of serum source for the in vitro replicative senescence of human bone marrow derived mesenchymal stem cells. *J Cell Physiol,* 226**,** 2908-15.

DUMONT, R. J., OKONKWO, D. O., VERMA, S., HURLBERT, R. J., BOULOS, P. T., ELLEGALA, D. B. & DUMONT, A. S. 2001. Acute spinal cord injury, part I: pathophysiologic mechanisms. *Clin Neuropharmacol,* 24**,** 254-64.

DVORAK, M. F., NOONAN, V. K., FALLAH, N., FISHER, C. G., FINKELSTEIN, J., KWON, B. K., RIVERS, C. S., AHN, H., PAQUET, J., TSAI, E. C., TOWNSON, A., ATTABIB, N., BAILEY, C. S., CHRISTIE, S. D., DREW, B., FOURNEY, D. R., FOX, R., HURLBERT, R. J., JOHNSON, M. G., LINASSI, A. G., PARENT, S. & FEHLINGS, M. G. 2015. The influence of time from injury to surgery on motor recovery and length of hospital stay in acute traumatic spinal cord injury: an observational Canadian cohort study. *J Neurotrauma,* 32**,** 645-54.

DWANE, S., DURACK, E. & KIELY, P. A. 2013. Optimising parameters for the differentiation of SH-SY5Y cells to study cell adhesion and cell migration. *BMC Research Notes,* 6**,** 366.

ECKER, T. M., KLEINSCHMIDT, M., MARTINOLLI, L., ZIMMERMANN, H. & EXADAKTYLOS, A. K. 2008. Clinical presentation of a traumatic cervical spine disc rupture in alpine sports: a case report. *Scandinavian Journal of Trauma, Resuscitation and Emergency Medicine,* 16**,** 14.

EDGELL, C. J., HAIZLIP, J. E., BAGNELL, C. R., PACKENHAM, J. P., HARRISON, P., WILBOURN, B. & MADDEN, V. J. 1990. Endothelium specific Weibel-Palade bodies in a continuous human cell line, EA.hy926. *In Vitro Cell Dev Biol,* 26**,** 1167-72.

EDGELL, C. J., MCDONALD, C. C. & GRAHAM, J. B. 1983. Permanent cell line expressing human factor VIII-related antigen established by hybridization. *Proceedings of the National Academy of Sciences of the United States of America,* 80**,** 3734-3737.

EGASHIRA, Y., SUGITANI, S., SUZUKI, Y., MISHIRO, K., TSURUMA, K., SHIMAZAWA, M., YOSHIMURA, S., IWAMA, T. & HARA, H. 2012. The conditioned medium of murine and human adipose-derived stem cells exerts neuroprotective effects against experimental stroke model. *Brain Res,* 1461**,** 87-95.

EL MASRI, W. 2006. Traumatic spinal cord injury: the relationship between pathology and clinical implications. *Trauma,* 8**,** 29-46.

EL MASRI, W. & KUMAR, N. 2017. Active physiological conservative management in traumatic spinal cord injuries–an evidence-based approach. *Trauma***,** 1460408617698508.

ELAHI, K. C., KLEIN, G., AVCI-ADALI, M., SIEVERT, K. D., MACNEIL, S. & AICHER, W. K. 2016. Human Mesenchymal Stromal Cells from Different Sources Diverge in Their Expression of Cell Surface Proteins and Display Distinct Differentiation Patterns. *Stem Cells International,* 2016**,** 5646384.

ESTRADA, R., LI, N. A., SAROJINI, H., AN, J. I. N., LEE, M.-J. & WANG, E. 2009. Secretome From Mesenchymal Stem Cells Induces Angiogenesis Via Cyr61. *Journal of cellular physiology,* 219**,** 563-571.

EVANIEW, N., NOONAN, V. K., FALLAH, N., KWON, B. K., RIVERS, C. S., AHN, H., BAILEY, C. S., CHRISTIE, S. D., FOURNEY, D. R., HURLBERT, R. J., LINASSI, A. G., FEHLINGS, M. G. & DVORAK, M. F. 2015. Methylprednisolone for the Treatment of Patients with Acute Spinal Cord Injuries: A Propensity Score-Matched Cohort Study from a Canadian Multi-Center Spinal Cord Injury Registry. *Journal of Neurotrauma,* 32**,** 1674-1683.

EVANS, M. J. & KAUFMAN, M. H. 1981. Establishment in culture of pluripotential cells from mouse embryos. *Nature,* 292**,** 154-6.

FARNDALE, R. W., BUTTLE, D. J. & BARRETT, A. J. 1986. Improved quantitation and discrimination of sulphated glycosaminoglycans by use of dimethylmethylene blue. *Biochim Biophys Acta,* 883**,** 173-7.

FARNDALE, R. W., SAYERS, C. A. & BARRETT, A. J. 1982. A direct spectrophotometric microassay for sulfated glycosaminoglycans in cartilage cultures. *Connect Tissue Res,* 9**,** 247-8.

FEHLINGS, M. G., THEODORE, N., HARROP, J., MAURAIS, G., KUNTZ, C., SHAFFREY, C. I., KWON, B. K., CHAPMAN, J., YEE, A., TIGHE, A. & MCKERRACHER, L. 2011. A phase I/IIa clinical trial of a recombinant Rho protein antagonist in acute spinal cord injury. *J Neurotrauma,* 28**,** 787-96.

FEHLINGS, M. G., WILSON, J. R., FRANKOWSKI, R. F., TOUPS, E. G., AARABI, B., HARROP, J. S., SHAFFREY, C. I., HARKEMA, S. J., GUEST, J. D., TATOR, C. H., BURAU, K. D., JOHNSON, M. W. & GROSSMAN, R. G. 2012. Riluzole for the treatment of acute traumatic spinal cord injury: rationale for and design of the NACTN Phase I clinical trial. *J Neurosurg Spine,* 17**,** 151-6.

FENG, H. & WANG, J. 2012. A new mechanism of stem cell differentiation through slow binding/unbinding of regulators to genes. *Scientific Reports,* 2**,** 550.

FENG, Y., HUANG, W., WANI, M., YU, X. & ASHRAF, M. 2014. Ischemic preconditioning potentiates the protective effect of stem cells through secretion of exosomes by targeting Mecp2 via miR-22. *PLoS One,* 9**,** e88685.

FENSTERMACHER, J., GROSS, P., SPOSITO, N., ACUFF, V., PETTERSEN, S. & GRUBER, K. 1988. Structural and functional variations in capillary systems within the brain. *Ann N Y Acad Sci,* 529**,** 21-30.

FERNYHOUGH, M. E., HAUSMAN, G. J., GUAN, L. L., OKINE, E., MOORE, S. S. & DODSON, M. V. 2008. Mature adipocytes may be a source of stem cells for tissue engineering. *Biochem Biophys Res Commun,* 368**,** 455-7.

FESTOFF, B. W., AMEENUDDIN, S., ARNOLD, P. M., WONG, A., SANTACRUZ, K. S. & CITRON, B. A. 2006. Minocycline neuroprotects, reduces microgliosis, and inhibits caspase protease expression early after spinal cord injury. *J Neurochem,* 97**,** 1314-26.

FINTANSHEERIN 2004. Spinal cord injury: anatomy and physiology of the spinal cord. *Emergency Nurse,* 12**,** 30-36.

FORTIER, L. A. 2005. Stem cells: classifications, controversies, and clinical applications. *Vet Surg,* 34**,** 415-23.

FRIEDENSTEIN, A. J., CHAILAKHJAN, R. K. & LALYKINA, K. S. 1970. The development of fibroblast colonies in monolayer cultures of guinea-pig bone marrow and spleen cells. *Cell Tissue Kinet,* 3**,** 393-403.

FRIEDENSTEIN, A. J., CHAILAKHYAN, R. K. & GERASIMOV, U. V. 1987. Bone marrow osteogenic stem cells: in vitro cultivation and transplantation in diffusion chambers. *Cell Tissue Kinet,* 20**,** 263-72.

FRIEDENSTEIN, A. J., LATZINIK, N. V., GORSKAYA, U. F. & SIDOROVICH, S. Y. 1981. Radiosensitivity and Postirradiation Changes of Bone Marrow Clonogenic Stromal Mechanocytes. *International Journal of Radiation Biology and Related Studies in Physics, Chemistry and Medicine,* 39**,** 537-546.

FRIEDENSTEIN, A. J., LATZINIK, N. W., GROSHEVA, A. G. & GORSKAYA, U. F. 1982. Marrow microenvironment transfer by heterotopic transplantation of freshly isolated and cultured cells in porous sponges. *Exp Hematol,* 10**,** 217-27.

FUJIKI, M., ZHANG, Z., GUTH, L. & STEWARD, O. 1996. Genetic influences on cellular reactions to spinal cord injury: activation of macrophages/microglia and astrocytes is delayed in mice carrying a mutation (WldS) that causes delayed Wallerian degeneration. *J Comp Neurol,* 371**,** 469-84.

FURLAN, J. C., NOONAN, V., CADOTTE, D. W. & FEHLINGS, M. G. 2011. Timing of decompressive surgery of spinal cord after traumatic spinal cord injury: an evidence-based examination of pre-clinical and clinical studies. *J Neurotrauma,* 28**,** 1371-99.

GANG, E. J., JEONG, J. A., HONG, S. H., HWANG, S. H., KIM, S. W., YANG, I. H., AHN, C., HAN, H. & KIM, H. 2004. Skeletal myogenic differentiation of mesenchymal stem cells isolated from human umbilical cord blood. *Stem Cells,* 22**,** 617-24.

GEFFNER, L. F., SANTACRUZ, P., IZURIETA, M., FLOR, L., MALDONADO, B., AUAD, A. H., MONTENEGRO, X., GONZALEZ, R. & SILVA, F. 2008. Administration of autologous bone marrow stem cells into spinal cord injury patients via multiple routes is safe and improves their quality of life: comprehensive case studies. *Cell Transplant,* 17**,** 1277-93.

GLASER, J., GONZALEZ, R., SADR, E. & KEIRSTEAD, H. S. 2006. Neutralization of the chemokine CXCL10 reduces apoptosis and increases axon sprouting after spinal cord injury. *J Neurosci Res,* 84**,** 724-34.

GOODELL, M. A., NGUYEN, H. & SHROYER, N. 2015. Somatic stem cell heterogeneity: diversity in the blood, skin and intestinal stem cell compartments. *Nat Rev Mol Cell Biol,* 16**,** 299-309.

GOODISON, S., URQUIDI, V. & TARIN, D. 1999. CD44 cell adhesion molecules. *Mol Pathol,* 52**,** 189-96.

GRANGER, N., BLAMIRES, H., FRANKLIN, R. J. M. & JEFFERY, N. D. 2012. Autologous olfactory mucosal cell transplants in clinical spinal cord injury: a randomized double-blinded trial in a canine translational model. *Brain,* 135**,** 3227-3237.

GRIESCHE, N., LUTTMANN, W., LUTTMANN, A., STAMMERMANN, T., GEIGER, H. & BAER, P. C. 2010. A simple modification of the separation method reduces heterogeneity of adipose-derived stem cells. *Cells Tissues Organs,* 192**,** 106-15.

GUHA, P., MORGAN, JOHN W., MOSTOSLAVSKY, G., RODRIGUES, NEIL P. & BOYD, ASHLEIGH S. 2013. Lack of Immune Response to Differentiated Cells Derived from Syngeneic Induced Pluripotent Stem Cells. *Cell Stem Cell,* 12**,** 407-412.

GUIDOLIN, D., VACCA, A., NUSSDORFER, G. G. & RIBATTI, D. 2004. A new image analysis method based on topological and fractal parameters to evaluate the angiostatic activity of docetaxel by using the Matrigel assay in vitro. *Microvascular research,* 67**,** 117-124.

GUPTA, P. K., CHULLIKANA, A., PARAKH, R., DESAI, S., DAS, A., GOTTIPAMULA, S., KRISHNAMURTHY, S., ANTHONY, N., PHERWANI, A. & MAJUMDAR, A. S. 2013. A double blind randomized placebo controlled phase I/II study assessing the safety and efficacy of allogeneic bone marrow derived mesenchymal stem cell in critical limb ischemia. *Journal of Translational Medicine,* 11**,** 143-143.

GUTH, L., ZHANG, Z. & STEWARD, O. 1999. The unique histopathological responses of the injured spinal cord. Implications for neuroprotective therapy. *Ann N Y Acad Sci,* 890**,** 366-84.

HANSEN, M. B., NIELSEN, S. E. & BERG, K. 1989. Re-examination and further development of a precise and rapid dye method for measuring cell growth/cell kill. *Journal of Immunological Methods,* 119**,** 203-210.

HARDING, J., ROBERTS, R. M. & MIROCHNITCHENKO, O. 2013. Large animal models for stem cell therapy. *Stem Cell Res Ther,* 4**,** 23.

HART, D. A. 2014. Why Mesenchymal Stem/Progenitor Cell Heterogeneity in Specific Environments?-Implications for Tissue Engineering Applications Following Injury or Degeneration of Connective Tissues. *Journal of Biomedical Science and Engineering,* 7**,** 526.

HASHIKAWA, T., TAKEDACHI, M., TERAKURA, M., SAHO, T., YAMADA, S., THOMPSON, L. F., SHIMABUKURO, Y. & MURAKAMI, S. 2003. Involvement of CD73 (ecto-5'-nucleotidase) in adenosine generation by human gingival fibroblasts. *J Dent Res,* 82**,** 888-92.

HASS, R., KASPER, C., BOHM, S. & JACOBS, R. 2011. Different populations and sources of human mesenchymal stem cells (MSC): A comparison of adult and neonatal tissue-derived MSC. *Cell Commun Signal,* 9**,** 12.

HAYNESWORTH, S. E., BABER, M. A. & CAPLAN, A. I. 1996. Cytokine expression by human marrow-derived mesenchymal progenitor cells in vitro: effects of dexamethasone and IL-1 alpha. *J Cell Physiol,* 166**,** 585-92.

HEMLER, M. E. 2003. Tetraspanin proteins mediate cellular penetration, invasion, and fusion events and define a novel type of membrane microdomain. *Annu Rev Cell Dev Biol,* 19**,** 397-422.

HICKS, J., PLATT, S., KENT, M. & HALEY, A. 2015. Canine brain tumours: a model for the human disease? *Veterinary and Comparative Oncology***,** n/a-n/a.

HICKSTEIN, D. D., OZOLS, J., WILLIAMS, S. A., BAENZIGER, J. U., LOCKSLEY, R. M. & ROTH, G. J. 1987. Isolation and characterization of the receptor on human neutrophils that mediates cellular adherence. *J Biol Chem,* 262**,** 5576-80.

HO, A. D., WAGNER, W. & FRANKE, W. 2008. Heterogeneity of mesenchymal stromal cell preparations. *Cytotherapy,* 10**,** 320-30.

HOCH, A. I., BINDER, B. Y., GENETOS, D. C. & LEACH, J. K. 2012. Differentiation-Dependent Secretion of Proangiogenic Factors by Mesenchymal Stem Cells. *PLOS ONE,* 7**,** e35579.

HONG, S. J., TRAKTUEV, D. O. & MARCH, K. L. 2010. Therapeutic potential of adipose-derived stem cells in vascular growth and tissue repair. *Curr Opin Organ Transplant,* 15**,** 86-91.

HOOGDUIJN, M. J. & DOR, F. J. M. F. 2013. Mesenchymal Stem Cells: Are We Ready for Clinical Application in Transplantation and Tissue Regeneration? *Frontiers in Immunology,* 4**,** 144.

HORN, P. A., MORRIS, J. C., NEFF, T. & KIEM, H. P. 2004. Stem cell gene transfer--efficacy and safety in large animal studies. *Mol Ther,* 10**,** 417-31.

HORWITZ, E. M., LE BLANC, K., DOMINICI, M., MUELLER, I., SLAPER-CORTENBACH, I., MARINI, F. C., DEANS, R. J., KRAUSE, D. S. & KEATING, A. 2005. Clarification of the nomenclature for MSC: The International Society for Cellular Therapy position statement. *Cytotherapy,* 7**,** 393-5.

HOWE, S. J., MANSOUR, M. R., SCHWARZWAELDER, K., BARTHOLOMAE, C., HUBANK, M., KEMPSKI, H., BRUGMAN, M. H., PIKE-OVERZET, K., CHATTERS, S. J., DE RIDDER, D., GILMOUR, K. C., ADAMS, S., THORNHILL, S. I., PARSLEY, K. L., STAAL, F. J., GALE, R. E., LINCH, D. C., BAYFORD, J., BROWN, L., QUAYE, M., KINNON, C., ANCLIFF, P., WEBB, D. K., SCHMIDT, M., VON KALLE, C., GASPAR, H. B. & THRASHER, A. J. 2008. Insertional mutagenesis combined with acquired somatic mutations causes leukemogenesis following gene therapy of SCID-X1 patients. *J Clin Invest,* 118**,** 3143-50.

HUGENHOLTZ, H. 2003. Methylprednisolone for acute spinal cord injury: not a standard of care. *Cmaj,* 168**,** 1145-6.

HUGHES, P., MARSHALL, D., REID, Y., PARKES, H. & GELBER, C. 2007. The costs of using unauthenticated, over-passaged cell lines: how much more data do we need? *Biotechniques,* 43**,** 575, 577-8, 581-2 passim.

HUR, J. W., CHO, T. H., PARK, D. H., LEE, J. B., PARK, J. Y. & CHUNG, Y. G. 2016. Intrathecal transplantation of autologous adipose-derived mesenchymal stem cells for treating spinal cord injury: A human trial. *J Spinal Cord Med,* 39**,** 655-664.

ILIC, D., DEVITO, L., MIERE, C. & CODOGNOTTO, S. 2015. Human embryonic and induced pluripotent stem cells in clinical trials. *Br Med Bull,* 116**,** 19-27.

ISAKSON, M., DE BLACAM, C., WHELAN, D., MCARDLE, A. & CLOVER, A. J. P. 2015. Mesenchymal Stem Cells and Cutaneous Wound Healing: Current Evidence and Future Potential. *Stem Cells International,* 2015**,** 831095.

JANSSON, L. C., LOUHIVUORI, L., WIGREN, H. K., NORDSTRÖM, T., LOUHIVUORI, V., CASTRÉN, M. L. & ÅKERMAN, K. E. 2012. Brain-derived neurotrophic factor increases the motility of a particular N-methyl-d-aspartate /GABA-responsive subset of neural progenitor cells. *Neuroscience,* 224**,** 223-234.

JARMALAVIČIŪTĖ, A. & PIVORIŪNAS, A. 2016. Neuroprotective properties of extracellular vesicles derived from mesenchymal stem cells. *Neural Regeneration Research,* 11**,** 904-905.

JAROCHA, D., LUKASIEWICZ, E. & MAJKA, M. 2008. Adventage of mesenchymal stem cells (MSC) expansion directly from purified bone marrow CD105+ and CD271+ cells. *Folia Histochem Cytobiol,* 46**,** 307-14.

JARVINEN, L., BADRI, L., WETTLAUFER, S., OHTSUKA, T., STANDIFORD, T. J., TOEWS, G. B., PINSKY, D. J., PETERS-GOLDEN, M. & LAMA, V. N. 2008. Lung resident mesenchymal stem cells isolated from human lung allografts inhibit T cell proliferation via a soluble mediator. *J Immunol,* 181**,** 4389-96.

JAYARAMAN, P., NATHAN, P., VASANTHAN, P., MUSA, S. & GOVINDASAMY, V. 2013. Stem cells conditioned medium: a new approach to skin wound healing management. *Cell Biol Int,* 37**,** 1122-8.

JEFFERY, N. D., SMITH, P. M., LAKATOS, A., IBANEZ, C., ITO, D. & FRANKLIN, R. J. 2006a. Clinical canine spinal cord injury provides an opportunity to examine the issues in translating laboratory techniques into practical therapy. *Spinal Cord,* 44**,** 584-93.

JEFFERY, N. D., SMITH, P. M., LAKATOS, A., IBANEZ, C., ITO, D. & FRANKLIN, R. J. M. 2006b. Clinical canine spinal cord injury provides an opportunity to examine the issues in translating laboratory techniques into practical therapy. *Spinal Cord,* 44**,** 584-593.

JIANG, T., LIU, W., LV, X., SUN, H., ZHANG, L., LIU, Y., ZHANG, W. J., CAO, Y. & ZHOU, G. 2010. Potent in vitro chondrogenesis of CD105 enriched human adipose-derived stem cells. *Biomaterials,* 31**,** 3564-71.

JIANG, X. X., ZHANG, Y., LIU, B., ZHANG, S. X., WU, Y., YU, X. D. & MAO, N. 2005. Human mesenchymal stem cells inhibit differentiation and function of monocyte-derived dendritic cells. *Blood,* 105**,** 4120-6.

JONES, E., ENGLISH, A., CHURCHMAN, S. M., KOUROUPIS, D., BOXALL, S. A., KINSEY, S., GIANNOUDIS, P. G., EMERY, P. & MCGONAGLE, D. 2010. Large-scale extraction and characterization of CD271+ multipotential stromal cells from trabecular bone in health and osteoarthritis: implications for bone regeneration strategies based on uncultured or minimally cultured multipotential stromal cells. *Arthritis Rheum,* 62**,** 1944-54.

JONES, E. & MCGONAGLE, D. 2008. Human bone marrow mesenchymal stem cells in vivo. *Rheumatology (Oxford),* 47**,** 126-31.

JONES, E. A., ENGLISH, A., KINSEY, S. E., STRASZYNSKI, L., EMERY, P., PONCHEL, F. & MCGONAGLE, D. 2006. Optimization of a flow cytometry-based protocol for detection and phenotypic characterization of multipotent mesenchymal stromal cells from human bone marrow. *Cytometry Part B: Clinical Cytometry,* 70B**,** 391-399.

JONES, E. A., KINSEY, S. E., ENGLISH, A., JONES, R. A., STRASZYNSKI, L., MEREDITH, D. M., MARKHAM, A. F., JACK, A., EMERY, P. & MCGONAGLE, D. 2002. Isolation and characterization of bone marrow multipotential mesenchymal progenitor cells. *Arthritis Rheum,* 46**,** 3349-60.

JUNG, D. I., HA, J., KANG, B. T., KIM, J. W., QUAN, F. S., LEE, J. H., WOO, E. J. & PARK, H. M. 2009. A comparison of autologous and allogenic bone marrow-derived mesenchymal stem cell transplantation in canine spinal cord injury. *J Neurol Sci,* 285**,** 67-77.

KAKABADZE, Z., KIPSHIDZE, N., MARDALEISHVILI, K., CHUTKERASHVILI, G., CHELISHVILI, I., HARDERS, A., LOLADZE, G., SHATIRISHVILI, G., KIPSHIDZE, N., CHAKHUNASHVILI, D. & CHUTKERASHVILI, K. 2016. Phase 1 Trial of Autologous Bone Marrow Stem Cell Transplantation in Patients with Spinal Cord Injury. *Stem Cells International,* 2016**,** 6768274.

KALININA, N., KHARLAMPIEVA, D., LOGUINOVA, M., BUTENKO, I., POBEGUTS, O., EFIMENKO, A., AGEEVA, L., SHARONOV, G., ISCHENKO, D., ALEKSEEV, D., GRIGORIEVA, O., SYSOEVA, V., RUBINA, K., LAZAREV, V. & GOVORUN, V. 2015. Characterization of secretomes provides evidence for adipose-derived mesenchymal stromal cells subtypes. *Stem Cell Res Ther,* 6**,** 221.

KANEKO, S., IWANAMI, A., NAKAMURA, M., KISHINO, A., KIKUCHI, K., SHIBATA, S., OKANO, H. J., IKEGAMI, T., MORIYA, A., KONISHI, O., NAKAYAMA, C., KUMAGAI, K., KIMURA, T., SATO, Y., GOSHIMA, Y., TANIGUCHI, M., ITO, M., HE, Z., TOYAMA, Y. & OKANO, H. 2006. A selective Sema3A inhibitor enhances regenerative responses and functional recovery of the injured spinal cord. *Nat Med,* 12**,** 1380-9.

KANG, S.-G., SHINOJIMA, N., HOSSAIN, A., GUMIN, J., YONG, R. L., COLMAN, H., MARINI, F., ANDREEFF, M. & LANG, F. F. 2010. Isolation and Perivascular Localization of Mesenchymal Stem Cells From Mouse Brain. *Neurosurgery,* 67**,** 711-720.

KANNO, H., PRESSMAN, Y., MOODY, A., BERG, R., MUIR, E. M., ROGERS, J. H., OZAWA, H., ITOI, E., PEARSE, D. D. & BUNGE, M. B. 2014. Combination of engineered Schwann cell grafts to secrete neurotrophin and chondroitinase promotes axonal regeneration and locomotion after spinal cord injury. *J Neurosci,* 34**,** 1838-55.

KAPUR, S. K. & KATZ, A. J. 2013. Review of the adipose derived stem cell secretome. *Biochimie,* 95**,** 2222-8.

KARIMI-ABDOLREZAEE, S., EFTEKHARPOUR, E., WANG, J., MORSHEAD, C. M. & FEHLINGS, M. G. 2006. Delayed transplantation of adult neural precursor cells promotes

remyelination and functional neurological recovery after spinal cord injury. *J Neurosci,* 26**,** 3377-89.

KEHAT, I., KENYAGIN-KARSENTI, D., SNIR, M., SEGEV, H., AMIT, M., GEPSTEIN, A., LIVNE, E., BINAH, O., ITSKOVITZ-ELDOR, J. & GEPSTEIN, L. 2001. Human embryonic stem cells can differentiate into myocytes with structural and functional properties of cardiomyocytes. *Journal of Clinical Investigation,* 108**,** 407-414.

KEIRSTEAD, H. S., NISTOR, G., BERNAL, G., TOTOIU, M., CLOUTIER, F., SHARP, K. & STEWARD, O. 2005. Human embryonic stem cell-derived oligodendrocyte progenitor cell transplants remyelinate and restore locomotion after spinal cord injury. *J Neurosci,* 25**,** 4694-705.

KHANNA, C., LINDBLAD-TOH, K., VAIL, D., LONDON, C., BERGMAN, P., BARBER, L., BREEN, M., KITCHELL, B., MCNEIL, E., MODIANO, J. F., NIEMI, S., COMSTOCK, K. E., OSTRANDER, E., WESTMORELAND, S. & WITHROW, S. 2006. The dog as a cancer model. *Nat Biotech,* 24**,** 1065-1066.

KHOO, C. P., MICKLEM, K. & WATT, S. M. 2011. A Comparison of Methods for Quantifying Angiogenesis in the Matrigel Assay In Vitro. *Tissue Engineering. Part C, Methods,* 17**,** 895-906.

KIM, D. K., NISHIDA, H., AN, S. Y., SHETTY, A. K., BARTOSH, T. J. & PROCKOP, D. J. 2016. Chromatographically isolated CD63+CD81+ extracellular vesicles from mesenchymal stromal cells rescue cognitive impairments after TBI. *Proc Natl Acad Sci U S A,* 113**,** 170-5.

KIM, H. O., CHOI, S.-M. & KIM, H.-S. 2013a. Mesenchymal stem cell-derived secretome and microvesicles as a cell-free therapeutics for neurodegenerative disorders. *Tissue Engineering and Regenerative Medicine,* 10**,** 93-101.

KIM, J. M., KIM, J., KIM, Y. H., KIM, K. T., RYU, S. H., LEE, T. G. & SUH, P. G. 2013b. Comparative secretome analysis of human bone marrow-derived mesenchymal stem cells during osteogenesis. *J Cell Physiol,* 228**,** 216-24.

KIM, N. & CHO, S.-G. 2013. Clinical applications of mesenchymal stem cells. *The Korean Journal of Internal Medicine,* 28**,** 387-402.

KIMBREL, E. A. & LANZA, R. 2015. Current status of pluripotent stem cells: moving the first therapies to the clinic. *Nat Rev Drug Discov,* 14**,** 681-92.

KINNAIRD, T., STABILE, E., BURNETT, M. S., LEE, C. W., BARR, S., FUCHS, S. & EPSTEIN, S. E. 2004. Marrow-derived stromal cells express genes encoding a broad spectrum of arteriogenic cytokines and promote in vitro and in vivo arteriogenesis through paracrine mechanisms. *Circ Res,* 94**,** 678-85.

KIRKNESS, E. F., BAFNA, V., HALPERN, A. L., LEVY, S., REMINGTON, K., RUSCH, D. B., DELCHER, A. L., POP, M., WANG, W., FRASER, C. M. & VENTER, J. C. 2003. The dog genome: survey sequencing and comparative analysis. *Science,* 301**,** 1898-903.

KIRSHBLUM, S. C., BURNS, S. P., BIERING-SORENSEN, F., DONOVAN, W., GRAVES, D. E., JHA, A., JOHANSEN, M., JONES, L., KRASSIOUKOV, A., MULCAHEY, M. J., SCHMIDT-READ, M. & WARING, W. 2011. International standards for neurological classification of spinal cord injury (Revised 2011). *The Journal of Spinal Cord Medicine,* 34**,** 535-546.

KOHLI, N., WRIGHT, K. T., SAMMONS, R. L., JEYS, L., SNOW, M. & JOHNSON, W. E. 2015. An In Vitro Comparison of the Incorporation, Growth, and Chondrogenic Potential of Human Bone Marrow versus Adipose Tissue Mesenchymal Stem Cells in Clinically Relevant Cell Scaffolds Used for Cartilage Repair. *Cartilage,* 6**,** 252-63.

KOLAR, M. K. 2014. The use of adipose derived stem cells in spinal cord and peripheral nerve repair.

KONALA, V. B., MAMIDI, M. K., BHONDE, R., DAS, A. K., POCHAMPALLY, R. & PAL, R. 2016. The current landscape of the mesenchymal stromal cell secretome: A new paradigm for cell-free regeneration. *Cytotherapy,* 18**,** 13-24.

KRAFTS, K. P. 2010. Tissue repair: The hidden drama. *Organogenesis,* 6**,** 225-33.

KRENGEL, W. F., 3RD, ANDERSON, P. A. & HENLEY, M. B. 1993. Early stabilization and decompression for incomplete paraplegia due to a thoracic-level spinal cord injury. *Spine (Phila Pa 1976),* 18**,** 2080-7.

KUNDI, S., BICKNELL, R. & AHMED, Z. 2013. The role of angiogenic and wound-healing factors after spinal cord injury in mammals. *Neurosci Res,* 76**,** 1-9.

KUO, C. K. & TUAN, R. S. 2008. Mechanoactive tenogenic differentiation of human mesenchymal stem cells. *Tissue Eng Part A,* 14**,** 1615-27.

KUPCOVA SKALNIKOVA, H. 2013. Proteomic techniques for characterisation of mesenchymal stem cell secretome. *Biochimie,* 95**,** 2196-2211.

LANDRY, D. W. & ZUCKER, H. A. 2004. Embryonic death and the creation of human embryonic stem cells. *J Clin Invest,* 114**,** 1184-6.

LARIJANI, B., ESFAHANI, E. N., AMINI, P., NIKBIN, B., ALIMOGHADDAM, K., AMIRI, S., MALEKZADEH, R., YAZDI, N. M., GHODSI, M., DOWLATI, Y., SAHRAIAN, M. A. & GHAVAMZADEH, A. 2012. Stem cell therapy in treatment of different diseases. *Acta Med Iran,* 50**,** 79-96.

LATIFI-PUPOVCI, H., KUÇI, Z., WEHNER, S., BÖNIG, H., LIEBERZ, R., KLINGEBIEL, T., BADER, P. & KUÇI, S. 2015. In vitro migration and proliferation ("wound healing") potential of mesenchymal stromal cells generated from human CD271(+) bone marrow mononuclear cells. *Journal of Translational Medicine,* 13**,** 315.

LAVOIE, J. R. & ROSU-MYLES, M. 2013. Uncovering the secretes of mesenchymal stem cells. *Biochimie,* 95**,** 2212-21.

LE BLANC, K. & PITTENGER, M. 2005. Mesenchymal stem cells: progress toward promise. *Cytotherapy,* 7**,** 36-45.

LECHLER, T. & FUCHS, E. 2005. Asymmetric cell divisions promote stratification and differentiation of mammalian skin. *Nature,* 437**,** 275-280.

LEE, S. M., LEE, S. C. & KIM, S. J. 2014. Contribution of human adipose tissue-derived stem cells and the secretome to the skin allograft survival in mice. *J Surg Res,* 188**,** 280-9.

LI, C. Y., WU, X. Y., TONG, J. B., YANG, X. X., ZHAO, J. L., ZHENG, Q. F., ZHAO, G. B. & MA, Z. J. 2015. Comparative analysis of human mesenchymal stem cells from bone marrow and adipose tissue under xeno-free conditions for cell therapy. *Stem Cell Res Ther,* 6**,** 55.

LI, J. & LEPSKI, G. 2013. Cell transplantation for spinal cord injury: a systematic review. *Biomed Res Int,* 2013**,** 786475.

LI, L. & XIE, T. 2005. Stem cell niche: structure and function. *Annu Rev Cell Dev Biol,* 21**,** 605-31.

LI, Z., ZHANG, C., WEINER, L. P., ZHANG, Y. & ZHONG, J. F. 2013. Molecular characterization of heterogeneous mesenchymal stem cells with single-cell transcriptomes. *Biotechnol Adv,* 31**,** 312-7.

LIEBSCHER, T., SCHNELL, L., SCHNELL, D., SCHOLL, J., SCHNEIDER, R., GULLO, M., FOUAD, K., MIR, A., RAUSCH, M., KINDLER, D., HAMERS, F. P. & SCHWAB, M. E. 2005. Nogo-A antibody improves regeneration and locomotion of spinal cord-injured rats. *Ann Neurol,* 58**,** 706-19.

LIM, J.-H., BYEON, Y.-E., RYU, H.-H., JEONG, Y.-H., LEE, Y.-W., KIM, W. H., KANG, K.-S. & KWEON, O.-K. 2007. Transplantation of canine umbilical cord blood-derived mesenchymal stem cells in experimentally induced spinal cord injured dogs. *Journal of Veterinary Science,* 8**,** 275-282.

LIN, H. 2008. Cell biology of stem cells: an enigma of asymmetry and self-renewal. *The Journal of Cell Biology,* 180**,** 257-260.

LINDBLAD-TOH, K., WADE, C. M., MIKKELSEN, T. S., KARLSSON, E. K., JAFFE, D. B., KAMAL, M., CLAMP, M., CHANG, J. L., KULBOKAS, E. J., ZODY, M. C., MAUCELI, E., XIE, X., BREEN, M., WAYNE, R. K., OSTRANDER, E. A., PONTING, C. P., GALIBERT, F., SMITH, D. R., DEJONG, P. J., KIRKNESS, E., ALVAREZ, P., BIAGI, T., BROCKMAN, W., BUTLER, J., CHIN, C.-W., COOK, A., CUFF, J., DALY, M. J., DECAPRIO, D., GNERRE, S., GRABHERR, M., KELLIS, M., KLEBER, M., BARDELEBEN, C., GOODSTADT, L., HEGER, A., HITTE, C., KIM, L., KOEPFLI, K.-

P., PARKER, H. G., POLLINGER, J. P., SEARLE, S. M. J., SUTTER, N. B., THOMAS, R., WEBBER, C. & LANDER, E. S. 2005. Genome sequence, comparative analysis and haplotype structure of the domestic dog. *Nature,* 438**,** 803-819.

LIU, J., MAO, J. J. & CHEN, L. 2011. Epithelial-mesenchymal interactions as a working concept for oral mucosa regeneration. *Tissue Eng Part B Rev,* 17**,** 25-31.

LIU, J., YANG, X., JIANG, L., WANG, C. & YANG, M. 2012. Neural plasticity after spinal cord injury. *Neural Regeneration Research,* 7**,** 386-391.

LIU, Z., LI, Y., ZHANG, Z. G., CUI, X., CUI, Y., LU, M., SAVANT-BHONSALE, S. & CHOPP, M. 2010. Bone marrow stromal cells enhance inter- and intracortical axonal connections after ischemic stroke in adult rats. *J Cereb Blood Flow Metab,* 30**,** 1288-95.

LOPATINA, T., BRUNO, S., TETTA, C., KALININA, N., PORTA, M. & CAMUSSI, G. 2014. Platelet-derived growth factor regulates the secretion of extracellular vesicles by adipose mesenchymal stem cells and enhances their angiogenic potential. *Cell Communication and Signaling : CCS,* 12**,** 26-26.

LOPATINA, T., KALININA, N., KARAGYAUR, M., STAMBOLSKY, D., RUBINA, K., REVISCHIN, A., PAVLOVA, G., PARFYONOVA, Y. & TKACHUK, V. 2011. Adipose-derived stem cells stimulate regeneration of peripheral nerves: BDNF secreted by these cells promotes nerve healing and axon growth de novo. *PLoS One,* 6**,** e17899.

LÓPEZ-IGLESIAS, P., BLÁZQUEZ-MARTÍNEZ, A., FERNÁNDEZ-DELGADO, J., REGADERA, J., NISTAL, M. & MIGUEL, M. P. D. 2011. Short and long term fate of human AMSC subcutaneously injected in mice. *World Journal of Stem Cells,* 3**,** 53-62.

LOY, D. N., CRAWFORD, C. H., DARNALL, J. B., BURKE, D. A., ONIFER, S. M. & WHITTEMORE, S. R. 2002. Temporal progression of angiogenesis and basal lamina deposition after contusive spinal cord injury in the adult rat. *J Comp Neurol,* 445**,** 308-24.

LUTTON, C., YOUNG, Y. W., WILLIAMS, R., MEEDENIYA, A. C., MACKAY-SIM, A. & GOSS, B. 2012. Combined VEGF and PDGF treatment reduces secondary degeneration after spinal cord injury. *J Neurotrauma,* 29**,** 957-70.

MADRIGAL, M., RAO, K. S. & RIORDAN, N. H. 2014. A review of therapeutic effects of mesenchymal stem cell secretions and induction of secretory modification by different culture methods. *Journal of Translational Medicine,* 12**,** 260.

MAJUMDAR, M. K., THIEDE, M. A., MOSCA, J. D., MOORMAN, M. & GERSON, S. L. 1998. Phenotypic and functional comparison of cultures of marrow-derived mesenchymal stem cells (MSCs) and stromal cells. *Journal of Cellular Physiology,* 176**,** 57-66.

MARIANI, E. & FACCHINI, A. 2012. Clinical applications and biosafety of human adult mesenchymal stem cells. *Curr Pharm Des,* 18**,** 1821-45.

MARIANO, E. D., TEIXEIRA, M. J., MARIE, S. K. N. & LEPSKI, G. 2015. Adult stem cells in neural repair: Current options, limitations and perspectives. *World Journal of Stem Cells,* 7**,** 477-482.

MARTIN, A. R., ALEKSANDEREK, I. & FEHLINGS, M. G. 2015. Diagnosis and Acute Management of Spinal Cord Injury: Current Best Practices and Emerging Therapies. *Current Trauma Reports,* 1**,** 169-181.

MARTIN, G. R. 1981. Isolation of a pluripotent cell line from early mouse embryos cultured in medium conditioned by teratocarcinoma stem cells. *Proc Natl Acad Sci U S A,* 78**,** 7634-8.

MARTÍN, M. & MENÉNDEZ, P. 2012. Biological Impact of Human Embryonic Stem Cells. *In:* LÓPEZ-LARREA, C., LÓPEZ-VÁZQUEZ, A. & SUÁREZ-ÁLVAREZ, B. (eds.) *Stem Cell Transplantation.* New York, NY: Springer US.

MASTER, Z., MCLEOD, M. & MENDEZ, I. 2007. Benefits, risks and ethical considerations in translation of stem cell research to clinical applications in Parkinson's disease. *Journal of Medical Ethics,* 33**,** 169-173.

MATNANI, R. G., STEWART, R. L., PULLIAM, J., JENNINGS, C. D. & KESLER, M. 2013. Peripheral T-Cell Lymphoma with Aberrant Expression of CD19, CD20, and CD79a: Case Report and Literature Review. *Case Reports in Hematology,* 2013**,** 5.

MATOS, A. C., LAROCCA, T., DE FREITAS, S. B., SOARES, M., MASCARENHAS, F. & SANTOS, R. 2016. 282 Bladder functional improvements after autologous transplantation of bone marrow mesenchymal stem cells In patients with chronic spinal cord injury: A phase I/II study. *European Urology Supplements,* 15**,** e282.

MAUTES, A. E., WEINZIERL, M. R., DONOVAN, F. & NOBLE, L. J. 2000. Vascular events after spinal cord injury: contribution to secondary pathogenesis. *Phys Ther,* 80**,** 673-87.

MCDONALD, J. W., LIU, X. Z., QU, Y., LIU, S., MICKEY, S. K., TURETSKY, D., GOTTLIEB, D. I. & CHOI, D. W. 1999. Transplanted embryonic stem cells survive, differentiate and promote recovery in injured rat spinal cord. *Nat Med,* 5**,** 1410-2.

MCMAHILL, B. G., BORJESSON, D. L., SIEBER-BLUM, M., NOLTA, J. A. & STURGES, B. K. 2015. Stem cells in canine spinal cord injury--promise for regenerative therapy in a large animal model of human disease. *Stem Cell Rev,* 11**,** 180-93.

MELTON, D. 2014. Chapter 2 - 'Stemness': Definitions, Criteria, and Standards. *Essentials of Stem Cell Biology (Third Edition).* Boston: Academic Press.

MENASCHE, P., VANNEAUX, V., FABREGUETTES, J. R., BEL, A., TOSCA, L., GARCIA, S., BELLAMY, V., FAROUZ, Y., POULY, J., DAMOUR, O., PERIER, M. C., DESNOS, M., HAGEGE, A., AGBULUT, O., BRUNEVAL, P., TACHDJIAN, G., TROUVIN, J. H. & LARGHERO, J. 2015. Towards a clinical use of human embryonic stem cell-derived cardiac progenitors: a translational experience. *Eur Heart J,* 36**,** 743-50.

MÉNDEZ-FERRER, S., MICHURINA, T. V., FERRARO, F., MAZLOOM, A. R., MACARTHUR, B. D., LIRA, S. A., SCADDEN, D. T., MA'AYAN, A., ENIKOLOPOV, G. N. & FRENETTE, P. S. 2010. Mesenchymal and haematopoietic stem cells form a unique bone marrow niche. *nature,* 466**,** 829-834.

MEYER, J. S., KATZ, M. L., MARUNIAK, J. A. & KIRK, M. D. 2004. Neural differentiation of mouse embryonic stem cells in vitro and after transplantation into eyes of mutant mice with rapid retinal degeneration. *Brain Res,* 1014**,** 131-44.

MIFUNE, Y., MATSUMOTO, T., MURASAWA, S., KAWAMOTO, A., KURODA, R., SHOJI, T., KURODA, T., FUKUI, T., KAWAKAMI, Y., KUROSAKA, M. & ASAHARA, T. 2013. Therapeutic superiority for cartilage repair by CD271-positive marrow stromal cell transplantation. *Cell Transplant,* 22**,** 1201-11.

MILTENYI, S., MULLER, W., WEICHEL, W. & RADBRUCH, A. 1990. High gradient magnetic cell separation with MACS. *Cytometry,* 11**,** 231-8.

MIRANVILLE, A., HEESCHEN, C., SENGENES, C., CURAT, C. A., BUSSE, R. & BOULOUMIE, A. 2004. Improvement of postnatal neovascularization by human adipose tissue-derived stem cells. *Circulation,* 110**,** 349-55.

MIZUNO, H., ZUK, P. A., ZHU, M., LORENZ, H. P., BENHAIM, P. & HEDRICK, M. H. 2002. Myogenic differentiation by human processed lipoaspirate cells. *Plast Reconstr Surg,* 109**,** 199-209; discussion 210-1.

MORANDO, S., VIGO, T., ESPOSITO, M., CASAZZA, S., NOVI, G., PRINCIPATO, M. C., FURLAN, R. & UCCELLI, A. 2012. The therapeutic effect of mesenchymal stem cell transplantation in experimental autoimmune encephalomyelitis is mediated by peripheral and central mechanisms. *Stem Cell Res Ther,* 3**,** 3.

MORGAN, D. M. L. 1998. Tetrazolium (MTT) Assay for Cellular Viability and Activity. *In:* MORGAN, D. M. L. (ed.) *Polyamine Protocols.* Totowa, NJ: Humana Press.

MORTE, M. I., CARREIRA, B. P., MACHADO, V., CARMO, A., NUNES-CORREIA, I., CARVALHO, C. M. & ARAUJO, I. M. 2013. Evaluation of proliferation of neural stem cells in vitro and in vivo. *Curr Protoc Stem Cell Biol,* Chapter 2**,** Unit 2D.14.

MOTHE, A. J. & TATOR, C. H. 2012. Advances in stem cell therapy for spinal cord injury. *J Clin Invest,* 122**,** 3824-34.

NEIRINCKX, V., AGIRMAN, G., COSTE, C., MARQUET, A., DION, V., ROGISTER, B., FRANZEN, R. & WISLET, S. 2015. Adult bone marrow mesenchymal and neural crest stem cells are chemoattractive and accelerate motor recovery in a mouse model of spinal cord injury. *Stem Cell Res Ther,* 6**,** 211.

NEUHUBER, B., TIMOTHY HIMES, B., SHUMSKY, J. S., GALLO, G. & FISCHER, I. 2005. Axon growth and recovery of function supported by human bone marrow stromal cells in the injured spinal cord exhibit donor variations. *Brain Research,* 1035**,** 73-85.

NG, M. T., STAMMERS, A. T. & KWON, B. K. 2011. Vascular disruption and the role of angiogenic proteins after spinal cord injury. *Transl Stroke Res,* 2**,** 474-91.

NIELSEN, J. S. & MCNAGNY, K. M. 2009. CD34 is a key regulator of hematopoietic stem cell trafficking to bone marrow and mast cell progenitor trafficking in the periphery. *Microcirculation,* 16**,** 487-96.

NOER, A., SØRENSEN, A. L., BOQUEST, A. C. & COLLAS, P. 2006. Stable CpG Hypomethylation of Adipogenic Promoters in Freshly Isolated, Cultured, and Differentiated Mesenchymal Stem Cells from Adipose Tissue. *Molecular Biology of the Cell,* 17**,** 3543-3556.

NORTON, K.-A. & POPEL, A. S. 2016. Effects of endothelial cell proliferation and migration rates in a computational model of sprouting angiogenesis. *Scientific Reports,* 6**,** 36992.

NOVOTNY, E., COMPTON, S., LIU, P. P., COLLINS, F. S. & CHANDRASEKHARAPPA, S. C. 2009. In vitro hematopoietic differentiation of mouse embryonic stem cells requires the tumor suppressor menin and is mediated by Hoxa9. *Mech Dev,* 126**,** 517-22.

ODORICO, J. S., KAUFMAN, D. S. & THOMSON, J. A. 2001. Multilineage differentiation from human embryonic stem cell lines. *Stem Cells,* 19**,** 193-204.

OH, J., LEE, K.-I., KIM, H.-T., YOU, Y., YOON, D. H., SONG, K. Y., CHEONG, E., HA, Y. & HWANG, D.-Y. 2015. Human-induced pluripotent stem cells generated from intervertebral disc cells improve neurologic functions in spinal cord injury. *Stem Cell Research & Therapy,* 6**,** 125.

OHTA, M., SUZUKI, Y., NODA, T., EJIRI, Y., DEZAWA, M., KATAOKA, K., CHOU, H., ISHIKAWA, N., MATSUMOTO, N., IWASHITA, Y., MIZUTA, E., KUNO, S. & IDE, C. 2004. Bone marrow stromal cells infused into the cerebrospinal fluid promote functional recovery of the injured rat spinal cord with reduced cavity formation. *Exp Neurol,* 187**,** 266-78.

OKITA, K., ICHISAKA, T. & YAMANAKA, S. 2007. Generation of germline-competent induced pluripotent stem cells. *Nature,* 448**,** 313-317.

OLIVERI, R. S., BELLO, S. & BIERING-SØRENSEN, F. 2014. Mesenchymal stem cells improve locomotor recovery in traumatic spinal cord injury: Systematic review with meta-analyses of rat models. *Neurobiology of Disease,* 62**,** 338-353.

OUDEGA, M. 2012. Molecular and cellular mechanisms underlying the role of blood vessels in spinal cord injury and repair. *Cell and Tissue Research,* 349**,** 269-288.

OYINBO, C. A. 2011. Secondary injury mechanisms in traumatic spinal cord injury: a nugget of this multiply cascade. *Acta Neurobiol Exp (Wars),* 71**,** 281-99.

PADOIN, A. V., BRAGA-SILVA, J., MARTINS, P., REZENDE, K., REZENDE, A. R., GRECHI, B., GEHLEN, D. & MACHADO, D. C. 2008. Sources of processed lipoaspirate cells: influence of donor site on cell concentration. *Plast Reconstr Surg,* 122**,** 614-8.

PALAZZOLO, G., HORVATH, P. & ZENOBI-WONG, M. 2012. The Flavonoid Isoquercitrin Promotes Neurite Elongation by Reducing RhoA Activity. *PLoS ONE,* 7**,** e49979.

PANDYA, N. M., DHALLA, N. S. & SANTANI, D. D. 2006. Angiogenesis--a new target for future therapy. *Vascul Pharmacol,* 44**,** 265-74.

PARK, D.-H., LEE, J.-H., BORLONGAN, C. V., SANBERG, P. R., CHUNG, Y.-G. & CHO, T.-H. 2011. Transplantation of Umbilical Cord Blood Stem Cells for Treating Spinal Cord Injury. *Stem Cell Reviews and Reports,* 7**,** 181-194.

PARK, J. H., KIM, D. Y., SUNG, I. Y., CHOI, G. H., JEON, M. H., KIM, K. K. & JEON, S. R. 2012a. Long-term results of spinal cord injury therapy using mesenchymal stem cells derived from bone marrow in humans. *Neurosurgery,* 70**,** 1238-47; discussion 1247.

PARK, J. S., WITHERS, S. S., MODIANO, J. F., KENT, M. S., CHEN, M., LUNA, J. I., CULP, W. T. N., SPARGER, E. E., REBHUN, R. B., MONJAZEB, A. M., MURPHY, W. J. &

CANTER, R. J. 2016. Canine cancer immunotherapy studies: linking mouse and human. *Journal for ImmunoTherapy of Cancer,* 4**,** 97.

PARK, S.-S., LEE, Y. J., LEE, S. H., LEE, D., CHOI, K., KIM, W.-H., KWEON, O.-K. & HAN, H. J. 2012b. Functional recovery after spinal cord injury in dogs treated with a combination of Matrigel and neural-induced adipose-derived mesenchymal Stem cells. *Cytotherapy,* 14**,** 584-597.

PARK, Y. B., KIM, Y. Y., OH, S. K., CHUNG, S. G., KU, S.-Y., KIM, S. H., CHOI, Y. M. & MOON, S. Y. 2008. Alterations of proliferative and differentiation potentials of human embryonic stem cells during long-term culture. *Experimental & Molecular Medicine,* 40**,** 98-108.

PATEL, D. M., SHAH, J. & SRIVASTAVA, A. S. 2013. Therapeutic Potential of Mesenchymal Stem Cells in Regenerative Medicine. *Stem Cells International,* 2013**,** 15.

PAUL, G. & ANISIMOV, S. V. 2013. The secretome of mesenchymal stem cells: potential implications for neuroregeneration. *Biochimie,* 95**,** 2246-56.

PENHA, E. M., MEIRA, C. S., GUIMAR, E. T., MENDONÇA, M. V. P., GRAVELY, F. A., PINHEIRO, C. M. B., PINHEIRO, T. M. B., BARROUIN-MELO, S. M., RIBEIRO-DOS-SANTOS, R. & SOARES, M. B. P. 2014. Use of Autologous Mesenchymal Stem Cells Derived from Bone Marrow for the Treatment of Naturally Injured Spinal Cord in Dogs. *Stem Cells International,* 2014**,** 8.

PEVSNER-FISCHER, M., LEVIN, S. & ZIPORI, D. 2011. The origins of mesenchymal stromal cell heterogeneity. *Stem Cell Rev,* 7**,** 560-8.

PHINNEY, D. G. 2012. Functional heterogeneity of mesenchymal stem cells: implications for cell therapy. *J Cell Biochem,* 113**,** 2806-12.

PIRES, A. O., NEVES-CARVALHO, A., SOUSA, N. & SALGADO, A. J. 2014. The Secretome of Bone Marrow and Wharton Jelly Derived Mesenchymal Stem Cells Induces Differentiation and Neurite Outgrowth in SH-SY5Y Cells. *Stem Cells International,* 2014**,** 438352.

PITTENGER, M. F., MACKAY, A. M., BECK, S. C., JAISWAL, R. K., DOUGLAS, R., MOSCA, J. D., MOORMAN, M. A., SIMONETTI, D. W., CRAIG, S. & MARSHAK, D. R. 1999. Multilineage potential of adult human mesenchymal stem cells. *Science,* 284**,** 143-7.

PLEWS, J. R., GU, M., LONGAKER, M. T. & WU, J. C. 2012. Large animal induced pluripotent stem cells as pre-clinical models for studying human disease. *J Cell Mol Med,* 16**,** 1196-202.

PLUCHINO, S. & COSSETTI, C. 2013. How stem cells speak with host immune cells in inflammatory brain diseases. *Glia,* 61**,** 1379-401.

PLUCHINO, S., ZANOTTI, L., ROSSI, B., BRAMBILLA, E., OTTOBONI, L., SALANI, G., MARTINELLO, M., CATTALINI, A., BERGAMI, A., FURLAN, R., COMI, G., CONSTANTIN, G. & MARTINO, G. 2005. Neurosphere-derived multipotent precursors promote neuroprotection by an immunomodulatory mechanism. *Nature,* 436**,** 266-71.

POLEJAEVA, I. & MITALIPOV, S. 2013. Stem cell potency and the ability to contribute to chimeric organisms. *Reproduction (Cambridge, England),* 145**,** R81-R88.

PONCE, M. L. 2001. In vitro matrigel angiogenesis assays. *Methods Mol Med,* 46**,** 205-9.

PONCE, M. L. 2009. Tube formation: an in vitro matrigel angiogenesis assay. *Methods Mol Biol,* 467**,** 183-8.

PONTA, H., SHERMAN, L. & HERRLICH, P. A. 2003. CD44: from adhesion molecules to signalling regulators. *Nat Rev Mol Cell Biol,* 4**,** 33-45.

POPOVICH, P. G., WEI, P. & STOKES, B. T. 1997. Cellular inflammatory response after spinal cord injury in Sprague-Dawley and Lewis rats. *J Comp Neurol,* 377**,** 443-64.

POTIAN, J. A., AVIV, H., PONZIO, N. M., HARRISON, J. S. & RAMESHWAR, P. 2003. Veto-like activity of mesenchymal stem cells: functional discrimination between cellular responses to alloantigens and recall antigens. *J Immunol,* 171**,** 3426-34.

QESKA, V., BAUMGARTNER, W. & BEINEKE, A. 2013. Species-specific properties and translational aspects of canine dendritic cells. *Vet Immunol Immunopathol,* 151**,** 181-92.

QU, J. & ZHANG, H. 2017. Roles of Mesenchymal Stem Cells in Spinal Cord Injury. *Stem Cells International,* 2017**,** 12.

QUERTAINMONT, R., CANTINIEAUX, D., BOTMAN, O., SID, S., SCHOENEN, J. & FRANZEN, R. 2012. Mesenchymal Stem Cell Graft Improves Recovery after Spinal Cord Injury in Adult Rats through Neurotrophic and Pro-Angiogenic Actions. *PLOS ONE,* 7**,** e39500.

QUIRICI, N., SOLIGO, D., BOSSOLASCO, P., SERVIDA, F., LUMINI, C. & DELILIERS, G. L. 2002. Isolation of bone marrow mesenchymal stem cells by anti-nerve growth factor receptor antibodies. *Exp Hematol,* 30**,** 783-91.

RAMAKRISHNAN, A., TOROK-STORB, B. & PILLAI, M. M. 2013. Primary marrow-derived stromal cells: isolation and manipulation. *Methods Mol Biol,* 1035**,** 75-101.

RAMIREZ-ZACARIAS, J. L., CASTRO-MUNOZLEDO, F. & KURI-HARCUCH, W. 1992. Quantitation of adipose conversion and triglycerides by staining intracytoplasmic lipids with Oil red O. *Histochemistry,* 97**,** 493-7.

RÄMÖ, O., KUMAR, D., GUCCIARDO, E., JOENSUU, M., SAAREKAS, M., VIHINEN, H., BELEVICH, I., SMOLANDER, O.-P., QIAN, K., AUVINEN, P. & JOKITALO, E. 2016. NOGO-A/RTN4A and NOGO-B/RTN4B are simultaneously expressed in epithelial, fibroblast and neuronal cells and maintain ER morphology. *Scientific Reports,* 6**,** 35969.

RANGANATH, S. H., LEVY, O., INAMDAR, M. S. & KARP, J. M. 2012. Harnessing the Mesenchymal Stem Cell Secretome for the Treatment of Cardiovascular Disease. *Cell Stem Cell,* 10**,** 244-258.

RATHINASABAPATHY, A., BRUCE, E., ESPEJO, A., HOROWITZ, A., SUDHAN, D. R., NAIR, A., GUZZO, D., FRANCIS, J., RAIZADA, M. K., SHENOY, V. & KATOVICH, M. J. 2016. Therapeutic potential of adipose stem cell-derived conditioned medium against pulmonary hypertension and lung fibrosis. *Br J Pharmacol,* 173**,** 2859-79.

RAUCH, M. F., HYNES, S. R., BERTRAM, J., REDMOND, A., ROBINSON, R., WILLIAMS, C., XU, H., MADRI, J. A. & LAVIK, E. B. 2009. Engineering angiogenesis following spinal cord injury: A coculture of neural progenitor and endothelial cells in a degradable polymer implant leads to an increase in vessel density and formation of the blood-spinal cord barrier. *The European journal of neuroscience,* 29**,** 132-145.

RAZEGHIAN JAHROMI, I., MEHRABANI, D., MOHAMMADI, A., DIANATPOUR, M., TAMADON, A., ZARE, S., GHAHREMANI SENO, M. & KHODABANDEH, Z. 2016. The effect of fetal rat brain extract on morphology of bone marrow-derived mesenchymal stem cells. *Comparative Clinical Pathology,* 25**,** 343-349.

REGE, T. A. & HAGOOD, J. S. 2006. Thy-1 as a regulator of cell-cell and cell-matrix interactions in axon regeneration, apoptosis, adhesion, migration, cancer, and fibrosis. *Faseb j,* 20**,** 1045-54.

RIBEIRO, C., SALGADO, A., FRAGA, J., SILVA, N., REIS, R. & SOUSA, N. 2011. The secretome of bone marrow mesenchymal stem cells-conditioned media varies with time and drives a distinct effect on mature neurons and glial cells (primary cultures). *Journal of tissue engineering and regenerative medicine,* 5**,** 668-672.

RIEBER, A. J., MARR, H. S., COMER, M. B. & EDGELL, C. J. 1993. Extent of differentiated gene expression in the human endothelium-derived EA.hy926 cell line. *Thromb Haemost,* 69**,** 476-80.

RONG, Z., FU, X., WANG, M. & XU, Y. 2012. A scalable approach to prevent teratoma formation of human embryonic stem cells. *J Biol Chem,* 287**,** 32338-45.

ROSENZWEIG, E. S., COURTINE, G., JINDRICH, D. L., BROCK, J. H., FERGUSON, A. R., STRAND, S. C., NOUT, Y. S., ROY, R. R., MILLER, D. M., BEATTIE, M. S., HAVTON, L. A., BRESNAHAN, J. C., EDGERTON, V. R. & TUSZYNSKI, M. H. 2010. Extensive spontaneous plasticity of corticospinal projections after primate spinal cord injury. *Nat Neurosci,* 13**,** 1505-1510.

ROSENZWEIG, E. S. & MCDONALD, J. W. 2004. Rodent models for treatment of spinal cord injury: research trends and progress toward useful repair. *Curr Opin Neurol,* 17**,** 121-31.

ROWELL, J. L., MCCARTHY, D. O. & ALVAREZ, C. E. 2011. Dog models of naturally occurring cancer. *Trends Mol Med,* 17**,** 380-8.

ROWLAND, J. W., HAWRYLUK, G. W., KWON, B. & FEHLINGS, M. G. 2008. Current status of acute spinal cord injury pathophysiology and emerging therapies: promise on the horizon. *Neurosurg Focus,* 25**,** E2.

SALEGIO, E. A., BRESNAHAN, J. C., SPARREY, C. J., CAMISA, W., FISCHER, J., LEASURE, J., BUCKLEY, J., NOUT-LOMAS, Y. S., ROSENZWEIG, E. S., MOSEANKO, R., STRAND, S., HAWBECKER, S., LEMOY, M. J., HAEFELI, J., MA, X., NIELSON, J. L., EDGERTON, V. R., FERGUSON, A. R., TUSZYNSKI, M. H. & BEATTIE, M. S. 2016. A Unilateral Cervical Spinal Cord Contusion Injury Model in Non-Human Primates (Macaca mulatta). *J Neurotrauma,* 33**,** 439-59.

SALEWSKI, R. P., MITCHELL, R. A., LI, L., SHEN, C., MILEKOVSKAIA, M., NAGY, A. & FEHLINGS, M. G. 2015. Transplantation of Induced Pluripotent Stem Cell-Derived Neural Stem Cells Mediate Functional Recovery Following Thoracic Spinal Cord Injury Through Remyelination of Axons. *Stem Cells Transl Med,* 4**,** 743-54.

SARMENTO, C. A. P., RODRIGUES, M. N., BOCABELLO, R. Z., MESS, A. M. & MIGLINO, M. A. 2014. Pilot study: bone marrow stem cells as a treatment for dogs with chronic spinal cord injury. *Regenerative Medicine Research,* 2**,** 9.

SASISEKHARAN, R., RAMAN, R. & PRABHAKAR, V. 2006. Glycomics approach to structure-function relationships of glycosaminoglycans. *Annu Rev Biomed Eng,* 8**,** 181-231.

SCHINKOTHE, T., BLOCH, W. & SCHMIDT, A. 2008. In vitro secreting profile of human mesenchymal stem cells. *Stem Cells Dev,* 17**,** 199-206.

SCHMITT, A. B., BUSS, A., BREUER, S., BROOK, G. A., PECH, K., MARTIN, D., SCHOENEN, J., NOTH, J., LOVE, S., SCHRODER, J. M., KREUTZBERG, G. W. & NACIMIENTO, W. 2000. Major histocompatibility complex class II expression by activated microglia caudal to lesions of descending tracts in the human spinal cord is not associated with a T cell response. *Acta Neuropathol,* 100**,** 528-36.

SCHNEIDER, M. R., WOLF, E., BRAUN, J., KOLB, H.-J. & ADLER, H. 2008. Canine embryo-derived stem cells and models for human diseases. *Human Molecular Genetics,* 17**,** R42-R47.

SCHWARTZ, S. D., HUBSCHMAN, J.-P., HEILWELL, G., FRANCO-CARDENAS, V., PAN, C. K., OSTRICK, R. M., MICKUNAS, E., GAY, R., KLIMANSKAYA, I. & LANZA, R. 2012. Embryonic stem cell trials for macular degeneration: a preliminary report. *The Lancet,* 379**,** 713-720.

SHAPIRO, H. M. 2004. The evolution of cytometers. *Cytometry A,* 58**,** 13-20.

SHARMA, M., KUMAR, R., DUBEY, P. K., VERMA, O. P., NATH, A., SAIKUMAR, G. & SHARMA, G. T. 2012. Expression and quantification of Oct-4 gene in blastocyst and embryonic stem cells derived from in vitro produced buffalo embryos. *In Vitro Cell Dev Biol Anim,* 48**,** 229-35.

SHUTTERSTOCK. 2003. *Fertilized egg development* [Online]. Available: https://www.shutterstock.com/image-vector/fertilized-egg-development-isolated-on-white-132798476 [Accessed 3.2.2016].

SIEGEL, G., KLUBA, T., HERMANUTZ-KLEIN, U., BIEBACK, K., NORTHOFF, H. & SCHÄFER, R. 2013. Phenotype, donor age and gender affect function of human bone marrow-derived mesenchymal stromal cells. *BMC Medicine,* 11**,** 146.

SILVA, N. A., SOUSA, N., REIS, R. L. & SALGADO, A. J. 2014. From basics to clinical: a comprehensive review on spinal cord injury. *Prog Neurobiol,* 114**,** 25-57.

SIVASUBRAMANIYAN, K., LEHNEN, D., GHAZANFARI, R., SOBIESIAK, M., HARICHANDAN, A., MORTHA, E., PETKOVA, N., GRIMM, S., CERABONA, F., DE ZWART, P., ABELE, H., AICHER, W. K., FAUL, C., KANZ, L. & BÜHRING, H.-J. 2012. Phenotypic and functional heterogeneity of human bone marrow– and amnion-derived MSC subsets. *Annals of the New York Academy of Sciences,* 1266**,** 94-106.

SKALNIKOVA, H., MOTLIK, J., GADHER, S. J. & KOVAROVA, H. 2011. Mapping of the secretome of primary isolates of mammalian cells, stem cells and derived cell lines. *Proteomics,* 11**,** 691-708.

SOTIROPOULOU, P. A., PEREZ, S. A., SALAGIANNI, M., BAXEVANIS, C. N. & PAPAMICHAIL, M. 2006. Characterization of the optimal culture conditions for clinical scale production of human mesenchymal stem cells. *Stem Cells,* 24**,** 462-71.

SPITZBARTH, I., BOCK, P., HAIST, V., STEIN, V. M., TIPOLD, A., WEWETZER, K., BAUMGARTNER, W. & BEINEKE, A. 2011. Prominent microglial activation in the early proinflammatory immune response in naturally occurring canine spinal cord injury. *J Neuropathol Exp Neurol,* 70**,** 703-14.

SPRADLING, A., DRUMMOND-BARBOSA, D. & KAI, T. 2001. Stem cells find their niche. *Nature,* 414**,** 98-104.

STARKEY, M. P., SCASE, T. J., MELLERSH, C. S. & MURPHY, S. 2005. Dogs really are man's best friend--canine genomics has applications in veterinary and human medicine! *Brief Funct Genomic Proteomic,* 4**,** 112-28.

ŠTEFKOVÁ, K., PROCHÁZKOVÁ, J. & PACHERNÍK, J. 2015. Alkaline phosphatase in stem cells. *Stem cells international,* 2015.

STEINHAUSER, C., HEIGL, U., TCHIKOV, V., SCHWARZ, J., GUTSMANN, T., SEEGER, K., BRANDENBURG, J., FRITSCH, J., SCHROEDER, J., WIESMULLER, K. H., ROSENKRANDS, I., WALTHER, P., POTT, J., KRAUSE, E., EHLERS, S., SCHNEIDER-BRACHERT, W., SCHUTZE, S. & REILING, N. 2013. Lipid-labeling facilitates a novel magnetic isolation procedure to characterize pathogen-containing phagosomes. *Traffic,* 14**,** 321-36.

STREM, B. M., HICOK, K. C., ZHU, M., WULUR, I., ALFONSO, Z., SCHREIBER, R. E., FRASER, J. K. & HEDRICK, M. H. 2005. Multipotential differentiation of adipose tissue-derived stem cells. *Keio J Med,* 54**,** 132-41.

STRIOGA, M., VISWANATHAN, S., DARINSKAS, A., SLABY, O. & MICHALEK, J. 2012. Same or not the same? Comparison of adipose tissue-derived versus bone marrow-derived mesenchymal stem and stromal cells. *Stem Cells Dev,* 21**,** 2724-52.

STUDENY, M., MARINI, F. C., DEMBINSKI, J. L., ZOMPETTA, C., CABREIRA-HANSEN, M., BEKELE, B. N., CHAMPLIN, R. E. & ANDREEFF, M. 2004. Mesenchymal stem cells: potential precursors for tumor stroma and targeted-delivery vehicles for anticancer agents. *J Natl Cancer Inst,* 96**,** 1593-603.

SUN, H., BÉNARDAIS, K., STANSLOWSKY, N., THAU-HABERMANN, N., HENSEL, N., HUANG, D., CLAUS, P., DENGLER, R., STANGEL, M. & PETRI, S. 2013. Therapeutic Potential of Mesenchymal Stromal Cells and MSC Conditioned Medium in Amyotrophic Lateral Sclerosis (ALS) - In Vitro Evidence from Primary Motor Neuron Cultures, NSC-34 Cells, Astrocytes and Microglia. *PLOS ONE,* 8**,** e72926.

SWIJNENBURG, R.-J., SCHREPFER, S., CAO, F., PEARL, J. I., XIE, X., CONNOLLY, A. J., ROBBINS, R. C. & WU, J. C. 2008. In Vivo Imaging of Embryonic Stem Cells Reveals Patterns of Survival and Immune Rejection Following Transplantation. *Stem Cells and Development,* 17**,** 1023-1029.

SWITONSKI, M. & SZCZERBAL, I. 2001. Comparing the Human and Canine Genomes. *eLS.* John Wiley & Sons, Ltd.

SYSTEM, H. A. 2016. *Anatomy Of Spine And Spinal Cord Spinal Anatomy Spinal Regions Bones And Discs Vertebrae* [Online]. Available: https://www.anatomylibrary.us/anatomy-of-spine-and-spinal-cord/anatomy-of-spine-and-spinal-cord-spinal-anatomy-spinal-regions-bones-and-discs-vertebrae-2/ [Accessed 15.6.2016].

TAKAHASHI, K. & YAMANAKA, S. 2006. Induction of Pluripotent Stem Cells from Mouse Embryonic and Adult Fibroblast Cultures by Defined Factors. *Cell,* 126**,** 663-676.

TALLONE, T., REALINI, C., BÖHMLER, A., KORNFELD, C., VASSALLI, G., MOCCETTI, T., BARDELLI, S. & SOLDATI, G. 2011. Adult Human Adipose Tissue Contains Several Types of Multipotent Cells. *Journal of Cardiovascular Translational Research,* 4**,** 200-210.

TATOR, C. H. 2006. Review of treatment trials in human spinal cord injury: issues, difficulties, and recommendations. *Neurosurgery,* 59**,** 957-82; discussion 982-7.

TAYLOR, C. J., BOLTON, E. M. & BRADLEY, J. A. 2011. Immunological considerations for embryonic and induced pluripotent stem cell banking. *Philosophical Transactions of the Royal Society B: Biological Sciences,* 366**,** 2312-2322.

TECHNIQUES, F. A. 2004. *Practical Applications Of Immunology* [Online]. Available: http://classes.midlandstech.edu/carterp/Courses/bio225/chap18/lecture6.htm [Accessed 25.6.2016].

TEIXEIRA, F. G., CARVALHO, M. M., SOUSA, N. & SALGADO, A. J. 2013. Mesenchymal stem cells secretome: a new paradigm for central nervous system regeneration? *Cellular and Molecular Life Sciences,* 70**,** 3871-3882.

TEIXEIRA, F. G., PANCHALINGAM, K. M., ASSUNÇÃO-SILVA, R., SERRA, S. C., MENDES-PINHEIRO, B., PATRÍCIO, P., JUNG, S., ANJO, S. I., MANADAS, B., PINTO, L., SOUSA, N., BEHIE, L. A. & SALGADO, A. J. 2016. Modulation of the Mesenchymal Stem Cell Secretome Using Computer-Controlled Bioreactors: Impact on Neuronal Cell Proliferation, Survival and Differentiation. *Scientific Reports,* 6**,** 27791.

THOMSON, J. A., ITSKOVITZ-ELDOR, J., SHAPIRO, S. S., WAKNITZ, M. A., SWIERGIEL, J. J., MARSHALL, V. S. & JONES, J. M. 1998. Embryonic stem cell lines derived from human blastocysts. *Science,* 282**,** 1145-7.

THURET, S., MOON, L. D. F. & GAGE, F. H. 2006. Therapeutic interventions after spinal cord injury. *Nat Rev Neurosci,* 7**,** 628-643.

TIMMERS, L., LIM, S. K., HOEFER, I. E., ARSLAN, F., LAI, R. C., VAN OORSCHOT, A. A. M., GOUMANS, M. J., STRIJDER, C., SZE, S. K., CHOO, A., PIEK, J. J., DOEVENDANS, P. A., PASTERKAMP, G. & DE KLEIJN, D. P. V. 2011. Human mesenchymal stem cell-conditioned medium improves cardiac function following myocardial infarction. *Stem Cell Research,* 6**,** 206-214.

TIPNIS, S., VISWANATHAN, C. & MAJUMDAR, A. S. 2010. Immunosuppressive properties of human umbilical cord-derived mesenchymal stem cells: role of B7-H1 and IDO. *Immunol Cell Biol,* 88**,** 795-806.

TOBIAS, P. S. & ULEVITCH, R. J. 1993. Lipopolysaccharide binding protein and CD14 in LPS dependent macrophage activation. *Immunobiology,* 187**,** 227-32.

TONDREAU, T., MEULEMAN, N., DELFORGE, A., DEJENEFFE, M., LEROY, R., MASSY, M., MORTIER, C., BRON, D. & LAGNEAUX, L. 2005. Mesenchymal stem cells derived from CD133-positive cells in mobilized peripheral blood and cord blood: proliferation, Oct4 expression, and plasticity. *Stem Cells,* 23**,** 1105-12.

TORMIN, A., LI, O., BRUNE, J. C., WALSH, S., SCHUTZ, B., EHINGER, M., DITZEL, N., KASSEM, M. & SCHEDING, S. 2011. CD146 expression on primary nonhematopoietic bone marrow stem cells is correlated with in situ localization. *Blood,* 117**,** 5067-77.

TOSH, D. & HORB, M. E. 2014. Chapter 9 - How Cells Change Their Phenotype. *Essentials of Stem Cell Biology (Third Edition).* Boston: Academic Press.

TROUNSON, A. & DEWITT, N. D. 2016. Pluripotent stem cells progressing to the clinic. *Nat Rev Mol Cell Biol,* 17**,** 194-200.

TSUJI, O., MIURA, K., FUJIYOSHI, K., MOMOSHIMA, S., NAKAMURA, M. & OKANO, H. 2011. Cell therapy for spinal cord injury by neural stem/progenitor cells derived from iPS/ES cells. *Neurotherapeutics,* 8**,** 668-76.

UCCELLI, A., MORETTA, L. & PISTOIA, V. 2008. Mesenchymal stem cells in health and disease. *Nat Rev Immunol,* 8**,** 726-36.

UCUZIAN, A. A. & GREISLER, H. P. 2007. In Vitro Models of Angiogenesis. *World Journal of Surgery,* 31**,** 654-663.

VALADI, H., EKSTROM, K., BOSSIOS, A., SJOSTRAND, M., LEE, J. J. & LOTVALL, J. O. 2007. Exosome-mediated transfer of mRNAs and microRNAs is a novel mechanism of genetic exchange between cells. *Nat Cell Biol,* 9**,** 654-9.

VAN NIEL, G., PORTO-CARREIRO, I., SIMOES, S. & RAPOSO, G. 2006. Exosomes: a common pathway for a specialized function. *J Biochem,* 140**,** 13-21.

VARMA, M. J., BREULS, R. G., SCHOUTEN, T. E., JURGENS, W. J., BONTKES, H. J., SCHUURHUIS, G. J., VAN HAM, S. M. & VAN MILLIGEN, F. J. 2007. Phenotypical and functional characterization of freshly isolated adipose tissue-derived stem cells. *Stem Cells Dev,* 16**,** 91-104.

VEGA, A., MARTIN-FERRERO, M. A., DEL CANTO, F., ALBERCA, M., GARCIA, V., MUNAR, A., OROZCO, L., SOLER, R., FUERTES, J. J., HUGUET, M., SANCHEZ, A. & GARCIA-SANCHO, J. 2015. Treatment of Knee Osteoarthritis With Allogeneic Bone Marrow Mesenchymal Stem Cells: A Randomized Controlled Trial. *Transplantation,* 99**,** 1681-90.

VILLATORO, A. J., FERNÁNDEZ, V., CLAROS, S., RICO-LLANOS, G. A., BECERRA, J. & ANDRADES, J. A. 2015. Use of adipose-derived mesenchymal stem cells in keratoconjunctivitis sicca in a canine model. *BioMed research international,* 2015.

WAGNER, J. L. & STORB, R. 1996. Preclinical large animal models for hematopoietic stem cell transplantation. *Curr Opin Hematol,* 3**,** 410-5.

WAKITANI, S., SAITO, T. & CAPLAN, A. I. 1995. Myogenic cells derived from rat bone marrow mesenchymal stem cells exposed to 5-azacytidine. *Muscle Nerve,* 18**,** 1417-26.

WALTER, M. N., WRIGHT, K. T., FULLER, H. R., MACNEIL, S. & JOHNSON, W. E. 2010. Mesenchymal stem cell-conditioned medium accelerates skin wound healing: an in vitro study of fibroblast and keratinocyte scratch assays. *Exp Cell Res,* 316**,** 1271-81.

WALTER, M. N. M., KOHLI, N., KHAN, N., MAJOR, T., FULLER, H., WRIGHT, K. T., KUIPER, J.-H. & JOHNSON, W. E. B. 2015. Human mesenchymal stem cells stimulate EaHy926 endothelial cell migration: combined proteomic and in vitro analysis of the influence of donor-donor variability. *Journal of Stem Cells & Regenerative Medicine,* 11**,** 18-24.

WANG, J. & PEARSE, D. 2015. Therapeutic Hypothermia in Spinal Cord Injury: The Status of Its Use and Open Questions. *International Journal of Molecular Sciences,* 16**,** 16848.

WANG, M., CRISOSTOMO, P. R., HERRING, C., MELDRUM, K. K. & MELDRUM, D. R. 2006. Human progenitor cells from bone marrow or adipose tissue produce VEGF, HGF, and IGF-I in response to TNF by a p38 MAPK-dependent mechanism. *Am J Physiol Regul Integr Comp Physiol,* 291**,** R880-4.

WARD, P. A. 2009. The sepsis seesaw: seeking a heart salve. *Nat Med,* 15**,** 497-498.

WEBB, A. A., NGAN, S. & FOWLER, J. D. 2010. Spinal cord injury I: A synopsis of the basic science. *The Canadian Veterinary Journal,* 51**,** 485-492.

WEBMD 2017. How to Figure Out Your Dog's Age.

WELLS, J. E., HURLBERT, R. J., FEHLINGS, M. G. & YONG, V. W. 2003. Neuroprotection by minocycline facilitates significant recovery from spinal cord injury in mice. *Brain,* 126**,** 1628-37.

WELLS, W. A. 2002. Is transdifferentiation in trouble? *J Cell Biol,* 157**,** 15-8.

WHETSTONE, W. D., HSU, J.-Y. C., EISENBERG, M., WERB, Z. & NOBLE-HAEUSSLEIN, L. J. 2003. Blood-Spinal Cord Barrier After Spinal Cord Injury: Relation to Revascularization and Wound Healing. *Journal of neuroscience research,* 74**,** 227-239.

WICHTERLE, H., LIEBERAM, I., PORTER, J. A. & JESSELL, T. M. 2002. Directed differentiation of embryonic stem cells into motor neurons. *Cell,* 110**,** 385-97.

WILKINS, A., KEMP, K., GINTY, M., HARES, K., MALLAM, E. & SCOLDING, N. 2009. Human bone marrow-derived mesenchymal stem cells secrete brain-derived neurotrophic factor which promotes neuronal survival in vitro. *Stem Cell Research,* 3**,** 63-70.

WRIGHT, K. T., EL MASRI, W., OSMAN, A., ROBERTS, S., CHAMBERLAIN, G., ASHTON, B. A. & JOHNSON, W. E. 2007. Bone marrow stromal cells stimulate neurite outgrowth over neural proteoglycans (CSPG), myelin associated glycoprotein and Nogo-A. *Biochem Biophys Res Commun,* 354**,** 559-66.

WRIGHT, K. T., GRIFFITHS, G. J. & JOHNSON, W. E. 2010. A comparison of high-content screening versus manual analysis to assay the effects of mesenchymal stem cell-conditioned medium on neurite outgrowth in vitro. *J Biomol Screen,* 15**,** 576-82.

WRIGHT, K. T., MASRI, W. E., OSMAN, A., CHOWDHURY, J. & JOHNSON, W. E. B. 2011. Concise Review: Bone Marrow for the Treatment of Spinal Cord Injury: Mechanisms and Clinical Applications. *Stem Cells (Dayton, Ohio),* 29**,** 169-178.

WRIGHT, K. T., MASRI, W. E., OSMAN, A., ROBERTS, S., TRIVEDI, J., ASHTON, B. A. & JOHNSON, W. E. 2008. The cell culture expansion of bone marrow stromal cells from humans with spinal cord injury: implications for future cell transplantation therapy. *Spinal Cord,* 46**,** 811-7.

WRIGHT, K. T., UCHIDA, K., BARA, J. J., ROBERTS, S., EL MASRI, W. & JOHNSON, W. E. 2014. Spinal motor neurite outgrowth over glial scar inhibitors is enhanced by coculture with bone marrow stromal cells. *Spine J,* 14**,** 1722-33.

WU, L., FU, J. & SHEN, S. H. 2002. SKAP55 coupled with CD45 positively regulates T-cell receptor-mediated gene transcription. *Mol Cell Biol,* 22**,** 2673-86.

XU, L., ZHANG, K. & WANG, J. 2014. Exploring the mechanisms of differentiation, dedifferentiation, reprogramming and transdifferentiation. *PLoS One,* 9**,** e105216.

XU, S., LI, X., ZHANG, J. & CHEN, J. 2015. Prognostic Value of CD11b Expression Level for Acute Myeloid Leukemia Patients: A Meta-Analysis. *PLoS One,* 10**,** e0135981.

YAMANAKA, S. 2009. Ekiden to iPS Cells. *Nat Med,* 15**,** 1145-1148.

YOUNG, R. G., BUTLER, D. L., WEBER, W., CAPLAN, A. I., GORDON, S. L. & FINK, D. J. 1998. Use of mesenchymal stem cells in a collagen matrix for achilles tendon repair. *Journal of Orthopaedic Research,* 16**,** 406-413.

YUSUF, M., LEUNG, K., MORRIS, K. J. & VOLPI, E. V. 2013. Comprehensive cytogenomic profile of the in vitro neuronal model SH-SY5Y. *Neurogenetics,* 14**,** 63-70.

ZAPATA, A. G., ALFARO, D. & GARCÍA-CECA, J. 2012. Biology of Stem Cells: The Role of Microenvironments. *In:* LÓPEZ-LARREA, C., LÓPEZ-VÁZQUEZ, A. & SUÁREZ-ÁLVAREZ, B. (eds.) *Stem Cell Transplantation.* New York, NY: Springer US.

ZHANG, N., DIETRICH, M. A. & LOPEZ, M. J. 2013a. Canine intra-articular multipotent stromal cells (MSC) from adipose tissue have the highest in vitro expansion rates, multipotentiality, and MSC immunophenotypes. *Vet Surg,* 42**,** 137-46.

ZHANG, T., LEE, Y. W., RUI, Y. F., CHENG, T. Y., JIANG, X. H. & LI, G. 2013b. Bone marrow-derived mesenchymal stem cells promote growth and angiogenesis of breast and prostate tumors. *Stem Cell Research & Therapy,* 4**,** 70-70.

ZHANG, Y., CHOPP, M., MENG, Y., KATAKOWSKI, M., XIN, H., MAHMOOD, A. & XIONG, Y. 2015. Effect of exosomes derived from multipluripotent mesenchymal stromal cells on functional recovery and neurovascular plasticity in rats after traumatic brain injury. *J Neurosurg,* 122**,** 856-67.

ZHAO, J., HU, L., LIU, J., GONG, N. & CHEN, L. 2013a. The Effects of Cytokines in Adipose Stem Cell-Conditioned Medium on the Migration and Proliferation of Skin Fibroblasts In Vitro. *BioMed Research International,* 2013**,** 11.

ZHAO, R. R., ANDREWS, M. R., WANG, D., WARREN, P., GULLO, M., SCHNELL, L., SCHWAB, M. E. & FAWCETT, J. W. 2013b. Combination treatment with anti-Nogo-A and chondroitinase ABC is more effective than single treatments at enhancing functional recovery after spinal cord injury. *Eur J Neurosci,* 38**,** 2946-61.

ZHOU, L. J., ORD, D. C., OMORI, S. A. & TEDDER, T. F. 1992. Structure of the genes encoding the CD19 antigen of human and mouse B lymphocytes. *Immunogenetics,* 35**,** 102-11.

ZHU, Y., LIU, T., SONG, K., FAN, X., MA, X. & CUI, Z. 2008. Adipose-derived stem cell: a better stem cell than BMSC. *Cell Biochem Funct,* 26**,** 664-75.

ZIMMERMANN, S., GLASER, S., KETTELER, R., WALLER, C. F., KLINGMULLER, U. & MARTENS, U. M. 2004. Effects of telomerase modulation in human hematopoietic progenitor cells. *Stem Cells,* 22**,** 741-9.

ZOLLER, M. 2009. Tetraspanins: push and pull in suppressing and promoting metastasis. *Nat Rev Cancer,* 9**,** 40-55.

ZORNER, B., FILLI, L., STARKEY, M. L., GONZENBACH, R., KASPER, H., ROTHLISBERGER, M., BOLLIGER, M. & SCHWAB, M. E. 2010. Profiling locomotor

recovery: comprehensive quantification of impairments after CNS damage in rodents. *Nat Meth,* 7**,** 701-708.

ZOU, Z., ZHANG, Y., HAO, L., WANG, F., LIU, D., SU, Y. & SUN, H. 2010. More insight into mesenchymal stem cells and their effects inside the body. *Expert Opin Biol Ther,* 10**,** 215-30.

ZUK, P. A., ZHU, M., ASHJIAN, P., DE UGARTE, D. A., HUANG, J. I., MIZUNO, H., ALFONSO, Z. C., FRASER, J. K., BENHAIM, P. & HEDRICK, M. H. 2002. Human adipose tissue is a source of multipotent stem cells. *Mol Biol Cell,* 13**,** 4279-95.

ZUK, P. A., ZHU, M., MIZUNO, H., HUANG, J., FUTRELL, J. W., KATZ, A. J., BENHAIM, P., LORENZ, H. P. & HEDRICK, M. H. 2001. Multilineage cells from human adipose tissue: implications for cell-based therapies. *Tissue Eng,* 7**,** 211-28.

7 Appendix

7.1 Quantification of exosomes concentration and measurement of their diameters

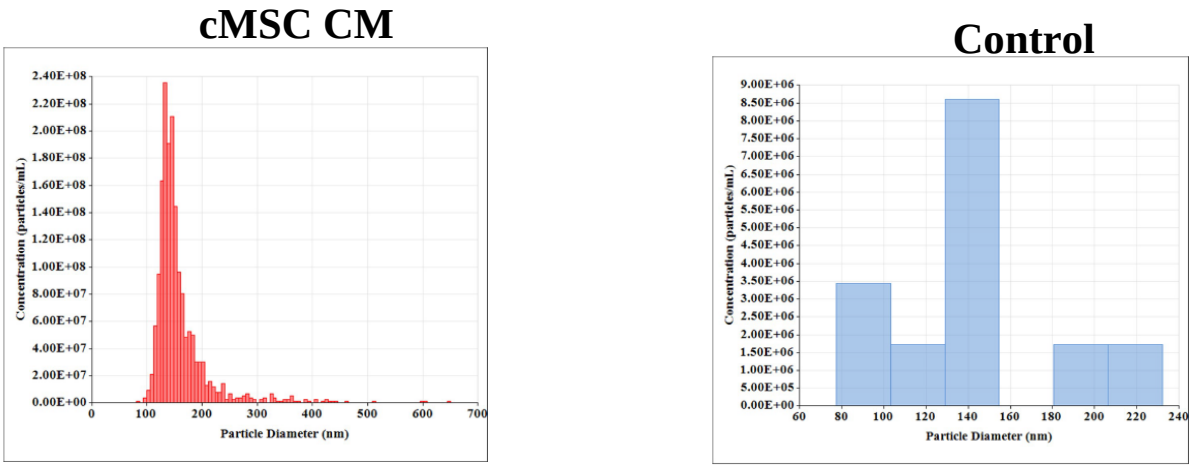

Figure 7:1 Measurements of the size and quantity of exosomes isolated from the secretomes of cMSCs.

The representative histograms show the concentration (y axis) and the diameter (x axis) of the extracellular vesicles from cMSC CM 2000 x*g supernatants* (left panel) and serum free medium as control (right panel, where the histogram show no presences of EVs). cMSC CM or serum free medium as controls were processed for EVs isolation by ultracentrifugation. Briefly, cMSC CM or control medium was centrifuged at 300 x*g* for 10 minutes. Then the collected supernatant was centrifuged at 2000xg for 20 minutes at 4 ºC. The supernatant was transferred to a special ultracentrifugation tube suitable for a SW 40 Ti rotor of optima L-100 ultracentrifuge (Beckman Coulter). This final supernatant was then ultra-centrifuged at 100,000 x*g* for 70 minutes. Then after removing the supernatant the pellets were re-suspended in 100 µl of PBS. The nanopore-based system q-Nano (IZON Science, Christchurch, New Zealand) was used to determine the size of extracellular vesicles in the MSC CM using a 200 nm nanopore membrane (IZON Science). The data was analysed using IZON software. Results suggest that cMSCs were secreting EVs in a relatively high concentration ($1.40x10^9$ particles/mL), where the majority of them fall within the diameter size range between 90 and 200 nm, commonly known to correspond to the exosomes (left panel). Serum free medium that should be EVs-free was also measured under the same conditions. Acquired data demonstrate the lack of characteristic EVs (right pane, l$3.26x10^7$ particles/mL) in serum free profiles as observed on the left panel, and it is due to the instrumental noise. It can be concluded that nanoparticles measured in cMSC CM preparations (left panel) are EVs derived from cells, and not from serum free medium (right panel).

7.2 List of publications

Al delfi, I. R., Sheard, J. J., Wood, C. R., Vernallis, A., Innes, J. F., Myint, P. & Johnson, W. E. 2016. Canine mesenchymal stem cells are neurotrophic and angiogenic: An in vitro assessment of their paracrine activity. Vet J, 217, 10-17.